https://doi.org/10.35662/unine-thesis-2958

Faculty of Science, Institute of Biology
Plant Physiology laboratory

Study of the physiological and molecular functions of ABC1K1 protein during early development of *Arabidopsis thaliana*

A dissertation submitted to the
University of Neuchâtel
For the degree of
Doctor of Philosophy in
Biological Sciences

Presented by

Joy Collombat

Thesis committee

Prof. Félix Kessler (Thesis director) – University of Neuchâtel
Dr. Fiamma Longoni (Co- thesis director) – University of Neuchâtel
Prof. Joop Vermeer – University of Neuchâtel
Dr. Michel Havaux – Aix Marseille University
Dr. Giovanni Finazzi – Grenoble Alpes University

Defended on January 20, 2022

UNIVERSITÉ DE NEUCHÂTEL

Faculté des Sciences
Secrétariat-décanat de Faculté
Rue Emile-Argand 11
2000 Neuchâtel – Suisse
Tél : + 41 (0)32 718 21 00
E-mail : secretariat.sciences@unine.ch

IMPRIMATUR POUR THESE DE DOCTORAT

La Faculté des sciences de l'Université de Neuchâtel autorise l'impression de la présente thèse soutenue par

Madame Joy COLLOMBAT

Titre:

"Study of physiological and molecular functions of ABC1K1 protein during early development of *Arabidopsis thaliana*"

sur le rapport des membres du jury composé comme suit:

- Prof. Felix Kessler, directeur de thèse, Université de Neuchâtel, Suisse
- Dre Fiamma Longoni, co-directrice de thèse, Université de Neuchâtel, Suisse
- Prof. Joop Vermeer, Université de Neuchâtel, Suisse
- Dr Michel Havaux, CEA, Cadarache, France
- Dr Giovanni Finazzi, CNRS, CEA, Grenoble, France

Neuchâtel, le 3 février 2022

Le Doyen, Prof. A. Bangerter

Abstract

Photosynthesis is a key bioenergetic mechanism allowing photosynthetic organisms such as plants or algae to convert sunlight energy into chemical energy to produce sugar, while releasing molecular oxygen. This process takes place in a specific cellular organelle called chloroplast. Inside the chloroplast, the components of the photosynthetic machinery required to perform the photochemical part of photosynthesis, are inserted in a highly dynamic structure, the thylakoid membrane. Plastoglobules, small lipoprotein particles (lipid droplets) associated with the thylakoid membrane, are essential for chloroplast lipid metabolism, thylakoid formation and photoprotection. These structures contain a large diversity of neutral lipids some of which have strong antioxidant properties, such as tocopherols, carotenoids or plastoquinone. Most of the plastoglobule proteins are involved in lipids metabolisms. Among them, the ABC1K proteins are involved in the regulation of neutral lipid metabolism and contribute to the maintenance of photosynthetic activity by plastoquinone homestasis. My PhD consists in the study of the physiological and molecular functions of ABC1K1 protein in the early development of *Arabidopsis thaliana*. In particular, we studied its role in early chloroplast biogenesis under stress-enhancing red and high light conditions.

We have discovered a new signaling mechanism in which ABC1K1 promotes the degradation of EX1, a singlet oxygen trigger ($^1O_2$), though the FTSH2 protease, particularly active under red light conditions. The accumulation of EX1 in *abc1k1* and *ftsh2* mutant led to the arrest of chloroplast biogenesis and a greening defect. Mutation of EX1 by CRISPR/Cas9 in the *abc1k1* background partially alleviated the greening defect observed in the *abc1k1* mutant (Chapter 2.1).

During my PhD, we also observed that *abc1k1* displayed a variegated phenotype under high light conditions, similarly to the *ftsh2* mutant. This result was integrated in the publication called "Plastoquinone homoeostasis by Arabidopsis proton gradient regulation 6 is essential for photosynthetic efficiency" published in the scientific journal "Communication Biology" in 2019 (Chapter 2.2).

Finally, we have shown that the dark re-oxidation of the photoactive plastoquinone pool is impaired in the *abc1k1* mutant suggesting a defect in the plastoquinone mobility. This defect is restored in the *abc1k1/abc1k3* double mutant. This result was integrated in the publication "Mutation of the Atypical Kinase ABC1K3 Partially Rescues the PROTON GRADIENT REGULATION 6 Phenotype in *Arabidopsis thaliana"* published in the scientific journal "Frontiers in Plant Science" in 2020 (Chapter 2.3).

This thesis provides new insight into the role of ABC1K1 and ABC1K3 proteins in the regulation of early chloroplast biogenesis and photosynthesis under stressful light conditions.

Keywords: Photosynthesis, Chloroplasts, plastoglobules, plastoquinone, ABC1K1, ABC1K3, Executer 1, signalling, singlet oxygen, chloroplast biogenesis, FTSH, red light.

Résumé

La photosynthèse est un mécanisme fondamental permettant aux organismes photosynthétiques comme les plantes ou les algues de convertir l'énergie lumineuse en énergie chimique dans le but de produit des sucres, en libérant de l'oxygène moléculaire. Ce processus se déroule dans une organelle spécifique appelé le chloroplaste. A l'intérieur du chloroplaste, tous les composants de la machinerie photosynthétique requis pour effectuer la phase photochimique de la photosynthèse sont insérés dans une structure hautement dynamique, la membrane des thylakoïdes. Les plastoglobules, de petites particules lipoprotéiques (« gouttelettes lipidiques ») associées à la membrane des thylakoïdes, sont essentiels pour le métabolisme du chloroplaste, la formation des thylakoïdes et la photo-protection. Ces structures contiennent une grande diversité de lipides neutres dont certains possèdent de fortes propriétés antioxydantes, comme les tocophérols, les caroténoïdes et la plastoquinone. La majorité des protéines du plastoglobule sont impliquées dans le métabolisme des lipides. Parmi elles, les protéines de la famille ABC1K sont impliquées dans la régulation du métabolisme des lipides neutres et contribuent au maintien de l'activité photosynthétique à travers l'homéostasie du plastoquinone.

Mon doctorat consiste à étudier les fonctions moléculaires et physiologiques de la protéine ABC1K1 dans le développement de jeunes plantules d'*Arabidopsis thaliana.* En particulier, nous avons étudié l'impact de la mutation d'*abc1k1* sur la biogénèse des chloroplastes en conditions de stress lumineux comme la lumière rouge ou la forte lumière blanche.

Nous avons découvert un nouveau mécanisme de signalisation dans lequel ABC1K1 stimule la dégradation de EX1, un senseur du singlet oxygène ($^1O_2$), à travers la protéase FTSH2 qui est particulièrement actif en conditions de lumière rouge. L'accumulation de EX1 dans les mutants *abc1k1* et *ftsh2* engendre l'arrêt de la biogénèse du chloroplaste qui donne un phénotype vert pâle aux plantules. La mutation de EX1, obtenue par CRISPR/Cas9 dans le mutant *abc1k1* permet de partiellement supprimer le phénotype pâle de *abc1k1* (Chapitre 2.1).

Durant ce doctorat, nous avons également observé que le mutant *abc1k1* présente un phénotype particulier quand il pousse sous forte intensité lumineuse appelé « variegated phenotype », de manière similaire au mutant *ftsh2*. Ce résultat a été intégré dans la publication appelée "Plastoquinone homoeostasis by Arabidopsis proton gradient regulation 6 is essential for photosynthetic efficiency" publiée dans le journal scientifique "Communication Biology" en 2019 (Chapitre 2.2). Finalement, nous avons montré que la ré-oxydation des plastoquinones au noir est affectée chez le mutant abc1k1, suggérant un défaut de mobilité ou d'homéostasis des plastoquinones. Ce défault est supprimé dans le double mutant abc1k1/abc1k3. Ces résultats ont été intégrés dans la publication appelée "Mutation of the Atypical Kinase ABC1K3 Partially Rescues the PROTON GRADIENT REGULATION 6 Phenotype in *Arabidopsis haliana"*publiée dans le journal scientifique "frontiers in Plant Science" en 2020 (Chapitre 2.3).

Cette thèse ouvre de nouvelles portes concernant le rôle de ABC1K1 et de ABC1K3 dans la régulation de la biogénèse des chloroplastes et de la photosynthèse en conditions de stress lumineux.

Mots-clés : Photosynthèse, chloroplastes, plastoglobules, ABC1K1, ABC1K3, Executer 1, signalisation, singlet oxygen, biogenèse du chloroplaste, FTSH, lumière rouge.

Table of content

Abbreviations

$^1O_2$	singlet oxygen
APKs	atypical protein kinases
ATP	adenosine triphosphate
ABC1K	activity of bc1 complex 1-like kinase
β-CC	β-cyclocitral
Bhlh	basic helix loop helix
CEF	cyclic electron flow
Chl	Chlorophyll
CHY2	β-carotene hydroxylases 2
CO2	carbon dioxide
COP1	Constitutive photomorphogenes1
cytb_6f	cytochrome b_6f
DGDG	Digalactosyldiacylglycerol
DMPBQ	dimethylphytylbenzoquinone
DNA	deoxyribonucleic acid
DP	Dipyridyl
ETC	electron transport chain
EX1	executer 1
FAR	far-red
FBN	Fibrillin
FC1	ferrochelatase 1
Fd	Ferredoxin
FM	maximum fluorescence in dark-adapted state
F0	minimum fluorescence in dark-adapted state
FV	variable fluorescence in dark-adapted state
FM’	maximum fluorescence in light

FNR	ferredoxin NADP+ reductase
FS	steady-state chlorophyll fluorescence in light
GM	grana margin
Gun	genomes uncoupled
H_2O_2	hydrogen peroxide
HL	high light
HPLC	high-performance liquid chromatography
HY5	elongated hypocotyl 5
kDa	kilodaltons
LCY	lycopene β-cyclase
LHC	light-harvesting complex
LHCBII	PSII light-harvesting chlorophyll a/b-binding protein 2
MPBQ	2-methyl-6-phytyl-1,4-benzoquinol
MGDG	monogalactosyldiacylglycerol
Mg-ProtoX	Mg-protoporphyrin X
NADPH	nicotinamide adenine dinucleotide phosphate
NDH	NAD(P)H dehydrogenase-like complex
NPQ	non-photochemical quenching
O2	molecular oxygen
OEC	oxygen evolving complex
OGE	organellar gene expression
PAP	3’-phosphoadenosine 5’-phosphosulfate
PC-8	plastochromanol-8
PC	plastocyanine
PETC	Photosynthetic electron transport chain
PG	plastogobule
PGR	proton gradient regulation

PhANG	photosynthesis-associated nuclear gene
Phy	Phytochrome
PIF	phtyochrome interacting factor
PKL	protein kinase-like
PLB	(paracrystalline) prolamellar body
PQ	Plastoquinone
PQH2	Plastoquinol
PSI	photosystem I
PSII	photosystem II
PTOX	plastid terminal oxidase / plastoquinone terminal oxidase
RL	red light
ROS	reactive oxygen species
STN	state transition kinase
SQDG	Sulfoquinovosyldiacylglycerol
TAG	Triacylglycerol
TIC	translocon at the inner chloroplast membrane
TOC	translocon at the outer chloroplast membrane
TMPBQ	Trimethylphytylbenzoquinone
VTE	vitamin E-deficient
WL	White light
WT	Wild type
ZDS	ζ-carotene desaturase
ΦMAX	maximum photosystem II efficiency
ΦPSII	photosystem II quantum yield

1. General introduction

1.1. Developmental plasticity of the plant

Plants are sessile organisms continuously challenged by environmental changes and stress factors, which require a strong capacity of acclimation. The plant phenotypic plasticity allows coping with environmental and developmental changes. It encompasses all the different phenotypes expressed by a single genotype in various environmental and stress conditions (Fusco and Minelli, 2010). Phenotypic plasticity is crucial for plant development, when many morphological and physiological changes occur. After germination in the dark, exposure of the seedling to light activates the de-etiolation process and plants undergo important phenotypic changes defined as the photomorphogenesis process.

1.1.1. Photomorphogenesis

Photomorphogenesis occurs upon illumination and is characterized by the opening of the cotyledons, arrest of the hypocotyl elongation and the full development of chloroplast ("greening"). This process is mostly under the control of photoreceptor families including the phytochromes (Phy). In *Arabidopsis thaliana*, five members of phytochrome family exist (Phy A, B, C, D and E). PhyA is involved in far red light signaling while the other Phy regulate red light signaling (Rockwell et al., 2006; Tripathi et al., 2019). Phytochromes are dimeric chromoproteins and exist in two forms: an active form (Pfr, active FR light-absorbing) and an inactive form (Pr, R light-absorbing) (Song et al., 2018). Upon red light illumination, the cytosolic inactive form of phytochrome (Pr) is converted into the active Pfr form and imported into the nucleus to regulate the expression of many light responsive genes. The main target of Pfr, is a group of basic helix loop helix (bHLH) transcription factors called PIFs, which act as negative regulators of photomorphogenesis (Martínez-García et al., 2000). It has been shown that phytochrome can phosphorylate PIFs leading to their degradation via the 26S proteasome pathway allowing photomorphogenesis to proceed (Park et al., 2018).

The E3 ubiquitin ligase COP1 (Constitutive photomorphogenesis protein 1) in complex with SPA1, is highly active in the dark and allows the degradation of many positive regulators of photomorphogenesis, such as HY5 (elongated hypocotyl 5) via the 26S proteasome pathway. HY5 is a transcription factor able to regulate many light-induced genes by binding to their promoters (Chattopadhyay et al., 1998). Upon illumination, COP1 is inactivated and Pfr (Phy B) can directly interact with SPA1 contributing to the dissociation of the COP1/SPA1 complex (Holm and Deng, 1999; Ponnu and Hoecker, 2021) allowing the accumulation of HY5 and the inhibition of hypocotyl elongation.

Light exposure of the seedling will also lead to modifications of plastid structure and metabolism resulting in a plastid designed for photosynthesis: the chloroplast.

1.1.2. Plastids are highly flexible plant organelles

Plastids are an essential family of organelles present in plant cells. They originated from an endosymbiotic event that occurred more than one billion years ago and involved a cyanobacterium and a eukaryotic cell (Gould et al., 2008; Reyes-Prieto et al., 2007; Yoon et al., 2004). These specialized organelles are highly versatile and possess a strong plasticity allowing them to differentiate and to perform many diverse functions.
The proplastid, an undifferentiated plastid, can differentiate into a leucoplast, etioplast or chloroplast according to the plant developmental stage and the environmental conditions. Leucoplasts are non-pigmented and serve mainly as storage compartments. Amyloplast and oleoplast are two types of leucoplasts, which accumulate starch and lipids, respectively. Two others types of plastids, the chromoplast and the gerontoplast generally differentiate from the chloroplast. Chromoplasts differentiate during fruit ripening and accumulate high levels of pigments, essentially carotenoids. In senescent leaves, the chloroplast thylakoid membrane is degraded resulting in gerontoplasts, which accumulate several thylakoid degradation products including triacylglycerol and phytol esters (Li and Yuan, 2013; Sadali et al., 2019). Chloroplast biogenesis requires light, which promotes the differentiation of the chloroplast precursor in the dark, the etioplast, into a photosynthetically active chloroplast. Chloroplasts possess their own genetic material and transcription/translation machinery. They are characterized by highly specific membrane structures, the thylakoids, allowing it to host the the photosynthetic electron transport chain.

1.2. The chloroplast, an essential plant organelle

1.2.1. The chloroplast structure

Three membrane systems define the chloroplast structure: an outer and an inner membrane, and a thylakoid membrane, where the light-driven photosynthetic reactions take place (Figure 1.1).

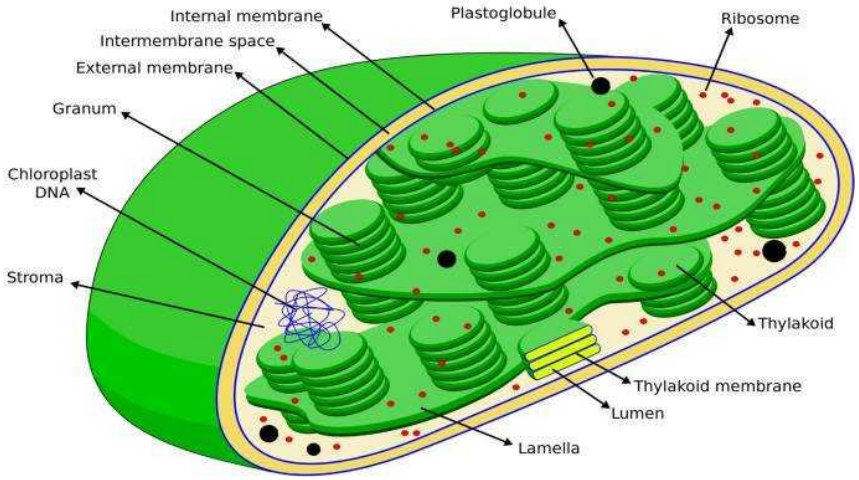

Figure 1.1. Schematic representation of the chloroplast structure (From burrosabio.net).

1.2.1.1. The outer and inner membrane of the chloroplast

The chloroplast is delimited by an envelope, consisting of an inner and an outer membrane, separated by an intermembrane space. These membranes are composed mainly of monogalactosyldiacylglycerol MGDG, digalactosyldiacylglycerol DGDG and include a low proportion of phosphatidylcholine (Block et al., 1983; Mackender and Leech, 1974).
Into theses membranes, the TIC and TOC complexes (translocons at the inner/outer chloroplast membranes) are inserted and responsible for the import of preproteins into the chloroplast (Paila et al., 2015; Richardson et al., 2014; Schnell et al., 1994). Preproteins are proteins encoded by the nucleus and carrying a transit peptide at their N-termini allowing their recognition and then their import by the TIC-TOC import machinery into the chloroplast (Keegstra and Cline, 1999; Keegstra and Froehlich, 1999; Kessler and Schnell, 2004; Lee et al., 2005; Smith et al., 2004). The TOC complex is located across the outer membrane and is mainly composed of three proteins: TOC 159, TOC 75 and TOC34. The TIC complex is composed of 5 proteins; TIC 110, TIC 20, TIC 40, TIC 21, TIC 22, and allows protein translocation across the inner membrane of the chloroplast (Andrès et al., 2010; Küchler et al., 2002; Schnell et al., 1997; Schnell et al., 1994) (Figure 1.2).

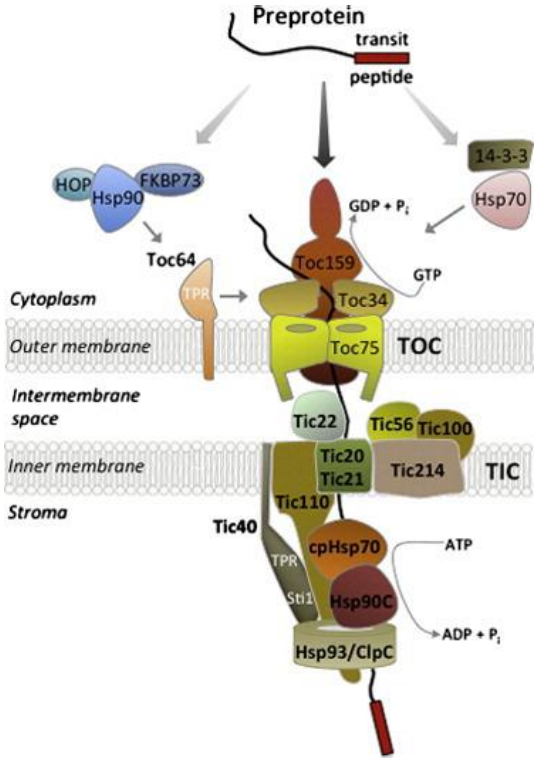

Figure 1.2. The TIC/TOC complex (translocon at the inner/outer membrane) (From Paila et al., 2015).

1.2.1.2. The thylakoid membrane of the chloroplast

The thylakoid membrane is a highly dynamic structure mostly arranged in stacks called grana (granal thylakoids) inside the chloroplast. The portion of the thylakoid membranes that is not stacked in grana is called stroma lamellae (stromal thylakoids) (Daum and Kühlbrandt, 2011) (Figure 1.1). This membrane is mainly composed of: two galactolipids monogalactosyldiacylglycerol (MGDG) and digalactosyldiacylglycerol (DGDG), a sulfolipid (sulfoquinovosyldiacylglycerol SQDG) and a low proportion of phosphoglycerolipids, mostly phosphatidylglycerol (PG), phosphatidylcholine (PC) and phosphatidylinositol (PI) (Boudière et al., 2014). Within the thylakoid membrane there are also several neutral lipids, which participate in the structure of the photosynthetic complexes and in electron transport between and within them (plastoquinone, phylloquinone). Some of these neutral lipids possess antioxidant properties that are critical for light acclimation such as β-carotene/xantophyll, plastoquinone, plastochromanol and tocopherols (Cazzaniga et al., 2012; Havaux et al., 2005; Latowski et al., 2011; Szymańska and Kruk, 2010). The photosynthetic complexes are inserted into the thylakoid lipid bilayer. This membrane separates two different compartments inside the chloroplast; the space comprised inside the thylakoids is referred to as the lumen while the stroma corresponds to the soluble phase outside the thylakoids (Figure 1.3). This separation is essential for the formation of a proton gradient across the membrane and thus for the functionality of the ATP synthase (Junesch and Gräber, 1991).
Small lipid droplets, with a radius from 30 to 100 nm (Lichtenthaler, 1968), are associated with certain regions of the thylakoid membrane, mostly the curved regions of the stromal thylakoids. These lipid droplets, called plastoglobules, are delimited by a lipid monolayer contiguous with the outer leaflet of the thylakoid membrane. Plastoglobules remain attached to the thylakoid after their formation (Austin et al., 2006a).

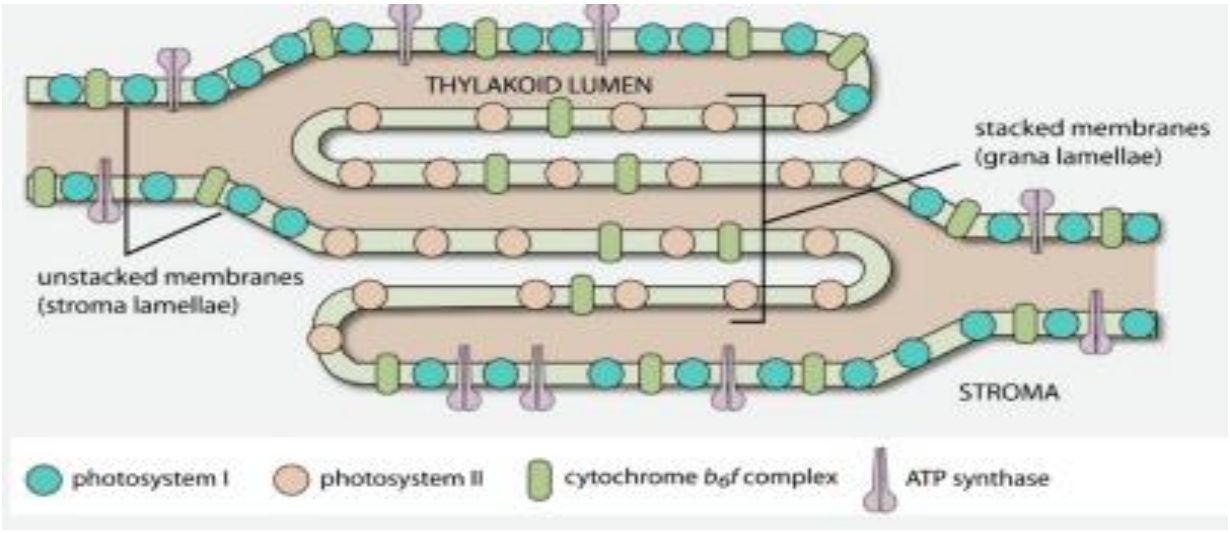

Figure 1.3. Schematic representation of thylakoids membrane and photosynthetic proteins (From Mirkovic et al., 2017).

1.2.2. Chloroplast biogenesis

1.2.2.1. From etioplast to chloroplast

In the dark, proplastids differentiate into precursors of the chloroplast called etioplasts (Solymosi and Schoefs, 2010). This plastid type is characterized by the absence of chlorophyll, an accumulation of its precursor, protochlorophyllide, and the presence of paracrystalline prolamellar bodies (PLB), which contain molecules essential for the biogenesis of the thylakoid membrane and the synthesis of chlorophyll (Blomqvist et al., 2008; Solymosi and Schoefs, 2010). Indeed, the PLB accumulates MGDG and DGDG, the two main components of the thylakoid membrane (Aronsson et al., 2008) and several proteins, linked to chlorophyll synthesis and the photosynthetic process (chlorophyll synthase, NADPH protochlorophyllide oxidoreductase, ATP synthase, cytochrome b6f). Upon illumination, lamellar prothylakoids emerge from the PLB, (Grzyb et al., 2013; Gunning, 2001) and the typical structure of the chloroplast, the thylakoid membrane, takes shape (Pipitone et al., 2021). At the same time, protochlorophyllide is converted into chlorophyll. The number of plastoglobules is higher in the etioplast and decreases during the conversion into the chloroplast (Lichtenthaler, 1968; Nacir and Brehelin, 2013; Sprey and Lichtenthaler, 1966). This decrease suggests that plastoglobules play an important role in the formation of thylakoid membranes during the conversion from etioplasts to chloroplasts.

1.2.2.2. Mutants defective in chloroplast biogenesis: the *im* and *var2* mutants

Chloroplast biogenesis is a highly complex process and involves many cytosolic and chloroplast proteins. It has been shown that mutation of different genes in *Arabidopsis thaliana* can lead to severe chloroplast biogenesis defects, among them, the *im* (*ptox*) and the *var2* (*ftsh2*) mutants have been well characterized. Both mutants display a variegated phenotype, characterized by green and albino leaf sectors (Rosso et al., 2009). The green sectors contain cells with normal chloroplasts whereas cells in white sectors contain abnormal chloroplasts with a lower pigment concentration (Aluru et al., 2001; Rédei, 1967).

The PTOX enzyme is responsible for electron transfer from PQH_2 to molecular oxygen producing water. This shows that PTOX contributes to the regeneration of oxidized PQ from its reduced form (PQH_2). Consequently, the *ptox* mutant (*im)* is characterized by an over-reduced plastoquinone pool, leading to a defect in the electron transport along the thylakoid membrane, in particular around PSI (Okegawa et al., 2010). The PTOX enzyme is indirectly involved in the desaturation reactions required for carotenoid production and the *ptox* mutant is characterized by the accumulation of the carotenoid precursor phytoene (Wetzel et al., 1994). The redox imbalance in the *im* mutant results in a variegated phenotype with green and white sectored leaves (Rosso et al., 2009). Studies on dark-grown seedlings suggest that PTOX has a central role in etioplast metabolism, specifically being involved in cyclic PSI electron flow mediated by PGR5 (PROTON GRADIENT REGULATION 5) and in plastoquinone redox regulation mediated by NDH (NAD(P)H dehydrogenase) (Kambakam et al., 2016). By acting

on the redox state of the plastoquinone pool, PTOX contributes to an important retrograde signal for the adaptation to stress conditions.

The *var2* (*ftsh2*) mutant also shows strong chloroplast biogenesis defects characterized by a variegated phenotype (Chen et al., 2000). This mutant lacks the FTSH2 chloroplast protease. FTSH2 is an ATP-dependent metalloprotease that belongs to the AAA (ATPase Associated with diverse cellular Activities) protein family and is part of the FTSH complex localized in the thylakoid membrane (Neuwald et al., 1999; Patel and Latterich, 1998). In *Arabidopsis thaliana*, nine out of 12 FTSH proteases are localized in chloroplast (FTSH 1,2,5,6,7,8,9,11,12) and three in mitochondria (Lindahl et al., 1996; Sakamoto et al., 2003; Yu et al., 2004; Yu et al., 2005). The most accumulated FTSH protease in *Arabidopsis thaliana* are FTSH2, FTSH5, FTSH8 and FTSH1 (Sinvany-Villalobo et al., 2004; Yu et al., 2004). These proteins form a hetero-complex composed of two types of subunits, A (FTSH1 and FTSH5) and B (FTSH2 and FTSH8). The proteins within a type are redundant, but the presence of both types is essential for the accumulation of a stable complex (Adam et al., 2006; Sakamoto et al., 2003; Yu et al., 2004; Zaltsman et al., 2005).
It is known that the FTSH complex is involved in the degradation of several photosynthetic complexes and proteins such as cytochrome b6f complex (Ostersetzer and Adam, 1997) and the damaged D1 proteins in the PSII repair cycle (Bailey et al., 2002; Nixon et al., 2005). This important process allows avoiding the accumulation of photodamaged D1 that can lead to photoinhibition. (Bailey et al., 2002; Sakamoto et al., 2002, 2004). Indeed, accumulation of ROS has been observed in *ftsh* mutants (Kato et al., 2009). However, no up-regulation of ROS related genes has been observed in theses mutants. (Miura et al., 2010). Knowing that ROS are important retrograde signaling molecules, these results suggest that FTSH protease may be involved in ROS signaling (Kato and Sakamoto, 2018).
Indeed, it has been shown that FTSH2 triggers $^1O2$ signalling through the proteolysis of EXECUTER 1 (EX1) (Dogra et al., 2017; Wang et al., 2016). EXECUTER1 (EX1) and EX2 are key components of the singlet oxygen signaling pathway (Lee et al., 2007; Zhang et al., 2014). Mutation of both EX1 and EX2 largely suppresses chloroplast $^1O_2$ signaling observed in the *flu* mutant (Kim and Apel, 2013; Kim et al., 2012; Wagner et al., 2004) and, in addition, *ex1/ex2* mutant was reported to have a defect in chloroplast biogenesis during embryo development (Kim et al., 2009).

1.2.3. The photosynthesis, the main plant bioenergetic mechanism

1.2.3.1. Generalities

Photosynthesis is a key bioenergetic mechanism allowing plants, algae and cyanobacteria to convert sunlight energy into chemical energy to be used to produce organic molecules. This process takes entirely place inside the chloroplast.
The photosynthetic process can be divided into two distinct phases. A first part called “light phase”, which is dependent on the light and results in the production of the high-energy molecules NADPH and ATP. A second part, which is called “dark phase”, is independent of

light and occurs in the stroma of the chloroplast and consists in the assimilation of CO_2 into organic molecules such as glucose. This is accomplished using the high energy molecules produced during the light phase in a process known as the Calvin cycle.

1.2.3.2. Structure, composition and functioning of the thylakoid photosynthetic machinery

The "light phase" of photosynthesis occurs at the thylakoid membrane and consists in the conversion of the light energy into chemical energy. This process is driven by an electron flow along a chain of photosynthetic complexes inserted in the thylakoid membrane and ultimately leads to the production of the two aforementioned high-energy molecules: NADPH and ATP.

The two main photosynthetic complexes are photosystem I (PSI) and photosystem II (PSII). The photosystems are separated in the thylakoid membrane: PSI is mainly localized in the stroma lamellae whereas the PSII is mainly found in the grana stacks. These complexes constitute a network of proteins and pigments and work in tandem to provide the energy needed for the Calvin cycle in the stroma. Membrane-bound peripheral light-harvesting complexes (LHC) surround the core of the PSII and PSI.

The PSII core is mainly present as a dimer in the stacked regions of the thylakoid membrane. It consists of a heterodimer of two proteins PsbA and PsbD, also called D1 and D2 respectively (Pagliano et al., 2014). These proteins contain the reaction center of the PSII enclosing a specialized pair of chlorophylls, the chlorophyll P680, which is involved in the electron transfer from water to the plastoquinone molecule Q_B bound to the PSII core during the light driven reactions of the photosynthesis. The PsbA and PsbD proteins of the PSII core are associated with two other major proteins, PsbB (CP47) and PsbC (CP43), which are inner PSII antenna proteins (Figure 1.4). Other proteins (PsbE, F, H, I, J, K, L, M, N, S, W, X) play a role in the stabilization of cofactors binding to the PSII core (Pagliano et al., 2013). PSII is also associated with the oxygen evolving complex (OEC) localized on the luminal side of the thylakoid membrane. This complex is composed of a Mn_4CaO_5 cluster surrounded by 4 PSII proteins: PsbO, PsbP, PsbQ and PsbR (Loll et al., 2005), and constitutes the catalytic center of PSII responsible of the oxidation of two H_2O molecules, leading to the release of one oxygen molecule, 4 protons (H^+) and 4 electrons (Vinyard and Brudvig, 2017). The majority of PSII proteins are encoded by the chloroplast genome except PsbO, P, Q, R, S, W, X, which are nuclear encoded proteins.

Peripheral antenna complexes transfer absorbed light energy in the form of chlorophyll excitation to the core of the PSII. This antenna system is composed of 6 isoforms of light-harvesting proteins (Lhcb1-6); Lhcb1, Lhcb2 and Lhcb3 form homo- and heterotrimers known as the major LHCII antenna. Lhcb4, Lhcb5 and Lhcb6 (CP29, CP26, and CP24 respectively) are located between LHCII trimers and the core complex as monomers (Xu et al., 2017). Each LHCB protein is associated with 11-14 chlorophyll molecules a or b and 2-4 carotenoid molecules (Liu et al., 2004; Pan et al., 2011; Standfuss et al., 2005). The size of the functional

antenna, its composition and organization can change in response to variations of light intensity and spectrum.

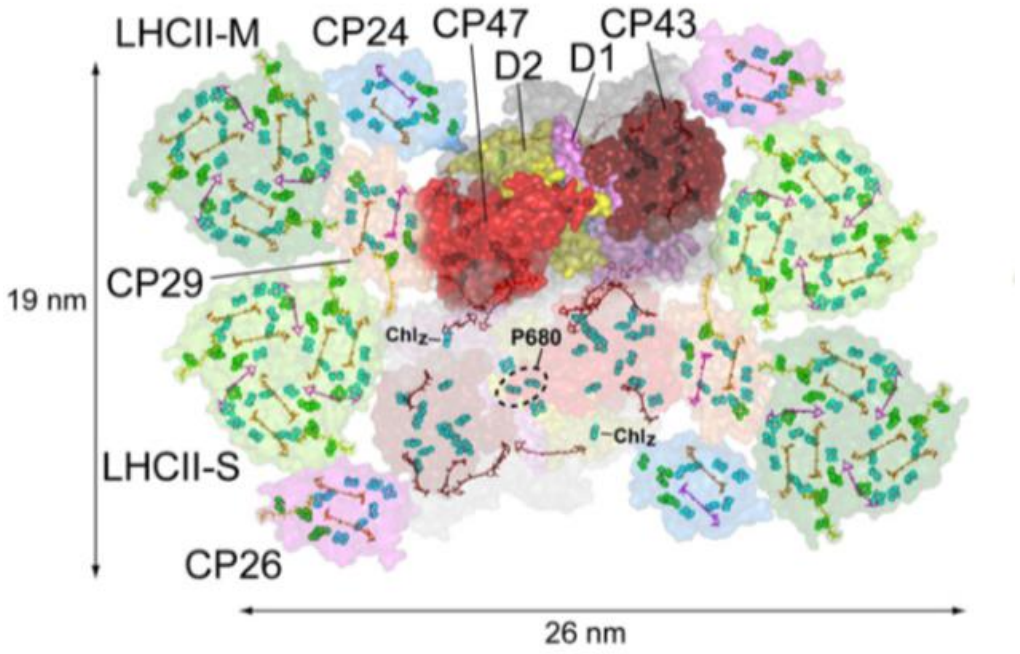

Figure 1.4. Representation of the PSII-LHCII supercomplex. (From Caffari et al., 2014).

PSI consists of a core complex composed of a heterodimer of the two major subunits, PsaA and PsaB, surrounded by 10 other structural proteins (PsaC, D, E, F, G, H, I, J, K, L and N) (Amunts et al., 2007) (Figure 1.5). Some of these proteins are encoded by the nucleus (PsaD, E, F, G, H, J, K, L, N) while the others are chloroplast encoded. The core complex contains approximatively 100 chlorophyll molecules. A specialized pair of chlorophyll, called P700, is located inside the reaction center of PSI and catalyzes the transfer of electrons from plastocyanin to the ferredoxin (Fd) to produce NADPH. The core of PSI is associated with protein pigment light-harvesting complexes consisting of four LHCI antennas (Lhca1-4). These antennas are composed of four proteins of the LHC family of chlorophyll a/b binding proteins, Lhca1-4. Lhca proteins are encoded by the nucleus and each protein contains 11-14 chlorophyll molecules (Amunts et al., 2007).

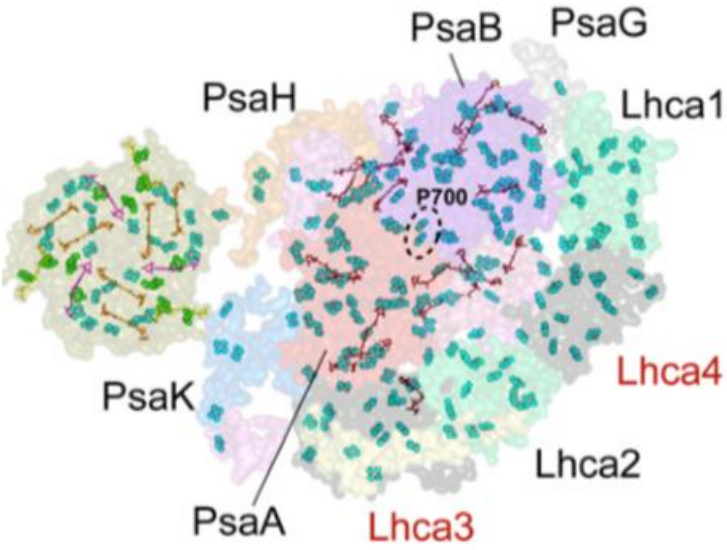

Figure 1.5. Representation of the PSI-LHCI super-complex (From Caffari et al.,2014).

The cytochrome *b*$_6$*f* complex (cyt*b*$_6$*f*) is functionally located between the PSII and the PSI. The structure of this complex has some analogies to that of its mitochondrial homologue the bc1 complex (Breyton, 2000). cyt*b*$_6$*f* is composed of 8 subunits; four large subunits PetA, PetB, PetC, PetD and four small subunits PetG, PetL, PetM and PetN (Whitelegge et al., 2002), and allows the electron transfer from the two electron-carrier plastoquinol PQH_2 to the lumenal single electron-carrier plastocyanine (PC) (Tikhonov, 2014).

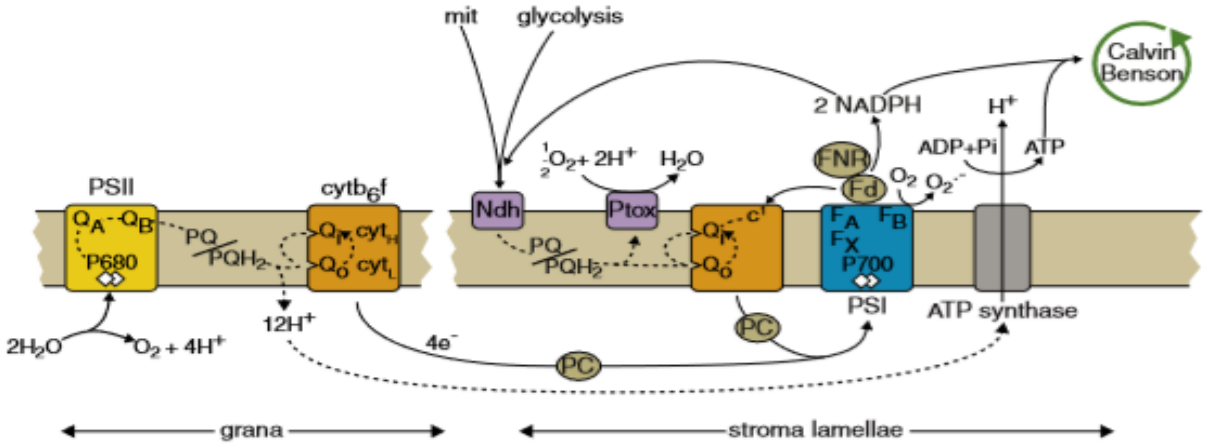

Figure 1.6. Schematic representation of the photosynthetic electron transport along the thylakoid membrane. (From Rochaix et al., 2011).

The capture of a photon by the chlorophylls in PSII antennas leads to an excitation of this molecule increasing its energy status. The excitation is transferred between chlorophylls through the antenna network until it reaches the specialized chlorophyll P680 pair in the PSII reaction center (Figure 1.6). Excitation of P680 results in the transfer of one electron from P680

to the plastoquinone molecule located in the Q_A site of the reaction center of the PSII. P680 thus becomes a strong oxidant capable of taking one electron provided by the OEC.
Then, the reduced quinone Q_A in the reaction center transfers its electrons to the quinone Q_B, which is released from PSII into the diffusible plastoquinone pool until it reaches the cyt*b*$_6$*f* complex.
The cyt*b*$_6$*f* complex catalyzes the transfer of one electron at a time from the plastoquinol (PQH_2) to the plastocyanine (PC), which can in turn transfer its electron to the oxidized chlorophyll P700 in the reaction center of the PSI. Finally, the P700 excited by the chlorophylls located in the associated antenna, will transfer one electron to the ferredoxin and then to the NADP+ to form NADPH (Rochaix, 2011; Tikhonov, 2014).
The linear electron transport produces also a proton gradient (ΔpH) across the thylakoid membrane. The accumulation of protons in the lumen of thylakoid allows the production of ATP by the ATP synthase complex located in the stroma lamellae portion of the thylakoid membrane.
In parallel to linear electron transport, PSI can also perform cyclic electron transport (CEF), which also contributes to the formation of the proton gradient across the thylakoid membrane (Fork and Herbert, 1993; Munekage et al., 2004). The cyclic transport system transfers electrons from reduced ferredoxin or NADPH back to the plastoquinone pool and subsequently to the cyt*b*$_6$*f* complex (Figure 1.6), allowing to produce ATP without the accumulation of NADPH (Shikanai and Yamamoto, 2017).

1.2.3.3. Photoprotection mechanisms: Non-photochemical quenching (NPQ), state transition and PSII repair cycle

The action of different complexes and molecules involved in the photochemical electron transport needs to be finely regulated in order to maximize the photosynthesis while avoiding the production of potentially harmful redox species (Pospíšil, 2016). This regulation is of particular relevance upon changes in light quality and intensity. In conditions of high light, there is an excess of energy that cannot be used for photochemistry. In particular, the over-excitation of P680 results in the production of triplet state chlorophyll (3Chl*) that can react with molecular oxygen producing singlet oxygen ($^1O_2$*) as well as other reactive oxygen species (ROS) which are toxic for the plant (Richter et al., 1990). To limit this problem, the photosynthetic machinery is capable of dissipating excess energy via an inducible process called non-photochemical quenching (NPQ). NPQ is activated by the acidification of the thylakoid lumen and involves PsbS, and the conversion of violaxanthin to zeaxanthin (Li et al., 2002; Li et al., 2000; Nilkens et al., 2010). This leads to a conformational change in LHCII antenna which promotes the non-photochemical dissipation of the excess energy (Chen and Gallie, 2012; Müller et al., 2001).

Another regulatory mechanism exists to tune the light harvesting between the two photosystems (PSI and PSII) known as state transitions. This process occurs when there is an imbalance of excitation between the two photosystems. When PSII is overexcited, a kinase (STN7) phosphorylates the LHCII antenna (Bellafiore et al., 2005). This phosphorylation leads to the

migration of a mobile part of the LHCII trimers from PSII to PSI. The LHCII redistribution equilibrates the light harvesting between the two photosystems. This state is called state II. The dephosphorylation of LHCII antenna by the PPH1/TAP38 phosphatase triggers the dissociation of LHCII antenna from PSI and its association back to PSII (state 1) (Shapiguzov et al., 2010). (Figure 1.7). It has been shown that this state transition process depends on the redox state of the photoactive plastoquinone pool since the reduction of this pool constitutes a signal for the activation of the STN7 kinase (Vener et al., 1997; Zito et al., 1999).

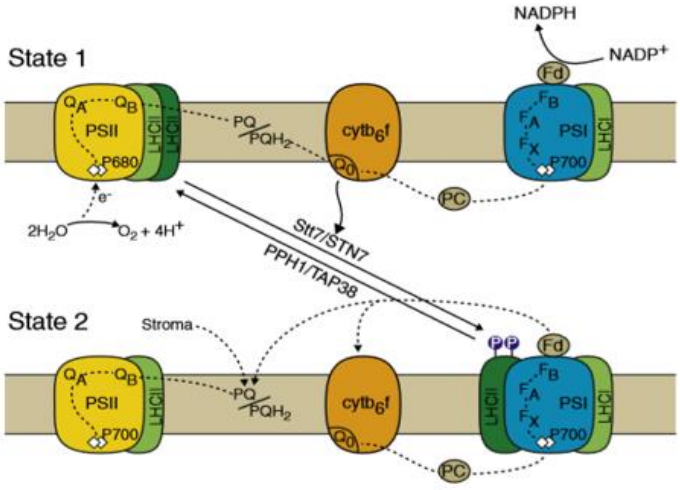

Figure 1.7. Schematic representation of the state transition process (From Rochaix et al., 2011).

During stress conditions, particularly under high light exposure, PSII can produce an excess of ROS. This can lead to photooxidative damage of the PSII core subunit D1 (PsbA) (Aro et al., 1993; Pospísil, 2009). To maintain PSII activity and the substitute damaged D1 protein, plants have a mechanism called PSII repair cycle, consisting in the light-dependent turnover of the D1 protein (figure 1.8).

This process is initiated by the phosphorylation of PSII core proteins, particularly D1, D2, CP43 and PsbH at their N-termini by the thylakoid state transition kinase homolog STN8. The phosphorylation facilitates the disassembly of the PSII supercomplexes in the grana stack and the migration of the PSII core monomer to the stroma lamellae (Herbstová et al., 2012; Tikkanen et al., 2008). Once there, the PSII core monomer is disassembled concomitantly with the release of CP43 and the oxygen evolving complex (OEC) and the D1 protein can be degraded. Two types of protein are involved in D1 degradation: The FTSH metalloprotease and Deg protease (Järvi et al., 2015; Kato and Sakamoto, 2009; Kato et al., 2012; Nixon et al., 2005).

After D1 degradation, a newly synthesized D1 protein is inserted into the PSII core monomer followed by the CP43 reassembly and by that of the OEC (van Wijk et al., 1997; Walter et al., 2015; Zhang et al., 1999). Finally, the repaired PSII core monomer can return back to the grana stack to be reassembled in a dimer and supercomplexes (Theis and Schroda, 2016).

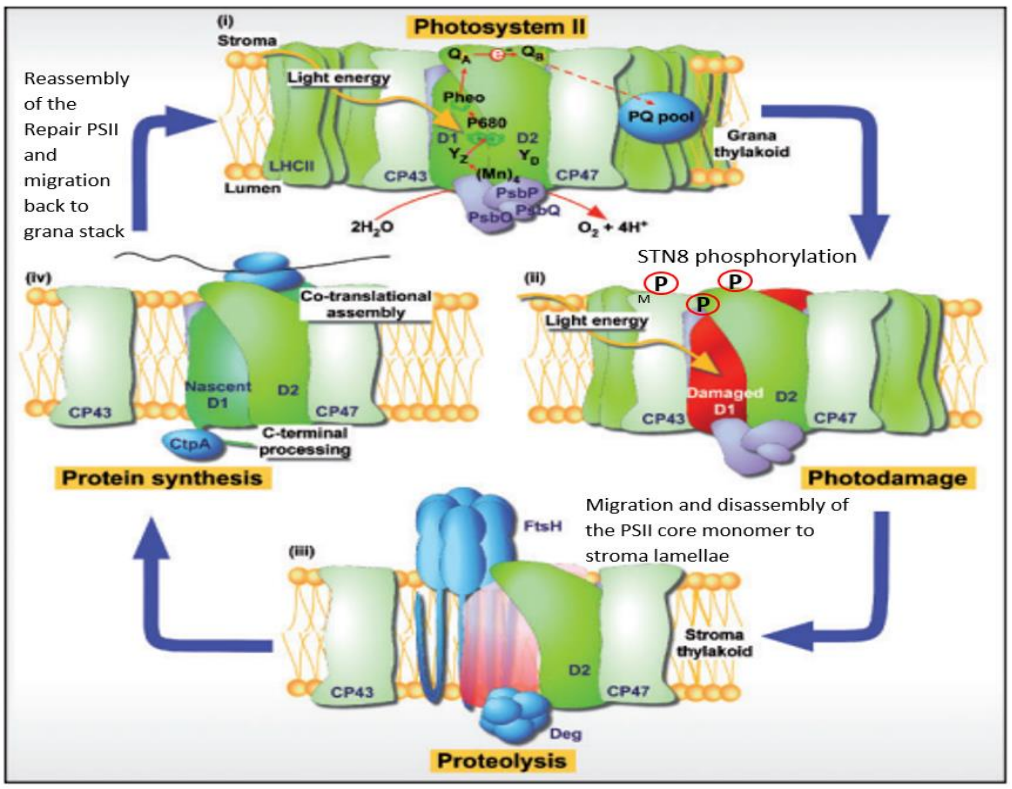

Figure 1.8. Schematic representation of the PSII repair cycle I) Functional PSII supercomplex in the grana stack of the thylakoid membrane. II) Photodamage of D1 core protein. The STN8-dependent phosphorylation of PSII proteins including damaged D1 induced the partial disassembly of the PSII complex and the migration of PSII core monomer to thylakoid stroma lamellae. III) The PSII core monomer is disassembled and FTSH and DEG protease degrade the photodamaged D1 protein. IV) After *De novo* synthesis of D1 protein, the PSII core is reassembled and migrate to the grana stack of the thylakoid membrane to form PSII-LHC supercomplexes. (Adapted from Kato and Sakamoto., 2009).

1.2.4. Communication between the chloroplast and the nucleus

1.2.4.1. Retrograde signalling, a key mechanism for plant acclimation

During evolution, a major part of the ancestral cyanobacterial genome (95%) has been lost or transferred to the genome of the eukaryotic host cell, so that only around 100 residual genes remain in the chloroplast (Martin et al., 2002; Martin et al., 1998; Sugiura, 1989; Timmis et al., 2004). Consequently, many of the chloroplast proteins are encoded by nuclear genes. The 117 chloroplast-encoded proteins are mainly related to organelle gene expression (OGE) or energy production whereas about 3000 plastid proteins with a wide variety of functions are imported from the cytosol (Jarvis, 2004; Keegstra and Froehlich, 1999; Kessler and Schnell, 2006). In order to coordinate the gene expression and the protein production between the nucleus and the chloroplast, the cell has evolved a retrograde/anterograde signaling system, allowing the communication between these two cellular compartments. This regulation is critical for the development of the plant and its stress resistance.

Nuclear genes encode the majority of proteins involved in OGE, thus allowing direct nuclear control of the OGE. This control is part of an anterograde signaling system. Conversely, the chloroplast can also modulate the expression of some nuclear genes through several retrograde signaling pathways.
The retrograde signaling allows the transmission of information about the physiological and developmental states of the chloroplast to the nucleus in order to modulate the expression of specific set of nuclear genes. The chloroplast retrograde signals are needed for the chloroplast and photosystem development, but also for the adaptation to environmental changes (Kleine and Leister, 2016).

1.2.4.2. Several molecules can act as retrograde signalling factors

Up to now, several sources of retrograde signaling have been identified and characterized:First, intermediates of the tetrapyrrole biosynthesis pathway have been reported to act as retrograde signaling molecules, leading to a modification of nuclear gene expression.

A genetic mutant screen using the bleaching herbicide norflurazon, an inhibitor of carotenoid biosynthesis, allowed the identification of some mutants affected in retrograde signaling, these mutants were called “Gun mutants” for *genome uncoupled* (*gun*) (Susek et al., 1993) (figure 1.9).
The *gun2* and *gun5* mutants are both impaired in enzymes involved in tetrapyrrole biosynthesis. The GUN5 locus encodes for the H-subunit of Mg-chelatase and *gun5* is characterized by a reduced level of Mg-protoporphyrin IX (Mg-ProtoIX) and therefore a reduced level of chlorophyll (Mochizuki et al., 2001). The GUN2 locus encodes a heme oxygenase, and the corresponding mutant displays a pale phenotype due to the accumulation of heme which is part of the feedback inhibition of the early step of tetrapyrrole biosynthesis (Terry and Kendrick, 1999). These mutants are both characterized by a reduced level of Mg-ProtoIX and by an impairment of retrograde signaling manifest in the expression of photosynthesis-associated nuclear genes (PhANG) even under norflurazon treatment when chloroplasts do not properly develop (Strand et al., 2003). In addition, treatment with norflurazon of wild type seedlings has been shown to increase the level of Mg-ProtoIX and down-regulate the expression of nuclear photosynthetic genes, supporting the hypothesis in which Mg-ProtoIX acts as a retrograde signaling molecule to repress the nuclear gene expression under stress condition such as norflurazon treatment (Strand et al., 2003).

Other intermediates of the tetrapyrrole biosynthetic pathway have been proposed to trigger retrograde signaling. In the *gun6-1D* mutant, which overexpressed the plastid ferrochelatase 1 (FC1, heme synthase) the PhANG expression is increased, suggesting that heme accumulation may act directly on PhANG expression (Woodson et al., 2011). However, it cannot be excluded that the heme-related signal acts indirectly on PhANG expression, by inducing the reduction of the level of Mg-ProtoIX. Interestingly, analysis of the *gun1* mutant, suggests that GUN1 is acting downstream of the Mg-ProtoIX signal. Indeed, treatment of norflurazon grown *gun1* seedlings with dipiridyl (DP), a compound known to increase the level of Mg-ProtoIX fails to restore the repression of Lhcb gene expression, while in *gun2* and *gun5* mutant, DP treatment

restores the PhANG. Moreover, ABAI4, a nuclear transcription factor, has been identify as a nuclear component of retrograde signaling.
The genetic analysis of the *aba1* mutant revealed an accumulation of Lhcb gene expression even when the chloroplast is impaired, similarly to *gun* mutants. Interestingly, overexpression of ABI4 restored the *gun1* phenotype, demonstrating that ABI4 acts downstream of GUN1 in retrograde signaling pathway (Koussevitzky et al., 2007; Zhang, 2007). Taken together, these results suggest that Mg-ProtoIX or heme signals may not directly trigger the retrograde signaling but rather be integrated in the GUN1-ABA14 pathway to repress PhANG.

Another well-described retrograde signaling pathway is the SAL1-PAP pathway. SAL1 is a phosphatase found in both mitochondria and chloroplast which negatively regulate the level of PAP (3'-phosphoadenosine 5'-phosphosulfate) by dephosphorylating PAP into AMP (adenosine monophosphate). Therefore, the *sal1* mutant is characterized by an accumulation of PAP. PAP has been shown to inhibit the exoribonuclease XRN2, 3 and 4 involved in the degradation of aberrant RNAs. It is proposed to act as retrograde signal since the level of PAP increased during high light or drought stress (Estavillo et al., 2011). This is consistent with the observation that *sal1* mutant (*alx8*) was reported to be drought tolerant (Rossel et al., 2006). Transgenic lines targeting the SLA1 protein either in the nucleus or the chloroplast in the *sal1* mutant restored the level of PAP suggesting that PAP is able to move between the nucleus and the chloroplast to relay retrograde signaling (Estavillo et al., 2011). Finally, analysis of global gene expression in the *sal1* mutant revealed an up-regulation of genes, many being involved in drought, heat, wounding and cold, demonstrating the involvement of SAL1-PAP pathway in stress-retrograde signaling (Wilson et al., 2009). More recently, the SAL1-PAP pathway has been shown to be involved in iron homeostasis since mutation of this pathway lead to the up-regulation of three ferritin genes AtFER1, AtFER3, and AtFER4 (Balparda et al., 2020).

A further source of retrograde signaling is associated with the redox state of the chloroplast. The over-accumulation of reactive oxygen species (ROS) such as hydrogen peroxide H_2O_2 or hydroxyl radicals (OH*), can also act as retrograde signals and modulates the expression of nuclear genes, especially during stress conditions (Galvez-Valdivieso and Mullineaux, 2010; Pogson et al., 2008; Rossel et al., 2002; Slesak et al., 2007). In particular, singlet oxygen ($^1O_2$) is responsible for most photosynthetic damage occurring inside the chloroplast under stress conditions (Triantaphylidès et al., 2008) and was reported to act as a retrograde signal modulating the expression of nuclear photosynthetic genes during cotyledon greening (Page et al., 2017). The role of $^1O_2$ in cell death signaling has been well characterized, in the *flu* mutant, a mutant that over-accumulates protochlorophyllide in the dark due to the absence of the FLU negative regulation of tetrapyrrole biosynthesis. Upon illumination, the accumulated free photosensitizing protochlorophyllide lead to the release of $^1O_2$ and therefore, to the bleaching of seedlings (Meskauskiene et al., 2001; op den Camp et al., 2003). Genetic screening allowed the identification of suppressors of the *flu* mutant, including the EXECUTER 1 and 2 protein (EX1) (Wagner et al., 2004). Mutation of EX1 and EX2 together largely suppress the upregulation of chloroplast $^1O_2$ signaling and the bleaching of seedlings observed in the *flu* mutant (Lee et al., 2007) showing that the bleaching of seedlings is not due to oxidative damage that the accumulation of $^1O_2$ may produce, but rather to the EX1/EX2 mediated signaling.

Interestingly, a genetic screen allowed the identification of a suppressor of the *flu/ex1* mutant with a flu-like phenotype, named SAFE1 (Wang et al., 2020). Whereas the up-regulation of $^1O_2$-induced signaling observed in *flu* mutant is suppressed in the *flux/ex1* mutant, the *flu/ex1/safe1* triple mutant shows $^1O_2$-induced signaling similar to those observed in *flu* single mutant. Moreover, analyses of the chloroplast ultrastructure showed chloroplast degradation in the *flu* mutant, which is suppressed in *flu/ex1* double mutant. Whereas the number and the size of plastoglobules is unaffected in *flu* and *flux/ex1* mutant after the release of $^1O_2$, *flux/ex1/safe1* displays a large increase in both size, number and fusion of to each other and with thylakoid stacks to form "dumbbell-shaped conglomerates on GMs". It was concluded that SAFE1 is a suppressor of the $^1O_2$-Induced EX1 independent pathway and protects grana margin from $^1O_2$.

Other molecules have been reported to be $^1O_2$ sensors in the grana core of the thylakoids such as some oxidation products of β-carotene. β-carotene plays a major role in the photoprotection of PSII thanks to its capacity to physically quench $^1O_2$ and triplet chlorophyll, the main source of $^1O_2$ in plant leaves. These molecules are able to deactivate $^1O_2$ to the unreactive ground state through a direct energy transfer between both molecules, and to dissipate its excess energy to the environment (Stahl and Sies, 2003). In addition to the physical quenching of $^1O_2$, β-carotene can perform chemical quenching, by being oxidized to various compounds such as aldehydes, ketones, endoperoxides, epoxides and lactones (Havaux, 2014; Ramel et al., 2012a). Among them, β-cyclocitral has been reported to act as an important signal molecule particulary under photoxidative stress (Ramel et al., 2012b). External addition of different concentrations of β-cyclocitral to *Arabidopsis* plants has revealed a strong induction of $^1O_2$ related genes, many of which are involved in oxidative stress response, cellular sensing and defense. Interestingly, according to the localization of the production site of $^1O_2$, grana core or grana margin, the $^1O_2$-induced signaling can follow two distinct pathways. In the first one, the light stress induced the production of $^1O_2$ in the PSII grana core and lead to the accumulation of β-cyclocitral which acted as a retrograde signaling molecule to allow plant acclimatation by activating genes involved in stress response and detoxification. In the second pathway, the accumulation of $^1O_2$ in the PSII thylakoid grana margin (GM) can be detected by the EX1 protein which is then degraded by FtsH to induce modification of nuclear gene expression leading to acclimation or cell death (Dogra and Kim, 2020) (figure 1.10).

Similarly, the redox state of the photoactive plastoquinone (PQ) pool, a molecule involved in photosynthetic electron transport, is also a major player in retrograde signaling. The redox state of this PQ pool plays the role of a "sensor" of photosynthetic efficiency, since it is directly affected by changes in environmental conditions, especially light variations (Jung and Mockler, 2014; Karpinski et al., 1999). It has been shown that the redox state of the PQ pool can affect the expression of about 750 nuclear genes, many of which are involved in the stress response (Jung et al., 2013), and can regulate nuclear alternative splicing (Petrillo et al., 2014).

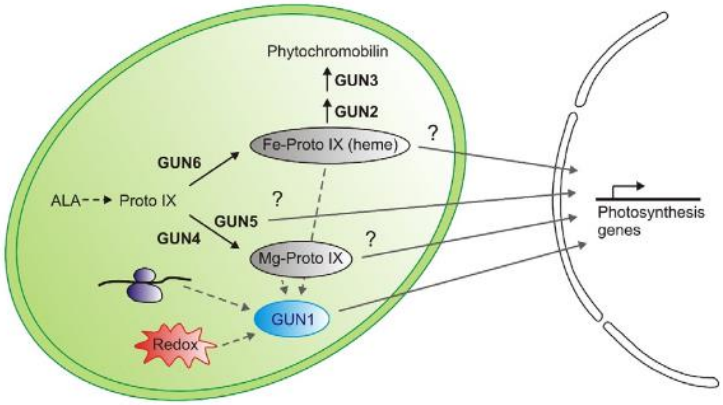

Figure 1.9. Schematic representation of GUN signaling in the tetrapyrrol biosynthetic pathway inside the chloroplast (from Kleine and Leister, 2016).

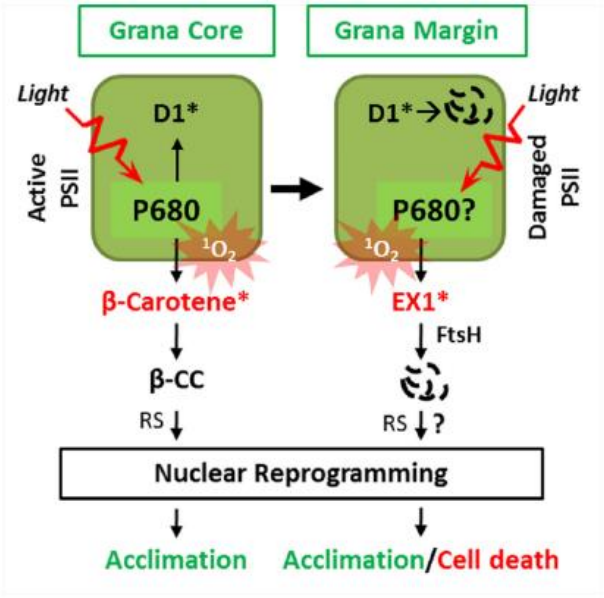

Figure 1.10. Schematic representation of singlet oxygen retrograde signalling in the grana core and grana margin of the thylakoid membrane (From Dogra et al., 2020)

1.3. Plastoglobuli constitute a highly dynamic microdomain of the thylakoid membrane

1.3.1. Structure and composition of plastoglobuli

The thylakoid membrane possesses microdomains known plastoglobules (PG) (Austin et al., 2006b). These globular structures were first observed in the 1960s. Owing to their osmiophilic properties due to the presence of unsaturated lipids they could easily be observed using electron microscopy. PG are lipid droplets ranging from 30 to 100 nm in diameter (Greenwood et al., 1963; Lichtenthaler, 1968; Spurr and Harris, 1968). These lipid droplets are delimited by a lipid monolayer that is contiguous with the outer leaflet of the thylakoid membrane. The structure of PG consists of a core of neutral lipids surrounded by a monolayer of polar lipids associated with proteins (Kessler et al., 1999). Biochemical studies revealed that the core of these lipid droplets

contained a variety of neutral lipids including prenylquinones (plastoquinone (PQ), phylloquinone (vitamin K1), plastochromanol-8 (PC8)), as well as tocopherols (vitamin E), carotenoids, phytylesters and triacylglycerol (TAG) (Gaude et al., 2007; Lichtenthaler and Peveling, 1966; Lippold et al., 2012; Tevini and Steinmüller, 1985; Vidi et al., 2006; Zbierzak et al., 2009). PG also contained a small amount of polar galactolipids and proteins, many being involved in lipid metabolism (Eugeni Piller et al., 2012a; Grennan, 2008; Ytterberg et al., 2006). The number, the size and the composition of PG fluctuate with the plastid type, the plastid developmental stage and the environmental conditions.

1.3.2. Role of plastoglobuli in chloroplast differentiation and metabolism

The decrease of PG number during the differentiation from etioplasts to chloroplasts suggested that these structures play an important role in the formation of thylakoid membranes probably by supplying chemical building blocks to thylakoid lipid biosynthesis such as that of MGDG (Rottet et al., 2015). Similarly, during chloroplast senescence, the disassembly of the thylakoid membrane and the increase of PG size and number can be observed, supporting the fact that PG and thylakoid membrane functionally interact (Tuquet and Newman, 1980).
PG are a major site of lipid metabolism and storage since most of the plastoglobular proteins are known or have been predicted to be involved in related processes. Similary, PG are involved in the final steps of the biosynthesis of plastochromanol (PC8), phylloquinone as well as α-tocopherol (Eugeni Piller et al., 2012b) (Figure 1.11). The tocopherol cyclase VTE1 (Vitamin E-deficient 1) is involved both in PC8 and tocopherol biosynthesis and shows how PG-embedded enzymes may interact with neutral lipids: a domain spanning the polar lipid monolayer allows it to contact the neutral lipids within the plastoglobule (Austin et al., 2006a; Mène-Saffrané et al., 2010).
In addition to their role in plastid differentiation and lipid metabolism, PG also play a role in stress responses. The number and the size of PG increases during various stress such as high light, heat, drought stress and nitrogen starvation, suggesting a role of PG in stress response and chloroplast acclimation (Ben Salem-Fnayou et al., 2011; Gaude et al., 2007; Zhang et al., 2010). The presence of antioxidant molecules inside PG such as carotenoids, plastoquinone or tocopherol may also play a protective role during stress exposure. PG also play a critical role during tomato fruit maturation and have been identified as a site of colored carotenoid biosynthesis. Four enzymes of the carotenoid biosynthesis pathway have been localized in red pepper PG: ζ-carotene desaturase (ZDS), lycopene β-cyclase (LCY) and two β-carotene hydroxylases 2 (CHY2) (Ytterberg et al., 2006). (Simkin et al., 2007b)

Although the role of PG has been relatively well studied, mechanisms regulating the PG proteome and its lipid composition as well as the role and mode of action of several PG-associated proteins remain largely unknown.

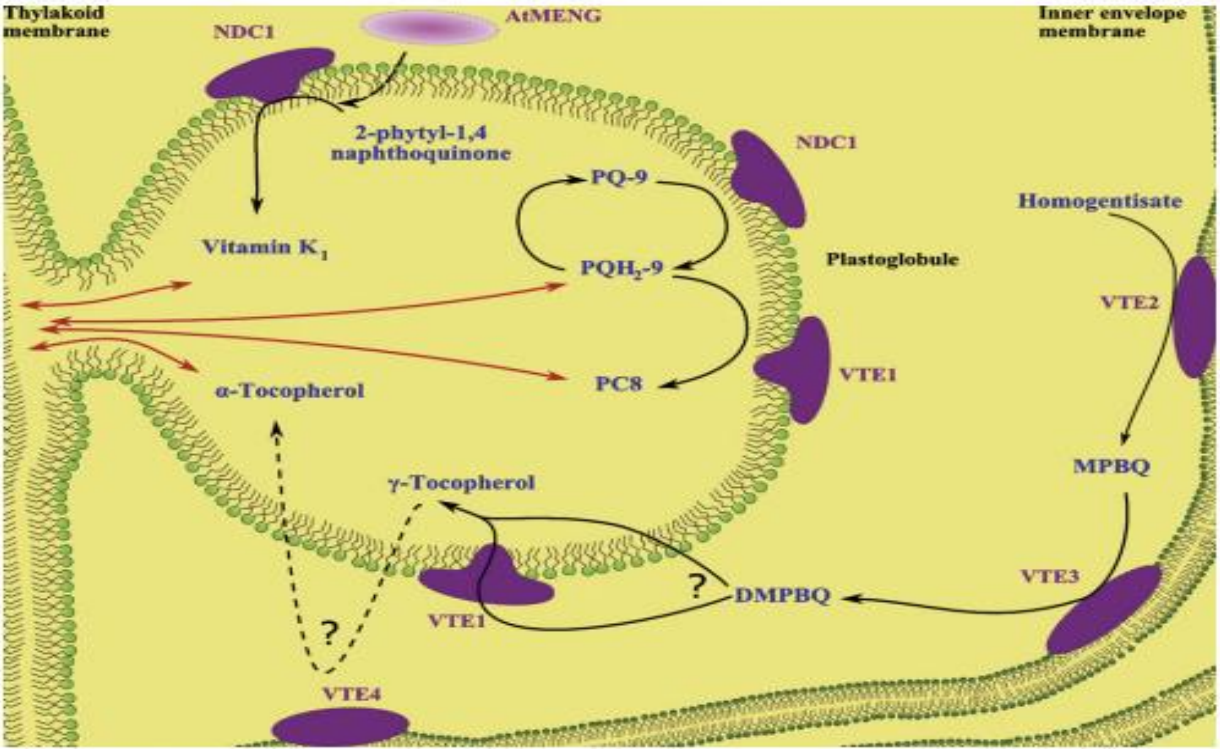

Figure 1.11. Prenylquinone metabolism inside chloroplast plastoglobules.
PQ-9, plastoquinone; PQH2-9, plastoquinol; PC8: plastochromanol-8; MPBQ, 2-methyl-6-phytyl-1,4-benzoquinol; DMPBQ, 2,3-dimethyl-5-phytyl-1,4-benzoquinol (From Eugeni Piller et al., 2012).

1.3.3. The plastoglobule as a lipoprotein particle

The core proteome of PG is composed of approximately 30 proteins (Lundquist et al., 2012b; Vidi et al., 2006; Ytterberg et al., 2006) among which, the most abundant are structural proteins called Fibrillins (FBN) and members of the Activity of BC1 complex Kinase (ABC1K) family (Table 1.1).

Accession Number	Protein Name
AT4G04020	Fibrillin 1a (FBN1a)
AT3G23400	Fibrillin 4 (FBN4)
AT4G22240	Fibrillin 1b (FBN1b)
AT2G35490	Fibrillin 2 (FBN2)
AT5G05200	ABC1K9
AT4G31390	ABC1K1
AT1G79600	ABC1K3
AT3G58010	Fibrillin 7a (FBN7a)
AT4G19170	Carotenoid dioxygenase 4 (CCD4)
AT4G32770	Tocopherol cyclase (VTE1)
AT1G54570	Diacylglycerol acyltransferase 3 (DGAT-3
AT5G08740	NAD(P)H dehydrogenase C1 (NDC1)
AT2G42130	Fibrillin 7b (FBN7b)
AT1G32220	Flavin reductase-related 1
AT4G13200	Unknown 1
AT3G10130	SOUL domain protein
AT2G46910	Fibrillin 8 (FBN8)
AT1G71810	ABC1K5
AT1G78140	UbiE methyltransferase-related 1
AT1G06690	Aldo/keto reductase
AT2G34460	Flavin reductase-related 2
AT2G41040	UbiE methyltransferase-related 2
AT3G26840	Diacylglycerol acyltransferase 4 (DGAT 4)
AT3G24190	ABC1K6
AT4G39730	PLAT/LH2–1
AT3G43540	Unknown 2 (DUF1350)
AT3G07700	ABC1K7
AT1G73750	Unknown SAG
AT3G27110	M48 protease
AT5G41120	Esterase 1
AT5G42650	Allene oxide synthase (AOS)
AT1G09340	Rap38/CSP41B
AT1G26090	Anion-transporting ATPase
AT1G28150	Unknown
AT4G01150	Unknown
AT3G63140	Rap41/CSP41A
AT5G01730	WAVE3
AT2G21330	FBPA-1
AT4G38970	FBPA-2
AT2G01140	FBPA-3
AT3G26060	PrxQ
AT1G52590	Unknown (DUF39)
AT3G26070	Fibrillin (FBN3a)

Table 1.1. List of identified plastoglobule proteins. (Adapted from Lundquist et al., 2012b).

FBN proteins are considered structural proteins and possess a predicted lipocalin motif, which may bind and facilitate transport of small hydrophobic molecules such as plastoquinone (Laizet et al., 2004; Simkin et al., 2007a; Singh et al., 2012; Singh and McNellis, 2011). Furthermore, some evidence shows that fibrillin proteins play a role in stress resistance and protection of the photosystem from photodamage (Otsubo et al., 2018; Singh et al., 2010; Torres-Romero et al., 2020).

ABC1K are atypical, predicted protein kinases conserved from prokaryotes (archaea and bacteria) to eukaryotes and possess a conserved kinase domain containing regions essential for ATP binding and phosphotransfer reaction (Scheeff and Bourne, 2005). In eukaryotes, these proteins are known to be localized in chloroplast and mitochondria (Lundquist et al., 2012a) . In mitochondria, ABC1Ks function in ubiquinone biosynthesis and is necessary for the respiratory chain (Bousquet et al., 1991; Brasseur et al., 1997; Do et al., 2001). In the chloroplast, the exact roles of ABC1Ks remain largely unknown, but the evidence so far suggests that they may be important regulators of chloroplast lipid metabolism and suborganellar distribution.

1.4. The role of ABC1-like kinase proteins in chloroplast metabolism

1.4.1. Overview of ABC1-like kinase proteins

1.4.1.1. ABC1K phylogeny from prokaryotes to eukaryotes

ABC1K homologs are found in bacteria, yeast, human and plants, and belong to the super family of the protein kinase-like (PKL), which can be divided into two groups: the ePKs (eukaryotic protein kinases) and the atypical protein kinases (aPKs). Among the group of aPKs, the ABC1-like kinase is classified as an eukaryotic protein kinase-like (ELKs) (Lundquist et al., 2012a) (Figure 1.12). Although there is no direct evidence of ABC1Ks mediated phosphorylation, some studies support the hypothesis that this protein has a kinase activity (Martinis et al., 2013; Xie et al., 2011).
The alignment of 100 full length ABC1K sequences from different angiosperm species revealed that the ABC1 kinase domain, containing 350 amino acids and twelve conserved motifs, is well conserved. Five of these motifs are also found in the ePK family (motif III, IVa, IVb, VIIb and VIII). Among these highly conserved motifs, III, IVa, and IVb are involved in ATP binding, the motif VIIb in catalysis and VIII in Mg^{2+} chelation.

Protein homologs of ABC1K in *Saccharomyces cerevisiae (*ABC1/Coq8 (coenzyme Q biosynthesis) and in *Escherichia coli* (YigR) are both required for the regulation of ubiquinone synthesis (Do et al., 2001; Poon et al., 2000; Xie et al., 2011). In yeast, ABC1/Coq8 protein regulates the redox activity of the mitochondrial bc1 complex involved in cellular respiration (Do et al., 2001). In humans, the ABC1-1 homolog CABC1 or ADCK3 is also required for the synthesis of ubiquinone and mutant of this protein leads to defect in the respiratory chain and causes severe neurological disorders (Mollet et al., 2008). Recently, It has been shown that additional ABC1K homologs in mitochondria are required for subcellular distribution of ubiquinone (Kemmerer et al., 2021). Although the role of ABC1 homologs has been studied in mitochondria and bacteria, comparatively little is known about the role of the plant ABC1K proteins localized in the chloroplast.

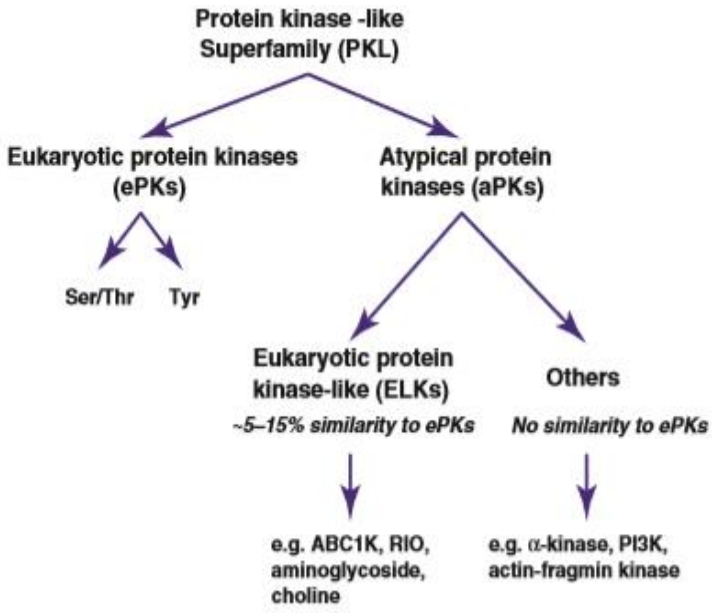

Figure 1.12. Classification of the protein kinase-like (PKL) family (From Lundquist et al., 2012a).

1.4.1.2. ABC1K homologs inside the chloroplast

Among the 17 members of the ABC1K family in Arabidopsis, eight localize in plastids and nine in mitochondria. Moreover, six of these eight ABC1Ks have been found in the plastoglobule proteome (1, 3, 5, 6, 7, 9) (Lundquist et al., 2012b; Vidi et al., 2006; Ytterberg et al., 2006). These conserved kinases are expected to have an important role in the regulation of chloroplast physiology potentially being involved in the coordination of plastoglobule functions with the rest of the chloroplast. For instance, ABC1K7 has been shown to be involved in chloroplast lipid metabolism, oxidative stress response, iron distribution and crosstalk between abscisic acid and ROS signaling (Manara et al., 2016; Manara et al., 2015; Manara et al., 2013). In Chlamydomonas, the ABC1K6 (EYE 3) homologue is involved in eyespot assembly (Boyd et al., 2011).

The colocalization of chloroplast ABC1K proteins with enzymes involved in prenylquinone metabolism inside the plastoglobule suggests that these kinases participate in their regulation. This is likely since ABC1Ks in bacteria and mitochondria of eukaryotes are involved in regulating ubiquinone biosynthesis (Do et al., 2001; Poon et al., 2000; Xie et al., 2011). However, still little is known about the molecular and physiological functions of this plastoglobular ABC1 kinase network. During my PhD, I will focus on the role of ABC1K1 and ABC1K3 proteins.

1.4.2. Role of ABC1K1 and ABC1K3

Several previous studies have investigated the role of the ABC1K1 and ABC1K3 in Arabidopsis, but the mode of action of these proteins remained elusive.

It has been shown that ABC1K1is required for the stability of chlorophyll-binding proteins in Arabidopsis. The *abc1k1* mutant shows an accumulation of chlorophyll degradation products after high light exposure and is, therefore, more sensitive to photooxidative stress (Lundquist et al., 2013; Yang et al., 2012). In addition, this mutation alters the chloroplast prenyl lipid composition (Lundquist et al., 2013; Martinis et al., 2013; Martinis et al., 2014). High light treatment induces a decrease in the level of α, γ and δ-tocopherol and an increase of α-tocopherol oxidation products in *abc1k1* compared to wild type, while the *abc1k3* mutant is only affected in plastochromanol PC-8 level. Knowing that α-tocopherol and PC-8 are synthesis by the VTE1 enzyme, these results suggested that VTE1 activities may be impaired in both mutants. Interestingly, *in vitro* analysis showed that these two kinases may act together to phosphorylate the tocopherol cyclase VTE1. Moreover, immunoprecipitation experiments suggested that ABC1K1 and ABC1K3 physically interact (Lundquist et al., 2013; Martinis et al., 2013). The *abc1k1* mutant also has a reduced level of β-carotene and is affected in starch and sugar metabolism.

ABC1K1 was originally identified as PGR6 (proton regulation 6) (Shikanai et al., 1999) and, like the other *pgr* mutants, is conditionally defective in non-photochemical quenching (NPQ) and photosynthetic electron transport, particularly under high light (Martinis et al., 2014). Recent data produced in our laboratory show that ABC1K1 is involved in maintaining the photoactive PQ pool, possibly by regulating its distribution between the thylakoid membrane and PG (Pralon et al., 2019). Interestingly, the *abc1k3* mutation allows a partial rescues of the pgr6 phenotype observed in *abc1k1* supporting the idea that these two kinases are functionally linked (Pralon et al., 2020). In summary, the evidence so far suggests the existence of a regulatory link between the photosynthetic activity and chloroplast metabolism, which could be mediated by ABC1K1 and ABC1K3.

Recently, it has been shown that ABC1K1 has an important role in regulating plant development under monochromatic red light light. Indeed, *abc1k1* mutant, under continuous red light, is characterized by a shorter hypocotyl, pale cotyledons, and a significant decrease in the expression of phytochrome-interacting Factors PIFs (1,3,4,5)(Yang et al., 2016). These transcription factors are involved in phytochrome-mediated developmental processes (Leivar and Monte, 2014; Pham et al., 2018) and the reduced PIF levels in *abc1k1* mutants suggests that ABC1K1 plays an upstream role in this signaling pathway. The two major photoreceptors perceiving far-red and red light are PhyA (phytochrome A) and PhyB (phytochrome B).

Analysis of the *phyB-9/abc1k1* double mutant in red light has shown that *abc1k1* mutation reduces the hypocotyl elongation typical of *phyB-9*, suggesting that ABC1K1 is involved in the regulation of plant development possibly independently or downstream of phyB in the red light signaling pathway (Yang et al., 2016).

Interestingly, analysis of hypocotyl elongation of *abc1k1/abc1k3* double and abc*1k1/abc1k3/phyB-9* triple mutants under red light strongly suggests that these two putative kinases have opposite activity. A tempting hypothesis was that ABC1K1 acts as a repressor of ABC1K3 activity. In fact, the mutation of ABC1K3 suppresses the short hypocotyl phenotype in *abc1k1/phyB-9* and *abc1k1* mutant (Huang et al., 2015; Yang et al., 2016). Taken together, these findings show that ABC1K1 plays an important role in chloroplast functions, and that it has a specific role in development; however, its phosphorylation targets and the signaling pathways are currently unknown.

1.5. Aim of this work

Whereas plastoglobules have been considered for a long time as simple lipid storage compartments, more and more studies revealed the importance of these lipoprotein particles for chloroplast metabolism and regulation. ABC1K like-kinase proteins inside the plastoglobule are necessary to maintain chloroplast lipid metabolism and photosynthesis; however, its phosphorylation targets and functional mechanisms are mostly unknown. In this context, the aim of this thesis is to investigate the physiological and molecular functions of ABC1K1 during the early development of *Arabidopsis thaliana* when the role of this kinase appears to be highly relevant. In particular, this work aims to characterize the molecular events leading to the chloroplast biogenesis defect observed in *abc1k1* seedlings when grown under red light.

To do that, several objectives have been established:

- The first objective is to study the impact of white high light (500 µE) and pure red light (60 µE, 680 nm) on the development of young seedlings, in particular by comparing *abc1k1* phenotypes and molecular defects with those of other mutants affected either in photosynthetic activity or chloroplast development. In particular, the *sps2* mutant, which is affected in the solanesyl diphosphate synthase 2 (SPS2) enzyme. This enzyme catalyzes the elongation of the PQ prenyl side chain (Block et al., 2013; Jun et al., 2004). Therefore, the *sps2* mutant has decreased total PQ levels and this limits the photoactive PQ pool and consequently electron transport chain (ETC) activity, similarly to *abc1k1 (Pralon et al., 2019).* However, the *sps2* mutant does not show the greening phenotype observed in *abc1k1* under red light. The comparison of *abc1k1* with *sps2* as well as other mutants should therefore allow us to distinguish between the phenotypes of *abc1k1* caused by the defect of the ETC activity from those related to chloroplast development.

- To determine whether ABC1K1 is involved in a specific retrograde signaling pathway, which could explain the chloroplast development defect observed in *abc1k1* under red light, analysis of ABC1K1 interaction partners will be performed. Candidate interaction partners will be confirmed using independent methods and further characterized with regard to their involvement in ABC1K1-dependent signaling.

- Finally, we would like to confirm and understand the functional link between ABC1K1 and ABC1K3. The objective is to narrow down the *abc1k1* molecular defects that can be complemented by the *abc1k3* mutation, separating them from those still present in the double

abc1k1/abc1k3 mutant. To do so, the *abc1k1/abc1k3* double mutant was compared to *abc1k1* when germinated under red light.

2. Results

2.1. Submitted manuscript: The atypical kinase ABC1K1 interacts with the EXECUTER pathway to promote chloroplast biogenesis.

Collombat Joy[1], Pralon Thibaut[1], Pego Magalhaes Jenny[1], Sarah Rottet[1,2], Ksas Brigitte[3], Gaetan Glauser[4] , Havaux Michel[3], Kessler Felix[1], Longoni Fiamma*[1]*

1. Laboratory of Plant Physiology, Institute of Biology, University of Neuchâtel, Neuchâtel, Switzerland.

2. Present adress: Division of Plant Sciences, Research School of Biology, The Australian National University, Canberra, Australia

3. Commissariat à l'Energie Atomique et aux Energies Alternatives (CEA), Cadarache, Centre National de la Recherche Scientifique (CNRS), UMR 7265, Institut de Biosciences et de Biotechnologies d'Aix-Marseille, Laboratoire d'Ecophysiologie Moléculaire des Plantes Aix Marseille Université, 13108, Saint-Paul-lez-Durance, France.

4. Neuchâtel Platform of Analytical Chemistry, University of Neuchâtel, Neuchâtel, Switzerland.

Corresponding authors: felix.kessler@unine.ch, fiamma.longoni@unine.ch

Contributions

In this paper, I contributed to the experimental design and performed all the experiments except the lipid peroxidation measurements. I participated actively in the writing of the manuscript.

Abstract

Multiple chloroplast-to-nucleus signaling pathways contribute to the regulation of chloroplast biogenesis during plant greening. Here, we provide evidence for the direct implication of the atypical kinase ABC1K1. ABC1K1 is required for sufficient plastoquinone (PQ) allocation to the photosynthetic electron transport chain. Unexpectedly, mutation of *abc1k1* suppresses greening and results in pale cotyledons under red light. This phenotype was not observed in other photosynthetic mutants and points to a specific signaling defect. Under red light, *abc1k1* accumulated EXECUTER1 (EX1), a trigger of singlet oxygen ($^1O_2$) signaling. Consistent with the role of the FTSH metalloprotease in chloroplast biogenesis and EX1 degradation, the FTSH2 mutant, mimicked the greening defect of *abc1k1* and accumulated EX1 under red light. We propose that this novel ABC1K1-dependent signal is required to promote chloroplast biogenesis in challenging light conditions.

Introduction

Photoautotrophic organisms depend on the conversion of light energy into chemical energy. In eukaryotes, this process, known as photosynthesis, takes place in a dedicated organelle: the chloroplast. Fully functional chloroplasts are therefore essential for survival of most higher plants. Plant embryos contain undifferentiated, non-photosynthetic proplastids. During the switch from heterotrophic to photoautotrophic growth they become functional chloroplasts (Waters and Langdale, 2009). Light is a key factor in this process and the initiation of the developmental process relies on signals conveyed by photoreceptors. In particular red light sensitive phytochromes together with the downstream PIF transcription factors play a central role. They activate chloroplast translation via an anterograde nucleus-to-chloroplast signal (Liebers et al., 2020; Yoo et al., 2019). However, the development of the chloroplast also requires retrograde signaling that is, at least partially, independent of PIF mediation (Martin et al., 2016). Five major retrograde signaling pathways have been reported: the tetrapyrrole biosynthesis pathway (TBP), plastid gene expression, reactive oxygen species (ROS), changes in photosynthetic electron transport chain (PETC) activity, and finally plastid metabolism (Hernandez-Verdeja and Strand, 2018). These signals are intricately interwoven and perturbation of one may have an impact on another as well as on different physiological processes. While there are existing reports chloroplast biogenesis impairement due to alteration of TBP signals via GUN1 (Martin et al., 2016; Tadini et al., 2020) and chloroplast gene expression (Liebers et al., 2020), little is known about the impact of a defective PETC signaling during seedling germination. Impaired PETC activity is often correlated with an increased production of ROS, such as hydrogen peroxide (H_2O_2), hydroxyl radicals (OH*) and singlet oxygen ($^1O_2$). $^1O_2$ has been reported to act as a retrograde signal modulating the expression of nuclear genes during cotyledon greening (Page et al., 2017). Key components of singlet oxygen signaling are EXECUTER1 (EX1) and EX2 (Lee et al., 2007; Wagner et al., 2004). Mutation of both EX1 and EX2 largely suppresses chloroplast $^1O_2$ signaling and the *ex1/ex2* mutant has been reported to have a defect in chloroplast biogenesis during embryo development (Kim et al., 2009). Further research revealed that the FTSH protease activates EX1-mediated signaling via EX1 proteolysis (Wang et al., 2016). FTSH also participates in the photosystem II (PSII) repair mechanism, thus linking $^1O_2$ signaling to the PETC activity (Kato et al., 2009). Furthermore, the mutation of single subunits of the FTSH protease complex leads to a variegated leaf phenotype due to the arrest of thylakoid development (Sakamoto et al., 2009). The arrest of thylakoid development has been reported to be light independent and not due to PSII photobleaching (Zaltsman et al., 2005a).

Among the PETC regulators, **A**ctivity of **B**c1 **C**omplex **K**inase **1** / **P**roton **G**radient **R**egulation 6 (ABC1K1) has a reported role in early plant development. Its mutation caused a conditional cotyledon greening defect and hampered hypocotyl elongation by acting on downstream effectors of the PHYB/HY5 pathway under monochromatic red light (Yang et al., 2016). ABC1K1 is required for plastoquinone (PQ) homeostasis balancing PQ between the PETC (photoactive PQ pool) and the plastoglobuli reservoir (non-photoactive PQ pool)(Pralon et al., 2020; Pralon et al., 2019). In particular, ABC1K1 is required to maintain the photoactive PQ pool when light is in excess over the PETC capacity and its mutation causes an over-reduction

and depletion of photoactive PQ (Ksas et al., 2015; Pralon et al., 2019). The limitation of the photoactive PQ pool, caused by the loss of ABC1K1, results in a defect in the induction of the photoprotective thermal dissipation (non-photochemical quenching; NPQ), in an imbalance of the PETC redox equilibrium and a limitation of electron flow (Pralon et al., 2019); the effects become phenotypic under high light intensity (Martinis et al., 2014). The lower level of photoactive PQ *in abc1k1* indirectly affects the phosphorylation of thylakoid proteins. In particular, diminished phosphorylation was reported for the targets of the state transition kinase 7 (STN7), such as the subunits of the light harvesting complex II (LHCII). STN7-dependent phosphorylation is a key component of PETC regulation and alters the LHCII organization around the photosystems (Bellafiore et al., 2005; Fristedt and Vener, 2011). PQ levels are also affected in *sps2*, the mutant of the solanesyl diphosphate synthase 2 (SPS2) enzyme, which catalyzes the elongation of the PQ prenyl side chain (Block et al., 2013; Jun et al., 2004). The *sps2* mutant mimics the defects in PETC activity observed in *abc1k1* (Pralon et al., 2019). The activity of ABC1K1 is counteracted by its homolog ABC1K3, as it was reported that both PETC activity and chloroplast biogenesis are partially restored under red light in the *abc1k1/abc1k3* double mutant (Huang et al., 2015; Pralon et al., 2020).

We observed that the greening defect of *abc1k1* is due to a chloroplast biogenesis arrest and separable from the perturbation of the PETC also caused by this mutation. The phenotype correlates with an over-accumulation of EX1 combined with diminished accumulation of the FTSH protease. Low concentrations of DCMU to produce $^1O_2$ elicited EX1 degradation and alleviated the chloroplast biogenesis arrest in *abc1k1*. This study demonstrates that ABC1K1 is a component of PETC signaling and enhances FTSH-dependent degradation of EX1, thereby regulating the progression of chloroplast biogenesis.

Results

The PETC defect is separable from the greening defect under red light.

To assess whether the greening defect, visible in *abc1k1* mutant lines germinated under red light, was caused by the PETC defect. We compared a panel of mutants affected in PETC with *abc1k1*: *stn7* (Bellafiore et al., 2005), *psaL* (Plochinger et al., 2016), *npq1* (Niyogi et al., 1998), *pgr5* (Munekage et al., 2002) and *sps2* (Pralon et al., 2019). All of these mutants, including *abc1k1*, are unable to relieve excess excitation pressure on PSII but none of them, except *abc1k1*, had a visible greening defect under red light (Figure 2.1a). However, all of the mutants including *abc1k1* had shorter hypocotyls under red light when compared to the WT (Figure 2.1b) while no differences were observed under white light except for *stn7* and *psal* (Supplementary figure S1). This indicated that hypocotyl elongation and the greening defect are separable phenomena. While hypocotyl elongation appears to be linked to photosynthetic activity, the greening defect may reflect impairment of a hypothetical ABC1K1-dependent signaling pathway.

To narrow down the time point at which cotyledon greening was affected in *abc1k1* we germinated the plants under white light for increasing durations before transferring them to red light. *abc1k1* mutant plants, germinated for 48h under white light and then shifted to red light,

had greener cotyledons than those germinated under constant red light, suggesting that *abc1k1* interferes with chloroplast biogenesis at a very early stage when exposed to red light. Consistently, *abc1k1* mutant plants germinated under red light for 72h (to compensate for the slower germination) before transfer to white light, remained compromised in cotyledon greening and occasionally resulting in albinism (Figure 2.1c).

Considering the early onset of this phenotype, the greening defect likely reflects a chloroplast biogenesis arrest (rather than bleaching) that is specifically induced in *abc1k1* by red light. We therefore investigated the possible role of ABC1K1 in chloroplast signaling.

ABC1K1 mutation increases Executer1 and decreases FTSH2 accumulation under red light

Affinity purification was carried out to identify potential signaling partners of ABC1K1 (Supplementary Table S1). To this end, *abc1k1* was complemented with a construct expressing a C-terminally YFP-HA-tagged version of ABC1K1 (ABC1K1:YFP-HA) under the control of the 35S promoter. As a negative control we used a WT line expressing a C-terminally GFP-HA-tagged version of the N-terminus of the small subunit of RuBisCO (pSSU::GFP-HA). Extracts were prepared from plants of these two lines grown under white as well as red light. The extracts were subjected to affinity purification (Supplementary Figure S2). A list of putative interactors was obtained by subtracting proteins identified in the pSSU::GFP-HA eluate from those in the ABC1K1:YFP-HA eluate from both light conditions. The resulting list was enriched in chloroplast proteins, and notably a number of subunits of the NDH complex (supplementary table S1). Among the subset of putative interactors of ABC1K1 identified only in the red light eluate, we found EX1. We considered EX1 a strong candidate as it is a known component of the $^1O_2$ chloroplast retrograde signaling pathway. Moreover, previous studies hinted at a possible function of EX1 in chloroplast biogenesis (Kim et al., 2012; Page et al., 2017).

A possible role of EX1 in ABC1K1 signaling may be reflected by its altered accumulation in the *abc1k1* background. Therefore, EX1 abundance relative to wildtype (WT) was assessed by immunoblotting. Among the PETC mutants *sps2* was selected as a negative control as it is the most similar to *abc1k1*, in terms of PETC defect, but has no greening defect under red light. Under red light, EX1 accumulated to higher levels in *abc1k1* than in WT (2.68±0.28 and 2.46±0.58 for *abc1k1-1* and *abc1k1-2* respectively) (Figure 2.2). An increased accumulation of EX1 under red light was also observed in the *abc1k1/abc1k3* background (2.08±0.29) while its level in *sps2* was comparable to WT (0.94±0.01). No significant difference in EX1 level was observed between these genotypes grown under white light (Figure 2.2). A previous report showed that the FTSH2 metalloprotease is involved in the degradation of EX1 and thereby contributes to the coordination of $^1O_2$-dependent retrograde signaling (Dogra et al., 2017). Therefore, diminished accumulation of this protease could explain the higher level of EX1 observed in the *abc1k1* mutants under red light. Abundance of FTSH2 and its close homolog FTSH5 were assessed by immunoblotting in *abc1k1*, *sps2* and *abc1k1/abc1k3* and compared to WT total protein extracts. Under white light, there were no major differences. However, under

red light, *abc1k1* mutant lines had a significantly lower level of both FTSH2 (0.37±0.11 and 0.35±0.02 for *abc1k1-1* and *abc1k1-2* respectively) and FTSH5 (0.33±0.06 and 0.50±0.09 for *abc1k1-1* and *abc1k1-2* respectively) compared to WT.

Eliciting EX1 degradation by $^1O_2$ restores chloroplast biogenesis in *abc1k1* under red light

$^1O_2$ has been shown to induce post-translational oxidation of Trp643 of EX1, which promotes EX1 degradation (Dogra et al., 2019b). To take advantage of this mechanism the production of $^1O_2$ in the plants was induced by a low dose of DCMU (12.5 nM). This increases the $^1O_2$ production from PSII without negatively affecting PETC function (Wagner et al., 2004). Measurement of the hydroxyoctadecatrienoic acids (HOTEs) leve indicated that the DCMU treatment increased lipid peroxidation, confirming the production of $^1O_2$, in the *abc1k1* background but not in WT (Supplementary Figure S3).

DCMU treatment resulted in partial recovery of chlorophyll accumulation in *abc1k1*, visible as cotyledon greening under red light, while there was no measurable effect on WT, *sps2* and *abc1k1/abc1k3* chlorophyll content (Figure 2.3a, 2.3b). We determined whether the greening recovery in *abc1k1* correlated with reduced levels of EX1: DCMU-treated *abc1k1* mutant plants under red light, showed diminished EX1 accumulation compared to the untreated *abc1k1* plants (0.57±0.19 and 0.81±0.26 for *acb1k1-1* and *abc1k1-2* respectively). In contrast, the DCMU treatment did not reduce EX1 accumulation in the *abc1k1/abc1k3* double mutant under red light (2.41±0.27 compared to WT) (Figure 2.2). The levels of FTSH5 and FTSH2 proteases after DCMU treatment were also addressed: The FTSH2 protein level had increased, reaching a level close to that of WT, in *abc1k1* plants treated with DCMU (0.72±0.19 and 0.72±0.13 for *abc1k1-1* and *abc1k1-2* respectively). The levels of FTSH5 were the same as in WT in both of the *abc1k1* mutant lines (1.01±0.23 and 1.07±0.38 for *abc1k1-1* and *abc1k1-2* respectively) (Figure 2.2).

To exclude that the observed changes in the EX1, FTSH5 and FTSH2 protein abundance were due to changes in gene expression, quantitative RT-PCR was carried out. The expression of all of these genes under red light was lower in the *abc1k1* mutant lines than in WT and was not affected by the DCMU treatment (Supplementary Figure S4). This indicates that ABC1K1 is implicated in posttranslational protein regulation within the chloroplast, possibly promoting the FTSH-dependent proteolysis of EX1, rather than in the regulation of the expression of the corresponding genes.

To assess the effect of the DCMU treatment on the recovery of the chloroplast biogenesis in *abc1k1*, the levels of thylakoid protein accumulation was determined by immunoblotting. Representative proteins for photosystem II (PsbA), photosystem I (PsaB, PsaD), cytochrome b_6f (PetB, PetC) and ATP synthase (ATPC) were analyzed in 5 days old seedlings. Under red light the accumulation of all tested proteins was higher in *abc1k1* seedlings treated with DCMU than in non-treated seedlings (Supplementary figure S5a). Analysis of PSII activity by chlorophyll fluorescence measurements, showed that the DCMU treatment alleviated the photosynthetic defect imposed by red light in *abc1k1* mutants, while it had no significant effect

on *abc1k1/abc1k3* and *sps2* (Supplementary figure S5b). Additional indicators for the progression of chloroplast biogenesis are the degradation of the early light-inducible proteins (ELIPs) (CRONSHAGEN and HERZFELD, 1990) and the accumulation of mono-galactosyldiacylglycerols (MGDG), which are membrane lipids almost exclusively present in the thylakoids (Pipitone et al., 2021). Both indicators support the hypothesis that DCMU treatment allows to overcome the arrest in chloroplast biogenesis: the ELIP protein accumulated in *abc1k1* under red light, but decreased when the plants were treated with DCMU (Supplementary figure S5a). The accumulation of MGDGs under red light in the *abc1k1* mutants was very low (679.15 ± 39.22 and 688.45 ± 156.30 µg/g FW for *abc1k1-1* and *abc1k1-2* respectively) compared to WT (1748.12 ± 156.18 µg/g FW). Under red light the DCMU treatment led to a partial recovery of the MGDG content in the *abc1k1* lines (1013.13 ± 129.96 and 874.02 ± 88.78 µg/g FW for *abc1k1-1* and *abc1k1-2* respectively). The MGDG content of the *abc1k1* lines treated with DCMU was thus similar to that of the untreated *sps2* line that has no phenotype under red light (1152.40 ± 89.83 µg/g FW). Furthermore, *abc1k1/abc1k3* plants under all light conditions also had a slightly lower level of MGDG compared to the WT despite the green phenotype of both lines (Figure 2.3c).

ABC1K1 genetically interacts with the executer pathway

Altered levels of FTSH2 and EX1 correlated with the greening phenotype in *abc1k1*. To establish whether they are directly implicated, T-DNA insertion lines for the FTSH5 and 2 proteases (*var1* and *var2*) and for the EXECUTER genes (*ex1* and *ex2*) were tested under red light. The *var2* mutant, which lacks the FTSH2 protease, displayed a greening defect and a short hypocotyl, phenotypically mimicking *abc1k1* under constant red light (Figure 2.4a).The FTSH5 mutant, *var1*, showed a milder greening defect. Finally, knockout mutations of *EX1* or *EX2* genes had no visible impact on the seedlings greening under red light.

To compare the effect of *var2* and *abc1k1* mutations on chloroplast biogenesis progression, ELIP accumulation was assessed. Both *var2* and *abc1k1* had higher levels of ELIP when grown under red light (Figure 2.4b). Furthermore, ELIP accumulated to a higher level also when *var2* and *abc1k1* mutants were germinated under high light (500 µmol photons m^{-2} s^{-1}). This suggests that *abc1k1* and *ftsh2* have related chloroplast biogenesis defects, also under other light conditions than red light. To investigate the relationship between the greening defect and EX1 accumulation, the levels of EX1 were assessed by immunoblotting. A higher level of EX1 was observed in the *var2* and *abc1k1* mutants compared to the WT, this effect was more evident under red light, while EX1 accumulated to a lower extent in plants germinated under high light, which correlates with a milder greening defect observed in high light for both lines (Figure 2.4c).

To obtain genetic evidence that the chloroplast biogenesis defect in *abc1k1* mutants was dependent on EX1 accumulation, the *EX1* gene was knocked out by CRISPR/Cas9 targeted mutation. Using two sgRNAs a portion of the *EX1* gene was deleted (Supplementary figure S6). This was detectable as a change in the fragment size of the diagnostic PCR amplicon (Supplementary figure S7a). Homozygous *abc1k1/ex1* double mutant lines were isolated and

verified by diagnostic PCR (Supplementary figure S7b). Homozygous double mutant lines were then challenged with red light. These double mutants partially recovered the greening phenotype when compared to *abc1k1*. However, the recovery was not complete and the phenotype of the double *abc1k1/ex1* mutants was similar to that of the *abc1k1* plants treated with DCMU under red light (Figure 2.5a). To confirm this observation, the chlorophyll content of WT, *abc1k1* and two *abc1k1/ex1* lines grown under white as well as red light was measured. The chlorophyll content observed in the double mutant was significantly higher than that of the *abc1k1* parental line in both light conditions (Figure 2.5b). The impact of *ex1* mutation in the *abc1k1* background on the accumulation of FTSH2 and LHCB1 was assessed by immunoblotting. The accumulation of these proteins correlated with the greening phenotype. Both proteins accumulated to higher levels in the *abc1k1/ex1* double mutant under red light when compared to *abc1k1* (Figure 2.5c). Consistently, the level of ELIP was lower in *abc1k1/ex1* lines compared to *abc1k1*.

Discussion

In this study, we show that the atypical kinase ABC1K1 plays a role in regulating the early phases of chloroplast biogenesis, as a potential relay between PSII activity and the regulation of the chloroplast biogenesis via the EX pathway. Under red light the loss of ABC1K1 results in an irreversible greening defect in the cotyledons and a short hypocotyl. We show here that these two phenotypes can be separated. The greening phenotype is specific for *abc1k1* whereas the short hypocotyl is a common trait in a panel of mutants affected in the regulation of the PETC. The defective elongation of the hypocotyl in *abc1k1* has been investigated previously and attributed to a perturbation in downstream phytochrome signaling (Yang et al., 2016). A possible explanation is that red light at 680nm overexcites PSII and that the mutants are unable to release the excitation pressure. Thereby, the PETC may generate a retrograde signal that ultimately converges with phytochrome pathway. Unlike the *abc1k1* mutant, the panel of photosynthetic mutants did not show a greening defect under red light suggesting that it is, at least partially, independent from the PETC. In the *abc1k1* mutant the photosynthetic defect has been attributed to a lack of PQ in the PETC. In this regard the *sps2* mutant, defective in PQ biosynthesis (Block et al., 2013), closely mimics the photosynthetic phenotype of *abc1k1* (Pralon et al., 2019) but not the greening defect under red light. For this reason, we used *sps2* as a reference, to isolate the photosynthetic defect from that of chloroplast biogenesis. Whereas SPS2 is simply a biosynthetic enzyme, ABC1K1 belongs to the family of atypical kinases that may have signaling functions beyond the allocation of PQ to the PETC.

Following up on potential signaling functions of ABC1K1, we identified EX1 as a potential interactor under red light in a co-isolation experiment (Supplementary table S1). In support of this notion, EX1 accumulated to higher levels in *abc1k1* of under red light than in the WT (Figure 2.2). However, the higher level of EX1 was not due to increased transcription (Supplementary figure S4). The phenotype of *abc1k1* in red light suggests that EX1 accumulation is linked to the arrest of chloroplast biogenesis visible as the greening defect. The hypothesis that EX1 could be involved in greening has also been explored by Page and coworkers (Page et al., 2017), which showed an increase in EX1 gene expression in seedlings

showing a chloroplast biogenesis arrest induced by far-red light pre-treatment. The factors promoting EX1 proteolysis in programmed cell death signaling: singlet oxygen (Wagner et al., 2004) and FTSH-dependent degradation (Dogra et al., 2017; Wang et al., 2016), are potentially involved also in EX1 proteolysis in seedlings germinating under red light. When *abc1k1* seedlings were germinated on DCMU, a herbicide inducing singlet oxygen production from the PSII by blocking the PETC (Trebst, 1980), the level of EX1 under red light decreased (Figure 2.2). Furthermore, the *ftsh2* mutant (*var2*) failed to degrade EX1 under red light (Figure 2.4c). However, the accumulation of EX1 alone did not appear to be sufficient to cause the greening phenotype; in fact, the *abc1k1/abc1k3* double mutant had no visible phenotype under red light, but still accumulated the EX1 protein (Figure 2.2). This suggests that the presence of ABC1K1 is required to promote EX1 degradation independently from a visible greening defect.

The observation that the *ftsh2* mutant (*var2*), had a similar greening defect as *abc1k1* under red light points to FTSH2 as a central component in the pathway (Figure 2.4a). Under red light the *abc1k1* mutant had a lower level of FTSH2. This would be expected to have a broader effect on chloroplast proteins than just regulating the level of EX1, as this metalloprotease has been reported to act on essential proteins of the PETC (reviewed in (Kato and Sakamoto, 2018). Our results are consistent with the FTSH threshold model, which proposes that the chloroplast biogenesis defect in the *ftsh* mutants is due to insufficient FTSH activity relative to the rate of protein synthesis (Chen et al., 2000; Yu et al., 2008; Zaltsman et al., 2005b). In fact, the *ftsh5* mutant (*var1)* had a milder greening defect under red light, and the greening recovery in the double *abc1k1/ex1* and *abc1k1/abc1k3* mutant correlates with higher accumulation of the FTSH metalloproteases (Figure 2.5c, figure 2.2).

To rationalize these results, we propose a model in which ABC1K1 enhances the proteolysis of EX1 by FTSH (Figure 2.6) potentially as a transient component of the signalosome proposed by (Dogra et al., 2019b). As ABC1K1 is also involved in the regulation of the PQ homeostasis (Pralon et al., 2019), it is tempting to suggest that the redox status of the photosynthetic PQ pool, and/or the concentration of photoactive PQ, may be factors regulating ABC1K1 signaling activity and/or its interaction with EX1. Thereby, ABC1K1 provides a link between the PETC and the executor pathway. The contribution of ABC1K1 during chloroplast biogenesis would thus act synergistically with the FTSH complex; both are involved in maintaining the PETC homeostasis, FTSH by acting on the PETC proteins (Järvi et al., 2016) and ABC1K1 on the photoactive PQ pool, and both are implicated in the chloroplast retrograde signaling via EX1. The complementation of *abc1k1* greening phenotype by the mutation of ABC1K3 would act by alleviating the PETC defect (Pralon et al., 2020) and thus the retrograde signals generated by a damaged PETC (Dogra et al., 2019a; Zaltsman et al., 2005a), rather than on the EX pathway. Therefore, the greening defect of *abc1k1* is the result of the combination of the PETC defect with the executor pathway defect.

In conclusion, we show that the *abc1k1* defect, as well as that of other PETC mutants, results in a suppression of the hypocotyl elongation under red light. However, ABC1K1 is also implicated in a separate signaling pathway that contributes to the regulation of the protein homeostasis during chloroplast biogenesis by the FTSH metalloprotease. The ABC1K1-

dependent signals elicit the degradation of EX1 by the FTSH metalloprotease. This signaling pathway is light dependent and becomes essential for chloroplast biogenesis in challenging light conditions.

Figures

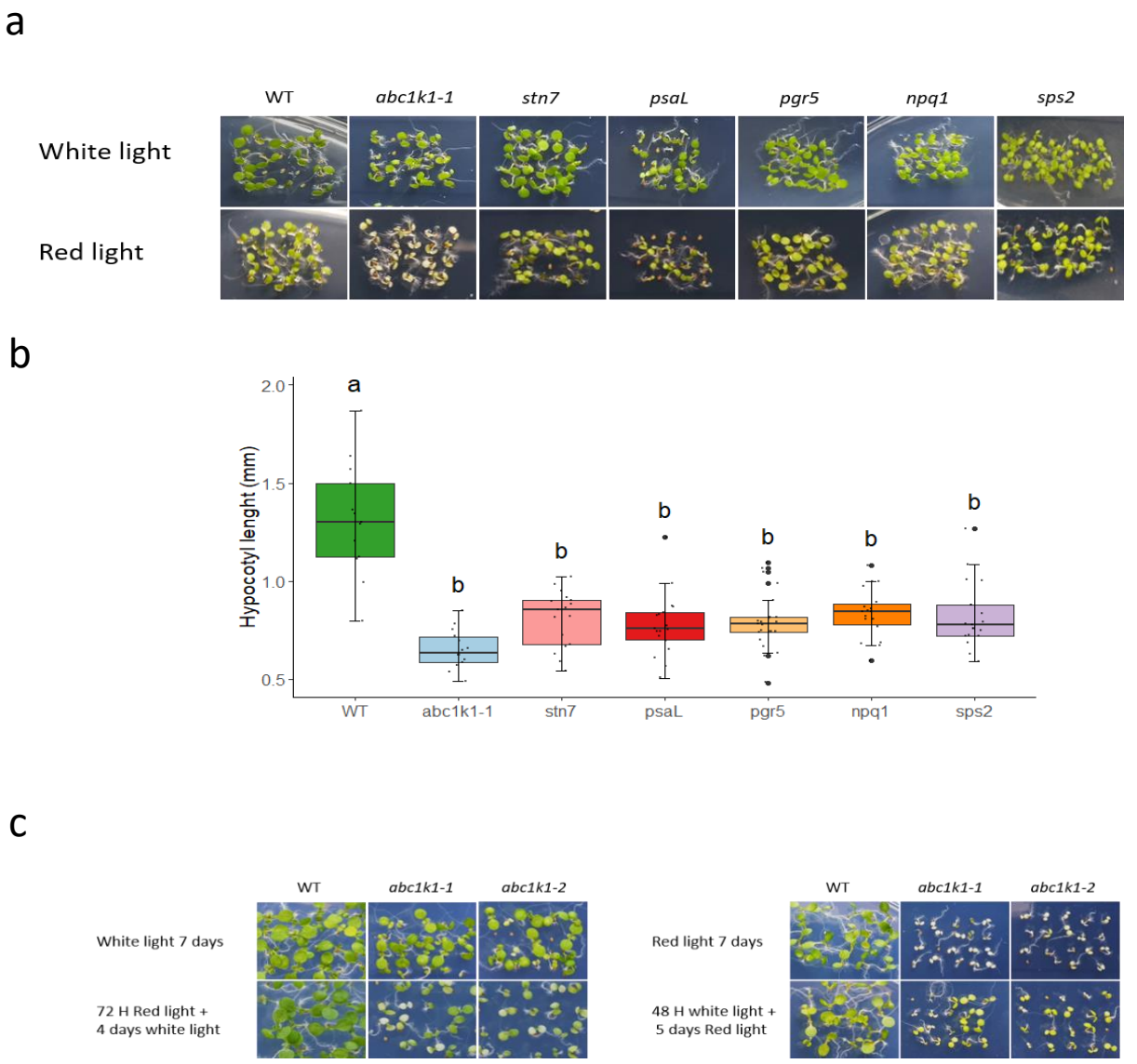

Figure 2.1. The photosynthetic defect of *abc1k1* mutants does not explain the pale green phenotype. WT, *abc1k1-1 stn7*, *psal*, *pgr5*, *npq1* and *sps2* seedlings grown on 0.5 X MS medium for 5 days under continuous white light (80 µE) or continuous red light (60 µE). a) Visible phenotype, b) Length of the hypocotyl by genotype of seedlings grown under continuous red light (60 µE). The whiskers and box plot shows the minimum, first quartile, median, average, third quartile and maximum of each dataset, points indicate individual samples, outliers are indicated by a bigger point (WT n=13, *abc1k1-1* n=14, , *stn7* n=17, *psal* n=18, *pgr5* n=23, *npq1 n*=18 and *sps2* n=19). The letters identify statistically different groups obtained by a Tukey-HSD post-hoc test (alpha =0.01). c) Phenotype of WT and *abc1k1* seedlings exposed to red light (left) or white light (right) until radicle emergence and then moved to the opposite light condition.

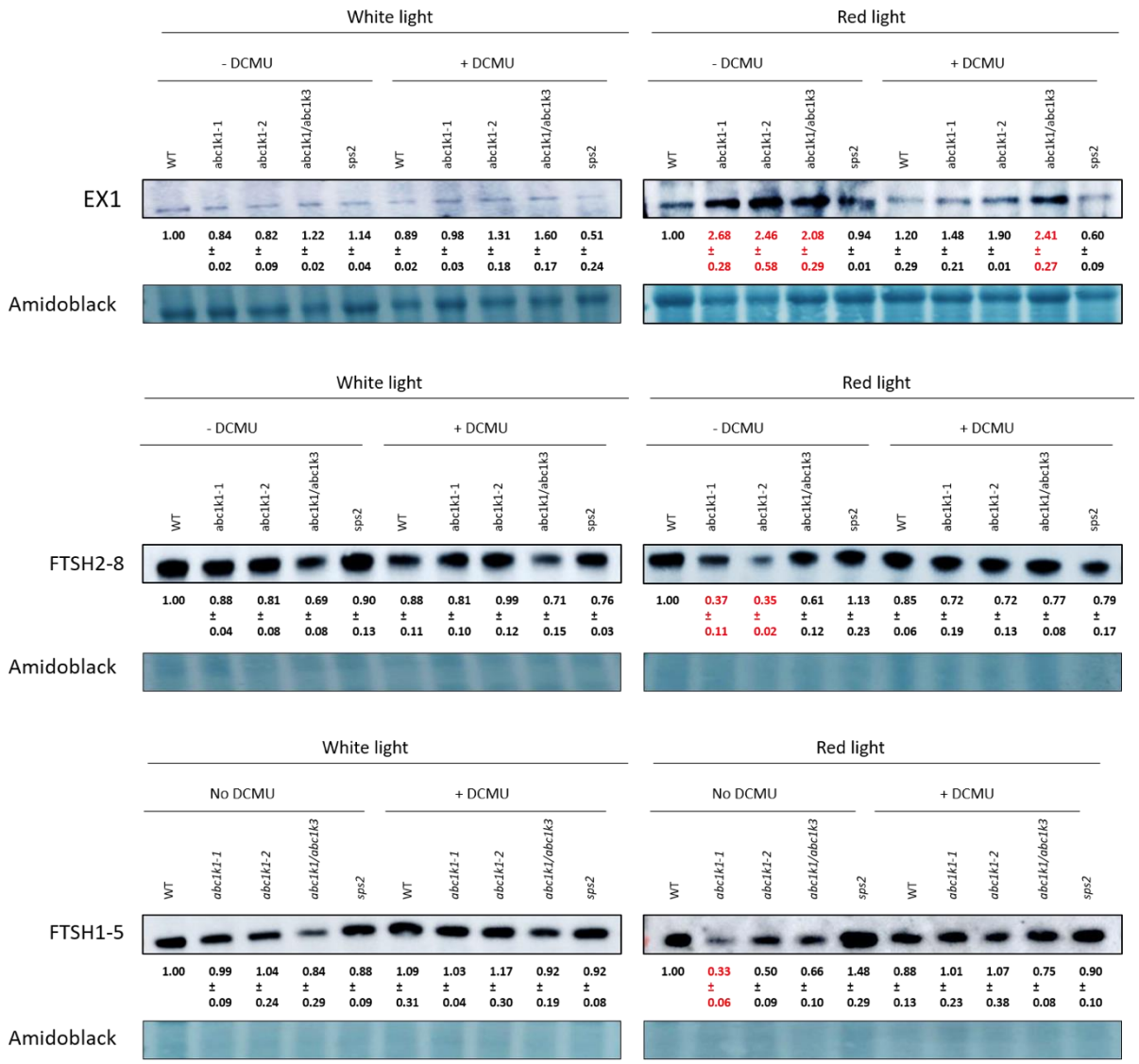

Figure 2.2. Changes in accumulation of protein EX1 and chloroplast FTSH proteases depending on genotype and light condition. Total protein extracts from five days old seedlings grown under constant white light (80 µE) or red light (60 µE) with or without 12.5 nM of DCMU were probed for the accumulation of Executer1 (EX1), and two different FTSH proteases, FTSH1-5 and FTSH2-8. The numbers below the immunoblot image show the average protein signal intensity compared to WT under white light ± the standard error between biological replicates (n=2 for EX1, n=3 for FTSH1-5 and FTSH2-8). In red are marked the samples showing a statistically significant difference from WT white light from a Tukey HSD post-hoc test following a Kruskal-Wallis test ($p<0.05$).

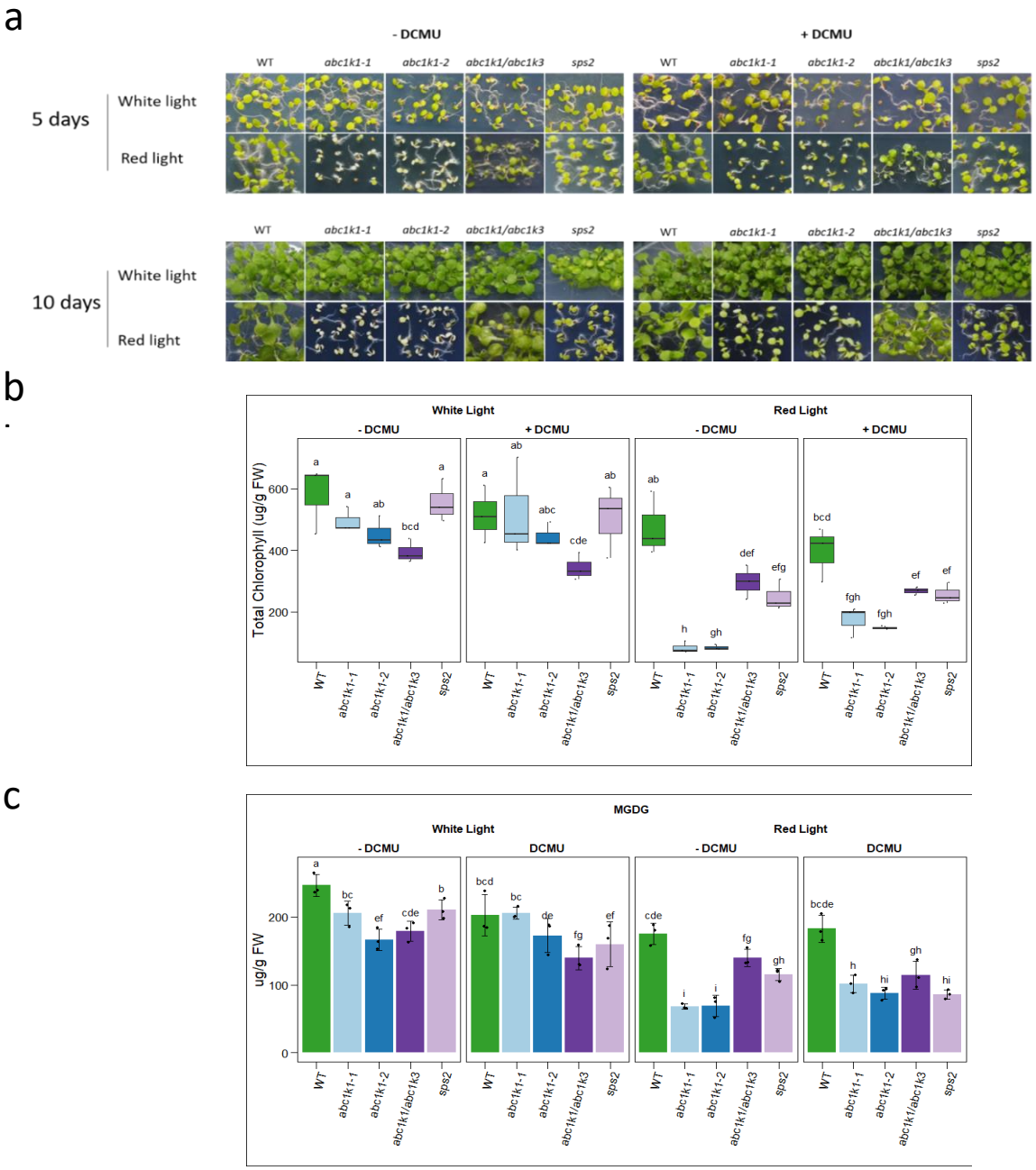

Figure 2.3. Effect of DCMU treatment on seedlings under white and red light. Col-0, *abc1k1-1*, *abc1k1-2*, *abc1k1/abc1k3* and *sps2* seedlings were grown under constant white light (80 µE) or constant red light (60 µE, peak 680nm) on standard 0.5x MS media or the same media supplemented with 12.5 nM DCMU a) Representative image of the phenotype of the seedlings 5 and 10 days after germination. b) Chlorophyll levels in seedlings 5 days after germination, the bar plot shows total chlorophyll, chlorophyll a and chlorophyll b concentrations. Error bars indicate ± SD (n=3). c) MGDG content in seedlings 5 days after germination, the bar plot shows total MGDG and Error bars indicate ± SD (n=3). The letters in b and c identify statistically different groups obtained by a post-hoc Fisher's analysis (alpha =0.05).

a

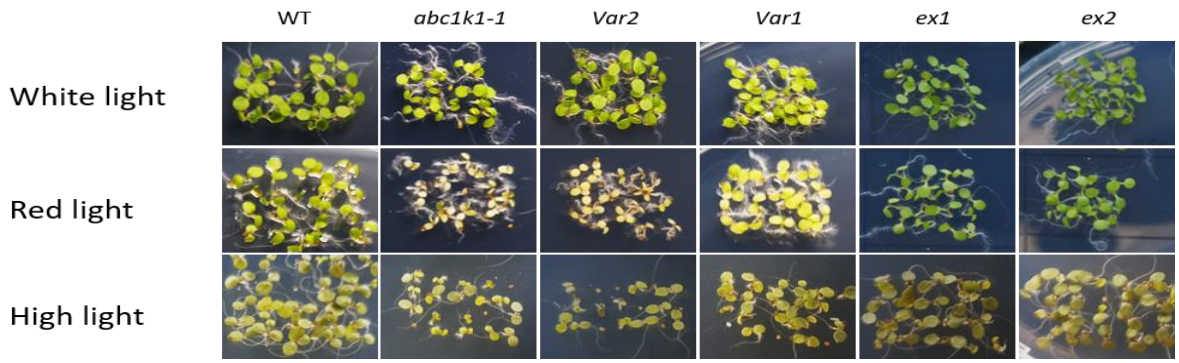

b

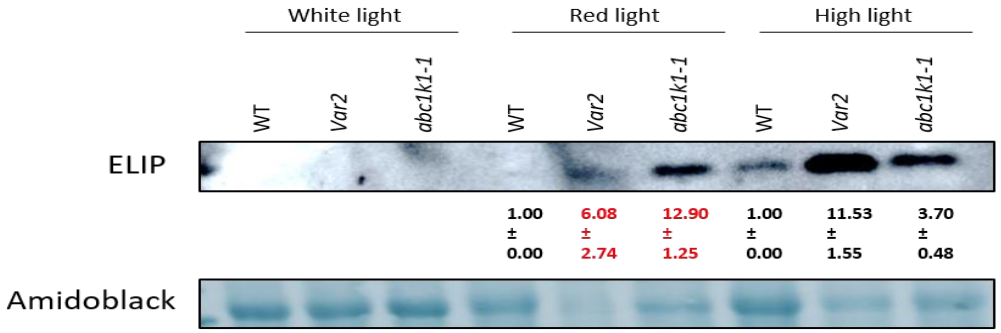

c

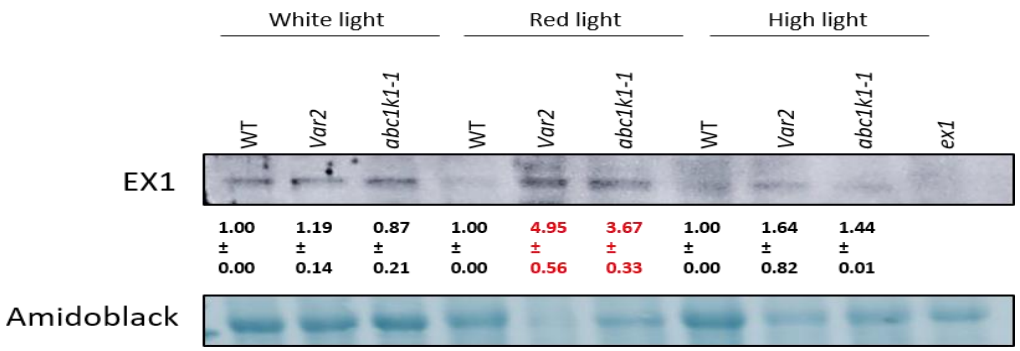

Figure 2.4. *abc1k1* and *ftsh2* have a similar defect in chloroplast biogenesis under light-induced stress. WT, *abc1k1-1*, *var2*, *var1*, *ex1* and *ex2* seeds were germinated under constant white (80 µE), constant red light (60 µE) or constant high light (500 µE). a) Visible phenotype of 5 days old seedlings for all the genotypes. b) representative image of immunoblot showing the levels of accumulation of ELIP and c) EX1 in WT, *abc1k1* and *var2* genotypes. The numbers below the band represents the signal intensity compared to WT for each light condition ± the standard error SE (n= 3 biologicallyindependent replicates). In red are marked the samples showing a statistically significant difference from WT red light from a post-hoc test following a Kruskal-Wallis test ($p<0.05$).

a

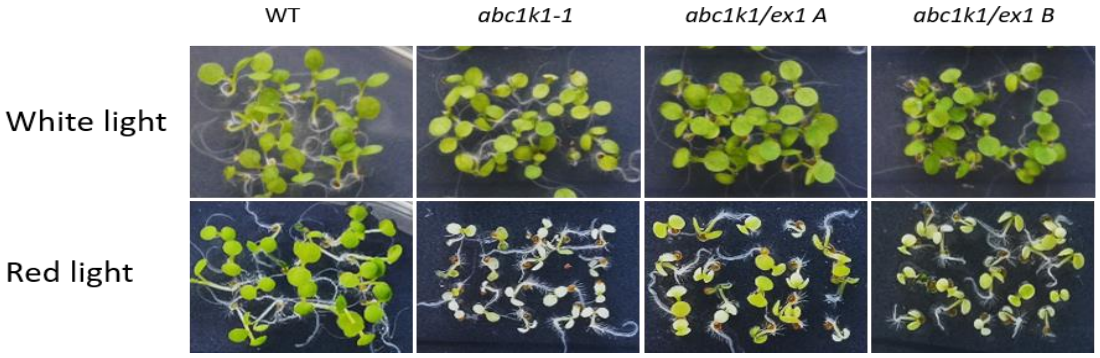

b

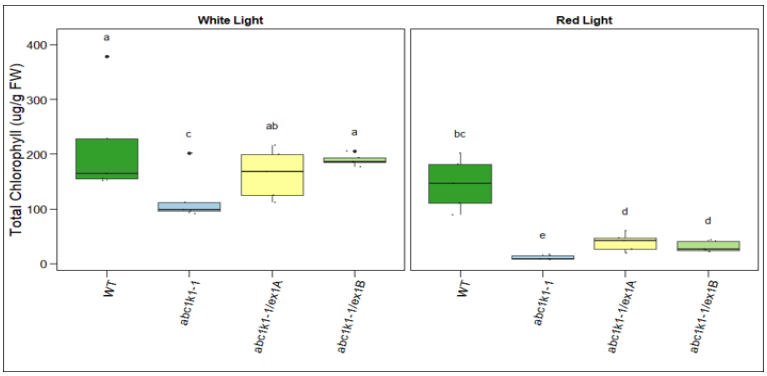

c

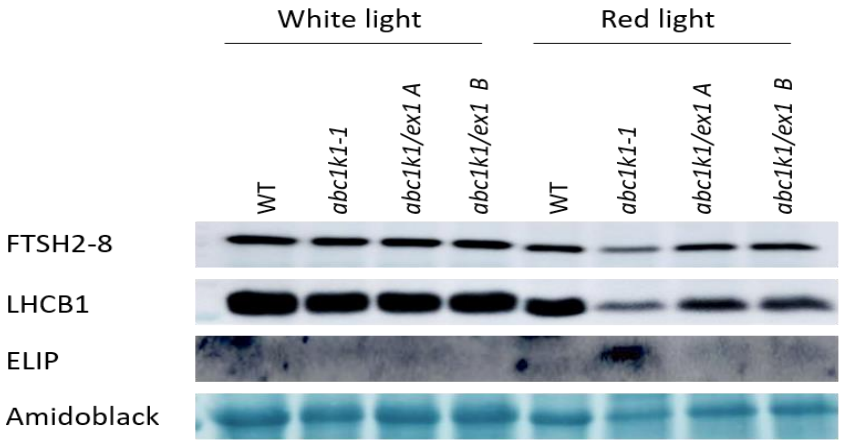

Figure 2.5. Mutation of the EX1 gene partially restores the *abc1k1* greening defect under red light. a) Visible phenotype of 5 days old seedlings of WT, *abc1k1*, and two independent *abc1k1/ex1* lines grown under constant red light (60 µE). b) Relative total chlorophyll levels of 5 days old WT, *abc1k1*, and *abc1k1/ex1 A*, *abc1k1/ex1 B* seedlings grown under constant white light (80 µE) or constant red light (60 µE). Error bars represent ± SD (n=2). The letters identify statistically different groups obtained by a post-hoc Fisher's analysis (alpha =0.1) c) Level of FTSH2-8, LHCB1 and ELIP protein analyzed by immunoblot in 5 days old seedlings of WT, *abc1k1* and *abc1k1/ex1 A*, *abc1k1/ex1 B* grown under constant white light (80 µE) or constant red light (60 µE).

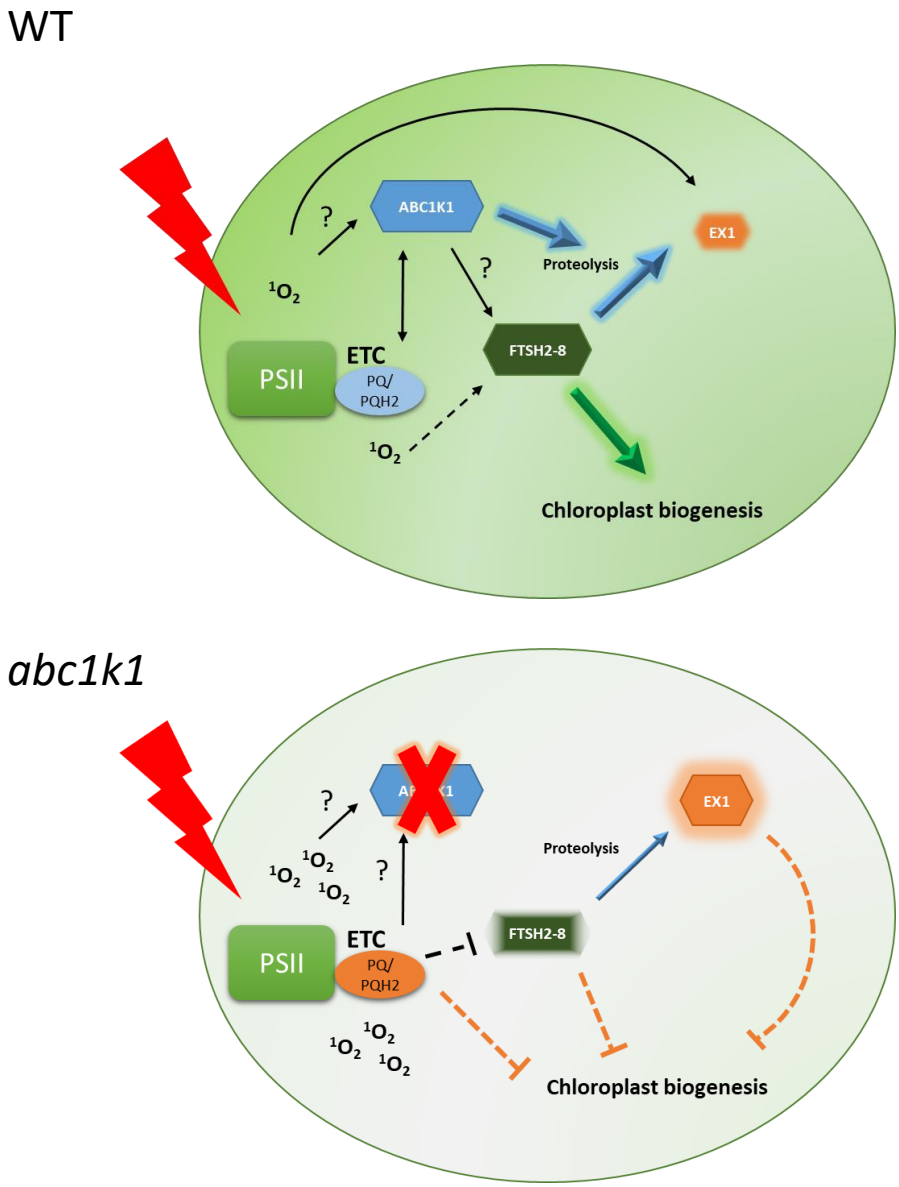

Figure 2.6. ABC1K1 interacts with EX1 signaling during chloroplast biogenesis. Under red light the pressure on the photosystem II (PSII) is increased leading to the production of singlet oxygen. This signal leads to the degradation of EX1 by FTSH and is integrated by the ABC1K1 dependent signal, the contribution of both signals leads to the degradation of EX1 that allows the progression of chloroplast biogenesis. In the absence of ABC1K1 a combination of multiple factors leads to the arrest of the chloroplast biogenesis. First, EX1 cannot be efficiently degraded and its accumulation is a first factor arresting the chloroplast biogenesis. Second, the photosynthetic electron transport is impaired, and its damage leads to a negative retrograde signaling, blocking the chloroplast biogenesis. Third, the FTSH protease is less accumulated, possibly damaged by the impaired PETC activity, leading to an imbalance in the chloroplast protein homeostasis and contributing to arrest the chloroplast biogenesis.

Materials and methods

Plant materials, growth conditions and treatments

Arabidopsis thaliana wild-type plant refers to var. Columbia-0 (Col-0). To analyze the effect of ABC1K1 knock-down, two T-DNA insertion lines (SALK_068628, SALK_130499C) were obtained from the Nottingham Arabidopsis Stock Centre (NASC, http://arabidopsis.info). The *abc1k1/abc1k3* double mutant was previously obtained by crossing (Pralon et al., 2020), the *sps2* mutant was a kind gift from Gilles Basset. The mutants used in this reports : *stn7* (N69602), *npq1* (N3771), *psaL* (N626585), *var1* (*ftsh5*, N271), *ex1*(N502088) and *ex2* (N521694) were obtained from NASC.The *pgr5* mutant was isolated as CE11-1-1 in a screen for high fluorescence mutants (Shikanai et al., 1999). The *var2* (*ftsh2*) mutant was a generous gift from Wataru Sakamoto. To generate the *abc1k1-1/ex1* double mutant, we introduced, by Agrobacterium-mediated nuclear transformation, a T-DNA construct containing two synthetic gRNAs (sgRNA) under the control of the U6 promoter, and the Cas9 gene under the control of the synthetic EC1 promoter that confers expression in the egg cells (Durr et al., 2018). The binary vector and the cloning method to insert two sgRNA were developed and described by Xing and coworkers (Xing et al., 2014). The chop chop software was used to design the sgRNA sequences targeting the EX1 coding sequence (Montague et al., 2014). The highest ranking sgRNA sequences were further analyzed with E-CRISP, and the two sequences with the highest efficacy score were chosen for the cloning (Heigwer et al., 2014).

The *abc1k1* mutant was complemented with 35S:ABC1K1-YFP-HA. The ABC1K1 coding sequence was synthetized directly in the pEarleyGate101 plant expression vector (Earley et al. 2006) by GeneCust (Boynes, France) between the constitutive 35S promoter and the YFP-HA tag resulting in pEarlyGate101-ABC1K1. The pEarlyGate101-ABC1K1 plasmid was introduced by electroporation into the Agrobacterium tumefaciens C58 strain. The resulting strain was used to transform *abc1k1-1* by floral dipping (Clough and Bent, 1998). Transgenic plants were selected on ½ MS agar medium supplemented with 30 mg/L glufosinate ammonium. Homozygous 35S:ABC1K1-YFP-HA lines with a single insertion of the transgene were selected by segregation analyses. Complemented plants, in which the protein expression was confirmed by immunoblot, were used for the following pull-down experiment. As a control, we produced a pSSU::YFP-HA line which overexpressed the YFP-HA-tag fused to the transit peptide of the Rubisco small subunit.To target the YFP-HA fusion to the chloroplast stroma, the chloroplast transit peptide (cTP) of the small subunit of Rubisco (SSU, At5g38430) was PCR-amplified with the primers list in table S2. The PCR product was inserted into the plant expression vector pEarleyGate 101, containing a C-terminal YFP-HA tag, using the Gateway recombination cloning system (Invitrogen) (Earley et al., 2006)

Sterilized seeds were spread on 0.5x MS plates with or without 12.5 nM of DCMU (3-(3,4-dichlorophenyl)-1, 1-dimethylurea), and were placed in the dark for 24 hours at 4°C. Seeds were moved to 22-24°C and exposed for 1 hour to white light (80 µmol m^{-2} s^{-1}), afterwards were kept for 5 days under continuous white light (80 µmol m^{-2} s^{-1}) or moved to continuous red light (60 µmol m^{-2} s^{-1}). 5 days old seedling were then collected under the light, immediately frozen in liquid nitrogen and stored at -20°C.

Chlorophyll quantification

Total chlorophyll was extracted from a minimum of 20 mg of fresh weight (FW) of 5 days old seedlings by adding 10 µl per mg FW of DMF (Dimethylformamide). Samples were centrifuged 1 minute at 16,000 g and stored overnight at 4°C in the dark. Extracts were further centrifuged 3 minutes at 16,000 g and the absorbance at 664 nm and 647 nm was measured with a Nanodrop spectrophotometer (NanoDrop ND-1000 spectrophotometer,Witec AG). Total chlorophyll, chlorophyll a and chlorophyll b concentrations were calculated according to (Porra et al., 1989).

Immunoblot analyses

Frozen 5 days old seedlings were ground in lysis buffer (100 mM Tris-HCl pH 8.5, 2% SDS, 10 mM NaF, 0.05% of protease inhibitor cocktail for plants (Sigma)) with a micro-pestle in a 1.7 ml microtubes. Samples were incubated at 37°C for 30 min and centrifuged for 15 minutes at 16,000 g at room temperature. Protein concentration was determined using the Pierce BCA protein assay kit (Thermo Scientific, cat. No. 23225) following manufacturer instructions. Proteins were precipitated using chloroform-methanol and resuspended in sample buffer (50 mM Tris-HCl pH 6.8, 100 mM Dithiothreitol, 2% SDS, 0.1% Bromophenol Blue, 10% Glycerol) at a final concentration of 1 µg/µl.; after denaturation for 10 minutes at 65°C, an aliquot of 5 µl was loaded on a 12% polyacrylamide SDS gel and proteins were separated by electrophoresis. Proteins were transferred to a nitrocellulose membrane for immunoanalysis using the following antibodies: anti-Lhcb1 (Agrisera, AS01 004), anti-Lhcb2-P (Agrisera, AS13 2705), anti-Lhcb1-P (Agrisera , AS13 2704) anti-D1 (PsbA) (Agrisera, AS05 084), anti-Lhca1 (Agrisera, AS01005), anti-PsaB (Agrisera, AS10 695), anti-PsaD (Agrisera, AS09 461), anti-PetB (Agrisera, AS18 4169), anti-PetC (Agrisera, AS08 330), anti-AtpC (Agrisera , AS08 312), anti-Elip (Agrisera , AS03 036), anti-Ftsh2-8 (Agrisera , AS16 3929), anti-Ftsh1-5 (Agrisera , AS16 3930), anti-Ex1 (Phytoab, PHY1693S). Primary antibodies were detected with horseradish peroxidase-conjugated anti-rabbit (Merck, AP132P) or anti-mouse (Sigma, A5278) antibodies. Chemiluminescent signals were generated by home-made reaction mixture (Luminol 1.25 mM, cumaric acid 0.20 mM, mixed with 0.01% H2O2 just before the reaction). Signals were revealed with a CCD camera (Amersham Imager 600, AmershamBiosciences, Inc.).

Real-time PCR analysis

Total RNA was extracted from multiple 5-days old seedlings using the RNeasy plant mini kit (Qiagen, cat. no. 74904) and cDNAs were synthetized from 1 µg of total RNA using GoScript™ Reverse Transcriptase kit (Promega, cat. no. A5001). Quantitative RT-PCR reactions were performed using the LightCycler 480 SYBR Green I Master mix (Roche, cat. no. 04887352001) and a LightCycler® 480 Instrument. The specific primers for each gene are listed in the supplementary table S2. The gene expression level was quantified using the $2^{-\Delta\Delta Ct}$ method (Livak and Schmittgen, 2001). The relative expression level of each gene was assessed using the Actin 2 gene (ACT2) as reference. All the reactions were performed in technical duplicates and the data shown come from two independent biological replicates.

Photosynthetic parameters

The chlorophyll fluorescence signal was measured with a Fluorcam MF800 (Photon System Instrument, Czech Republic, http://www.psi.cz). The actinic light for the light curve induction was provided by blue LEDs (470nm). At the beginning of the protocol, the maximum yield of PSII was measured: $\Phi_{max} = (F_M–F_O)/F_M$ where F_M is the maximal fluorescence in dark acclimated plants, measured during a saturating light pulse, and F_O the fluorescence recorded in the dark. For each light intensity step we estimated the fraction of open PS II centers based on a "lake" model by $qL = [(F_M'–F_S)/ (F_M'–F_O')]* (F_O'–F_S)$ (Kramer et al., 2004), the quantum yield of PSII $\Phi_{PSII} = (F_M'–F_S)/F_M'$ and the non-photochemical quenching $NPQ = (F_M – F_M')/F_M'$. F_M' is the maximal fluorescence at the end of each light intensity step, F_S the steady state fluorescence at the end of each light step and F_O' the fluorescence in the dark measured after 2 seconds of exposition to far-red light at the end of each light phase. The experiment was repeated on four independent biological replicates composed by 9 to 12, 5-days old seedlings per genotype.

Lipid profile analysis

Extraction of total lipids was performed on pools of 5-days old seedlings for each genotype obtained from three independent experiments. In brief, after grinding, the lipids were extracted with 10 µl of tetrahydrofuran:methanol 50:50 (v/v) per mg of FW, the debris were separated by centrifugation (3 min, 14,000 g), and the supernatant transferred to an HPLC vial. 2.5 µl of the sample were loaded on a reverse-phase Acquity BEH C18 column (50 × 2.1 mm, 1.7 µm) maintained at 60°C, and analysed by ultra-high pressure liquid chromatography coupled to atmospheric pressure chemical ionization-quadrupole time-of-flight mass spectrometry (UHPLC-APCI-QTOF-MS) as previously described (Spicher et al., 2016). Data were acquired using MassLynx version 4.1 (Waters) and further processed with TargetLynx (Waters). Compound identity was determined based on reference standards that were also used for the quantification curve (Spicher et al., 2016). For the identification of the galactolipids a commercial MGDG mix (Avanti Polar Lipids) was used as a standard, the linearity of the detection was assessed as previously reported (Sattari Vayghan et al., 2020).

Lipid peroxidation analysis

Lipid peroxidation was measured by quantifying HOTEs (hydroxyoctadecatrienoic acids, C18:3-OH), oxidation products of linolenic acid (C18:3), the major fatty acid in Arabidopsis, as described elsewhere (D'Alessandro et al., 2018; Montillet et al., 2004). Lipids were extracted from about 0.3 g of frozen Arabidopsis seedlings. The samples were ground in an equivolume of methanol/chloroform solution containing 5 mM triphenyl phosphine, 1 mM 2,6-tert-butyl-p-cresol (5 mL g^{-1} fresh weight), and citric acid (2.5 mL g^{-1} fresh weight), using an Ultra-Turrax blender. Internal standard 15-HEDE was added to a final concentration 100 nmol g^{-1} fresh weight. After centrifugation at 1000 g and 4 °C for 5 min, the lower organic phase was carefully taken out with the help of a glass syringe into a glass tube. The solvent was evaporated under N_2 gas at 40 °C. The residues were recovered in 1.25 mL of absolute ethanol and 1.25 mL of 3.5 N NaOH and hydrolyzed at 80 °C for 30 min. The ethanol was evaporated under N_2 gas at

40 °C for 10 min. After cooling to 25 °C, pH was adjusted between 4 and 5 with citric acid. Hydroxy fatty acids were extracted with hexane/ether (v/v). The organic phase was analyzed by straight phase HPLC-UV, as previously described (Montillet et al., 2004). HOTE isomers (9-, 12-, 13-, and 16-HOTE) were quantified based on the 15-HEDE internal standard.

Affinity purification

Affinity isolation of ABC1K1 interactors was performed using the 35S:ABC1K1-YFP-HA line. As control, we used the pSSU::YFP-HA line. The pull down was performed using the µMACS HA Tagged protein isolation kit (Miltenyi Biotec, cat. no. 130-091-122). Briefly, 1 g of 5 days old seedlings grown under white light (80 µE) or pure red light (60 µE) were ground in 2 ml of lysis buffer and centrifuged 10 min at 16 000 g to remove the cell debris. Then, 50 µl of HA-beads were added to the supernatant and incubated for 45 min at 4°C. The samples were loaded on a µ column, Miltenyi Biotec, cat. no. 130-042-701). The column was washed and proteins eluted. Eluates were analyzed by mass spectrometry at the Protein Analysis Facility, Center for Integrative Genomics, Faculty of Biology and Medecine, University of Lausanne, Switzerland. The obtained peptides were identified using the MASCOT/SCAFFOLD algorithm. The peptides corresponding to proteins identified only in the eluates from ABC1K1-YFP-HA extracts and not in the pSSU::YFP-HA control are listed in the supplementary table S1. The mass spectrometry proteomics data have been deposited to the ProteomeXchange Consortium via the PRIDE (Perez-Riverol et al., 2019) partner repository with the dataset identifier PXD030243 and 10.6019/PXD030243.

Statistical Analysis

The normal distribution of the residuals of each data set was tested before any other statistical analysis. If this assumption was met, an ANOVA model was utilized; otherwise, a Kruskal–Wallis rank sum test was performed to assess statistically significant differences between the data groups. If the result was significant, we used post hoc Tukey's HSD test for multiple comparisons. The reported p-values, corrected by the false discovery rate (Benjamini and Hochberg, 1995), were obtained with the latter, the classes in the figures were defined as distinct by an alpha score of 0.05, unless otherwise specified. The calculations were performed with RStudio with the package agricola (Version 1.2.5019 RStudio Inc).

Acknowledgements

This work was supported the University of Neuchâtel and SNF grants 31003A_176191 to FK and 31003A_179417 to FL. We thank Veronique Douet for her technical assistance.

Contributions

J.C., F.L. and F.K. designed the experiments. J.C., F.L., M.H., and F.K wrote the manuscript. J.C., F.L. and J.P.M. performed all experiments. T.P. and S.R. produced the complemented lines and the pSSU-HA line. M.H. and B.K. did the HOTEs analysis. G.G. did the lipid profile analysis.

References

Bellafiore, S., Barneche, F., Peltier, G., and Rochaix, J.D. (2005). State transitions and light adaptation require chloroplast thylakoid protein kinase STN7. Nature *433*, 892-895.

Benjamini, Y., and Hochberg, Y. (1995). Controlling the False Discovery Rate: A Practical and Powerful Approach to Multiple Testing. Journal of the Royal Statistical Society: Series B (Methodological) *57*, 289-300.

Block, A., Fristedt, R., Rogers, S., Kumar, J., Barnes, B., Barnes, J., Elowsky, C.G., Wamboldt, Y., Mackenzie, S.A., Redding, K., *et al.* (2013). Functional modeling identifies paralogous solanesyl-diphosphate synthases that assemble the side chain of plastoquinone-9 in plastids. J Biol Chem *288*, 27594-27606.

Chen, M., Choi, Y., Voytas, D.F., and Rodermel, S. (2000). Mutations in the Arabidopsis VAR2 locus cause leaf variegation due to the loss of a chloroplast FtsH protease. Plant J *22*, 303-313.

Clough, S.J., and Bent, A.F. (1998). Floral dip: a simplified method for Agrobacterium-mediated transformation of Arabidopsis thaliana. The Plant journal : for cell and molecular biology *16*, 735-743.

CRONSHAGEN, U., and HERZFELD, F. (1990). Distribution of the early light-inducible protein in the thylakoids of developing pea chloroplasts. European journal of biochemistry *193*, 361-366.

D'Alessandro, S., Ksas, B., and Havaux, M. (2018). Decoding β-Cyclocitral-Mediated Retrograde Signaling Reveals the Role of a Detoxification Response in Plant Tolerance to Photooxidative Stress. The Plant cell *30*, 2495-2511.

Dogra, V., Duan, J., Lee, K.P., and Kim, C. (2019a). Impaired PSII proteostasis triggers a UPR-like response in the var2 mutant of Arabidopsis. J Exp Bot *70*, 3075-3088.

Dogra, V., Duan, J., Lee, K.P., Lv, S., Liu, R., and Kim, C. (2017). FtsH2-Dependent Proteolysis of EXECUTER1 Is Essential in Mediating Singlet Oxygen-Triggered Retrograde Signaling in Arabidopsis thaliana. Front Plant Sci *8*, 1145.

Dogra, V., Li, M., Singh, S., Li, M., and Kim, C. (2019b). Oxidative post-translational modification of EXECUTER1 is required for singlet oxygen sensing in plastids. Nat Commun *10*, 2834.

Durr, J., Papareddy, R., Nakajima, K., and Gutierrez-Marcos, J. (2018). Highly efficient heritable targeted deletions of gene clusters and non-coding regulatory regions in Arabidopsis using CRISPR/Cas9. Scientific reports *8*, 1-11.

Fristedt, R., and Vener, A.V. (2011). High light induced disassembly of photosystem II supercomplexes in Arabidopsis requires STN7-dependent phosphorylation of CP29. PLoS One *6*, e24565.

Heigwer, F., Kerr, G., and Boutros, M. (2014). E-CRISP: fast CRISPR target site identification. Nature methods *11*, 122-123.

Hernandez-Verdeja, T., and Strand, A. (2018). Retrograde Signals Navigate the Path to Chloroplast Development. Plant Physiol *176*, 967-976.

Huang, H., Yang, M., Su, Y., Qu, L., and Deng, X.W. (2015). Arabidopsis Atypical Kinases ABC1K1 and ABC1K3 Act Oppositely to Cope with Photodamage Under Red Light. Mol Plant *8*, 1122-1124.

Järvi, S., Suorsa, M., Tadini, L., Ivanauskaite, A., Rantala, S., Allahverdiyeva, Y., Leister, D., and Aro, E.-M. (2016). Thylakoid-bound FtsH proteins facilitate proper biosynthesis of photosystem I. Plant physiology *171*, 1333-1343.

Jun, L., Saiki, R., Tatsumi, K., Nakagawa, T., and Kawamukai, M. (2004). Identification and subcellular localization of two solanesyl diphosphate synthases from Arabidopsis thaliana. Plant Cell Physiol *45*, 1882-1888.

Kato, Y., Miura, E., Ido, K., Ifuku, K., and Sakamoto, W. (2009). The Variegated Mutants Lacking Chloroplastic FtsHs Are Defective in D1 Degradation and Accumulate Reactive Oxygen Species. Plant Physiology *151*, 1790-1801.

Kato, Y., and Sakamoto, W. (2018). FtsH Protease in the Thylakoid Membrane: Physiological Functions and the Regulation of Protease Activity. Front Plant Sci *9*, 855.

Kim, C., Lee, K.P., Baruah, A., Nater, M., Gobel, C., Feussner, I., and Apel, K. (2009). (1)O2-mediated retrograde signaling during late embryogenesis predetermines plastid differentiation in seedlings by recruiting abscisic acid. Proc Natl Acad Sci U S A *106*, 9920-9924.

Kim, C., Meskauskiene, R., Zhang, S., Lee, K.P., Lakshmanan Ashok, M., Blajecka, K., Herrfurth, C., Feussner, I., and Apel, K. (2012). Chloroplasts of Arabidopsis are the source and a primary target of a plant-specific programmed cell death signaling pathway. Plant Cell *24*, 3026-3039.

Kramer, D.M., Johnson, G., Kiirats, O., and Edwards, G.E. (2004). New Fluorescence Parameters for the Determination of QA Redox State and Excitation Energy Fluxes. Photosynth Res *79*, 209.

Ksas, B., Becuwe, N., Chevalier, A., and Havaux, M. (2015). Plant tolerance to excess light energy and photooxidative damage relies on plastoquinone biosynthesis. Sci Rep *5*, 10919.

Lee, K.P., Kim, C., Landgraf, F., and Apel, K. (2007). EXECUTER1- and EXECUTER2-dependent transfer of stress-related signals from the plastid to the nucleus of Arabidopsis thaliana. Proc Natl Acad Sci U S A *104*, 10270-10275.

Liebers, M., Gillet, F.X., Israel, A., Pounot, K., Chambon, L., Chieb, M., Chevalier, F., Ruedas, R., Favier, A., Gans, P., *et al.* (2020). Nucleo-plastidic PAP8/pTAC6 couples chloroplast formation with photomorphogenesis. EMBO J *39*, e104941.

Livak, K.J., and Schmittgen, T.D. (2001). Analysis of relative gene expression data using real-time quantitative PCR and the 2− ΔΔCT method. methods *25*, 402-408.

Martin, G., Leivar, P., Ludevid, D., Tepperman, J.M., Quail, P.H., and Monte, E. (2016). Phytochrome and retrograde signalling pathways converge to antagonistically regulate a light-induced transcriptional network. Nat Commun *7*, 11431.

Martinis, J., Glauser, G., Valimareanu, S., Stettler, M., Zeeman, S.C., Yamamoto, H., Shikanai, T., and Kessler, F. (2014). ABC 1 K 1/PGR 6 kinase: a regulatory link between photosynthetic activity and chloroplast metabolism. The Plant Journal *77*, 269-283.

Montague, T.G., Cruz, J.M., Gagnon, J.A., Church, G.M., and Valen, E. (2014). CHOPCHOP: a CRISPR/Cas9 and TALEN web tool for genome editing. Nucleic acids research *42*, W401-W407.

Montillet, J.-L., Cacas, J.-L., Garnier, L., Montané, M.-H., Douki, T., Bessoule, J.-J., Polkowska-Kowalczyk, L., Maciejewska, U., Agnel, J.-P., Vial, A., *et al.* (2004). The upstream oxylipin profile of Arabidopsis thaliana: a tool to scan for oxidative stresses. The Plant Journal *40*, 439-451.

Munekage, Y., Hojo, M., Meurer, J., Endo, T., Tasaka, M., and Shikanai, T. (2002). PGR5 is involved in cyclic electron flow around photosystem I and is essential for photoprotection in Arabidopsis. Cell *110*, 361-371.

Niyogi, K.K., Grossman, A.R., and Bjorkman, O. (1998). Arabidopsis mutants define a central role for the xanthophyll cycle in the regulation of photosynthetic energy conversion. Plant Cell *10*, 1121-1134.

Page, M.T., McCormac, A.C., Smith, A.G., and Terry, M.J. (2017). Singlet oxygen initiates a plastid signal controlling photosynthetic gene expression. New Phytol *213*, 1168-1180.

Pipitone, R., Eicke, S., Pfister, B., Glauser, G., Falconet, D., Uwizeye, C., Pralon, T., Zeeman, S.C., Kessler, F., and Demarsy, E. (2021). A multifaceted analysis reveals two distinct phases of chloroplast biogenesis during de-etiolation in Arabidopsis. Elife *10*.

Plochinger, M., Torabi, S., Rantala, M., Tikkanen, M., Suorsa, M., Jensen, P.E., Aro, E.M., and Meurer, J. (2016). The Low Molecular Weight Protein PsaI Stabilizes the Light-Harvesting Complex II Docking Site of Photosystem I. Plant Physiol *172*, 450-463.

Porra, R., Thompson, W., and Kriedemann, P. (1989). Determination of accurate extinction coefficients and simultaneous equations for assaying chlorophylls a and b extracted with four different solvents: verification of the concentration of chlorophyll standards by atomic absorption spectroscopy. Biochimica et Biophysica Acta (BBA)-Bioenergetics *975*, 384-394.

Pralon, T., Collombat, J., Pipitone, R., Ksas, B., Shanmugabalaji, V., Havaux, M., Finazzi, G., Longoni, P., and Kessler, F. (2020). Mutation of the Atypical Kinase ABC1K3 Partially Rescues the PROTON GRADIENT REGULATION 6 Phenotype in Arabidopsis thaliana. Front Plant Sci *11*, 337.

Pralon, T., Shanmugabalaji, V., Longoni, P., Glauser, G., Ksas, B., Collombat, J., Desmeules, S., Havaux, M., Finazzi, G., and Kessler, F. (2019). Plastoquinone homoeostasis by Arabidopsis proton gradient regulation 6 is essential for photosynthetic efficiency. Commun Biol *2*, 220.

Sakamoto, W., Uno, Y., Zhang, Q., Miura, E., Kato, Y., and Sodmergen (2009). Arrested Differentiation of Proplastids into Chloroplasts in Variegated Leaves Characterized by Plastid Ultrastructure and Nucleoid Morphology. Plant and Cell Physiology *50*, 2069-2083.

Sattari Vayghan, H., Tavalaei, S., Grillon, A., Meyer, L., Ballabani, G., Glauser, G., and Longoni, P. (2020). Growth Temperature Influence on Lipids and Photosynthesis in Lepidium sativum. Frontiers in plant science *11*, 745.

Shikanai, T., Munekage, Y., Shimizu, K., Endo, T., and Hashimoto, T. (1999). Identification and characterization of Arabidopsis mutants with reduced quenching of chlorophyll fluorescence. Plant Cell Physiol *40*, 1134-1142.

Spicher, L., Glauser, G., and Kessler, F. (2016). Lipid antioxidant and galactolipid remodeling under temperature stress in tomato plants. Frontiers in Plant Science *7*, 167.

Tadini, L., Peracchio, C., Trotta, A., Colombo, M., Mancini, I., Jeran, N., Costa, A., Faoro, F., Marsoni, M., Vannini, C., *et al.* (2020). GUN1 influences the accumulation of NEP-dependent transcripts and chloroplast protein import in Arabidopsis cotyledons upon perturbation of chloroplast protein homeostasis. Plant J *101*, 1198-1220.

Trebst, A. (1980). Inhibitors in electron flow: Tools for the functional and structural localization of carriers and energy conservation sites. In Methods in Enzymology, A. San Pietro, ed. (Academic Press), pp. 675-715.

Wagner, D., Przybyla, D., Op den Camp, R., Kim, C., Landgraf, F., Lee, K.P., Wursch, M., Laloi, C., Nater, M., Hideg, E., *et al.* (2004). The genetic basis of singlet oxygen-induced stress responses of Arabidopsis thaliana. Science *306*, 1183-1185.

Wang, L., Kim, C., Xu, X., Piskurewicz, U., Dogra, V., Singh, S., Mahler, H., and Apel, K. (2016). Singlet oxygen- and EXECUTER1-mediated signaling is initiated in grana margins and depends on the protease FtsH2. Proc Natl Acad Sci U S A *113*, E3792-3800.

Waters, M.T., and Langdale, J.A. (2009). The making of a chloroplast. EMBO J *28*, 2861-2873.

Xing, H.L., Dong, L., Wang, Z.P., Zhang, H.Y., Han, C.Y., Liu, B., Wang, X.C., and Chen, Q.J. (2014). A CRISPR/Cas9 toolkit for multiplex genome editing in plants. BMC Plant Biol *14*, 327.

Yang, M., Huang, H., Zhang, C., Wang, Z., Su, Y., Zhu, P., Guo, Y., and Deng, X.W. (2016). Arabidopsis atypical kinase ABC1K1 is involved in red light-mediated development. Plant Cell Rep *35*, 1213-1220.

Yoo, C.Y., Pasoreck, E.K., Wang, H., Cao, J., Blaha, G.M., Weigel, D., and Chen, M. (2019). Phytochrome activates the plastid-encoded RNA polymerase for chloroplast biogenesis via nucleus-to-plastid signaling. Nat Commun *10*, 2629.

Yu, F., Liu, X., Alsheikh, M., Park, S., and Rodermel, S. (2008). Mutations in SUPPRESSOR OF VARIEGATION1, a factor required for normal chloroplast translation, suppress var2-mediated leaf variegation in Arabidopsis. Plant Cell *20*, 1786-1804.

Zaltsman, A., Feder, A., and Adam, Z. (2005a). Developmental and light effects on the accumulation of FtsH protease in Arabidopsis chloroplasts--implications for thylakoid formation and photosystem II maintenance. Plant J *42*, 609-617.

Zaltsman, A., Ori, N., and Adam, Z. (2005b). Two types of FtsH protease subunits are required for chloroplast biogenesis and Photosystem II repair in Arabidopsis. Plant Cell *17*, 2782-2790.

Supplementary figures

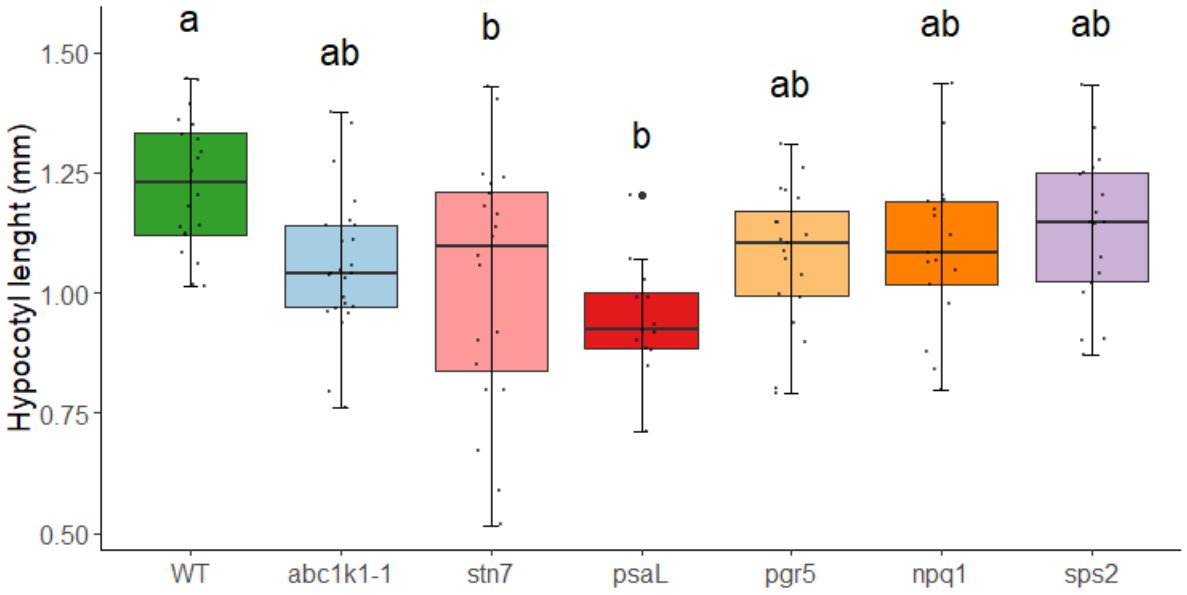

Figure S1: Length of the hypocotyl by genotype of seedlings grown under continuous white light (80 µE). The whiskers and box plot shows the minimum, first quartile, median, average, third quartile and maximum of each dataset, points indicate individual samples, outliers are indicated by a bigger point. (WT n=20, *abc1k1-1* n=24, *stn7* n=20, *psaL* n=12, *pgr5* n=19, *npq1* n=17 and *sps2* n=18). The letters identify statistically different groups obtained by a Tukey-HSD post-hoc test (alpha =0.01).

Identified Proteins	Accession Number	Alternate ID	CTL WL	K1 WL	CTL RL	K1 RL	Localization
Found in the eluate of ABC1K1 in normal light and red light							
AT3g24190/MUJ8_17 OS=Arabidopsis thaliana OX=3702 GN=At3g24190 PE=2 SV=1	Q9LRN0	At3g24190	0	2	0	15	Chloroplast
LETM1-like protein OS=Arabidopsis thaliana OX=3702 GN=MBL20.10 PE=4 SV=1	A0A1P8B9X6	At5g06220	0	5	0	11	Chloroplast, chloroplast envelope, mitochondrial inner membrane
Oligouridylate-binding protein 1C OS=Arabidopsis thaliana OX=3702 GN=UBP1C PE=1 SV=1	Q9LJH8	At3g14100	0	5	0	11	Cytoplasme, nucleus
Amino acid kinase family protein OS=Arabidopsis thaliana OX=3702 GN=At3g18680 PE=1 SV=1	A0A1I9LRT3 (+1)	At3g18680	0	3	0	11	Chloroplast
NAD(P)H-quinone oxidoreductase subunit K, chloroplastic OS=Arabidopsis thaliana OX=3702 GN=ndhK PE=3 SV=1	P56756	Atcg00430	0	12	0	10	Chloroplast, plastid
NAD(P)H-quinone oxidoreductase subunit 1, chloroplastic OS=Arabidopsis thaliana OX=3702 GN=ndhA PE=3 SV=2	Q37165	Atcg01100	0	11	0	10	Chloroplast
Probable plastid-lipid-associated protein 10, chloroplastic OS=Arabidopsis thaliana OX=3702 GN=PAP10 PE=1 SV=1	Q8W4F1	At2g46910	0	7	0	10	Chloroplast, cytosol, plastoglobule
Protein MITOFERRINLIKE 1, chloroplastic OS=Arabidopsis thaliana OX=3702 GN=MFL1 PE=2 SV=1	Q9FHX2	At5g42130	0	4	0	10	Chloroplast, chloroplast envelope, mitochondrion, plastid
Thioredoxin family protein OS=Arabidopsis thaliana OX=3702 GN=At4g10000 PE=4 SV=1	F4JKW0	At4g10000	0	3	0	9	Chloroplast
Thioredoxin-like protein HCF164, chloroplastic OS=Arabidopsis thaliana OX=3702 GN=HCF164 PE=1 SV=2	O23166	At4g37200	0	4	0	9	Chloroplast thylakoid membrane
Jacalin-related lectin 8 OS=Arabidopsis thaliana OX=3702 GN=JAL8 PE=3 SV=1	F4IB94	At1g52050	0	4	0	8	Extracellular regions
Alpha/beta-Hydrolases superfamily protein OS=Arabidopsis thaliana OX=3702 GN=At1g74640 PE=2 SV=1	Q8L475	At1g74640	0	4	0	8	Chloroplast, chloroplast envelope, chloroplast thylakoid membrane
NAD(P)H-quinone oxidoreductase subunit M, chloroplastic OS=Arabidopsis thaliana OX=3702 GN=ndhM PE=2 SV=1	Q2V2S7	At4g37925	0	7	0	7	Chloroplast, chloroplast thylakoid membrane, plasma membrane
CBS domain-containing protein CBSCBSPB5 OS=Arabidopsis thaliana OX=3702 GN=CBSCBSPB5 PE=1 SV=1	P0DH79 (+1)	At5g50640	0	3	0	7	Plastid
Mitochondrial transcription termination factor family protein OS=Arabidopsis thaliana OX=3702 GN=At5g07900 PE=2 SV=1	Q9SD94	At5g07900	0	5	0	7	Chloroplast
GDP-L-fucose synthase 1 OS=Arabidopsis thaliana OX=3702 GN=GER1 PE=1 SV=3	O49213	At1g73250	0	2	0	7	Cytoplasm
Protein kinase superfamily protein OS=Arabidopsis thaliana OX=3702 GN=At3g61080 PE=4 SV=1	A0A1I9LR17 (+1)	At3g61080	0	4	0	6	Chloroplast, mitochondrion
Conserved oligomeric Golgi complex subunit 4 OS=Arabidopsis thaliana OX=3702 GN=COG4 PE=1 SV=1	Q8L838	At4g01395	0	3	0	6	Golgi apparatus
P-type ATPase of Arabidopsis 2 OS=Arabidopsis thaliana OX=3702 GN=PAA2 PE=3 SV=1	A0A1P8BE56 (+1)	AT5G21930	0	3	0	6	Chloroplast, chloroplast thylakoid membrane
Putative septum site-determining protein minD homolog, chloroplastic OS=Arabidopsis thaliana OX=3702 GN=MIND1 PE=1 SV=1	Q9MBA2	At5g24020	0	2	0	6	Chloroplast, chloroplast envelope, chloroplast stroma
Cytochrome P450 705A5 OS=Arabidopsis thaliana OX=3702 GN=CYP705A5 PE=2 SV=1	Q9FI39	At5g47990	0	2	0	5	Endoplasmic reticulum, mitochondrion
Mitochondrial import inner membrane translocase subunit TIM17-2 OS=Arabidopsis thaliana OX=3702 GN=TIM17-2 PE=1 SV=2	Q9SP35	At2g37410	0	4	0	5	Endoplasmic reticulum, mitochondrial inner/outer membrane, mitochondrion
UPF0051 protein ABCI8, chloroplastic OS=Arabidopsis thaliana OX=3702 GN=ABCI8 PE=2 SV=1	Q9ZS97	At4g04770	0	3	0	5	Chloroplast, chloroplast stroma
Uncharacterized methyltransferase At2g41040, chloroplastic OS=Arabidopsis thaliana OX=3702 GN=At2g41040 PE=1 SV=1	Q0WPT7	At2g41040	0	4	0	5	Chloroplast, plastoglobule
AT3g23700/MYM9_3 OS=Arabidopsis thaliana OX=3702 GN=At3g23700 PE=2 SV=1	Q9LK47	At3g23700	0	3	0	5	Chloroplast, Chloroplast stroma, nucleus
AmmeMemoRadiSam system protein B OS=Arabidopsis thaliana OX=3702 GN=At2g25280 PE=2 SV=1	Q9SIR5	At2g25280	0	3	0	5	Nucleus
Lycopene beta cyclase, chloroplastic OS=Arabidopsis thaliana OX=3702 GN=LCY1 PE=1 SV=1	Q38933	At3g10230	0	2	0	5	Chloroplast
Ycf3-interacting protein 1, chloroplastic OS=Arabidopsis thaliana OX=3702 GN=Y3IP1 PE=1 SV=1	Q9LU01	At5g44650	0	5	0	4	Chlorplast, chloroplast thylakoid membrane
Sulfoquinovosyl transferase SQD2 OS=Arabidopsis thaliana OX=3702 GN=SQD2 PE=1 SV=1	Q8S4F6	At5g01220	0	5	0	3	Chloroplast, chloroplast envelope, plasma membrane, plastid
NAD(P)H-quinone oxidoreductase subunit I, chloroplastic OS=Arabidopsis thaliana OX=3702 GN=ndhI PE=2 SV=1	Q9CAC5	At1g70760	0	5	0	3	Chloroplast, chloroplast thylakoid membrane
NAD(P)H-quinone oxidoreductase subunit N, chloroplastic OS=Arabidopsis thaliana OX=3702 GN=ndhN PE=2 SV=1	Q9LVM2	At5g58260	0	9	0	0	Chloroplast, chloroplast envelope, chloroplast thylakoid membrane
Found in the eluate of ABC1K1 only in red light							
LETM1-like protein OS=Arabidopsis thaliana OX=3702 GN=MBL20.10 PE=4 SV=1	F4K2D7	At5g06220	0	0	0	11	Chloroplast, chloroplast envelope, mitochondrial inner membrane
Aspartokinase 2, chloroplastic OS=Arabidopsis thaliana OX=3702 GN=AK2 PE=1 SV=2	O23653	At5g14060	0	0	0	11	Chloroplast, chloroplast stroma
Serine/threonine-protein kinase SRK2B OS=Arabidopsis thaliana OX=3702 GN=SRK2B PE=1 SV=1	Q9C958	At1g60940	0	0	0	8	nucleus
P-loop containing nucleoside triphosphate hydrolases superfamily protein OS=Arabidopsis thaliana OX=3702 GN=SPD1 PE=4 SV=1	F4I3R7	At3g10420	0	0	0	7	Chloroplast, chloroplast envelope, chloroplast intermembrane space
Isopentenyltransferase 9 OS=Arabidopsis thaliana OX=3702 GN=IPT9 PE=3 SV=1	F4KZQ7 (+1)	At5g20040	0	0	0	7	Nucleus
Probable galactinol--sucrose galactosyltransferase 2 OS=Arabidopsis thaliana OX=3702 GN=RFS2 PE=2 SV=2	Q94A08	At3g57520	0	0	0	7	Cytoplasme, plasmodesma
Protein EXECUTER 1, chloroplastic OS=Arabidopsis thaliana OX=3702 GN=EX1 PE=1 SV=1	Q93YW0	At4g33630	0	0	0	6	Chloroplast, thylakoid membrane
Thermosome subunit gamma OS=Arabidopsis thaliana OX=3702 GN=DY1 PE=2 SV=1	Q949W7	At5g19540	0	0	0	6	Chloroplast, chloroplast stroma
Cytochrome P450 71B5 OS=Arabidopsis thaliana OX=3702 GN=CYP71B5 PE=2 SV=1	O65784	At3g53280	0	0	0	6	Chloroplast
Arogenate dehydratase/prephenate dehydratase 6, chloroplastic OS=Arabidopsis thaliana OX=3702 GN=ADT6 PE=1 SV=1	Q9SGD6	At1g08250	0	0	0	6	Chloroplast
Insulinase (Peptidase family M16) protein OS=Arabidopsis thaliana OX=3702 GN=MIK19.18 PE=1 SV=1	A0A2H1ZE93	At5g56730	0	0	0	6	Chloroplast, mitochondrion, plastid

Table S1: List of ABC1K1 interaction candidates. The proteins identified by mass spectrometry in the co-immunoprecipitation eluate with ABC1K1::HA are shown in the table (spectral count >4). The protein identification was based on TAIR database, from which the protein description and the corresponding accession number were taken. The corresponding gene locus was also obtained from TAIR. The peptide counts are shown in the column for the negative control and the ABC1K1:HA samples (CTL and K1 respectively) prepared from plants grown under constant white light (NL) or red light (RL). Protein localization, as annotated in TAIR, is reported in the last column. The top part of the table shows proteins identified in both growth conditions, while the bottom part shows the proteins identified in the protein samples obtained only from plants grown under red light.

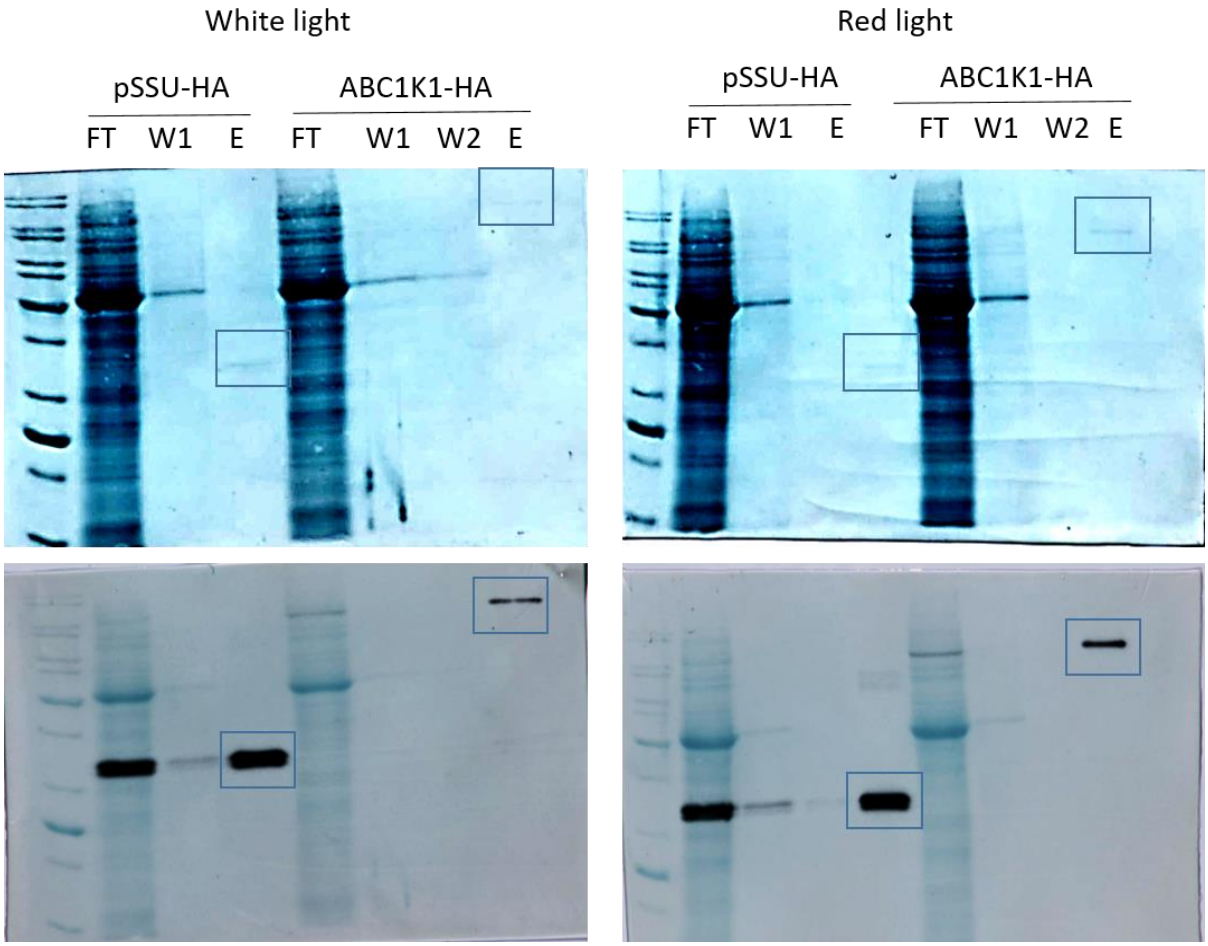

Figure S2: **Co-immuno purification of ABC1K1-HA with putative interaction partners.** Total protein extracts were prepared from 5 days old seedling of pSSU-HA control line and ABC1K1-HA complemented line, grown under white light (80 µE) or pure red light (60 µE). The extracts were loaded on affinity chromatography, the picture shows the protein staining (top membrane) of the flow through (FT), the first washing (W1), the second washing (W2) and the eluate (E), of the isolation process for the two lines and the two light condition. On the bottom membrane is shown the chemioluminescent signal obtained by the decoration of the membrane with an antibody anti-HA. The bands corresponding to pSSU-HA and ABC1K1-HA in the respective eluates, are framed in blue.

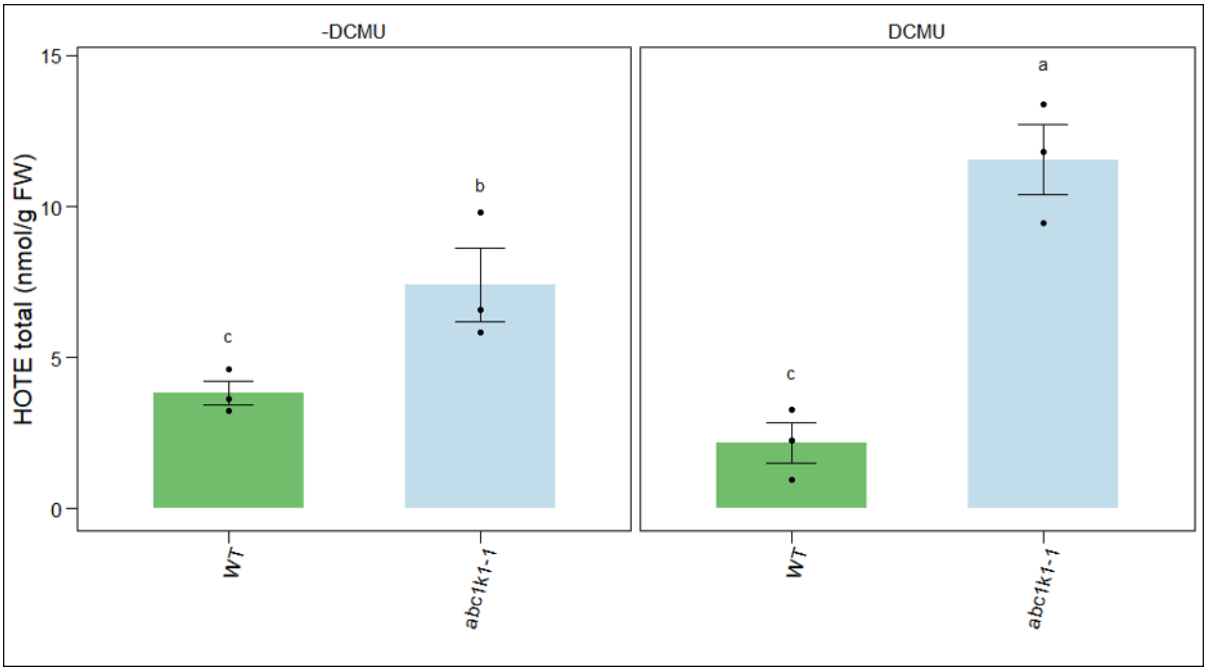

Figure S3: **DCMU treatment increases lipid peroxidation in *abc1k1-1*.** The lipid peroxidation was measured by the hydroxy-octodecatrienoic acid levels (HOTEs), in 5 days old WT and *abc1k1* seedlings grown under white light (80 µE) in the presence or absence of 12.5nM DCMU (n=3). The different letters represent statistically different groups (alpha=0.05) as identified by a Tukey HSD test.

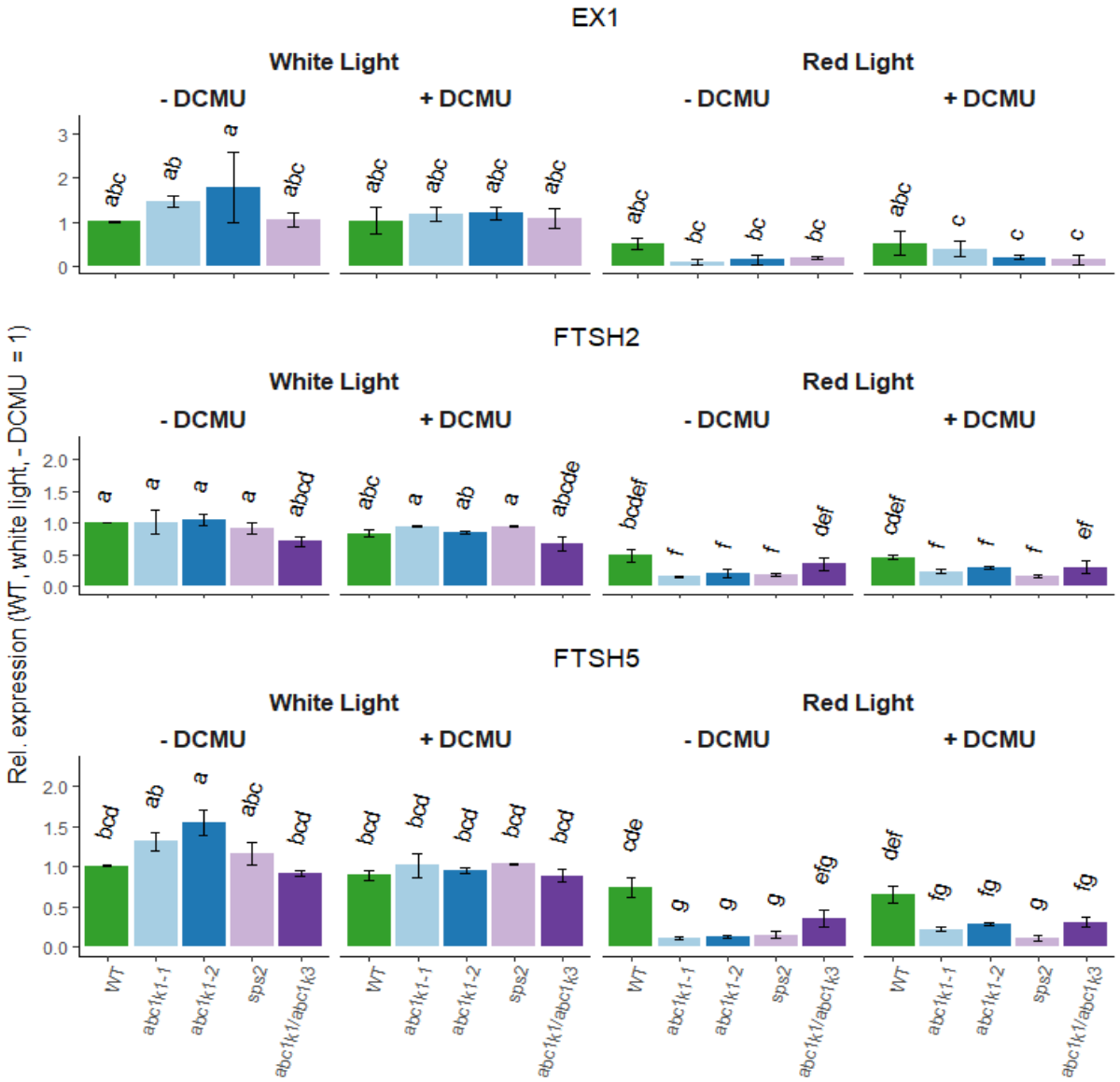

Figure S4: **Gene expression of EX1 and FTSH proteases in various genotypes and light conditions**. Transcript levels of Ex1 (At4g33630), ftsh2 (At2g30950) and ftsh5 (At5g42270) analyzed by quantitative PCR (qRT-PCR) of 5 days old WT, *abc1k1-1, abc1k1-2*, and *sps2* seedlings grown under white light (80 µE) or red light (60 µE) with or without 12.5 nM of DCMU. Error bars indicate the standard error (n= 2). The different letters represent statistically different groups (alpha=0.05) as identified by a Tukey HSD test.

a

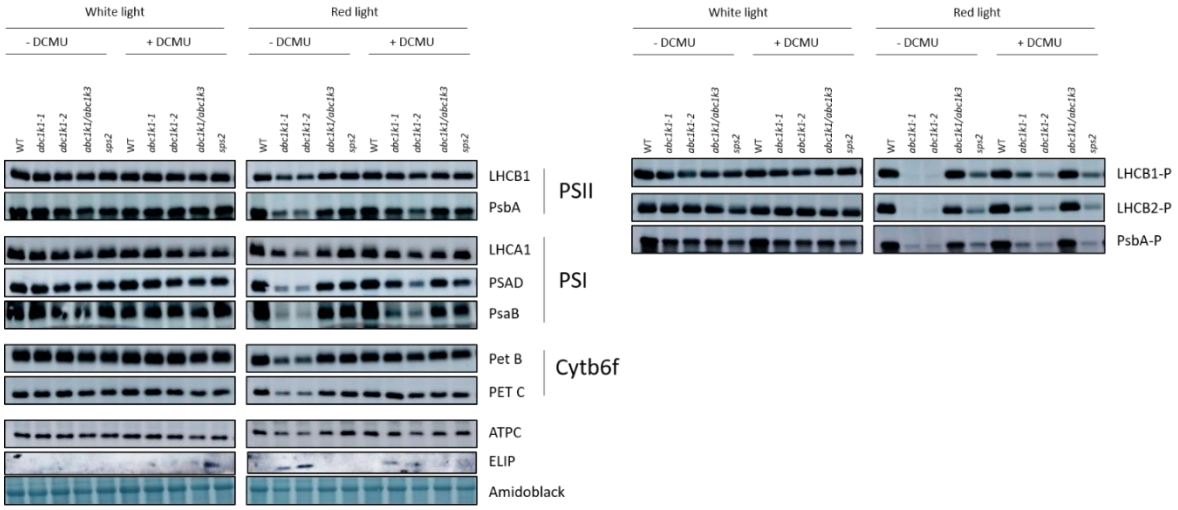

b

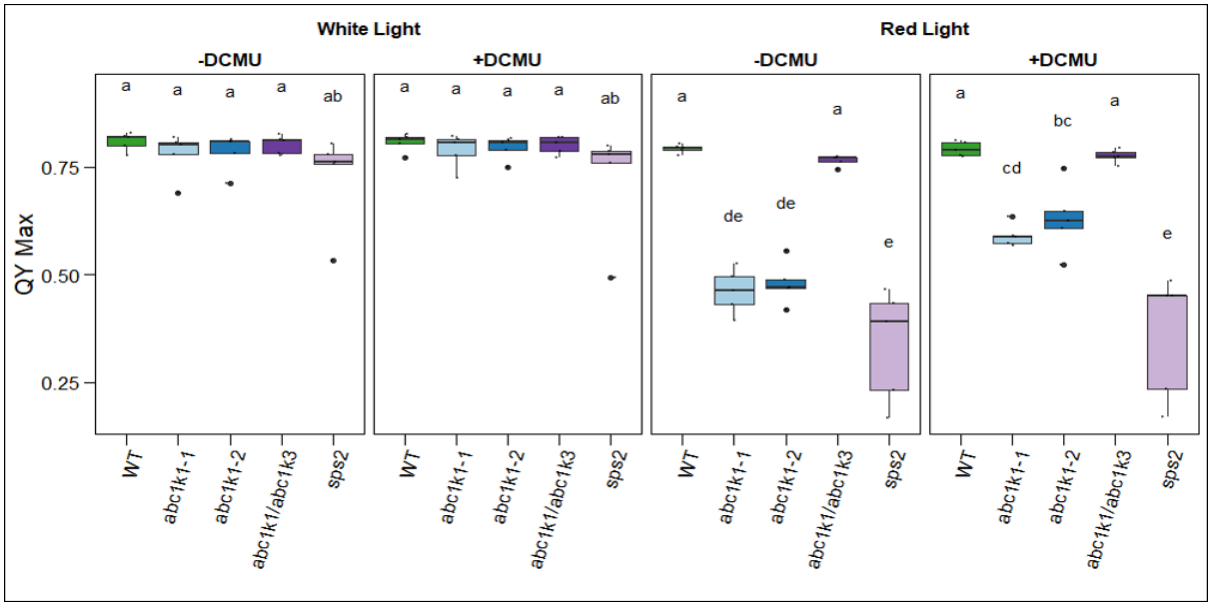

Figure S5: DCMU treatment partially restored the level of photosynthesis-associated proteins and the maximum quantum yield in *abc1k1* under red light.
a) Representative immunoblot image showing the accumulation of photosynthetic proteins representative of the electron transport chain complexes in 5 days old seedling grown under four tested conditions: White light, red light, with and without DCMU. The phosphorylation level of LHCII and PSII was assessed with antibodies recognizing the main phosphorylated peptide of these proteins. Amidoblack staining of the membrane is showed as the loading control. b) PSII maximum quantum yield (QY MAX = FV/FM) measured in 5 days old seedlings, whiskers and box plot shows the minimum, first quartile, median, average, third quartile and maximum of each dataset, outlier measures are plotted as separated points. (n=4).

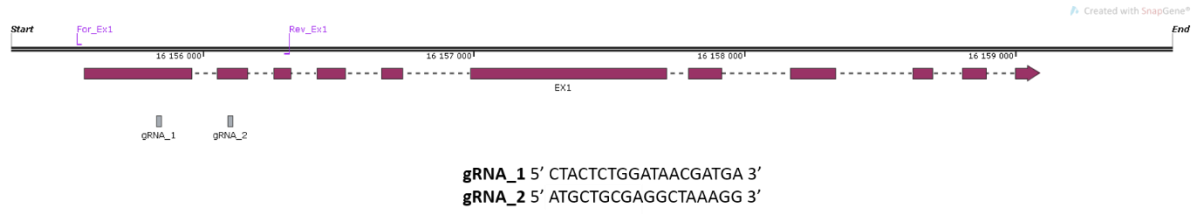

Figure S6: Schematic representation of the *ex1* gene showing the position of the two guide RNAs and primers used for CRISPR/Cas 9 mutation and validation. The sequences of the two gRNAs used for the targeted mutation are reported below the scheme.

a

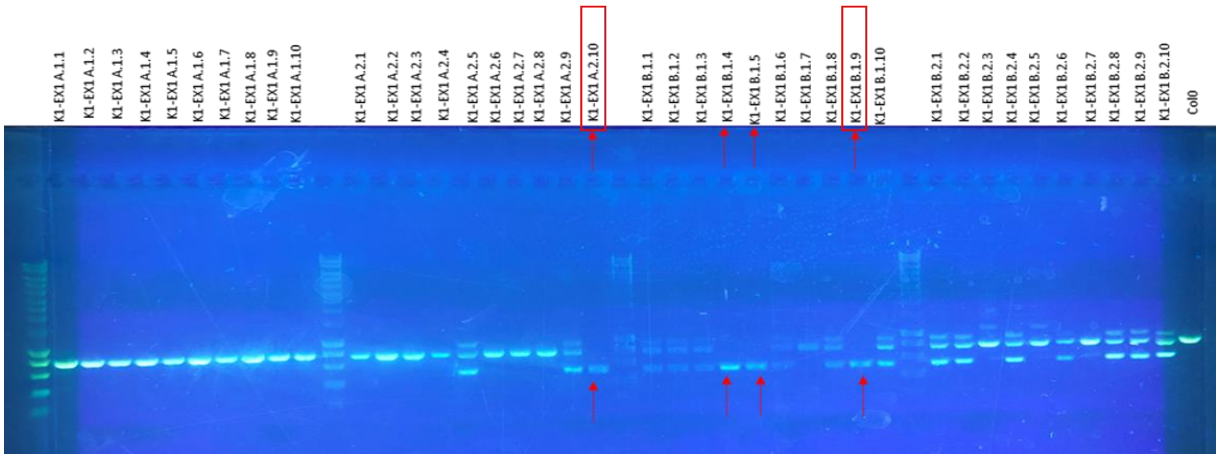

b

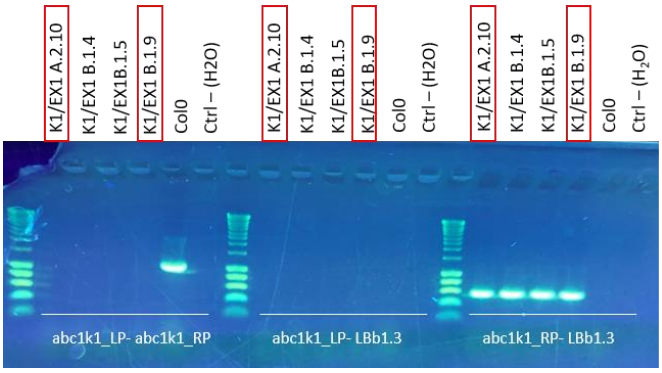

Figure S7: Screening by genomic PCR of the double *abc1k1/ex1* CRISPR/Cas9 mutants. Total genomic DNA was extracted from WT (Col-0) and multiple *abc1k1/ex1* CRISPR/Cas9 lines originated from two transformed plants and tested by PCR a) using primers listed in table S3 and represented in figure S6. The *abc1k1/ex1 A2 10*, *abc1k1/ex1 B1 4*, *5* and *9* (red arrow) show only one band at about 400 bp which confirms the homozygous mutation of the *EX1* gene. b) The presence of the T-DNA insert in the *ABC1K1* gene mutation was confirmed by PCR using primers abc1k1_LP, abc1k1_RP and LBb1.3 listed in table s3. In red squares, *the abc1k1/ex1* lines used for experiments.

Gene name	Primer ID	Nucleotide sequences 5' -> 3'	References
qRT-PCR			
EX1	At4g33630-For	CTACTGCTACTAATGATGCTGTTG	Page et al., 2016
	At4g33630-Rev	GACATCTTCCGAAATACCAGAC	
FTSH2	At2g30950-For	GTGTGTGGAACATTGACTCCAG	
	At2g30950-Rev	GGTGATCTGTTGTAAGTCACC	
FTSH5	At5g42270-For	GCTTACCATGAGGCTGGG	
	At5g42270-Rev	GCAACAGCCATTTGGTTCTC	
ACT2	At3g18780-For	CTTGCACCAAGCAGCATGAA	Yang et al., 2016
	At3g18780-Rev	CCGATCCAGACACTGTACTTCCTT	
Genotyping			
ABC1K1	abc1k1-1_LP	AGCTGATTCATCATCTGTCGG	
	abc1k1-1_RP	TCCCTTCCCACACTAAAAGTG	
EX1	Ex1-For	CCACACGCTCTCACATCTCT	
	Ex1-Rev	ACCAGCTTTGTCTCGCAAGT	
Cloning			
EX1	Ex1g1-BsF	ATATATGGTCTCGATTGCTACTCTGGATAACGATGAGTT	
	Ex1g1-F0	TGCTACTCTGGATAACGATGAGTTTTAGAGCTAGAAATAGC	
	Ex1g2-R0	AACCCTTTAGCCTCGCAGCATCCAATCTCTTAGTCGACTCTAC	
	Ex1g2-BsR	ATTATTGGTCTCGAAACCCTTTAGCCTCGCAGCATCCAA	
pSSU, At5g38430	RBCS1B-For	GGGGACAAGTTTGTACAAAAAAGCAGGCTATGGCTTCCTCTATGCTCTCC	
	RBCS1B-Rev	GGGGACCACTTTGTACAAGAAAGCTGGGTGCTTCTTTCCGATTGGTGGCCA	

Table S2: List of the oligonucleotides used in this report

2.2. Plastoquinone homoeostasis by *Arabidopsis* proton gradient regulation 6 is essential for photosynthetic efficiency

Contributions

My contribution to this paper is the discovery of the variegated phenotype of *abc1k1* under high light. The discovery of the pale-green phenotype of *abc1k1* seedlings under red light exposure by Yang et al in 2016 raised many questions about ABC1K1 function during the early development of *Arabidopsis thaliana*. Until then, the *abc1k1* mutant had been characterized mainly under high light stress and only in adult plants. Consequently, little was known about the impact of the *abc1k1* mutation on chloroplast biogenesis and development in young seedling. In this context, I wanted to test the phenotype of *abc1k1* seedlings, germinated and grown 12 days under high light. I observed that *abc1k1* mutants displayed a variegated phenotype, with green and white leave sectors, which was not the case in the related mutants *abc1k3*, *abc1k1/abc1k3* and *sps2*. This result suggested that ABC1K1 plays a specific role in chloroplast biogenesis under light stress conditions.

COMMUNICATIONS BIOLOGY

ARTICLE

https://doi.org/10.1038/s42003-019-0477-4 OPEN

Plastoquinone homoeostasis by *Arabidopsis* proton gradient regulation 6 is essential for photosynthetic efficiency

Thibaut Pralon[1], Venkatasalam Shanmugabalaji[1], Paolo Longoni[1], Gaetan Glauser[1,2], Brigitte Ksas[3], Joy Collombat[1], Saskia Desmeules[1], Michel Havaux[3], Giovanni Finazzi[4] & Felix Kessler[1]

Photosynthesis produces organic carbon via a light-driven electron flow from H_2O to CO_2 that passes through a pool of plastoquinone molecules. These molecules are either present in the photosynthetic thylakoid membranes, participating in photochemistry (photoactive pool), or stored (non-photoactive pool) in thylakoid-attached lipid droplets, the plastoglobules. The photoactive pool acts also as a signal of photosynthetic activity allowing the adaptation to changes in light condition. Here we show that, in *Arabidopsis thaliana*, proton gradient regulation 6 (PGR6), a predicted atypical kinase located at plastoglobules, is required for plastoquinone homoeostasis, i.e. to maintain the photoactive plastoquinone pool. In a *pgr6* mutant, the photoactive pool is depleted and becomes limiting under high light, affecting short-term acclimation and photosynthetic efficiency. In the long term, *pgr6* seedlings fail to adapt to high light and develop a conditional variegated leaf phenotype. Therefore, PGR6 activity, by regulating plastoquinone homoeostasis, is required to cope with high light.

[1] Faculty of Sciences, Laboratory of Plant Physiology, University of Neuchâtel, 2000 Neuchâtel, Switzerland. [2] Faculty of Sciences, Chemical Analytical Service of the Swiss Plant Science Web, Neuchâtel Platform for Analytical Chemistry (NPAC), University of Neuchâtel, 2000 Neuchâtel, Switzerland. [3] Commissariat à l'Energie Atomique et aux Energies Alternatives (CEA), Cadarache, Centre National de la Recherche Scientifique (CNRS), UMR 7265, Institut de Biosciences et de Biotechnologies d'Aix-Marseille, Laboratoire d'Ecophysiologie Moléculaire des Plantes Aix Marseille Université, 13108 Saint-Paul-lez-Durance, France. [4] Laboratoire de Physiologie Cellulaire et Végétale, UMR 5168, Centre National de la Recherche Scientifique (CNRS), Commissariat à l'Energie Atomique et aux Energies Alternatives (CEA), Institut National de la Recherche Agronomique (INRA), Institut de Biosciences et Biotechnologie de Grenoble (BIG), CEA-Grenoble Université Grenoble Alpes (UGA), 38000 Grenoble, France. Correspondence and requests for materials should be addressed to P.L. (email: paolo.longoni@unine.ch) or to F.K. (email: felix.kessler@unine.ch)

Oxygenic photosynthesis exploits light energy to generate an electron flow from H_2O to NADPH, which is used for the production of organic molecules from CO_2. This process requires the coordinated activity of several membrane embedded complexes: photosystem II (PSII), the cytochrome b_6f and photosystem I (PSI), which are functionally connected by diffusible electron carriers[1,2]. A membrane-soluble prenyl quinone, plastoquinone (PQ), ensures the electron transport between PSII and cytochrome b_6f[1–3]. High light intensities generate stress at the photosynthetic apparatus with PSII being particularly exposed to damage. By transferring electrons to cytochrome b_6f PQ releases the light excitation pressure on PSII and as a consequence, prevents light-induced damage on the photosynthetic apparatus. However, only part of the total PQ participates in electron flow. This portion (the photoactive PQ pool) can be quantified by measuring its reduction by PSII[4,5] or its oxidation by PSI[6] via the cytochrome b_6f complex upon light exposure. The remaining portion of the total PQ is not directly involved in photochemistry. This is defined as the non-photoactive PQ pool since it cannot be reduced by PSII or oxidised by PSI. This second pool of PQ is largely stored in lipid droplets associated with the thylakoid membranes: the plastoglobules[7]. The non-photoactive pool is involved in biosynthetic pathways occurring within the chloroplast (e.g. plastochromanol-8 biosynthesis[8]) and at the same time acts as an indispensable reservoir of PQ to refill the photoactive pool. In fact, when a plant experiences light intensities exceeding its electron transport capacity (high light), the photoactive PQ pool is damaged[9,10]. By replenishing it, the presence of a sufficient non-photoactive PQ pool reservoir ensures photosynthetic efficiency under prolonged stressful light conditions[4,11,12].

The proton gradient regulation (PGR) family comprises mutants displaying a perturbation of photosynthetic electron transport[13], which in turn compromises the formation of a proton gradient across the thylakoid membranes. The proton gradient not only aliments ATP synthesis but also induces non-photochemical quenching (NPQ) of chlorophyll fluorescence upon high light exposure. *PGR6* codes for a predicted atypical **a**ctivity of **b**c1 **c**omplex kinase 1 that is localised inside the chloroplast and associated with plastoglobules[14–16]. The *pgr6* mutant is defective in NPQ and maximal photosynthetic electron transport rate[13,17]. Moreover, loss of PGR6 leads to developmental defects such as impaired cotyledon greening and hypocotyl elongation under pure red light, which were reported to be independent from phytochrome-dependent light signalling pathways[18]. Upon several days of high light exposure, the *pgr6* mutant is characterised by growth and specific metabolic defects, such as low carotenoid accumulation and impaired sugar metabolism, which have been reported for adult plants[17,19].

In this study, we show that the *pgr6* primary defect consists in the misregulation of the homoeostatic relationship between the photoactive PQ pool and the non-photoactive PQ pool. By relating photophysiological measurements to the analysis of photochemically active and non-active PQ pools in wild type, *pgr6* and a mutant of PQ biosynthesis, we conclude that PGR6 is required to maintain the balance between the two pools already during a short (3 h) exposure to high light. This primary *pgr6* phenotype brings on the downstream defects in chloroplast physiology and plant development, which result in leaf variegation in high light exposed seedlings.

Results

Short-term photosynthetic defects in *pgr6*. Phenotypic observation of young seedlings grown under continuous high light (500μmol m^{-2} s^{-1}) revealed that the *pgr6* mutation resulted in a chloroplast developmental issue that became visible as a conditional variegation of young leaves (Fig. 1a). Conversely, the same mutant plants did not show any visible phenotype when grown under continuous low light intensity (80μmol m^{-2} s^{-1}). This variegation is reminiscent of the phenotype previously reported in plants affected in protein turnover[20], reoxidation of PQ[21] or chloroplast to nucleus signalling[22]. Thus, this observation suggests that PGR6 is part of a mechanism essential for chloroplast development under high light.

To pinpoint the *pgr6* primary defect, while limiting the secondary effects that may arise from this initial perturbation[17,19], we grew wild type and mutant plants under moderate light conditions (120μmol m^{-2} s^{-1}, 8 h light/16 h dark) for 5 weeks and then exposed them to a relatively short high light treatment (3 h, 500 μmol m^{-2} s^{-1}). This did not cause lasting damage to the photosynthetic apparatus, as shown by the maximum PSII efficiency ($\Phi_{MAX} = F_V/F_M$), which remained similar in both *pgr6* lines and wild-type plants (Fig. 1b). However, both the PSII quantum yield (Φ_{PSII}) and the NPQ were clearly lower in both *pgr6* mutant lines compared to wild type (Fig. 1c, d). The photosynthetic defects observed in *pgr6* after 3-h high light were not due to alterations in the composition and/or abundance of photosynthetic complexes that were present at comparable levels of representative subunits of PSII (D1 (PsbA) and PsbO), PSI (PsaD and PsaC), light harvesting complex (LHCII) (Lhcb2), cytochrome b_6f (cyt*b6f*) (PetC) and the ATPase (AtpC) (Supplementary Fig. 1).

Loss of PGR6 affects state transition kinases activity. When shifted to high light plants acclimate via changes in the phosphorylation patterns of their photosynthetic protein complexes. High light leads to the inactivation of state transition kinase 7 (STN7) that phosphorylates the PSII antenna and a concomitant increase in the phosphorylation of the PSII core proteins by state transition kinase 8 (STN8)[23]. Since PGR6 is a predicted atypical kinase that may phosphorylate chloroplast proteins[14–17], we investigated whether the observed modifications in the Φ_{PSII} and NPQ parameters reflect a modification in the phosphorylation of the photosynthetic complexes. We analysed the phosphorylation patterns of major thylakoid proteins in wild type, *pgr6-1* and *pgr6-2* by anti-phosphothreonine immunoblotting and discovered that phosphorylation of both LHCII and PSII was clearly lower in both *pgr6* lines after 3-h high light compared to wild type (Fig. 2a), while there was no visible difference under moderate light. We found that the phosphorylation of the two major LHCII subunits (Lhcb1 and Lhcb2), as assessed by phosphorylation-dependent band shift using Phostag™-gels, was severely decreased in *pgr6* upon high light exposure. This result suggests that in *pgr6*, the activity of the STN7 kinase is more severely downregulated compared to wild type (Fig. 2b). Indeed, STN7 is the principal responsible for the phosphorylation of the trimeric LHCII, triggering the migration of mobile LHCII trimers between the two PSs in a process known as state transitions[24]. STN7 activity depends on the reduction of photoactive PQ at cytb_6f,[25–27] and PGR6 is associated with plastoglobules (thylakoid-attached lipid droplets) that are believed to function as PQ reservoir[7,14–16]. We therefore reasoned that the observed changes in the phosphorylation patterns might reflect a perturbation in PQ redox state and/or availability in this mutant rather than a direct effect of PGR6 kinase activity.

We thus investigated the impact of the *pgr6* mutation on state transitions. To follow the antenna movement in vivo, we measured the chlorophyll fluorescence at room temperature in plants while switching from red supplemented with far-red (FAR) light (which triggers LHCII dephosphorylation leading to state 1) to red light only (which enhances phosphorylation in state 2)[28].

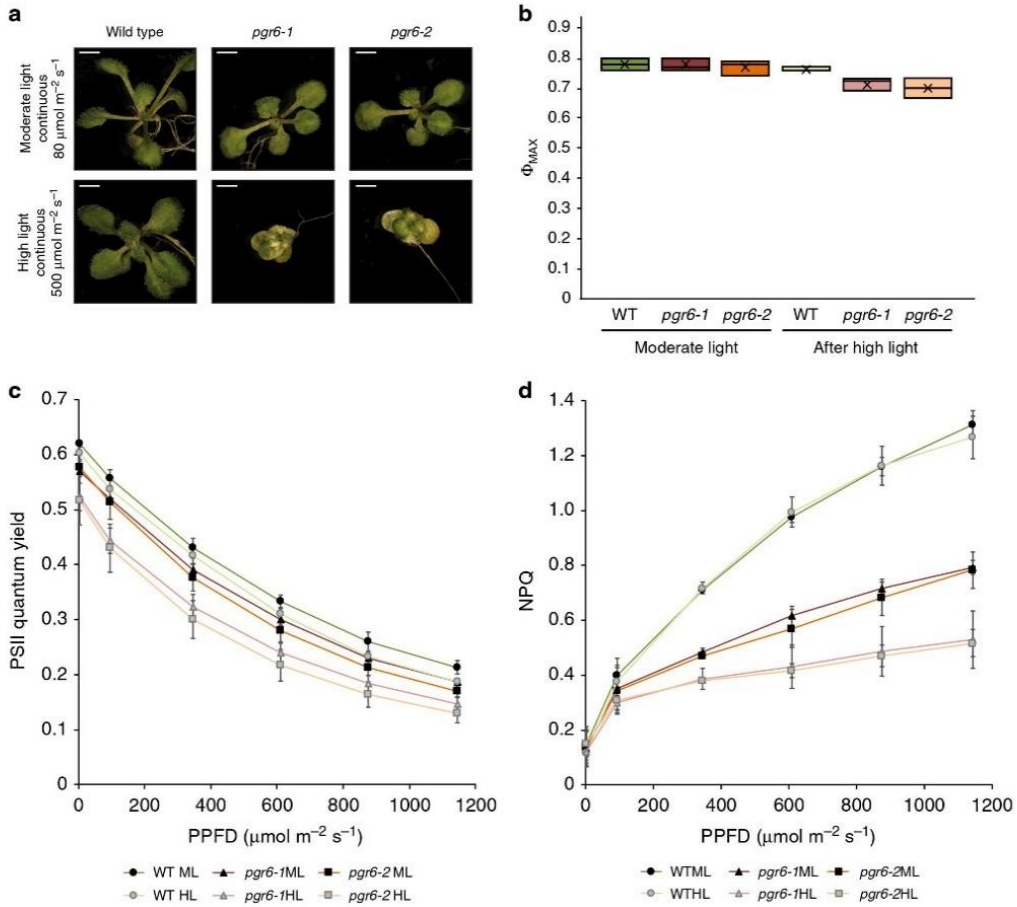

Fig. 1 The *pgr6* mutant has a conditional variegated phenotype and is affected in photosystem II efficiency. **a** Visible phenotype of 14 days seedlings of wild type, *pgr6-1* and *pgr6-2* mutants grown on 0.5 × MS medium under 80µmol m^{-2} s^{-1} and 500µmol m^{-2} s^{-1} in 24 h continuous light; scale bar = 2 mm. Twenty-four-day-old plants grown on soil in short day cycle (8 h light /16 h dark) were used to assess the photosynthetic efficiency of wild type (WT), *pgr6-1* and *pgr6−2* under moderate light (120µmol m^{-2} s^{-1}) (ML, dark colours) and after 3 h of high light (500 µmol m^{-2} s^{-1}) (HL, light colours). After 10 min of dark relaxation, variable room temperature chlorophyll fluorescence was measured on whole plants exposed to these light conditions to determine the following parameters: **b** PSII maximum quantum yield ($\Phi_{MAX} = F_V/F_M$). **c** PSII quantum yield ($\Phi_{PSII} = (F_M'-F_S)/F_M'$) at increasing light intensities, whiskers and box plot shows the minimum, first quartile, median, average, third quartile and maximum of each dataset. **d** Non-photochemical quenching (NPQ = (F_M – F_M')/F_M') after 1 min of exposure at different light intensities. These measures were performed with a Fluorcam (MF800 – PSI) with blue light LEDs (470 nm). Each value represents the average of a pot containing 2–3 plants. Error bars indicate ± SD ($n = 3$ biologically independent samples). Data points for the items **b–d** are available in Supplementary data 1

Decrease in the fluorescence level upon light switch is a proxy for the antenna movement and is absent in the state transition mutant *stn7*[24]. Consistent with the phosphorylation data, we found that both *pgr6* and wild type have the same capacity to undergo the state 1 to state 2 transition, when grown under and exposed only to moderate light (Fig. 2c). However, the transition from state 1 to state 2 was inhibited in *pgr6* but not in wild type after 3-h high light (Fig. 2c, d), supporting the idea that the loss of PGR6 causes a conditional state transition defect, which may be observed only after high light exposure.

It has been reported that the activation of STN7 kinase involves its own phosphorylation[26,27]. Therefore, we analysed the phosphorylation pattern of the STN7 protein using Phostag™ gels, and found that it was less phosphorylated in *pgr6* after high light treatment (Fig. 2e), once again in agreement with a perturbation of state transitions (i.e. STN7 activity). Interestingly, the phosphorylation of the PSII reaction centre proteins (i.e. D1 (PsbA) and D2 (PsbD)), which mostly depends on STN8[24,29], was also affected in *pgr6*. Three-hour high light exposure resulted in a lower phosphorylation level of D1 (PsbA) and D2 (PsbD) in *pgr6* compared to wild type (Fig. 2a and Supplementary Fig. 2). Although the regulation of STN8 has not been fully clarified yet, this observation suggests that the activities of the two state transition kinases are linked and possibly both dependent on the status of the photosynthetic electron transport chain (ETC) or that they have overlapping target proteins[30]. A decrease in PSII phosphorylation may affect the repair cycle of the core protein D1 (PsbA) thereby decreasing the maximum efficiency of PSII[31]. This did not appear to be the underlying cause of the long-term *pgr6* phenotype, as short high light exposure did not cause a measurable decrease in the maximum yield of PSII (Fig. 1b) or increase of the basal level of fluorescence in the dark (F_0). Both parameters are dependent on PSII activity and are affected if there is a defect in its repair cycle[32] (Supplementary Fig. 2).

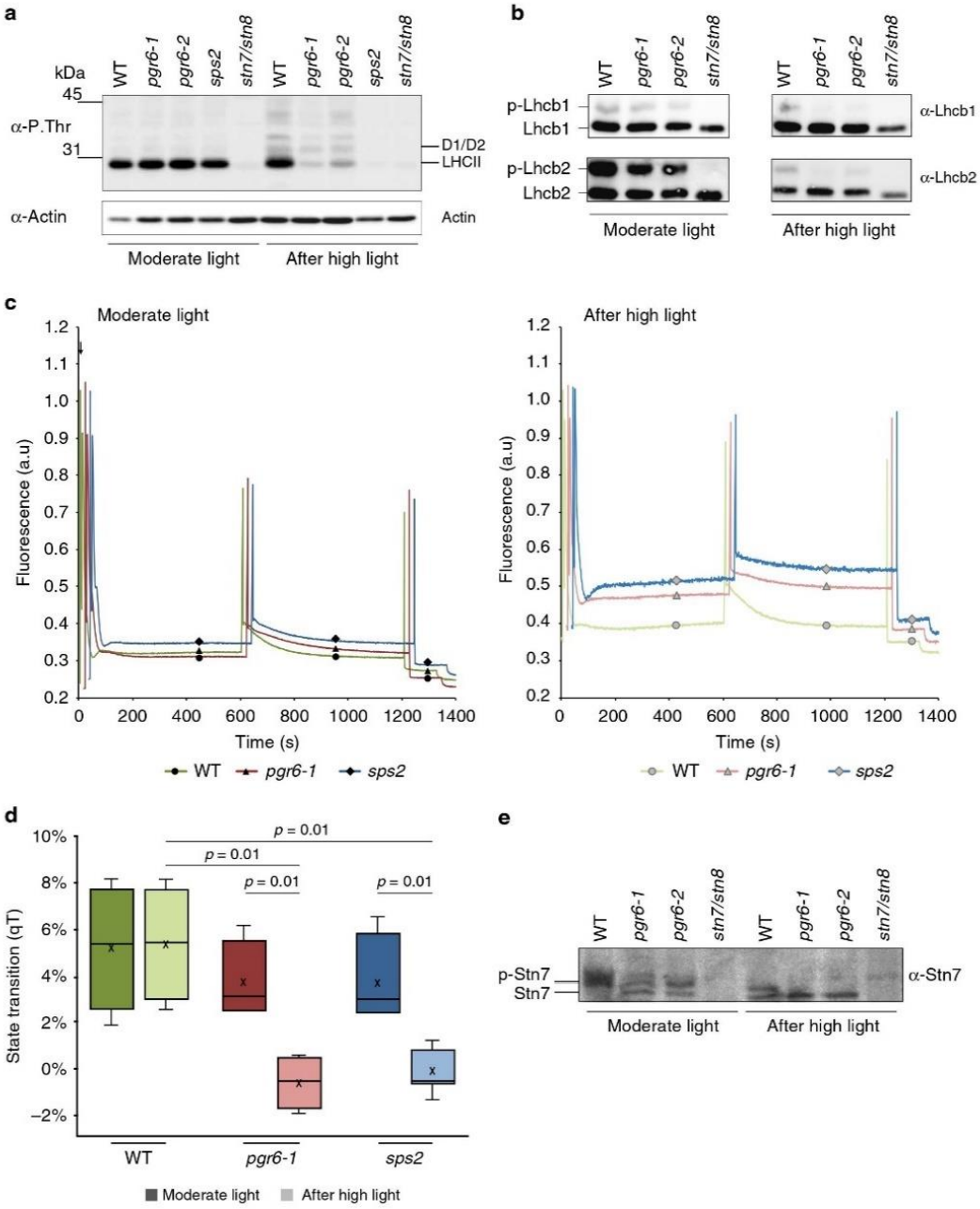

Loss of PGR6 affects the photoactive PQ pool. To address whether the defects in protein phosphorylation and state transitions are linked to a decrease in PQ availability, we compared the photosynthetic behaviour of *pgr6* to that of *sps2* (solanesyl phosphate synthase 2 mutant). In *sps*2, a mutant partially defective in PQ biosynthesis, the total PQ and, as a consequence, the photoactive PQ pools are decreased[4]. In particular, the shortage of photoactive PQ should diminish the electron capacity of the ETC affecting the photosynthetic efficiency. This would result in lower electron transport rate, and therefore a reduced quantum yield of the PSII (Φ_{PSII}) and NPQ induction[4] (Supplementary Fig. 3). Since *sps2* by its nature is PQ-limited, it can be used as a term of comparison to pinpoint a *pgr6* defect due to PQ availability. The first observation was that in *sps2*, as in *pgr6*, the thylakoid proteins are strongly dephosphorylated after 3-h high light (Fig. 2a). This result supports the hypothesis linking the downregulation of the STN7 and STN8 activity and perturbation of PQ availability. To directly assess the capacity of the ETC, we measured chlorophyll *a* fluorescence induction kinetics and calculated the electron transport capacity from the normalised area above the fluorescence traces[33] (Fig. 3a). The rationale for this choice is that the area above the fluorescence kinetics is a proxy of the average number of turnovers of each PSII reaction centre, i.e. of the number of electrons that this photosystem is able to inject

Fig. 2 Thylakoid protein phosphorylation and state transitions are disturbed after high light treatment in *pgr6* background. **a** Total protein extracts of 4-week-old wild type (WT), *pgr6-1*, *pgr6−2*, *sps2* and *stn7/stn8* analysed by immunoblotting with anti-phosphothreonine antibody; the principal thylakoid phospho proteins are indicated on the right according to their size. Core photosystem II proteins D1 (PsbA) and D2 (PsbD) are indicated as a single band due to their poor resolution. Actin was used as a loading control. **b** Lhcb1 and Lhcb2 phosphorylation levels were visualised after separation on Phostag™-pendant acrylamide gels. The upper band corresponds to the phosphorylated form (p-), *stn7/stn8* double mutant is a non-phosphorylated control. **c** Average transient of the variable room temperature chlorophyll fluorescence measured during the transition from red (660nm) supplemented with far-red light (720nm) state 1 to pure red light state 2 ($n = 4$ independent pots containing 2–3 plants). The fluorescence curves from *pgr6* and *sps2* are shifted on the *x*-axis to allow visualising the F_MST1 and F_MST2 values. The *x*-axis time scale refers to the wild-type curve. **d** Calculated quenching related to state transition ($qT = (F_MST1 - F_MST2)/F_M$), expressed as the percentage of F_M that is dissipated by the state 1 to state 2 transition, of wild type (WT), *pgr6−1* and *sps2* under moderate light (120µmol m^{-2} s^{-1}) (ML) and after 3 h of high light (500µmol m^{-2} s^{-1}) (HL). Whiskers and box plot shows the minimum, first quartile, median, average, third quartile and maximum of each dataset ($n = 4$ biologically independent samples); *p*-values are calculated via a two-tailed Student's *t* test. **e** STN7 phosphorylation level visualised after separation on Phostag™-pendant acrylamide gels. The upper band corresponds to the phosphorylated form (p-), a protein sample from *stn7/stn8* double mutant was loaded as a control for the antibody specificity. Uncropped images of the membranes displayed in **a**, **b** and **e** are available as Supplementary Fig. 11. Data points for items **c**, **d** are available as Supplementary data 2

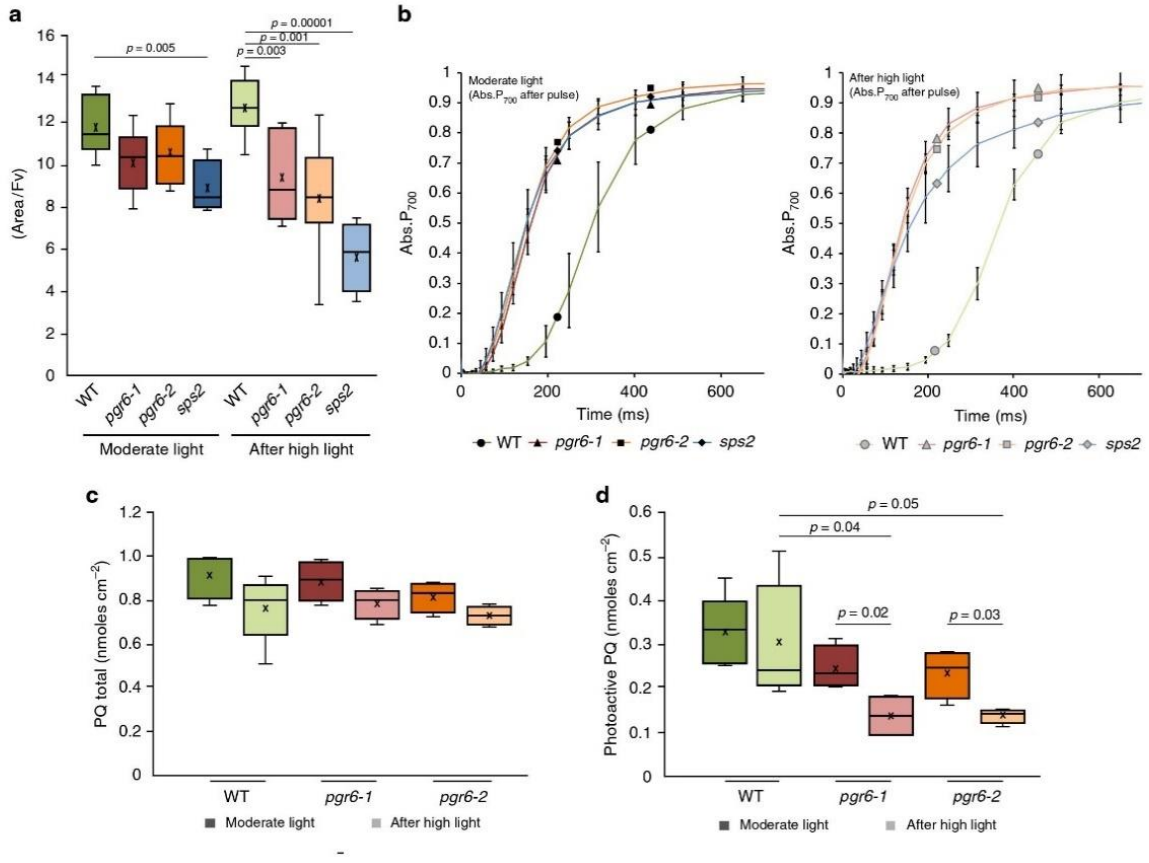

Fig. 3 The *pgr6* mutant shows a limitation in photosynthetic electron carriers. Wild type (WT), *pgr6-1*, *pgr6−2* and *sps2* plants were grown under moderate light intensity and sampled under growth light conditions (moderate light) or after the exposure to 3 h at 500µmol m^{-2} s^{-1} (after high light). **a** Normalised area above the rapid fluorescence induction curve measured after 15 min of incubation in dark. This value estimates the number of available electron carriers per reaction centre (area/Fv). Error bars indicate ± SD ($n = 8$ for wild type, *pgr6−2*, $n = 6$ for *pgr6−1*, $n = 4$ for *sps2* biologically independent samples). **b** Analysis of P_{700} re-oxidation kinetics induced by far-red light after a saturating light pulse (Time 0 = far-red ON). The oxidation status was measured by the increase in absorption at 810 nm on fully expanded leaves of each genotype. Error bars indicate ± SD ($n = 9$ biologically independent samples). **c** Leaf discs from wild type (WT), *pgr6-1* and *pgr6-2* plants were collected under moderate light (120µmol m^{-2} s^{-1}) and after 3 h of high light (500µmol m^{-2} s^{-1}), the average total plastoquinone (oxidised + reduced PQ) content was measured in nmoles cm^{-2}. **d** The oxidised and reduced PQ amount was measured in leaf discs exposed either to 2min far-red light (5.5µmol m^{-2} s^{-1}) to fully oxidise the photoactive PQ pool or to 15 s saturating flash (2000µmol m^{-2} s^{-1}) to fully reduce the photoactive PQ. The total photoactive PQ pool was calculated from the difference between these two conditions. Average values are reported as PQ nmoles cm^{-2}. Whiskers and box plot shows the minimum, first quartile, median, average, third quartile and maximum of each dataset ($n = 4$ biologically independent samples); *p*-values are calculated via a two-tailed Student's *t* test. Data points for item **a** are available as Supplementary data 3; data points for item **b** are available as Supplementary data 4; data points for items **c**, **d** are available as Supplementary data 6

Table 1 The electron transport capacity per photosystem I is limited in *pgr6*

Moderate light

	Wild type	*pgr6-1*	*pgr6−2*	*sps2*
Lag time after far red (ms)	8.78 ± 0.79	9.89 ± 1.06	8.57 ± 1.15	7.32 ± 1.06
Lag time after pulse (ms)	165.88 ± 2.93[a]	**74.34 ± 5.93[b]**	**69.38 ± 5.81[b]**	**64.54 ± 5.92[b]**
Calculated pulse e^- number	19.35 ± 1.95[f]	**7.53 ± 0.41[g]**	**8.16 ± 0.68[g]**	**9.19 ± 2.23[g]**

After high light

	Wild type	*pgr6-1*	*pgr6-2*	*sps2*
Lag time after far red (ms)	17.14 ± 4.37	15.68 ± 2.94	15.01 ± 2.69	17.67 ± 0.98
Lag time after pulse (ms)	213.03 ± 12.68[c]	**54.04 ± 13.72[d]**	**47.36 ± 14.05[d,e]**	**14.75 ± 3.27[e]**
Calculated pulse e^- number	13.21 ± 2.33[h]	**3.69 ± 1.51[i]**	**3.30 ± 1.31[i]**	**0.83 ± 0.16[i]**

Electron (e^-) capacity of the electron transport chain per photosystem I calculated from the P_{700} oxidation lag time after a saturation pulse normalised over the lag time of the oxidation after dark. Values statistically different from the wild type for each condition are in bold. Superscript letters are used to indicate statistically different groups by Student's *t* test ($p < 0.05$) ($n = 4$ for wild type, *pgr6-1* and $n = 3$ for *pgr6−2*, *sps2* biologically independent samples). Data points are available in Supplementary data 4

into the ETC. It thus provides quantitative data on all the ETC electron acceptors, including the PSII internal electron acceptors (Q_A and Pheophytin), the plastocyanin downstream of the cytochrome b_6f complex and the PQ connected to PSII (the photochemically active pool). Using this approach, we found that the ETC electron capacity is not different between *pgr6* and wild type when plants were grown under moderate light. This suggests that the photoactive PQ pool has the same electron capacity in *pgr6* and wild type at least under moderate light. On the other hand, we detected a smaller electron capacity in *sps2* mutant, consistent with a constitutive lack of PQ in this line. Upon 3 h of high light exposure, both *pgr6* and *sps2* mutants showed a diminished electron transport capacity (Fig. 3a). This finding suggests that increasing light intensity diminishes the photoactive PQ pool in *pgr6*, thus the phenotype was similar to *sps2* from a functional point of view. To substantiate the hypothesis that the changes in the ETC observed after 3 h of high light are linked to the lack of photoactive PQ, we quantified changes in the electron fluxes in the different genotypes using a previously established kinetic model based on fluorescence induction kinetics (the JIP test)[33,34]. We found that the maximum quantum yield of primary photochemistry in PSII (ΦPo) did not vary between wild type and *pgr6* under moderate light (Supplementary Fig. 4), consistent with the previous measurements (Fig. 1b). However, the quantum yield of the electron transport flux after Q_A (ΦET2o) and the yield of electron transport to PSI electron acceptors (ΦRE1o) were already lower in *pgr6* mutants compared to wild type. After 3 h of high light exposure, the maximum yield was again not affected by the *pgr6* mutation, however both parameters related to the transport from PSII to PSI (ΦET2o and ΦRE1o) were even further decreased in the two *pgr6* mutant lines (ΦET2o: 0.28 ± 0.04; 0.28 ± 0.07) (ΦRE1o: 0.08 ± 0.02; 0.07 ± 0.03) compared to wild type (ΦET2o: 0.38 ± 0.03; ΦRE1o: 0.13 ± 0.02). Similarly, the PQ-limited *sps2* plants showed lower electron transport efficiency (lower ΦET2o and ΦRE1o) under both light conditions (Supplementary Fig. 4). This analysis points to a constitutive lower capacity of the mutants to perform electron transport from PSII to PSI, which is consistent with a perturbation of the photoactive PQ pool in *pgr6*. However, this defect becomes symptomatic only upon exposure to high light. A direct measurement in *pgr6* of the fraction of the PSII reaction centres incapable of transferring electrons to the ETC (closed) by variable room temperature fluorescence upon exposure to increasing light intensities[35] also supports this hypothesis. In fact, the steady-state fluorescence was higher in the mutant confirming that the PSII reaction centres were systematically more closed in *pgr6* than in the wild type (Supplementary Fig. 5). Closure of PSII reaction centres is the expected consequence of a limitation of the electron transfer to the photoactive PQ pool[35]. It is worth noting that said effect is already measurable in plants not exposed to high light, suggesting that the electron transport efficiency is constitutively defective in *pgr6*.

A limitation in the size of the photoactive PQ pool should also have a downstream effect on PSI, by decreasing the number of electrons available to reduce its primary electron donor (P_{700}) upon light-driven oxidation. This hypothesis can be tested by comparing the lag time of P_{700}^+ oxidation in conditions under which the ETC is completely oxidised (devoid of transportable electrons so that only the one electron present inside the PSI will account for the delay) or fully reduced by a saturating flash. The ratio between these two values provides the number of electrons contained in the whole ETC per PSI[6]. We measured these parameters using time resolved redox spectroscopy to quantify the *pgr6*-induced defect[6]. Wild-type plants, acclimated to moderate light, had a maximum of 19 ± 2 electrons per PSI, which is a number consistent with previous reports estimating the number of electron carriers[36], whereas in both *pgr6* lines background there were only 8 ± 1 electrons per PSI. After 3 h of high light exposure, the ETC of the wild-type plant contained 13 ± 2 electrons per PSI, while only 4 ± 1 and 3 ± 1 were present in *pgr6-1* and *pgr6-2*, respectively (Fig. 3b and Table 1). These results demonstrate that the ETC capacity is limited in *pgr6* and that this defect is accentuated by the high light treatment. Interestingly, the same effect was observed in the *sps2* background (Table 1).

In summary, the spectroscopic data for both *pgr6* and *sps2* are consistent with a scenario in which the limitation of photoactive PQ results in diminished electron transport. Importantly, also, the cytochrome b_6f turnover rate[37] was affected in neither *pgr6* nor in *sps2*, featuring wild-type kinetics after exposure to 3 h of high light (Supplementary Fig. 6). This indicates that the very high affinity of this complex for PQ in vivo ensures maximum turnover even under conditions when the PQ pool is lowered[38].

To biochemically determine the size of the photoactive PQ pool, the amounts of reduced and oxidised PQ were measured by HPLC in leaves in which the photoactive PQ was either fully oxidised by 2min of FAR light or fully reduced by saturating white light[4,5,11,12]. Total PQ in *pgr6* was indistinguishable from the wild type (Fig. 3c), and the photoactive PQ was 0.33 ± 0.08 nmoles cm^{-2} in wild type and 0.24 ± 0.05 and 0.23 ± 0.06 nmoles cm^{-2} in *pgr6-1* and *pgr6-2*, respectively, under moderate light (Fig. 3d). However, after 3-h high light, the photoactive PQ in *pgr6* mutants decreased significantly (Student *t* test, $p = 0.05$) to 0.14 ± 0.05 nmoles cm^{-2} and 0.14 ±

0.02 nmoles cm^{-2}, while the wild-type photoactive PQ pool remained stable around 0.30 ± 0.13 nmoles cm^{-2} (Fig. 3d). Furthermore, no major difference was observed in the levels of the hydroxyl-PQ, a molecule that accumulates when PQ is depleted by oxidative stress, between wild type, *pgr6* and *sps2*[12] (Supplementary Fig. 7). These results demonstrate that high light treatment depletes photoactive PQ in *pgr6*. Since total PQ was not measurably different under either moderate or high light conditions, no accumulation of the oxidation product hydroxyl-PQ had occurred and the photoactive pool was smaller, we expected the non-photoactive PQ pool in the plastoglobules to be increased. Consistently, higher levels of PQ were present in the plastoglobules isolated from *pgr6* and this difference was accentuated after 3-h high light (Supplementary Fig. 8).

Discussion

Knockout mutants of *PGR6* are characterised by conditional defects in growth and development, including the pale cotyledon phenotype previously reported under constant red light[18] and the variegated phenotype under high light reported here (Fig. 1a). So far, no molecular explanation for the observed defects was provided besides proposing that either the lower photosynthetic efficiency[17] or the misregulation of the prenyl-lipid metabolism[19] in *pgr6* are the cause of the biochemical phenotype upon prolonged high light. In this work, we analysed plants grown under moderate non-phenotype-inducing light and assessed their photosynthetic traits after a limited exposure to high light. We observed that 3 h of high light were sufficient to trigger a clear photosynthetic defect in *pgr6*, suggesting that the underlying cause was either already present before the treatment or could be attributed to the lack of fast adaptive responses. Photosynthetic complexes were affected neither in amount nor in activity, suggesting that the defect is not a direct consequence of protein perturbation (Supplementary Figs. 1 and 6).

A first level of response to photosynthetic imbalance is through the phosphorylation network of the thylakoid proteins controlled, mostly, by the kinases STN7 and STN8 and their counteracting phosphatases[23,30]. Due to the STN7- and STN8-dependent phosphorylation, the photosynthetic apparatus is capable to cope with rapid changes in the environmental conditions by maintaining an optimal photosynthetic efficiency (e.g. state transitions) and cope with damages to the photosystems (e.g. regulation of D1 repair cycle)[39,40]. In high light, the overall thylakoid protein phosphorylation was decreased in *pgr6* compared to the wild type. Lower activity of the STN7 kinase is expected in plants shifted to high light, however, the analysis of the phosphorylation pattern indicated lower activities of both STN7 and STN8 kinases in *pgr6* (Fig. 2). The activity of both STN kinases is linked to the redox status of the PQ pool. Therefore, this defect can potentially be explained by an influence of PGR6 on PQ. Although we cannot fully exclude that PGR6 is a direct regulator of the STN kinases, this scenario seems a rather unlikely explanation for the photosynthetic defects observed in *pgr6*. Indeed, even the double knockout mutant of the STN kinases (*stn7/stn8*), which has an even lower level of phosphorylation of the target proteins than *pgr6*, does not display a defect in electron transport comparable to that of *pgr6* (Supplementary Fig. 2). Furthermore, *sps2*, which is genetically deprived of PQ, displays a phosphorylation defect similar to *pgr6* (Fig. 2).

The evidence so far points toward PQ as a key molecule regulated by PGR6 activity. Biochemical and biophysical analyses were performed to assess whether there is a limitation of the photoactive PQ pool in *pgr6* (Fig. 3). The comparison between wild type, *pgr6* and *sps2* offers a suitable experimental system to test this model. Indeed, when the photoactive PQ pool is genetically limited, as in *sps2*, the PSII input will be in excess over the electron capacity of the PQ pool at lower light intensity than in wild type (Supplementary Fig. 3). As a result, the fraction of closed PSII, unable to donate electrons to the photoactive PQ, will increase and thus limit the photosynthetic efficiency compared to wild type.

These data show that here the role of PGR6 is to maintain the size of the photoactive PQ pool, i.e. the PQ available for the photosynthetic ETC. The lack of PGR6 does not result in a visible phenotype under moderate light indicating that its activity is not essential under this light condition[13]. This can be rationalised assuming that the loss of photoactive PQ depends on the electron flux from the PSII. The electron flow is the result of the photon input (i.e. light intensity) minus the portion of absorbed photons dissipated as heat (NPQ)[41]. It is only during high light that the photoactive PQ pool will receive electrons in excess of the electron flow capacity and therefore an efficient supply of PQ from a reservoir (non-photoactive PQ pool) is required for its homoeostasis[12]. In this model, the role of PGR6 is to ensure a rapid refill of the photoactive PQ pool, which is essential in high electron fluencies (high light) (Fig. 4). Consequently, in a *pgr6* mutant upon high light exposure, the photoactive PQ pool will be depleted limiting the amount of the electron carriers available for photosynthesis. Hydroxylation of the photoactive PQ may be the cause of said depletion, which becomes phenotypic when combined with an inefficient supply of newly synthesised PQ from storage compartments to the photoactive pool[12]. However, no detectable difference in the level of accumulation of the hydroxyl-PQ has been observed between *pgr6* and the wild type (Supplementary Fig. 7). Although the most likely storage compartments capable of efficiently and quickly refilling the photoactive PQ are the plastoglobules, the contribution of the envelope-located PQ cannot be excluded.

The depletion of the photoactive PQ pool observed in *pgr6* upon exposure to 3-h high light may account for the reported electron transport limitation and resembles that of *sps2*. The observation that total PQ is not affected and there is no accumulation of hydroxyl-PQ in *pgr6* after 3 h of high light supports the model in which the cause for photoactive PQ pool depletion is the lack of an efficient refill from the PQ reservoir[12]. The lower refill ratio can be explained by a lower mobility of PQ in *pgr6*. PQ mobility constraints would also explain the measurable increase in the fraction of closed PSII reaction centres (1-qP) and NPQ observed in *pgr6* plants grown under moderate light, where the photoactive PQ pool size is unaffected (Figs. 1, 3 and Supplementary Fig. 5) and the lower yield of electron transport from PSII to PQ (ΦET2o) (Supplementary Fig. 4). Additional evidence comes from measuring the electron transport as the output of the ETC at the level of P_{700} (PSI) oxidation. The output defect of *pgr6* and *sps2* appears to be much larger than the lack of photoactive PQ measured biochemically. This is exceedingly evident in the *sps2* mutant, where the depletion of PQ caused by high light resulted in a drop of the measured electron transport to less than 1 electron, suggesting that the ETC is almost completely blocked (Table 1). However, there is still a measurable amount of available electron acceptors for PSII and therefore of available PQ molecules (Fig. 3a). The observation is consistent with previous studies on the *sps2* mutant[4] and becomes highly relevant in the context of the defect in *pgr6*: the photoactive PQ pool appears only slightly diminished (Fig. 3d), but electron transport is disproportionately affected (Figs. 1c and 3a, b). This is consistent with the previous model, showing that a lower concentration of PQ in the photoactive pool cannot efficiently overcome the diffusion barriers affecting its access to the photosynthetic complexes[42]. Furthermore, by limiting its own mobility in the thylakoid membranes[42], the exchange with the non-photoactive PQ pool will be impaired. Therefore, a combination of adequate photoactive PQ pool size,

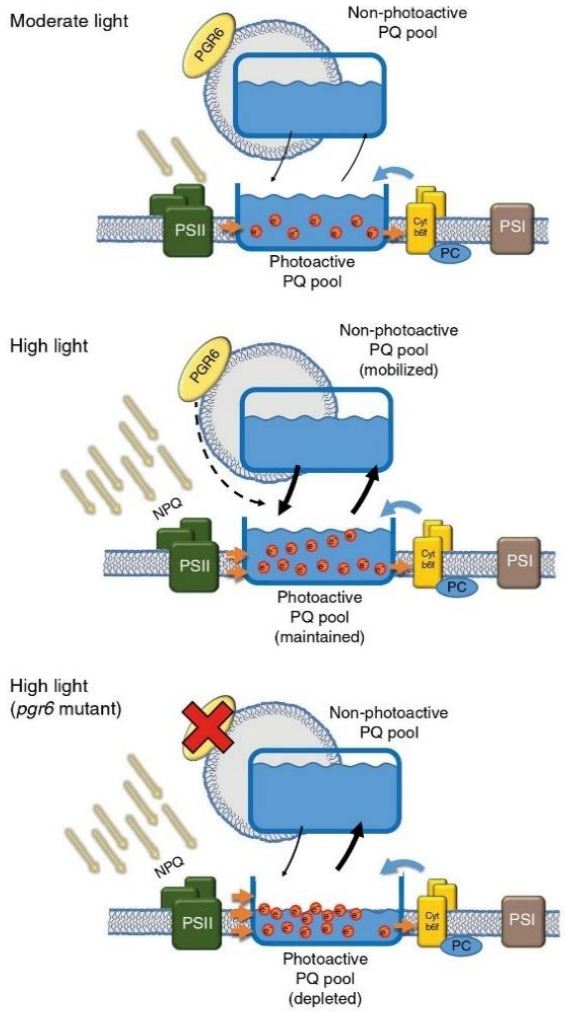

Fig. 4 Schematic representation of the regulation mediated by PGR6. Under moderate light intensity, the electron input from the PSII is compensated by the activity of cytochrome b_6f complex. Under this condition, the action of the two complexes is in equilibrium and maintains the photoactive PQ pool in balance thus allowing a continuous electron transport. When the light exceeds the electron transport capacity (high light), the electron input from the PSII is higher than the output from the cytochrome b_6f, this effect is partially mitigated by the thermal dissipation of light excess (NPQ). Under high light, the maintenance of the photoactive PQ depends as well on the mobilisation of the reservoir, i.e. the PQ stored in the non-photoactive pool. This mobilisation is possible thanks to the activity of PGR6, which regulates this redistribution thus allowing the preservation of the photoactive PQ pool under high light. In the absence of PGR6, the input from the non-photoactive pool is limited and therefore insufficient to replenish the photoactive PQ pool, furthermore, the lower NPQ induction causes an even stronger overreduction of the PQ pool, which further increases the loss of the photoactive PQ. These combined defects result in a reduction of growth and in developmental issues observed in *pgr6* mutant plants. Orange dots represent the electrons contained inside the pool, orange arrows represent the movement of the reduced PQ and blue arrows represent the movement of the oxidised form, while black arrows represent the rate of exchange between the photoactive and the non-photoactive PQ pools

PQ mobility and refill rate are required to ensure PQ homoeostasis and photosynthetic efficiency. Perturbation of the electron flow through the photoactive PQ, which is also the molecular vector for proton transfer across the thylakoid membrane, will limit the trans-thylakoid proton gradient needed to activate the thermal dissipation of excess absorbed light (NPQ)[43]. With a lower NPQ, the ETC will become even more overreduced since the electron input from PSII cannot be adequately controlled. This creates a negative loop that will further exacerbate the electron transport defect. The finding that both *pgr6* and *sps2* share common defects at the level of electron transport and NPQ (Fig. 1 and Supplementary Fig. 3) is also in accordance with this model. In the long term (i.e. several days of high light), these combined defects increase the high light dependent degradation of PQ[12] and will result in the depletion of the total PQ that was previously reported in *sps2*[11,12] and *pgr6*[17].

A defect in PQ mobility and availability may also explain the previously reported defect in carotenoid accumulation in *pgr6*[17,19]: Oxidised PQ functions as a sink for the electrons removed during the desaturase reactions of carotenoid biosynthesis; a limitation in the access, mobility and/or concentration of PQ may hamper this process and would lead to a lower level of carotenoid production. The consequence of this scenario would be similar to the one of *immutans* that lacks the terminal PQ oxidase[21]. Interestingly, this mutant is also characterised by a variegated light-dependent phenotype similar to the one observed in *pgr6* exposed to high light. Finally, alteration of the size (and accessibility) of the photoactive PQ pool would explain long-term effects of *pgr6* on chloroplast to nucleus communication, thus providing a rationale for the pale cotyledon phenotype reported when grown under constant red light[44].

In conclusion, our results indicate that in order to maintain photoactive PQ as well as photosynthetic efficiency while preventing long-term photodamage[17,19] under high light, plants have evolved a PQ homoeostasis mechanism controlled by the PGR6 kinase (Fig. 4). The observed depletion of photoactive PQ in *pgr6* after 3-h high light explains the diminished STN7 activity on LHCII together with the measured effects on state transitions. Also, the proton gradient regulation phenotype considering that the lack of photoactive PQ will generate a smaller trans-thylakoid proton gradient, which is needed to activate the NPQ mechanism[43], and the lack of this protective mechanism results in increased chlorophyll fluorescence, which is the signature phenotype of all *pgr* mutants[13]. Considering its subcellular localisation on plastoglobules, it is tempting to hypothesise that the role of PGR6 is to control the release of PQ from plastoglobules supplying the ETC in the thylakoid membrane[12]. In support of this model, there was a measurable increase in PQ concentration in *pgr6* plastoglobules compared to wild type suggesting PQ trapping in the non-photoactive pool (Supplementary Fig. 8).

Methods

Plants material and treatments. *Arabidopsis thaliana* wild-type plant refers to var. Columbia-0 (Col-0). *pgr6-1* T-DNA insertion line (SALK_068628) and *pgr6-2* T-DNA insertion line (SALK_130499C) were purchased at Nottingham Arabidopsis Stock Centre (NASC, http://arabidopsis.info). *stn7*/*stn8* and *sps2* were gifts from Prof. Goldschmidt-Clermont and from Prof. Basset, respectively.

Seedlings were grown for 14 days in 0.5× MS plates under continuous light condition (80µmol m^{-2} s^{-1} for control and 500µmol m^{-2} s^{-1} for the high light). Plants were grown on soil with solbac (Andermatt) under moderate light conditions (120µmol m^{-2} s^{-1}, 20–22 °C and 8 h light/16 h dark) in a controlled environment room. For high light treatment, 4–5-week-old plants were exposed to 500µmol m^{-2} s^{-1}, 20–22 °C, for 3 h.

Samples were collected under light, directly frozen in liquid nitrogen and stored at −20 °C.

Photosynthetic parameters. Maximum quantum yield of PSII (Φ_{MAX}), quantum yield of PSII (Φ_{PSII}) and NPQ were determined using Fluorcam (Photon System Instrument, Czech Republic, http://www.psi.cz) with blue light LED (470nm). Plants were dark adapted for 10min before measurements. $\Phi_{MAX} = (F_V/F_M)$; $\Phi_{PSII} = (F_M'-F_S)/F_M'$; and $NPQ = (F_M-F_M')/F_M'$; where F_M is maximum fluorescence; F_0 is minimum fluorescence; F_V is the variable fluorescence (F_M-F_0) in dark-adapted state; F_M' is maximum fluorescence; and F_S is steady-state chlorophyll fluorescence in the light[35]. The employed PPFD, (photosynthetic photon flux density), measured by LI-189 photometer (LI-COR), are 2.5–95–347–610–876–1145μmol m^{-2} s^{-1}. State transitions were measured with the same instrument. After measurement of the F_0 and F_M, plants were exposed to 10min red light (50μmol m^{-2} s^{-1} 660nm peak measured as PPFD) supplemented with far red (17μmol m^{-2} s^{-1} calculated from the 733nm peak area considering values between 500 and 800nm). At the end of this phase, the F_M' (F_MST1) was measured, and then the FAR light were turned off. The transition from state 1 to state 2 was followed during 10min, then again the F_M' (F_MST2) was measured. Quenching related to state transition (qT) was calculated as $qT = (F_M ST1 - F_M ST2)/F_M$.

Chlorophyll a fluorescence curve kinetics (OJIP, JIP test). Fast chlorophyll, *a* fluorescence induction (OJIP, JIP-test) kinetics, were measured at room temperature using a plant efficiency analyser (Handy-PEA; Hansatech Ltd., King's Lynn, Norfolk, England), following manufacturer instructions. Plants were dark adapted for 10min before measurements. Measured data were extracted with the WinPEA software (Hansatech) and analysed with JIP-test according to Strasser et al. (2010)[33] and Kalaji et al. (2014)[34]. In detail, ΦPo (maximum quantum yield of primary PSII photochemistry) was calculated as $1- F_0/F_M$. ΦET2o (quantum yield of the electron transport from Q_A to Q_B) as $((F_M-F_0)/F_M)$ $(1-(F_{2ms}-F_0)/(F_M-F_0))$. ΦRE1o (quantum yield of the electron transport until the PSI electron acceptors) as $((F_M-F_0)/F_M)$ $(1-(F_{30ms}-F_0)/(F_M-F_0))$. Where F_M is the maximum fluorescence, F_0 the minimal fluorescence calculated by the Handy-PEA, $F_{2\,ms}$ and $F_{30\,ms}$ are the fluorescence levels measured at 2 and 30ms, respectively.

P_{700} oxidation. The kinetics of PSI photoxidation were measured on detached leaves using a JTS-10 LED spectrometer (BioLogic Science Instruments) in absorbance mode.

P_{700} oxidation was assessed by increase in absorption at 810nm (after deconvolution of plastocyanin absorption, as described in Joliot and Joliot[6]). FAR illumination was provided by a LED peaking at 735 nm, filtered through three Wratten filters 55 that block wavelengths shorter than 700nm. When needed, the maximum extent of P_{700}^+ was estimated by imposing a white light saturating flash on top of the FAR. A red LED provided actinic light peaking at 640nm[45]. In order to measure the number of electrons present in the ETC per PSI, the plants were incubated 2min under strong white light (500μmol m^{-2} s^{-1}) in order to reduce the contribution of the cyclic electron flow by activating CO_2 assimilation in the leaves[6]. Reactivation of cyclic flow only occurs after a long period of dark[6,45]. Therefore, after a short dark adaptation, electrons available to P_{700}^+ are only reflecting the reduction level of the PSI donors including the PQ pool. We exposed the leaf to FAR for 2min to oxidise the ETC and, after 2 s of dark adaptation to allow P_{700} reduction, we followed its reoxidation induced by FAR either in the presence or in the absence of a short saturating flash of actinic light (1000μmol m^{-2} s^{-1} for 100 μs) to fully reduce the ETC. The time interval between the beginning of FAR illumination and the beginning of P_{700} oxidation was measured after a saturating pulse (PSI electron donors reduced) and after dark incubation (PSI electron donors oxidised). The ratio between these two values is used as a proxy for the number of available electrons per PSI (Supplementary Fig. 9).

Immunoblot analysis. Total proteins were extracted from *Arabidopsis* light-exposed leaves and homogenised in 400μL of lysis buffer (100mM Tris-HCl pH 8.5, 2% SDS, 10mM NaF and 0.05% of protease inhibitor cocktail for plant (Sigma)) with a micro pestle in a 1.5mL microtube. Proteins were denatured at 37 °C for 30minu, then centrifuged for 5 min at 16,000 *g* at room temperature. Two hundred microliters of supernatant were precipitated by chloroform–methanol, then resuspended in sample buffer (50mM Tris-HCl pH 6.8, 100mM dithiothreitol, 2% SDS, 0.1% bromophenol blue and 10% Glycerol) at 0.5 μg chlorophyll per μL and denatured at 65 °C for 10 min. Five–ten microliters of supernatant was mixed with 1mL of 80% acetone and chlorophylls concentration was determined according to Arnon (1949)[46]. An amount of thylakoids equivalent to 2 μg of chlorophyll were loaded. Proteins were separated by 12% SDS-PAGE and transferred onto a nitrocellulose membrane for western blotting.

For Phostag™-pendant acrylamide gels, we followed the protocol for the antenna proteins previously described in Longoni et al.[47]. For the detection of PSII core subunits and STN7 phopshorylation, the protocol was modified as follows: a Phostag™ gradient (0 to 25μM) and $Zn(NO_3)_2$ (0 to50 μM) was made in the upper half of the resolving 7% acrylamide in 0.35 M Bis-Tris pH 6.8 gel. The stacking gel (4% acrylamide and 0.35 M Bis-Tris pH 6.8) was casted above the resolving gel. The gels were incubated at room temperature for at least 3 h before loading. Samples were prepared as previously described in Longoni et al.[47]. Briefly, total leaf protein were ground in liquid nitrogen and resuspend in lysis buffer (100mM Tris HCl pH 7.8, 2% SDS, 10 mM NaF, 1× cOmplete™ and EDTA-free protease inhibitor cocktail (Roche)). Following incubation at 37 °C for 30′ in agitation (1000 r.p.m Eppendorf thermomixer) protein content was measured with the Bicinchoninic Acid Protein Assay Kit (Sigma-Aldrich) and samples were diluted to equal protein concentration (0.5μg/μL). Samples were further diluted in 2× lithium dodecyl sulfate (LDS) loading buffer (10% glycerol, 244mM Tris HCl pH 8.5, 2% LDS, 0.33 mM Coomassie Brilliant Blue G-250 and 100mM dithiothreitol) and heated for 5 min at 70 °C before loading.

Immunodetections were performed using anti-Actin (Sigma, A 0480) at 1/3000 dilution in 5% fat free milk/PBS, anti-Lhcb1 (Agrisera, AS09 522), anti-Lhcb2 (Agrisera, AS01 003), anti-D1 (PsbA) (Agrisera, AS05 084), anti-PsbO (Agrisera, AS14 2825), anti-PetC (Agrisera, AS08 330); anti-PsaD (Agrisera, AS09 461), anti-PsaC (Agrisera, AS04 042P), anti-AtpC (Agrisera, AS08 312); anti-STN7 (Agrisera, AS16 4098), anti-PsbD (Agrisera, AS06 146) at 1/5000 dilution in 5% fat free milk/TBS and anti-Phosphothreonine (Cell Signaling Technology, #9381) at 1/10'000 in 3% BSA/TBS Tween20 0.1%. Secondary antibodies (anti-rabbit (Merck, AP132P) or anti-mouse (Sigma, A5278) at 1/3000) conjugated with HRP allow the detection of proteins of interest with 1mL of enhanced chemiluminescence and 3.3μL of H_2O_2 3% using an imager for chemiluminescence (Amersham Imager 600, Amersham Biosciences, Inc).

PQ analysis. Small leaf discs (0.8cm diameter) were taken from 5-week-old plants. Total lipids were extracted after 15 s of saturating white light (2000μmol m^{-2} s^{-1}) using a fibre-optic system allowing a maximal reduction of the PQ pool. Samples were directly flash frozen in liquid nitrogen at the end of the light treatment while still illuminated. A second disc from the same leaf was treated with FAR light (735nm and 5.5 μmol m^{-2} s^{-1}) for 2 min allowing a maximal oxidation of the PQ pool. For prenyl lipid determination, samples were grinded immediately in the frozen state and extracted with cold ethyl acetate. This step as well as the analyses were performed as described in Kruk and Karpinski[5] and Ksas et al.[11,12]. The photoactive PQ pool was determined from the difference between the reduced PQ after 2 min of FAR light, upon which all the photoactive pool is oxidised, and the reduced PQ after a high irradiance light flash, upon which all the photoactive pool is reduced. Plastoglobule isolation from chloroplasts and prenyl lipid analysis were performed according to Martinis et al. [48] and Eugeni-Piller et al.[49]. Intact chloroplast were extracted from entire leaves by grinding in HB buffer (Sorbitol 450mM, Tricine-KOH pH 8.4 20mM, EDTA pH 8.4 10mM, $NaHCO_3$ 10mM, $MnCl_2$ 1mM, Na-ascorbate 5mM and PMSF 1mM). The chloroplast were filtered through two layers of miracloth (Merck Millipore) and collected by centrifugation (5600 × *g*). The chloroplasts were lysate by osmotic shock in TED buffer (Tricine pH 7.5 50mM, EDTA-Na_2 2mM and dithiothreitol 2mM) supplemented with 0.6 M sucrose. Chloroplasts were diluted to a concentration of 2 mg/ml of chlorophyll and incubated for 10′ on ice to allow a complete lysis and further incubated for 2 h at −80 °C. The samples were diluted four times in TED buffer. The sample was homogenate 20 times with a Dounce homogeniser (PTFE Tissue grinder 50cm3, VWR®). The membranes and plastoglobules were separated from the stroma by ultracentrifugation (60′ 100,000 × *g* at 4 °C). The pellet was dissolved in TED buffer supplemented with 45% sucrose to a concentration of 2–3mg/mL of chlorophyll. Further homogenisation of the sample was performed with a Dounce homogeniser (20 times). This solution was used as a lower phase of a discontinuous sucrose gradient. The gradient was assembled in TED buffer with the following sucrose concentrations: 15ml of sample in 45% sucrose, 6mL of 38% sucrose, 6mL of 20% sucrose, 4mL of 15% sucrose and 8mL of 5% sucrose. The gradient was centrifuged to allow the fractionation by flotation (16 h, 100,000 × *g* at 4 °C). One-milliliter fractions were collected from the top of the gradient. The lipids from each fraction were extracted with ethyl -acetate (0.75 volumes, 2 times), the ethyl-acetate phase was recovered upon centrifugation (1′ 10,000 × *g*) and dried in a speedvac. The dried pellet was solubilized in a tetrahydrofuran–methanol (1:1) solution, and used for UHPLC-APCI-MS-QTOF analysis.

Statistics and reproducibility. The sample size was determined empirically for each experiment (minimum of three independent organism and two experimental replicates), on the basis of experience with similar assays and from sample sizes generally used by other investigators. No data were excluded from the analysis. The experiment were replicated at least two times, the results were reproducible when the plants were not stressed before the experiment. When testing light condition, the position of the plants of different genotypes was changed randomly in order to reduce any possible positioning effect. The data were compared for statistical difference by a two-tailed, heteroscedastic Student's *t* test (Excel 2016).

Reporting Summary. Further information on research design is available in the Nature Research Reporting Summary linked to this article.

Data availability

The datasets analysed in this paper are included in this published article (and its supplementary information files). Further datasets generated during the current study are available from the corresponding author on reasonable request.

Received: 5 February 2019 Accepted: 17 May 2019
Published online: 20 June 2019

References

1. Tikhonov, A. N. pH-dependent regulation of electron transport and ATP synthesis in chloroplasts. *Photosynth. Res.* **116**, 511–534 (2013).
2. Rochaix, J. D. Regulation of photosynthetic electron transport. *Biochim. Biophys. Acta* **1807**, 375–383 (2011).
3. Van Eerden, F. J., Melo, M. N., Frederix, P., Periole, X. & Marrink, S. J. Exchange pathways of plastoquinone and plastoquinol in the photosystem II complex. *Nat. Commun.* **8**, 15214 (2017).
4. Block, A. et al. Functional modeling identifies paralogous solanesyl-diphosphate synthases that assemble the side chain of plastoquinone-9 in plastids. *J. Biol. Chem.* **288**, 27594–27606 (2013).
5. Kruk, J. & Karpinski, S. An HPLC-based method of estimation of the total redox state of plastoquinone in chloroplasts, the size of the photochemically active plastoquinone-pool and its redox state in thylakoids of *Arabidopsis*. *Biochim. Biophys. Acta* **1757**, 1669–1675 (2006).
6. Joliot, P. & Joliot, A. Cyclic electron flow in C3 plants. *Biochim. Biophys. Acta* **1757**, 362–368 (2006).
7. van Wijk, K. J. & Kessler, F. Plastoglobuli: plastid microcompartments with integrated functions in metabolism, plastid developmental transitions, and environmental adaptation. *Annu. Rev. Plant Biol.* **68**, 253–289 (2017).
8. Kruk, J., Szymanska, R., Cela, J. & Munne-Bosch, S. Plastochromanol-8: fifty years of research. *Phytochemistry* **108**, 9–16 (2014).
9. Giacometti, G. M., Barbato, R., Chiaramonte, S., Friso, G. & Rigoni, F. Effects of ultraviolet-B radiation on photosystem II of the cyanobacterium *Synechocystis* sp. PCC 6083. *Eur. J. Biochem.* **242**, 799–806 (1996).
10. Trebst, A. & Pistorius, E. Photosynthetische reaktionen in UV-bestrahlten chloroplasten. *Z. für Naturforschung B* **20**, 885–889 (1965).
11. Ksas, B., Becuwe, N., Chevalier, A. & Havaux, M. Plant tolerance to excess light energy and photooxidative damage relies on plastoquinone biosynthesis. *Sci. Rep.* **5**, 10919 (2015).
12. Ksas, B. et al. The plastoquinone pool outside the thylakoid membrane serves in plant photoprotection as a reservoir of singlet oxygen scavengers. *Plant Cell Environ.* **41**, 2277–2287 (2018).
13. Shikanai, T., Munekage, Y., Shimizu, K., Endo, T. & Hashimoto, T. Identification and characterization of *Arabidopsis* mutants with reduced quenching of chlorophyll fluorescence. *Plant Cell Physiol.* **40**, 1134–1142 (1999).
14. Lundquist, P. K. et al. The functional network of the *Arabidopsis* plastoglobule proteome based on quantitative proteomics and genome-wide coexpression analysis. *Plant Physiol.* **158**, 1172–1192 (2012).
15. Vidi, P. A. et al. Tocopherol cyclase (VTE1) localization and vitamin E accumulation in chloroplast plastoglobule lipoprotein particles. *J. Biol. Chem.* **281**, 11225–11234 (2006).
16. Ytterberg, A. J., Peltier, J. B. & van Wijk, K. J. Protein profiling of plastoglobules in chloroplasts and chromoplasts. A surprising site for differential accumulation of metabolic enzymes. *Plant Physiol.* **140**, 984–997 (2006).
17. Martinis, J. et al. ABC1K1/PGR6 kinase: a regulatory link between photosynthetic activity and chloroplast metabolism. *Plant J.* **77**, 269–283 (2014).
18. Yang, M. et al. *Arabidopsis* atypical kinase ABC1K1 is involved in red light-mediated development. *Plant Cell Rep.* **35**, 1213–1220 (2016).
19. Lundquist, P. K. et al. Loss of plastoglobule kinases ABC1K1 and ABC1K3 causes conditional degreening, modified prenyl-lipids, and recruitment of the jasmonic acid pathway. *Plant Cell* **25**, 1818–1839 (2013).
20. Kato, Y., Miura, E., Ido, K., Ifuku, K. & Sakamoto, W. The variegated mutants lacking chloroplastic FtsHs are defective in D1 degradation and accumulate reactive oxygen species. *Plant Physiol.* **151**, 1790–1801 (2009).
21. Wetzel, C. M., Jiang, C. Z., Meehan, L. J., Voytas, D. F. & Rodermel, S. R. Nuclear-organelle interactions: the immutans variegation mutant of *Arabidopsis* is plastid autonomous and impaired in carotenoid biosynthesis. *Plant J.* **6**, 161–175 (1994).
22. Zagari, N. et al. SNOWY COTYLEDON 2 promotes chloroplast development and has a role in leaf variegation in both lotus *japonicus* and *Arabidopsis* thaliana. *Mol. Plant* **10**, 721–734 (2017).
23. Mekala, N. R., Suorsa, M., Rantala, M., Aro, E. M. & Tikkanen, M. Plants actively avoid state transitions upon changes in light intensity: role of light-harvesting complex II protein dephosphorylation in high light. *Plant Physiol.* **168**, 721–734 (2015).
24. Bellafiore, S., Barneche, F., Peltier, G. & Rochaix, J. D. State transitions and light adaptation require chloroplast thylakoid protein kinase STN7. *Nature* **433**, 892–895 (2005).
25. Rochaix, J. D. Redox regulation of thylakoid protein kinases and photosynthetic gene expression. *Antioxid. Redox Signal.* **18**, 2184–2201 (2013).
26. Shapiguzov, A. et al. Activation of the Stt7/STN7 kinase through dynamic interactions with the cytochrome b6f complex. *Plant Physiol.* **171**, 82–92 (2016).
27. Trotta, A., Suorsa, M., Rantala, M., Lundin, B. & Aro, E. M. Serine and threonine residues of plant STN7 kinase are differentially phosphorylated upon changing light conditions and specifically influence the activity and stability of the kinase. *Plant J.* **87**, 484–494 (2016).
28. Pietrzykowska, M. et al. The light-harvesting chlorophyll a/b binding proteins Lhcb1 and Lhcb2 play complementary roles during state transitions in *Arabidopsis*. *Plant Cell* **26**, 3646–3660 (2014).
29. Bonardi, V. et al. Photosystem II core phosphorylation and photosynthetic acclimation require two different protein kinases. *Nature* **437**, 1179–1182 (2005).
30. Schonberg, A. et al. Identification of STN7/STN8 kinase targets reveals connections between electron transport, metabolism and gene expression. *Plant J.* **90**, 1176–1186 (2017).
31. Tikkanen, M., Nurmi, M., Kangasjarvi, S. & Aro, E. M. Core protein phosphorylation facilitates the repair of photodamaged photosystem II at high light. *Biochim. Biophys. Acta* **1777**, 1432–1437 (2008).
32. Bailey, S. et al. A critical role for the Var2 FtsH homologue of *Arabidopsis* thaliana in the photosystem II repair cycle in vivo. *J. Biol. Chem.* **277**, 2006–2011 (2002).
33. Strasser, R. J., Tsimilli-Michael, M., Qiang, S. & Goltsev, V. Simultaneous in vivo recording of prompt and delayed fluorescence and 820-nm reflection changes during drying and after rehydration of the resurrection plant *Haberlea* rhodopensis. *Biochim. Biophys. Acta* **1797**, 1313–1326 (2010).
34. Kalaji, H. M. et al. Identification of nutrient deficiency in maize and tomato plants by in vivo chlorophyll a fluorescence measurements. *Plant Physiol. Biochem.* **81**, 16–25 (2014).
35. Maxwell, K. & Johnson, G. N. Chlorophyll fluorescence--a practical guide. *J. Exp. Bot.* **51**, 659–668 (2000).
36. Graan, T. & Ort, D. R. Quantitation of the rapid electron donors to P700, the functional plastoquinone pool, and the ratio of the photosystems in spinach chloroplasts. *J. Biol. Chem.* **259**, 14003–14010 (1984).
37. Finazzi, G. et al. Involvement of state transitions in the switch between linear and cyclic electron flow in *Chlamydomonas* reinhardtii. *EMBO Rep.* **3**, 280–285 (2002).
38. Finazzi, G. et al. Function-directed mutagenesis of the cytochrome b6f complex in *Chlamydomonas* reinhardtii: involvement of the CD loop of cytochrome b6 in quinol binding to the Q(o) site. *Biochemistry* **36**, 2867–2874 (1997).
39. Pesaresi, P., Pribil, M., Wunder, T. & Leister, D. Dynamics of reversible protein phosphorylation in thylakoids of flowering plants: the roles of STN7, STN8 and TAP38. *Biochim. Biophys. Acta* **1807**, 887–896 (2011).
40. Tikkanen, M., Grieco, M., Kangasjarvi, S. & Aro, E. M. Thylakoid protein phosphorylation in higher plant chloroplasts optimizes electron transfer under fluctuating light. *Plant Physiol.* **152**, 723–735 (2010).
41. Genty, B., Harbinson, J., Briantais, J. M. & Baker, N. R. The relationship between non-photochemical quenching of chlorophyll fluorescence and the rate of photosystem 2 photochemistry in leaves. *Photosynth. Res.* **25**, 249–257 (1990).
42. Lavergne, J. & Joliot, P. Restricted diffusion in photosynthetic membranes. *Trends Biochem. Sci.* **16**, 129–134 (1991).
43. Müller, P., Li, X. P. & Niyogi, K. K. Non-photochemical quenching. A response to excess light energy. *Plant Physiol.* **125**, 1558–1566 (2001).
44. Huang, H., Yang, M., Su, Y., Qu, L. & Deng, X. W. *Arabidopsis* atypical kinases ABC1K1 and ABC1K3 act oppositely to cope with photodamage under red light. *Mol. Plant* **8**, 1122–1124 (2015).
45. Trouillard, M. et al. Kinetic properties and physiological role of the plastoquinone terminal oxidase (PTOX) in a vascular plant. *Biochim. Biophys. Acta* **1817**, 2140–2148 (2012).
46. Arnon, D. I. Copper enzymes in isolated chloroplasts. polyphenoloxidase in *Beta* vulgaris. *Plant Physiol.* **24**, 1–15 (1949).
47. Longoni, P., Douchi, D., Cariti, F., Fucile, G. & Goldschmidt-Clermont, M. Phosphorylation of the light-harvesting complex II isoform Lhcb2 is central to state transitions. *Plant Physiol.* **169**, 2874–2883 (2015).
48. Martinis, J., Kessler, F. & Glauser, G. A novel method for prenylquinone profiling in plant tissues by ultra-high pressure liquid chromatography-mass spectrometry. *Plant Methods* **7**, 23 (2011).
49. Eugeni-Piller, L., Glauser, G., Kessler, F. & Besagni, C. Role of plastoglobules in metabolite repair in the tocopherol redox cycle. *Front. Plant Sci.* 5, 10.3389/Fpls.2014.00298 (2014).

Acknowledgements

This work was supported by the Swiss National Science Foundation (SNSF) grants 31003A_156998 and 31003A_176191. G.F. acknowledges funding by the HFSP RGP0052 project and the INRA AAP project PURIST funds form the GRAL (ANR-10-LABX-49–01) labex. We thank Prof. Goldschmidt-Clermont for his helpful discussion and support during the project.

Author contributions

T.P., V.S., P.L. and F.K. designed experiments. T.P., P.L., G.G., B.K., J.C., S.D., M.H. and G.F. performed all experiments. T.P., V.S., P.L., M.H., G.F. and F.K. contributed to the

analysis and the interpretation of the results. T.P., V.S., P.L., M.H., G.F. and F.K. wrote the manuscript.

Additional information

Supplementary information accompanies this paper at https://doi.org/10.1038/s42003-019-0477-4.

Competing interests: The authors declare no competing interests.

Reprints and permission information is available online at http://npg.nature.com/reprintsandpermissions/

Publisher's note: Springer Nature remains neutral with regard to jurisdictional claims in published maps and institutional affiliations.

2.3. Mutation of the Atypical Kinase ABC1K3 Partially Rescues the PROTON GRADIENT REGULATION 6 Phenotype in *Arabidopsis Thaliana*

Contributions

In this paper, I measured Dark and Far Red PQ re-oxidation in Col-0, *abc1k1-1*, *abc1k1-2*, *abc1k1/abc1k3* and *sps2* under moderate light and high light. The previous discovery of the *abc1k1* variegated phenotype under high light lead us to analyze other mutants displaying a similar phenotype. Variegated phenotypes have been observed in several mutants, among them, *ptox*. Yet, the causes of variegation remain poorly understood (Carol et al., 1999). PTOX is an oxidase localized in the stroma lamellae of the thylakoid membrane and is responsible of the light-independent oxidation of the plastoquinone. PTOX activity provides oxidized plastoquinone as a co-factor in the desaturation reactions required for carotenoid synthesis. In agreement with the fact that the *abc1k1* mutant has a defect in the homeostasis of the plastoquinone pool and also displays a variegated phenotype, we hypothesized that PTOX function may be impaired in the *abc1k1* mutant. We therefore analyzed the red/ox state of the photoactive plastoquinone pool in *abc1k1*, *abc1k3*, *abc1k1/abc1k3*, *sps2* and *ptox*, and we observed that the dark re-oxidation of the plastoquinone pool is impaired in *abc1k1*, despite the presence of the PTOX protein, suggesting a defect in the mobility of plastoquinone molecules.

frontiers in Plant Science

ORIGINAL RESEARCH
published: 25 March 2020
doi: 10.3389/fpls.2020.00337

Mutation of the Atypical Kinase ABC1K3 Partially Rescues the PROTON GRADIENT REGULATION 6 Phenotype in *Arabidopsis thaliana*

Thibaut Pralon[1], Joy Collombat[1], Rosa Pipitone[1], Brigitte Ksas[2], Venkatasalam Shanmugabalaji[1], Michel Havaux[2], Giovanni Finazzi[3], Paolo Longoni[1] and Felix Kessler[1]**

[1] *Laboratory of Plant Physiology, Institute Biology, University of Neuchâtel, Neuchâtel, Switzerland,* [2] *Aix Marseille University, Centre National de la Recherche Scientifique (CNRS), Commissariat à l'Énergie Atomique et aux Énergies Alternatives (CEA), UMR 7265, Biosciences et Biotechnologies Institute of Aix-Marseille, Saint-Paul-lez-Durance, France,* [3] *Université Grenoble Alpes, Centre National de la Recherche Scientifique (CNRS), Commissariat à l'Énergie Atomique et aux Énergies Alternatives (CEA), Institut National de la Recherche Agromique (INRA), Interdisciplinary Research Institute of Grenoble - Cell and Plant Physiology Laboratory (IRIG-LPCV), Grenoble, France*

OPEN ACCESS

Edited by:
Przemysław Malec, Jagiellonian University, Poland

Reviewed by:
Claire Remacle, University of Liège, Belgium
Peter J. Gollan, University of Turku, Finland

***Correspondence:**
Paolo Longoni
paolo.longoni@unine.ch
Felix Kessler
felix.kessler@unine.ch

Specialty section:
This article was submitted to Plant Physiology, a section of the journal Frontiers in Plant Science

Received: *27 November 2019*
Accepted: *06 March 2020*
Published: *25 March 2020*

Citation:
Pralon T, Collombat J, Pipitone R, Ksas B, Shanmugabalaji V, Havaux M, Finazzi G, Longoni P and Kessler F (2020) Mutation of the Atypical Kinase ABC1K3 Partially Rescues the PROTON GRADIENT REGULATION 6 Phenotype in Arabidopsis thaliana. Front. Plant Sci. 11:337. doi: 10.3389/fpls.2020.00337

Photosynthesis is an essential pathway providing the chemical energy and reducing equivalents that sustain higher plant metabolism. It relies on sunlight, which is an inconstant source of energy that fluctuates in both intensity and spectrum. The fine and rapid tuning of the photosynthetic apparatus is essential to cope with changing light conditions and increase plant fitness. Recently PROTON GRADIENT REGULATION 6 (PGR6-ABC1K1), an atypical plastoglobule-associated kinase, was shown to regulate a new mechanism of light response by controlling the homeostasis of photoactive plastoquinone (PQ). PQ is a crucial electron carrier existing as a free neutral lipid in the photosynthetic thylakoid membrane. Perturbed homeostasis of PQ impairs photosynthesis and plant acclimation to high light. Here we show that a homologous kinase, ABC1K3, which like PGR6-ABC1K1 is associated with plastoglobules, also contributes to the homeostasis of the photoactive PQ pool. Contrary to PGR6-ABC1K1, ABC1K3 disfavors PQ availability for photosynthetic electron transport. In fact, in the *abc1k1/abc1k3* double mutant the *pgr6*(*abc1k1*) the photosynthetic defect seen in the *abc1k1* mutant is mitigated. However, the PQ concentration in the photoactive pool of the double mutant is comparable to that of *abc1k1* mutant. An increase of the PQ mobility, inferred from the kinetics of its oxidation in dark, contributes to the mitigation of the *pgr6*(*abc1k1*) photosynthetic defect. Our results also demonstrate that ABC1K3 contributes to the regulation of other mechanisms involved in the adaptation of the photosynthetic apparatus to changes in light quality and intensity such as the induction of thermal dissipation and state transitions. Overall, we suggests that, besides the absolute concentration of PQ, its mobility and exchange between storage and active pools are critical for light acclimation in plants.

Keywords: photosynthetic electron transport, plastoquinone pool, plastoglobule, high light acclimation, NPQ

INTRODUCTION

The photosynthetic conversion of light energy into chemical energy occurs via a series of redox reactions resulting in electron transport along the thylakoid membrane. The linear electron transport begins with water splitting at the level of photosystem II (PSII) and ends at photosystem I (PSI) with the reduction of $NADP^+$ by ferredoxin. Both PSII and PSI utilize photonic energy to fuel the redox reactions. Electrons are transferred from PSII to PSI via the cytochrome *b6f* complex (cyt *b6f*). At the Q_B site of PSII, a molecule of plastoquinone (PQ) is reduced twice and protonated to form plastoquinol (PQH_2). The PQH_2 can then diffuse within the thylakoid membrane to reach the Q_O site of cyt *b6f*. Oxidation of PQH_2 at cyt *b6f* occurs through the Q-cycle that releases protons into the thylakoid lumen contributing to the formation of the trans-thylakoid proton gradient. In addition, two electrons are released, one of which returns to PQ pool, while the other is transferred via the plastocyanin to PSI (Tikhonov, 2014). The proportion of PQ that participates in electron transport in the thylakoid membrane is considered as the photoactive PQ pool; whereas the remaining proportion, which is approximately 60–70% of the total PQ, constitutes the non-photoactive pool and is largely stored inside thylakoid-associated lipid droplets known as plastoglobules (PG) (Kruk and Karpinski, 2006; Block et al., 2013; Ksas et al., 2018).

To shuttle electrons, PQ has to rapidly navigate in the thylakoid lipid bilayer (Blackwell et al., 1994). However, the thylakoid membrane is crowded with integral proteins, covering up to 70% of the surface in the grana stacks, which drastically restrict PQ diffusion, especially at the long-range (Kirchhoff et al., 2000). Thylakoid membranes are close to the percolation threshold, therefore it has been suggested that the organization of the protein supercomplexes creates lipid microdomains that facilitate PQ mobility and thus electron shuttling between PSII and cyt *b6f* (Lavergne and Joliot, 1991; Kirchhoff et al., 2000; Kirchhoff, 2014). On the other hand, long-range mobility of the PQ is also important, for instance to mobilize the non-photoactive pool when damaged PQ molecules have to be replaced as it was proposed to occur during high light stress (Ksas et al., 2018). Therefore, the mobility of plastoquinone/ol molecules within the thylakoid lipid bilayer is a critical parameter to ensure electron transport and maintain the photosynthetic electron transport chain (ETC).

Apart from the role of PQ as electron carrier, its redox state is an important signal in the regulation of many physiological processes within the chloroplast such as state transitions (as described below), gene expression, carotenoid biosynthesis, and antioxidant activity (Karpinski et al., 1999; Li et al., 2009; Suzuki et al., 2012). A rapid readout of the PQ redox state allows photosynthetic adaptation to changes in environmental conditions and therefore increases plant fitness in the natural environment. The adaptation to such varying light conditions is essential for plants to maintain the highest photosynthetic efficiency while avoiding photo-induced damage. To alleviate the negative effects of an imbalance between the activity of the two photosystems, plants have developed a short-term adaptive mechanism: the state transitions. This process allows the re-equilibration of the light energy input between the two photosystems on a time scale of a few minutes by re-allocating part of the mobile light-harvesting complexes II (LHCII) (Allen et al., 1981; Rochaix, 2007, 2013). Phosphorylation of LHCII by the STN7 kinase, the activity of which is dependent on the PQ redox state, allows its movement from PSII to PSI (state 2) (Bellafiore et al., 2005; Shapiguzov et al., 2016; Dumas et al., 2017). The process is reverted by the dephosphorylation of LHCII, operated by the PPH1/TAP38 phosphatase (state 1) (Pesaresi et al., 2010, 2011; Shapiguzov et al., 2010; Trotta et al., 2016). To prevent harmful effects of excess light, plants can dissipate the energy excess as heat by a set of regulated mechanisms summarily referred to as non-photochemical quenching (NPQ). These mechanisms include the rapid rearrangement to a "quenched" state of the LHCII antenna dependent on the PSBS protein and the conversion of the xanthophylls associated to LHCII from violaxanthin to zeaxanthin. The sum of all components creates a system with differential kinetics activated within a few seconds to hours (Dall'Osto et al., 2005; Joliot and Finazzi, 2010; Nilkens et al., 2010; Sylak-Glassman et al., 2014; Ruban, 2016, 2018). Nonetheless, upon continuous light stress, ROS can be produced at the PSII reaction center leading to loss of the PSII activity by damaging the core protein D1 (PsbA). Loss of PSII activity, known as photoinhibition (qI), contributes to the dissipation of excess light (Gong and Ohad, 1991; Miyao, 1994; Vasilikiotis and Melis, 1994). To restore PSII activity after inhibition there is an efficient repair cycle (Aro et al., 1993; Rintamaki et al., 1996, 1997; Theis and Schroda, 2016). The replacement of damaged D1 (PsbA) is facilitated by the phosphorylation of the core proteins of the PSII reaction center by STN8 kinase and requires PSII to migrate from the grana to the stroma lamellae (Aro et al., 1993; Bonardi et al., 2005; Tikkanen et al., 2008; Theis and Schroda, 2016; Li et al., 2018). Photo oxidative stress also triggers other responses allowing the chloroplast to alleviate the damage. These responses involve regulation of gene expression (Pfannschmidt et al., 1999; Pfannschmidt, 2003), structural changes of the thylakoids (Moejes et al., 2017) and synthesis of antioxidant molecules (Munné-Bosch and Alegre, 2002; Kanwischer et al., 2005; Gruszka et al., 2008; Nowicka and Kruk, 2012; Block et al., 2013; Martinis et al., 2014; Ksas et al., 2015, 2018; Spicher et al., 2016; Ferretti et al., 2018).

An important player in the plant stress response is the plastoglobule (PG). PGs are small lipid droplets, attached to the outer lipid leaflet of the thylakoid membrane, delimited by a membrane lipid monolayer consisting mostly of galactolipids and coated with proteins (Austin et al., 2006). Several neutral lipids including prenylquinones, carotenoids, triacylglycerols, phytolesters fill the plastoglobule (Lichtenthaler and Peveling, 1966; Steinmuller and Tevini, 1985; Gaude et al., 2007; Zbierzak et al., 2010; Lippold et al., 2012; Lundquist et al., 2013; Rottet et al., 2016; van Wijk and Kessler, 2017). In response to various stresses PGs increase in size and number (Taylor and Craig, 1971; Hall et al., 1972; Gaude et al., 2007; Martinis et al., 2014; Zechmann, 2019). Physical connections between PG and the thylakoid membranes suggest bidirectional lipid

trafficking between these two compartments (Austin et al., 2006). Besides being a lipid storage site, the PG proteome revealed the presence of specific proteins, several of which are involved in prenylquinone metabolism (Vidi et al., 2006; Ytterberg et al., 2006; Lundquist et al., 2012).

After fibrillins (Lundquist et al., 2012), the second most abundant protein family in PG is composed of homologs of the ABC1 (Activity of BC1 complex) atypical kinases (Lundquist et al., 2012). The ABC1 domain has been conserved through evolution, suggesting that it has a crucial role (Lohscheider and Rio Bartulos, 2016). In microorganisms as well as in human cells, ABC1 proteins were shown to be essential in ubiquinone synthesis and in mitochondrial electron transport (Bousquet et al., 1991; Brasseur et al., 1997; Poon et al., 2000; Mollet et al., 2008). Six members of the ABC1-like kinase family are found in the PG proteome. A member of this family, ABC1K1 (At4g31390), was identified as *PGR6* in a genetic screen to identify mutants affected in proton gradient formation (PGR) (Shikanai et al., 1999). PGR mutants are characterized by high chlorophyll fluorescence and reduced NPQ under different light conditions (from 50 to 500 μmol of photons m^{-2} s^{-1}) (Shikanai et al., 1999; Martinis et al., 2014; Yamori and Shikanai, 2016). In the *abc1k1* mutant, the electron transport rate as well as NPQ are constitutively limited in a light fluency dependent manner when compared to the wild type. Under prolonged exposure to high light, *abc1k1* adult plants exhibited almost complete photoinhibition during the early days of treatment and after several days PSII maximum efficiency recovered despite the plants still being still exposed to high light (Martinis et al., 2014). Nonetheless, the metabolic profile of *abc1k1* was profoundly altered. In particular, plants displayed a decrease in tocopherol accumulation and a shift from starch production to soluble sugars (Martinis et al., 2014).

ABC1K1 was identified as BDR1 (Bleached dwarf under red light) (Huang et al., 2015; Yang et al., 2016). During early seedling development under continuous red light, the mutant is severely stunted and has white cotyledons. Since the bleaching phenotype was accompanied by a specific diminishment of the photosystem D1 (PsbA) protein but not that of other photosynthetic proteins tested [D2 (PsbD); PsbC; PsbB] the pale phenotype was attributed to photobleaching (Huang et al., 2015; Yang et al., 2016). A repressor of the *bdr1* mutation, RBD1 (repressor of *bdr1*) was also identified as the ABC1K1 homolog ABC1K3. As the *abc1k3* mutation repressed the *bdr1*(*abc1k1*) phenotype, it led to the hypothesis that the two homologs have opposing functions (Huang et al., 2015). Furthermore, *abc1k3* adult plants are not severely affected by prolonged high light and they showed a decreased plastochromanol accumulation (Martinis et al., 2013). However, previous investigations on adult plants reported that the double *abc1k1/abc1k3* mutation results in an additive, senescence-like phenotype characterized by conditional degreening, including the loss of chlorophyll and photosystem proteins, and recruitment of the jasmonate pathway to PG under prolonged high light treatment (Lundquist et al., 2013). Furthermore, ABC1K1 and ABC1K3 may interact and form a complex that may be involved in the stabilization of plastoglobule proteins (Lundquist et al., 2013; Martinis et al., 2013).

Recently, a molecular mechanism explaining the *pgr6*(*abc1k1*) defect was proposed: ABC1K1 would be required for the homeostasis of photoactive PQ. Indeed, upon high light, the photoactive PQ pool in *abc1k1* mutant becomes limiting and this can explain the diminished linear electron transport and NPQ, the dephosphorylation of the LHCII antenna and perturbation of the state transitions; all these leading to an overall decrease in the photosynthetic efficiency (Pralon et al., 2019).

In this study, we investigated the impact of the *abc1k3* mutation in the *pgr6(abc1k1)* mutant background. In particular we focused on the capacity of a double mutant, lacking both *ABC1K1* and *ABC1K3*, to acclimate to a short high light treatment (3 h, 500 $\mu mol \cdot m^{-2} \cdot s^{-1}$). We found that the *abc1k3* mutant has no photosynthetic defect compared to the wild type under the tested conditions. However, by stacking this mutation with *abc1k1* we observe a partial alleviation of all the photosynthetic defects previously reported in *abc1k1* (Shikanai et al., 1999; Martinis et al., 2014; Pralon et al., 2019). Surprisingly, the phenotype complementation does not originate from an effect on the size of the photoactive PQ pool but rather from an effect on PQ mobility in the thylakoid membrane. This evidence suggests that there is a push-pull relationship of ABC1K1 and ABC1K3 with regard to the mobility of PQ, and that this regulated process is fundamental to ensure the photosynthetic efficiency under high light.

MATERIALS AND METHODS

Plants Material and Treatments

The wild type *Arabidopsis thaliana* refers to var. Columbia-0 (Col-0). *abc1k1.1* (Salk_068628), *abc1k1.2* (Salk_130499C) *abc1k3.1* (Salk_128696), or with *abc1k3.2* (Sail_918_E10) T-DNA insertion lines were purchased at Nottingham Arabidopsis Stock Centre (NASC)[1]. The double mutant lines *abc1k1/akc1k3.1* and *abc1k1/akc1k3.2* were produced by crossing *abc1k1.1* mutant with *abc1k3.1* and *abc1k3.2*, respectively. TDNA insertion was verified by PCR, and primers were listed in **Supplementary Table 1**. The mutant lines *stn7/stn8* (Fristedt et al., 2009) and *sps2* (Block et al., 2013) were kindly provided by the respective research groups. The *ptox* mutant was obtained from NASC, and corresponds to the previously characterized immutans variegation mutant (Wetzel et al., 1994).

Plants were grown in pots on soil pre-treated with solbac (Andermatt) with standard light conditions (120 μmol m^{-2} s^{-1}, 8 h light/16 h dark) in a controlled environment room maintaining a daily temperature of 22 ± 1°C. For high light treatment, 4–5 weeks old plants were exposed for 3 h to 500 μmol m^{-2} s^{-1} of white light (FutureLED), always at 22 ± 1°C.

Leaf samples were collected directly under the light in the growth chamber, and immediately snap frozen in liquid nitrogen, and stored at −20°C.

[1]http://arabidopsis.info

Photosynthetic Parameters

Before measuring the photosynthetic performance, the plants were kept in the dark for at least 10 min. The measurements were performed using a Fluorcam (Photon System Instrument, Czech Republic)[2] with a modified light curve protocol. Briefly, after measuring the minimal fluorescence (F_0) and the maximal fluorescence during a saturating pulse (F_M) in dark, the plants were exposed to increasing blue light (470 nm) intensities for 1 min following this scheme: 2.5–95–347–610–876–1145 μmol m^{-2} s^{-1}. At the end of every light period, a saturating flash was used to measure the maximal fluorescence in light (F_M'). The fluorescence recorded before the peak were used as F_S (steady-state chlorophyll fluorescence in the light). Three parameters were calculated from the above values: Maximum quantum yield of photosystem II $\Phi_{MAX} = (F_V/F_M)$; quantum yield of photosystem II $\Phi_{PSII} = (F_M' - F_S)/F_M'$ and Non-Photochemical Quenching $NPQ = (F_M - F_M')/F_M'$. To assess the extent of the "state transitions" the plants were exposed to 10 min red light (50 μmol m^{-2} s^{-1} 660 nm peak measured as PPFD) supplemented with far-red (17 μmol m^{-2} s^{-1} calculated from the 733 nm peak area considering values between 500 and 800 nm) followed by 10 min of the red light only. The maximal fluorescence in the light was measured at the end of both 10 min periods to obtain F_MST1 when far-red was supplemented and "state I" promoted and F_MST2 after 10 min of pure red, which promotes the transition toward "state II." The extent of the quenching related to state transition (qT) was calculated as $qT = (F_M ST1 - F_M ST2)/F_M$.

P_{700} Oxidation

The photooxidation of the photosystem I reaction center (P_{700}) was assessed by the increase in absorption at 810 nm after deconvolution of the plastocyanin absorption as previously described (Joliot and Joliot, 2006). The measurement was performed with a JTS-10 LED spectrometer (BioLogic Science Instruments) in absorbance mode equipped with a Far-red (FAR) LED peaking at 735 nm filtered through three Wratten filters 55 to block the wavelengths shorter than 700 nm, a red LED, peaking at 640 nm, was used for the actinic light. To estimate maximum extent of P_{700}^+ a saturating white light flash was superimposed on the top of the FAR. The measurement of the maximum number of electrons contained in the electron transport chain (ETC) per PSI was performed as follows. The plants were pre-incubated 2 min under a strong white light (500 μmol m^{-2} s^{-1}) to activate CO_2 assimilation in the leaves and thus reduce the contribution of the cyclic electron flow (Joliot and Joliot, 2006), which can only be reactivated after prolonged dark incubation (Joliot and Joliot, 2006; Trouillard et al., 2012). This allows only electrons from the linear ETC, including the photoactive PQ pool, to be available for PSI reduction. Detached leaves were put inside the holder and subjected to 2 min of FAR to oxidize the ETC followed by 2 s of dark allowing the reduction of P_{700}. The kinetic of the subsequent reoxidation induced by FAR were followed with a saturating flash of actinic light (1000 μmol m^{-2} s^{-1} for 100 μs) to fully reduce the ETC or without so that the ETC was fully oxidized. The ratio between the lag times between the FAR onset and the beginning of the P_{700} oxidation in these two conditions is used as a proxy for the number of available electrons per PSI (Pralon et al., 2019).

[2]http://www.psi.cz

Chlorophyll *a* Fluorescence Curve Kinetics (OJIP, JIP-Test)

Plants were dark-adapted for at least 10 min before measurements and then a single leaf detached in dark and put in a clip holder for the Plant Efficiency Analyzer (M-PEA 2; Hansatech Ltd.). The chlorophyll *a* fluorescence induction curve was recorded and the JIP-parameters recovered with M-PEA software Hansatech Ltd. The measurement was automatically repeated after increasing intervals of dark (4, 8, 12, 16, 20, 24 s) and far-red light (0.05, 0.1, 0.2, 0.4, 0.8, 1.6 s). The parameters extracted from the first pulse after the dark incubation were used to assess the steady state of the ETC after moderate light or 3 h of high light (Stirbet et al., 2018). The yield of the electron transport from Q_A to Q_B (ΦET2o) and the yield of the transport to final PSI acceptors (ΦRE1o) were calculated according to the JIP-Model described in Strasser et al. (2010) and Kalaji et al. (2014a,b). The variable fluorescence at 3 ms ($V_J = F_J/F_M$) value was used as a proxy of the redox state of the photoactive plastoquinone (Tóth et al., 2007). The data points of V_J over time were interpolated with a logarithmic function with RStudio (RStudio, Inc.).

Plastoquinone Analysis

The analysis of the photoactive PQ pool, and of the total pool were performed as previously described (Pralon et al., 2019). Briefly, leaf disks of 0.8 cm of diameter were collected from 5 weeks old plants. The disks were exposed either to 15 s of saturating light (2000 μmol m^{-2} s^{-1}) or to 2 min of far-red light (735 nm, 5.5 μmol m^{-2} s^{-1}). The samples were flash frozen and used for total lipid analysis as described in Kruk and Karpinski (2006) and Ksas et al. (2015, 2018). The photoactive PQ pool was determined from the difference between the reduced PQ after high light (maximal reduction of the photoactive PQ pool) and the amount measured after far-red light (maximal oxidation of the photoactive PQ pool).

Immunoblot Analysis

Fully expanded leaves of adult plants (at least 4 weeks old) were collected under the relevant light condition and flash frozen in liquid nitrogen. The leaves were ground to a fine powder in a 1.5 mL microtube with a micro-pestle. Four hundred mircroliter of lysis buffer [100 mM Tris-HCl pH 8.5, 2% SDS, 10 mM NaF, 0.05% of protease inhibitor cocktail for plant (Sigma)] was add to the powder and the material incubated at 37°C for 30 min, debris were removed by centrifugation (5 min at 16,000 g) at room temperature. The chlorophyll concentration of the sample was determined according to Arnon (1949). Proteins were precipitated in chloroform-methanol and the pellet solubilized directly in the gel loading buffer (50 mM Tris-HCl pH 6.8, 100 mM Dithiothreitol, 2% SDS, 0.1% Bromophenol Blue, 10% Glycerol) to a concentration of 0.5 μg chlorophyll/μL.

Following denaturation at 65°C for 10 min, 4 μL of each sample were loaded into a 12% Acrylamide SDS gel. After separation by electrophoresis the proteins were transferred to a nitrocellulose membrane. The membrane was decorated using the following antibodies: anti-Actin (Sigma, A 0480) at 1/3000 dilution in 5% fat free milk/PBS, anti-Lhcb2 (Agrisera, AS01 003), anti-D1 (PsbA) (Agrisera, AS05 084), anti-PetC (Agrisera, AS08 330); anti-PsaD (Agrisera, AS09 461), anti-PsaC (Agrisera, AS04 042P), anti-AtpC (Agrisera, AS08 312); at 1/5000 dilution in 5% fat free milk/TBS, and anti-Phosphothreonine (Cell Signaling Technology, #9381) at 1/10,000 in 3% BSA/TBS Tween20 0.1%; anti-PTOX (Agrisera, AS16 3692) at 1/2000 in 6% BSA/TBS Tween20 0.05%. Secondary antibodies (anti-rabbit (Merck, AP132P) or anti-mouse (Sigma, A5278) at 1/3000) conjugated with HRP allow the detection of proteins of interest with 1 mL of enhanced chemiluminescence and 3.3 μL of H_2O_2 3% using an imager for chemiluminescence (Amersham Imager 600, Amersham Biosciences, Inc.).

RESULTS

Isolation and Selection of abc1k1/abc1k3 Double Mutants

ABC1K1 and ABC1K3 are two homologous, atypical kinases located at plastoglobules and share 31.6% identity at the level of the global amino acid sequence (**Supplementary Figure 1**). To analyze potential interactions between ABC1K1 and ABC1K3 in the regulation of photosynthesis, two double mutant *abc1k1/abc1k3* lines were produced by crossing *abc1k1.1* (Salk_068628) with *abc1k3.1* (Salk_128696) or with *abc1k3.2* (Sail_918_E10). Double *abc1k1/abc1k3* mutant lines were selected and verified by PCR. The genotyping confirmed the presence of TDNA insertions in both genes (**Figure 1**).

Thermal Dissipation and Electron Transport Capacities Are Partially Recovered in abc1k1/abc1k3

Independent studies indicate that *abc1k1* is impaired in NPQ as well as electron transport (Shikanai et al., 1999; Martinis et al., 2014; Pralon et al., 2019), while the *abc1k3* mutant did not show defects in those parameters even after prolonged high light exposure (Martinis et al., 2013). To further characterize the *abc1k1/abc1k3* double mutant, we measured photosynthetic parameters such as PSII maximum efficiency [φ_{MAX} (= F_V/F_M)], NPQ as well as electron capacity of the ETC in 4–5 weeks old plants grown under moderate light (120 μmol m^{-2} s^{-1}) (ML) and after 3 h of high light (500 μmol m^{-2} s^{-1}).

The maximum quantum yield of the PSII (φ_{MAX}) in wild type (WT), *abc1k1*, *abc1k3*, and *abc1k1/abc1k3* slightly decreased after 3 h of high light but without any significant difference between the lines (**Figure 2A**). Furthermore, after 3 h of high light, there was no major impact on the PSII yield, and this allowed the measurement of the efficiency of the ETC avoiding potential bias caused by PSII photodamage.

Short-term high light treatment affected NPQ induction, which decreased in all the tested genotypes compared to moderate light conditions. Nonetheless, the NPQ in WT and in *abc1k3* was always higher than the one measured in *abc1k1* lines. Intriguingly, both under moderate light and after high light, the double mutants showed greater NPQ compared to *abc1k1* lines but still less than the WT level (**Figure 2B**), suggesting a partial rescue of the *pgr6*(*abc1k1*) phenotype in the double mutant.

Starting from P_{700} oxidation kinetics (Joliot and Joliot, 2006) and the JIP-test (Strasser et al., 2010; Kalaji et al., 2014a,b), we evaluated the ETC capacity at the PSI and PSII sides under moderate light and after exposure to high light to determine whether the rescued NPQ in *abc1k1/abc1k3* correlated with an increase in the electron capacity of the ETC.

P_{700} oxidation kinetics were analyzed after full reduction of the ETC by a saturating flash and its full oxidation by far-red illumination (**Figure 3A**; Joliot and Joliot, 2006; Pralon et al., 2019). The maximum number of electrons (e^-) present in the electron transport chain per PSI was assessed from P_{700} oxidation kinetic curves: by dividing the lag time after a strong light pulse (time required to oxidize P_{700} when ETC is fully reduced) by the lag time after far-red exposure (oxidation time of a single electron present in P_{700} reaction center) (Joliot and Joliot, 2006). When sampled under moderate light, *abc1k3* and WT ETC had the same electron capacity per PSI (20 ± 3 and 20 ± 4 electrons respectively), whereas the *abc1k1* ETC carried fewer electrons per PSI (8 ± 1 electrons) (**Figure 3B**). In the *abc1k1/abc1k3* mutant grown under moderate light the number of electrons carried by the ETC per PSI (16 ± 5) was intermediate between *abc1k1* and the WT. The measure was repeated on plants kept 3 h under high light. After high light treatment, in the WT the number of electrons carried by the ETC per PSI was 13 ± 3, thus it decreased in comparison to the same genotype sampled under moderate light. Similarly, in *abc1k1* as well as *abc1k1/abc1k3* the number of electrons per PSI dropped after high light treatment to 4 ± 2 and 8 ± 1 respectively. The measured electron transport capacity in *abc1k1/abc1k3* was double than that in *abc1k1*, indicating partial rescue of the ETC capacity. The *abc1k3* mutant displayed only a very slight decrease in the number of the ETC carriers per PSI (18 ± 4) upon shifting from moderate light to high light for 3 h, thus more ETC carriers than WT in this condition (**Figure 3B**).

The ETC capacity, before and after the high light treatment, was also estimated using fast chlorophyll *a* fluorescence (JIP-test) by normalizing the area above curve over variable fluorescence [Area/(F_M-F_O)] (Strasser et al., 2010; Kalaji et al., 2014a,b). This area positively correlates with the number of turnovers of the Q_A site of PSII before being fully closed. Since each turnover corresponds to a single electron injected in the ETC, the area offers a proxy of the number of available electron acceptors per PSII. These acceptors are internal to PSII, pheophytin and Q_A, or external, PQ molecules of the photoactive plastoquinone pool, the cyt *b6f* complex and plastocyanin. Under moderate light, the electron capacity estimated by the normalized area, was bigger in *abc1k3* than in WT (17 ± 2), while it was smaller in both *abc1k1* lines (15 ± 1; 14 ± 1). In the two

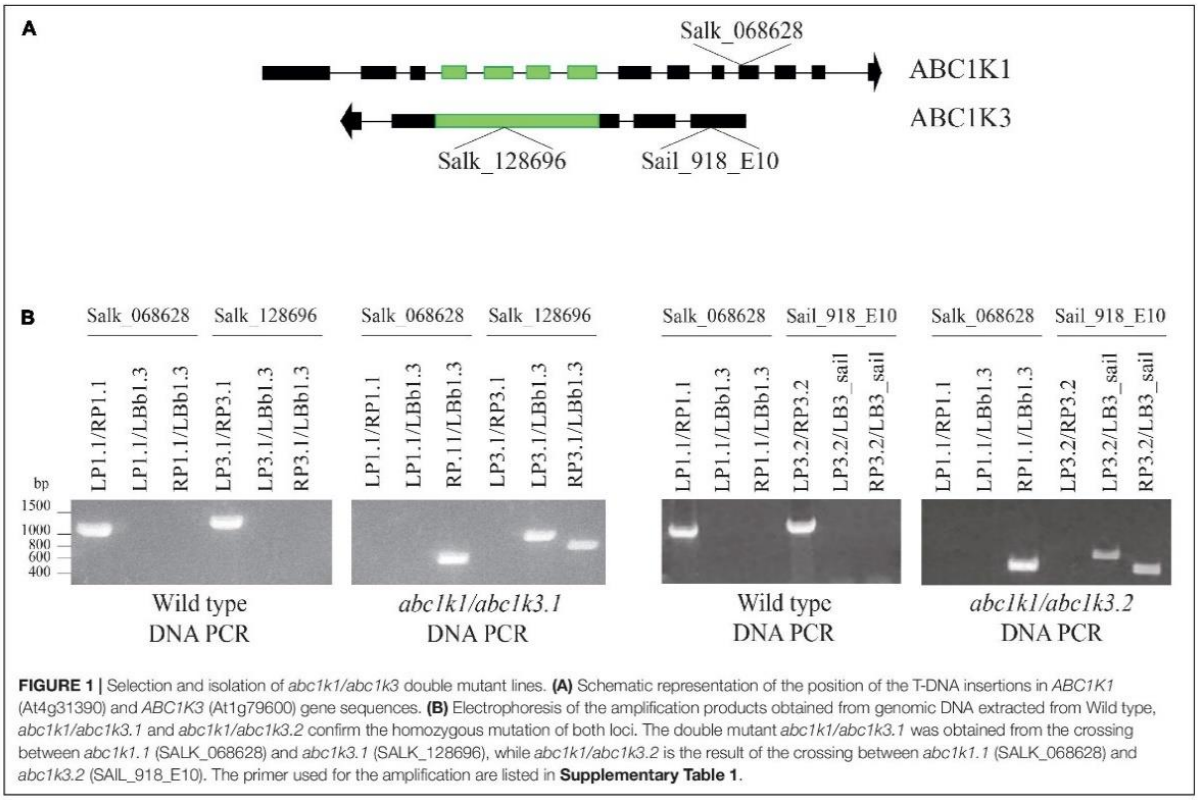

FIGURE 1 | Selection and isolation of *abc1k1/abc1k3* double mutant lines. **(A)** Schematic representation of the position of the T-DNA insertions in *ABC1K1* (At4g31390) and *ABC1K3* (At1g79600) gene sequences. **(B)** Electrophoresis of the amplification products obtained from genomic DNA extracted from Wild type, *abc1k1/abc1k3.1* and *abc1k1/abc1k3.2* confirm the homozygous mutation of both loci. The double mutant *abc1k1/abc1k3.1* was obtained from the crossing between *abc1k1.1* (SALK_068628) and *abc1k3.1* (SALK_128696), while *abc1k1/abc1k3.2* is the result of the crossing between *abc1k1.1* (SALK_068628) and *abc1k3.2* (SAIL_918_E10). The primer used for the amplification are listed in **Supplementary Table 1**.

abc1k1/abc1k3 lines the estimated electron capacity (18 ± 2; 20 ± 3) was comparable to WT (**Figure 4A**). A second measurement was performed on leaves sampled after 3 h of high light, in this sample, compared to the moderate light condition, the availability of the electron acceptors per PSII remained essentially unchanged in WT (19 ± 2) and in both *abc1k1/abc1k3* lines (19 ± 2; 18 ± 3). In the two *abc1k1* lines, after high light treatment, the electron transport capacity was diminished (13 ± 1; 11 ± 2) compared to the moderate light conditions. In contrast, both *abc1k3* lines showed a tendency toward an increase in electron carriers (22 ± 2; 24 ± 3) when comparing leaves sampled after 3 h of high light with those harvested in moderate light condition (**Figure 4A**).

To obtain an indication of the impact of the mutations on different components of the electron transport chain, we calculated the quantum yields of the electron transport flux from Q_A^- to PQ (ΦET2o) and to the PSI electron acceptors (ΦRE1o) by analyzing chlorophyll fluorescence inductions of JIP-curves at 3 ms (F_J) and 30 ms (F_I).

In leaves collected under moderate light, ΦET2o was lower in *abc1k1/abc1k3* and *abc1k1* compared to WT and *abc1k3*. After challenging the plants with 3 h of high light, the measurement revealed that ΦET2o dropped in all lines, with the most severe decrease in *abc1k1* lines followed by *abc1k1/abc1k3* (**Figure 4B**).

The quantum yield of electron transport to PSI final acceptors (ΦRE1o), in plants maintained under moderate light, was similar in WT and *abc1k1/abc1k3*, lower in *abc1k1* and higher in *abc1k3*. After 3 h of high light, ΦRE1o in *abc1k1*diminished even further, while it remained essentially unchanged in *abc1k1/abc1k3* when compared to moderate light. Therefore, *abc1k1/abc1k3* quantum yield was comparable to the WT in both light condition. For this parameter, the double mutation appears to partially attenuate the photosynthetic defects due to the *abc1k1* mutation. Finally, after high light, ΦRE1o in *abc1k3* did not change compared to moderate light, thus being always higher than in the WT (**Figure 4C**).

To verify whether the recovery of photosynthetic parameters in *abc1k1/abc1k3* as well as the higher photosynthetic capacities measured in *abc1k3*, were due to an increased cytochrome *b6f* activity, the turnover rate was measured (Finazzi et al., 2002). The measurement showed that there was no negative impact on the level of activity among all the tested lines (**Supplementary Figure 2**).

Together, these results indicate that the mutation of *abc1k3* has no negative impact the electron transport between the photosynthetic complexes, since the transport efficiency in this mutant line was elevated also after exposure to high light. Conversely, the electron transport in *abc1k1* was impaired in the moderate light condition and worsened upon exposure of the plants to 3 h of high light. The double mutation of *abc1k1* and

A

Maximum PSII Quantum Yield (ΦMAX)

	WT	*abc1k1.1*	*abc1k1.2*	*abc1k3.1*	*abc1k3.2*	*abc1k1/abc1k3.1*	*abc1k1/abc1k3.2*
ML	0.830 ± 0.010 ^{a}	0.817 ± 0.023 ^{a}	0.823 ± 0.006 ^{a}	0.830 ± 0.000 ^{a}	0.827 ± 0.015 ^{a}	0.817 ± 0.023 ^{a}	0.830 ± 0.000 ^{a}
HL 3h	0.773 ± 0.006 ^{b}	0.743 ± 0.031 ^{b}	0.723 ± 0.031 ^{b}	0.727 ± 0.012 ^{b}	0.763 ± 0.006 ^{b}	0.767 ± 0.017 ^{b}	0.740 ± 0.017 ^{b}

B

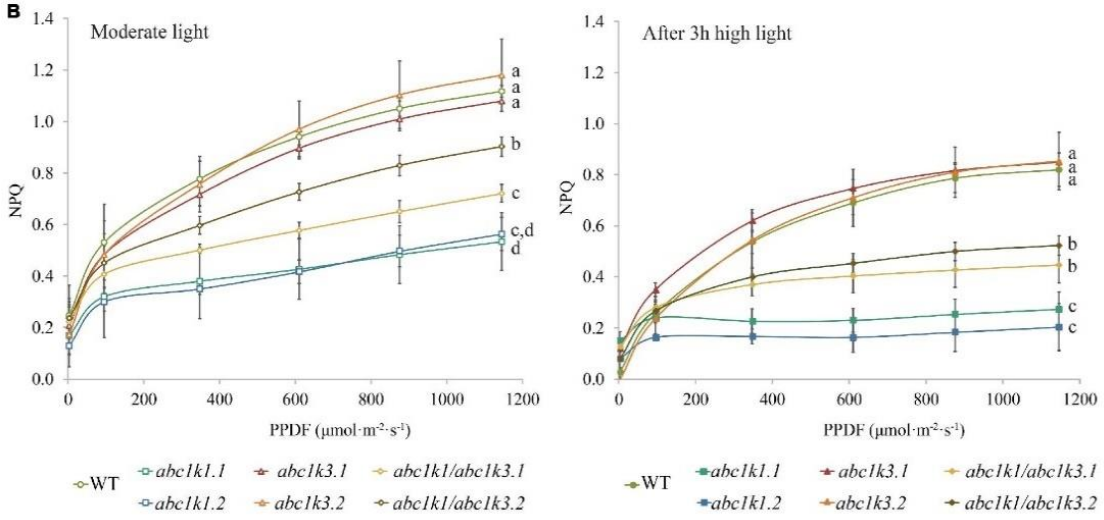

FIGURE 2 | Non-photochemical quenching is partially recovered in *abc1k1/abc1k3* lines compared to *abc1k1*. **(A)** PSII maximum quantum efficiency (ΦPSII = (FM – FO)/FM) and **(B)** non-photochemical quenching (NPQ) of 4–5 weeks old plants of wild type (WT), *abc1k1.1, -2, abc1k3.1, -2* and *abc1k1/abc1k3.1, -2* under moderate light and after 3 h of high light. Plants were dark-adapted 10 min before measurement. Non-photochemical quenching (NPQ = (FM – FM')/FM') was calculated from the maximal fluorescence at room temperature recorded after 1 min of exposure at increasing blue light intensities (470 nm). These measures were performed with a Fluorcam (MF800 – PSI). Each value represents the average of a pot containing 2–3 plants. Superscript letters are used to indicate statistically different groups ($p < 0.05$) by paired Student's *t*-test. Error bars indicate ± SD between different pots ($n = 3$).

abc1k3 resulted in a partial recovery of the electron transport and NPQ to WT levels when compared to *abc1k1*.

Mutation of abc1k3 Has No Effect on the Photoactive PQ Pool Size

The level of NPQ and the electron acceptor capacity of the ETC may be related to the size of the photoactive PQ pool (Block et al., 2013; Pralon et al., 2019). Therefore, we examined whether the partial rescue of the electron transport and NPQ capacities in *abc1k1/abc1k3* compared to *abc1k1* can be attributed to the size of the photoactive plastoquinone pool (i.e., the number of PQ molecules readily available per PSII). For this, we measured the total PQ (nmol cm^{-2}) and the relative photoactive PQ pool (in% of total PQ pool) in 4–5 weeks old plants under moderate light and after 3 h of high light exposure. The photoactive PQ pool is defined as the fraction of total PQ that is rapidly reduced during a saturating light pulse and oxidized when the sample is exposed to far-red light. To measure this fraction, PQH_2 and PQ amounts were analyzed by HPLC-MS on leaves illuminated either with a strong light flash in order to completely reduce the photoactive PQ pool, or with far-red to obtain its complete oxidation (Kruk and Karpinski, 2006; Block et al., 2013; Ksas et al., 2018; Pralon et al., 2019). The difference between the amount of reduced PQ after the saturating flash and that measured after far-red illumination determines the photoactive PQ pool.

Total plastoquinone levels (photoactive PQ pool + non-photoactive PQ pool) in *abc1k1* and in *abc1k1/abc1k3* lines were similar when compared to WT and decreased only slightly after 3 h of high light exposure. Conversely, the total PQ level was lower in *abc1k3* compared to WT (**Figure 5A**). The photoactive PQ pool (photoactive PQ/total PQ) measured in *abc1k3* was larger under moderate light condition and identical to the WT after 3 h of high light (**Figure 5B**). Whereas, in *abc1k1* after 3 h of high light, the photoactive PQ pool was strongly diminished compared to WT. Although the double mutant was not severely impaired in either ETC capacity or NPQ (**Figures 2**, **4**), the relative photoactive PQ pool, measured in plants grown under moderate light, in *abc1k1/abc1k3* was unexpectedly small and similar to the one of *abc1k1*. High light had no negative effect on the size of the photoactive PQ pool in the *abc1k1/abc1k3* double mutant. However, after 3 h of high light, its photoactive PQ pool size was smaller than that of the WT or *abc1k3*, and comparable to *abc1k1* (**Figure 5B**).

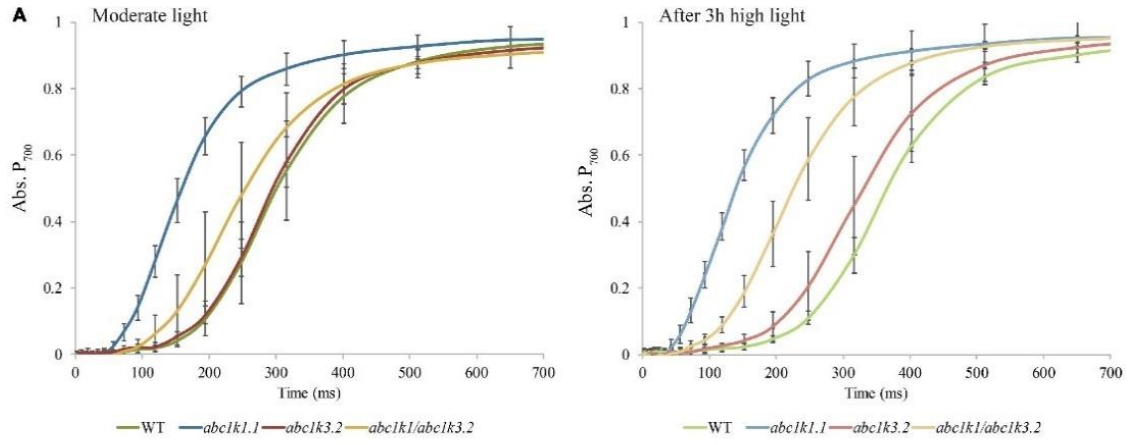

B

Moderate light	WT	*abc1k1.1*	*abc1k3.2*	*abc1k1/abc1k3.2*
Lag time after FAR (ms)	8.68	10.07	8.79	9.49
Lag time after pulse (ms)	173.68	75.22*	170.44	139.90*
Calculated pulse e^- number	20 ± 1	**8 ± 2***	20 ± 3	**16 ± 5***

After 3h high light	WT	*abc1k1.1*	*abc1k3.2*	*abc1k1/abc1k3.2*
Lag time after FAR (ms)	17.87	15.92	11.68	14.47
Lag time after pulse (ms)	215.14	49.85*	200.60	109.84*
Calculated pulse e^- number	13 ± 4	**4 ± 2***	18 ± 4	**8 ± 1***

FIGURE 3 | The shortage of electron carriers per photosystem I of *abc1k1* is partially recovered in *abc1k1/abc1k3*. **(A)** Kinetics of P_{700} re-oxidation induced by far-red light were recorded after a saturating light pulse (Time 0 = far-red ON) in wild type, *abc1k1.1*, *abc1k3.2*, and *abc1k1/abc1k3.2* kept under moderate light and after 3 h of high light. The P_{700} oxidation status was measured by the increase in absorption at 810 nm on fully expanded leaves of each genotype. **(B)** Electron (e^-) carried by the electron transport chain per photosystem I calculated from the lag time of P_{700} oxidation after a saturating pulse divided by the lag time of the oxidation after dark. Asterisk are used to indicate statistically different groups by Student's *t*-test ($p < 0.05$) ($n = 4$ biologically independent samples).

The analysis of the photoactive PQ pool suggests that the complementation of the *pgr6*(*abc1k1*) photosynthetic phenotype, induced by the *abc1k3* mutation, does not simply arise from a change of the amount of PQ readily available at PSII.

Mutation of ABC1K1 and ABC1K3 Impacts the Kinetics of PQ Re-oxidation in the Dark

The redox state of PQ in the light is dependent on the activity of the PSII, which will reduce the photoactive pool, and on that of the cytochrome *b6f*, which oxidizes the PQ pool transferring electrons along the ETC toward PSI. However, the photosynthetic complexes are inactive in the dark and therefore the redox state of PQ is mostly dependent on light-independent electron routes alternative to the cytochrome *b6f*. In the transition from light to dark the photoactive PQ pool will tend to start in a reduced form and be re-oxidized. The principal actor of this re-oxidation is PTOX. This enzyme, in Arabidopsis, is mostly located in the stroma lamellae fraction of the thylakoid membrane (Joet et al., 2002; Lennon et al., 2003; Houyoux et al., 2011). PSII being more abundant in the grana stacks, and considering the timescale of the mobility of PQ (Kirchhoff, 2014), we may assume that a large portion of the photoactive PQ pool is located within the grana stacks. Therefore, in order to be oxidized by PTOX the photoactive PQ has to migrate from the grana stacks to the stroma lamellae and then return to the grana stacks. Considering this, the kinetics of the oxidation of the photoactive PQ pool represents a proxy of the mobility of the PQ across the different portions of the thylakoid membrane. To estimate the redox state of the photoactive PQ pool we used the rapid chlorophyll *a* fluorescence induction, we based the analysis on the relative fluorescence at 3 ms (VJ). It has been shown that the fluorescence recorded at this time interval correlates with the redox state of the photoactive PQ pool (Strasser et al., 2010; Kalaji et al.,

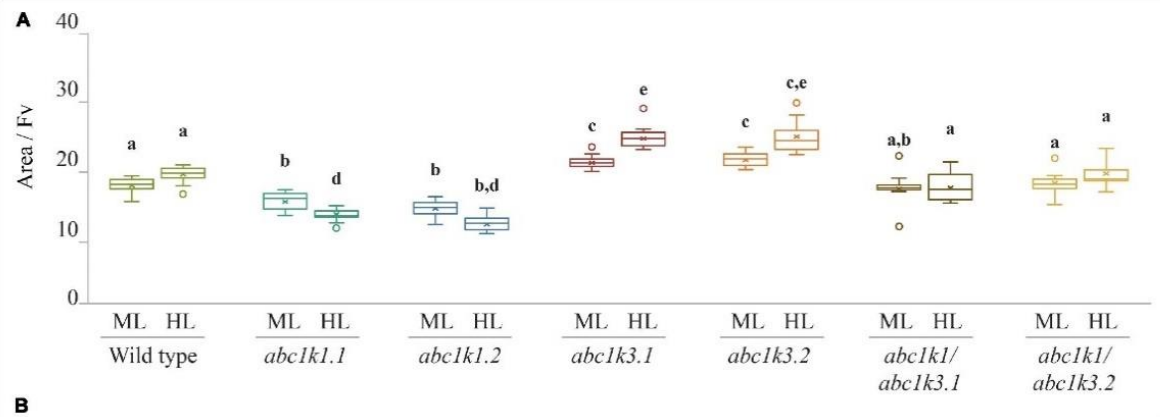

B

φET2o

	WT	*abc1k1.1*	*abc1k1.2*	*abc1k3.1*	*abc1k3.2*	*abc1k1/abc1k3.1*	*abc1k1/abc1k3.2*
ML	0.48 ± 0.02 ^{a}	**0.42 ± 0.03** ^{b}	**0.38 ± 0.04** ^{c}	0.48 ± 0.01 ^{a}	0.49 ± 0.01 ^{a}	**0.44 ± 0.02** ^{b}	**0.43 ± 0.03** ^{b}
HL 3h	0.42 ± 0.04 ^{b,c}	**0.31 ± 0.04** ^{d,e}	**0.26 ± 0.07** ^{e}	0.40 ± 0.03 ^{b,c}	0.40 ± 0.03 ^{b,c}	**0.32 ± 0.02** ^{d}	**0.33 ± 0.03** ^{d}

C

φRE1o

	WT	*abc1k1.1*	*abc1k1.2*	*abc1k3.1*	*abc1k3.2*	*abc1k1/abc1k3.1*	*abc1k1/abc1k3.2*
ML	0.14 ± 0.03 ^{a}	**0.11 ± 0.02** ^{b}	**0.10 ± 0.02** ^{b}	**0.18 ± 0.01** ^{c}	**0.18 ± 0.02** ^{c}	0.14 ± 0.02 ^{a}	0.13 ± 0.03 ^{a}
HL 3h	0.15 ± 0.02 ^{a}	**0.08 ± 0.01** ^{d}	**0.06 ± 0.02** ^{d}	**0.18 ± 0.02** ^{c}	**0.17 ± 0.02** ^{c}	0.11 ± 0.02 ^{a,b}	0.12 ± 0.02 ^{a,b}

FIGURE 4 | High light as a moderate impact on photosynthetic electron transport fluxes in *abc1k1/abc1k3*. Fully expanded leaves from Wild type (WT), *abc1k1.1, -2, abc1k3.1, -2,* and *abc1k1/abc1k3.1, -2* plants were collected under moderate light conditions (120 μmol of photons m^{-2} s^{-1}) (ML) and after 3 h of high light (500 μmol of photons m^{-2} s^{-1}) (HL). **(A)** Normalized area (Area/Fv) above the chlorophyll fluorescence induction curve measured after 15 min of dark incubation. This value estimates the number of available electron carriers per PSII reaction center. **(B)** Quantum electron transport yield from Q_A to PQ pool (ΦET2o), and **(C)** until the PSI electron acceptors (ΦRE1o). These measures were performed with Handy-PEA (Hansatech Instruments). Whiskers and box plot shows the minimum, first quartile, median, average, third quartile, and maximum of each data set (n = 12 biologically independent samples). Superscript letters are used to indicate statistically different groups by paired Student's t-test ($p < 0.05$).

2014a). A high V_J value is recorded in samples where the photoactive PQ pool is mostly reduced, and it decreases with its oxidation (Tóth et al., 2007). The chlorophyll *a* fluorescence induction was measured at increasing time intervals of dark incubation after a saturating light pulse. The results show that the measured oxidation, which appears to be almost completely PTOX dependent, is faster in the *abc1k3* mutants, while severely impaired in *abc1k1* (**Figure 6A**).

A limitation of total PQ, as in the *sps2* mutant (Block et al., 2013; Pralon et al., 2019), resulted in a slower oxidation in the dark as well. The PQ oxidation in the *abc1k1/abc1k3* double mutant progressed more rapidly than in the *abc1k1* single mutant (**Figure 6A**). The dark re-oxidation of the photoactive PQ pool is independent on the photosynthetic ETC. In fact, all the tested mutant lines displayed the same kinetics when the PQ oxidation was performed by the cytochrome *b6f*, as observed when PSI was excited with far-red light (**Figure 6B**). The kinetics of PQ oxidation in the dark may be influenced by the level of accumulation of the PTOX protein (Ivanov et al., 2012). We therefore used immunodetection to test the PTOX accumulation in total protein samples from the different mutants. The result showed no differences at the protein level, which appeared to be uniform among the lines (**Supplementary Figure 3**). After 3 h under high light the dark re-oxidation of the photoactive PQ in the *abc1k1* mutant is almost completely blocked, and it is slower overall in all lines analyzed. Once again, the defect was milder in the *abc1k1/abc1k3* double mutant (**Supplementary Figure 4**). It is worth noting that after 3 h of high light the oxidation kinetics under far-red light were also affected in *abc1k1*, suggesting that 3 h of high light exposure induce a perturbation of the ETC, consistently with the previous report (Pralon et al., 2019).

This experiment shows that *abc1k1* is impaired in the regulation of the photoactive PQ redox state independently of the activity of the ETC. Considering the specific localization and identical protein levels of PTOX, this supports a model

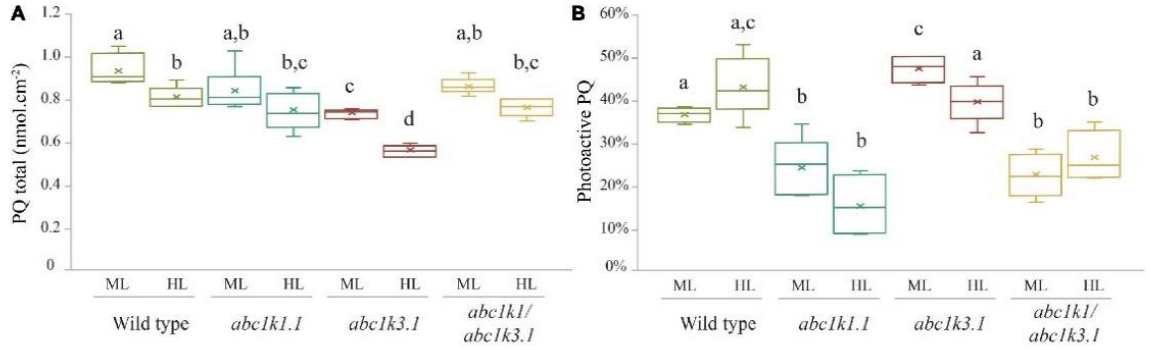

FIGURE 5 | Photoactive PQ pool is smaller in all the lines containing the *abc1k1* mutation. **(A)** Total plastoquinone content (nmol cm^{-2}) and **(B)** photoactive plastoquinone pool (as% of total PQ) were analyzed from leaves of Wild type, *abc1k1.1*, *abc1k3.2*, and *abc1k1/abc1k3.2* under moderate light and after 3 h high light. The photoactive plastoquinone pool was determined by the difference of the plastoquinol (PQH_2) amount measured when the PQ pool is maximally reduced by strong white light pulse (15 s at 2,000 m^{-2} s^{-1}), and the amount of PQH_2 measured when the PQ pool is fully oxidized after far-red illumination (2 min at 5.5 µmol of photons m^{-2} s^{-1}). Whiskers and box plot shows the minimum, first quartile, median, average, third quartile, and maximum of each data set ($n = 4$ biologically independent samples). Superscript letters are used to indicate statistically different groups by paired Student's *t*-test ($p < 0.05$).

of limited mobility of PQ. Interestingly, said defect is partially complemented by *abc1k3* mutation.

Major Thylakoid Membrane Protein Phosphorylation and State Transitions Are Partially Restored in abc1k1/abc1k3

A smaller photoactive PQ pool (**Figure 5B**) should be prone to over-reduction or at least to "mimic" a condition of over-reduction as fewer PQ molecules are available (**Figure 4B**). This would be expected to perturb state transitions (Bellafiore et al., 2005; Shapiguzov et al., 2010, 2016; Tikkanen et al., 2012; Trotta et al., 2016; Pralon et al., 2019). Cytochrome *b6f* activity is dependent on the redox state of PQ and regulates the activation of STN7, the principal kinase involved in LHCII phosphorylation. Therefore, we evaluated the phosphorylation status of the major thylakoid membrane proteins by immunodetection. Moreover, we measured the re-allocation of the mobile light harvesting complex II (LHCII) between the two photosystems by room temperature chlorophyll fluorescence in *abc1k1/abc1k3* during state 1 to state 2 transition induced by changes in the light spectrum. Both approaches were used as proxies to assess the redox state of the PQ pool *in vivo*.

The phosphorylation status of the thylakoid protein was assessed by anti-phosphothreonine immunoblotting on total protein extracts from leaves collected under moderate light and after 3 h high light exposure. Under moderate light, the thylakoid phosphoprotein pattern was similar among all the lines tested (**Figure 7A**). Compared to the moderate light, after 3 h of high light exposure PSII core proteins D1 (PsbA) and D2 (PsbD) were only slightly more phosphorylated in *abc1k1*, while their phosphorylation increased markedly in WT, *abc1k3* as well as in *abc1k1/abc1k3*. Similarly, after the high light stress, the LHCII proteins were highly phosphorylated in *abc1k3*, *abc1k1/abc1k3*, and WT, while the LHCII phosphorylation was clearly lower in *abc1k1* (**Figure 7A**). This suggests that, despite the shortage of photoactive PQ in *abc1k1/abc1k3* (**Figure 5B**), the STN7 kinase maintains its activity toward LHCII even after exposure to high light. Furthermore, neither the change in total PQ nor in the photoactive fraction had an impact on the abundance of selected photosynthetic proteins after 3 h of high light (**Figure 7B**).

To determine whether thylakoid protein phosphorylation observed in *abc1k1/abc1k3* correlated with the ability to perform state transitions we followed and measured room temperature chlorophyll *a* fluorescence kinetics on dark-adapted plants by switching red light supplemented with far-red light (State 1) to red light only (State 2). The quenching (fluorescence decline) caused by state transitions (qT), was calculated as the difference between the maximal fluorescence (FM) after "State 1" illumination (FM_ST1) and the one after "State 2" light (FM_ST2) normalized on maximal fluorescence (FM) (qT = (FM_ST1 – FM_ST2)/FM), which reflects the dissociation of antenna from PSII and its association with PSI.

Under moderate light, the qT in all genotypes was comparable to the WT, indicating their ability to perform transition from State 1 to State 2 and only *abc1k1* lines appeared to be slightly impaired (**Figure 7C**). *stn7/stn8*, which is completely unable to perform state transitions, was used as a negative control. After 3 h of high light exposure, *abc1k3* and WT maintained their capacity to perform state transitions, while *abc1k1* lines were defective in state transitions. After 3 h of high light, state transitions in *abc1k1/abc1k3* lines exhibited a level of quenching comparable to WT and *abc1k3* (**Figure 7C**). This shows that LHCII phosphorylation, and thus the activity of the STN7 kinase, which is maintained in *abc1k1/abc1k3* mutants, allows the state transitions after high light exposure.

DISCUSSION

The photosynthetic apparatus has to adapt to photo-oxidative stress induced by excess light in order to prevent thylakoid

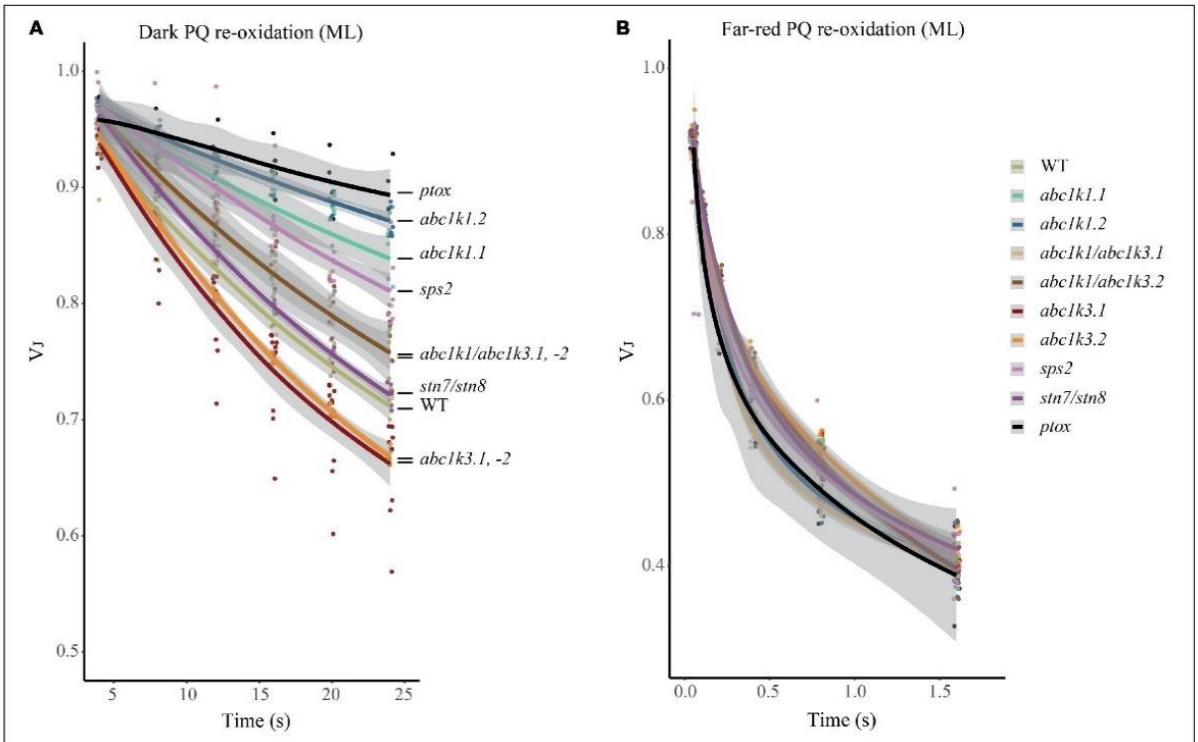

FIGURE 6 | Mutations of ABC1K1 and ABC1K3 influence the dark re-oxidation kinetic of the photoactive plastoquinone. The relative fluorescence after 3 ms (VJ) is plotted over the time from the previous saturating pulse. The sample was incubated in dark **(A)** or with far-red light **(B)**. Kinetics of the re-oxidation are shown by interpolation of the data points with a logarithmic curve with the deviation of the model in gray (R-Studio) for wild type (WT) *abc1k1.1, -2, abc1k3.1, -2,* and *abc1k1/abc1k3.1, -2, sps2, stn7/stn8, ptox* plants grown under moderate light (ML). These measures were performed with Handy-PEA (Hansatech Instruments) on detached leaves incubated for 10 min in dark.

membrane damage and maintain photosynthetic efficiency. Photo-protective strategies comprise adjustment of electron transport capacity (ETC) (Rochaix, 2011), equilibration of energy between photosystems (state transitions) (Rochaix, 2007) and induction of NPQ (Müller et al., 2001; Ruban, 2016). All three mechanisms are directly or indirectly related to the activity of the plastoquinone as an electron carrier. Recently, it has been demonstrated that ABC1K1 is implicated in photosynthesis regulation by homeostasis of photoactive PQ under high light (Pralon et al., 2019). In this study, we describe the involvement of ABC1K3 (Lundquist et al., 2013; Martinis et al., 2013; Huang et al., 2015), a close homolog of ABC1K1, in the same process.

We tested two *abc1k3* mutant lines for their ability to induce NPQ under increasing light intensities. Contrary to *abc1k1,* this mutation did not cause any perturbation in NPQ induction when compared with the WT (**Figure 2**). A previous report shows that, during several days of exposure to high light (500 μmol of photons m^{-2} s^{-1}), *abc1k3* had a tendency to induce slightly less NPQ compared to WT, however this difference was not statistically significant nor constant over the time course (Martinis et al., 2013). This suggests that the NPQ parameter alone is not sufficient to discriminate the photosynthetic adaptation of *abc1k3* from WT. In fact, the differences between WT and *abc1k3* are significant only when the photosynthetic ETC capacity is analyzed in detail (**Figures 3**, **4**). To further address the role of *abc1k3* in the photosynthetic regulation, we crossed this mutant with *abc1k1* to obtain *abc1k1/abc1k3* double mutant plants (**Figure 1**). The *abc1k3* mutation was capable to partially alleviate the NPQ defect observed in *abc1k1*; while the NPQ level in *abc1k1/abc1k3* was higher than in the single *abc1k1* mutant, it remained lower than in the WT (**Figure 2**).

In order to confirm that the NPQ perturbation is due to a lack of transport through the ETC, we measured the number of electrons transported per PSI after a saturating light pulse by analyzing the lag time of PSI oxidation. As expected from previous reports (Shikanai et al., 1999; Martinis et al., 2014; Pralon et al., 2019), *abc1k1* transfers less electrons to PSI, and the difference compared to the WT increases after exposure to 3 h high light. On the contrary, *abc1k3* was not impaired and appeared capable of maintaining a high level of electron transfer after 3 h of high light (**Figure 3**). In *abc1k1/abc1k3*, the electron transport capacity was still lower than the WT, however, more electrons were transferred per PSI compared to *abc1k1* and the decrease after 3 h of high light was comparable to the one observed in the WT (**Figure 3**). This finding suggests that the defect in the photosynthetic electron carriers of *abc1k1* was

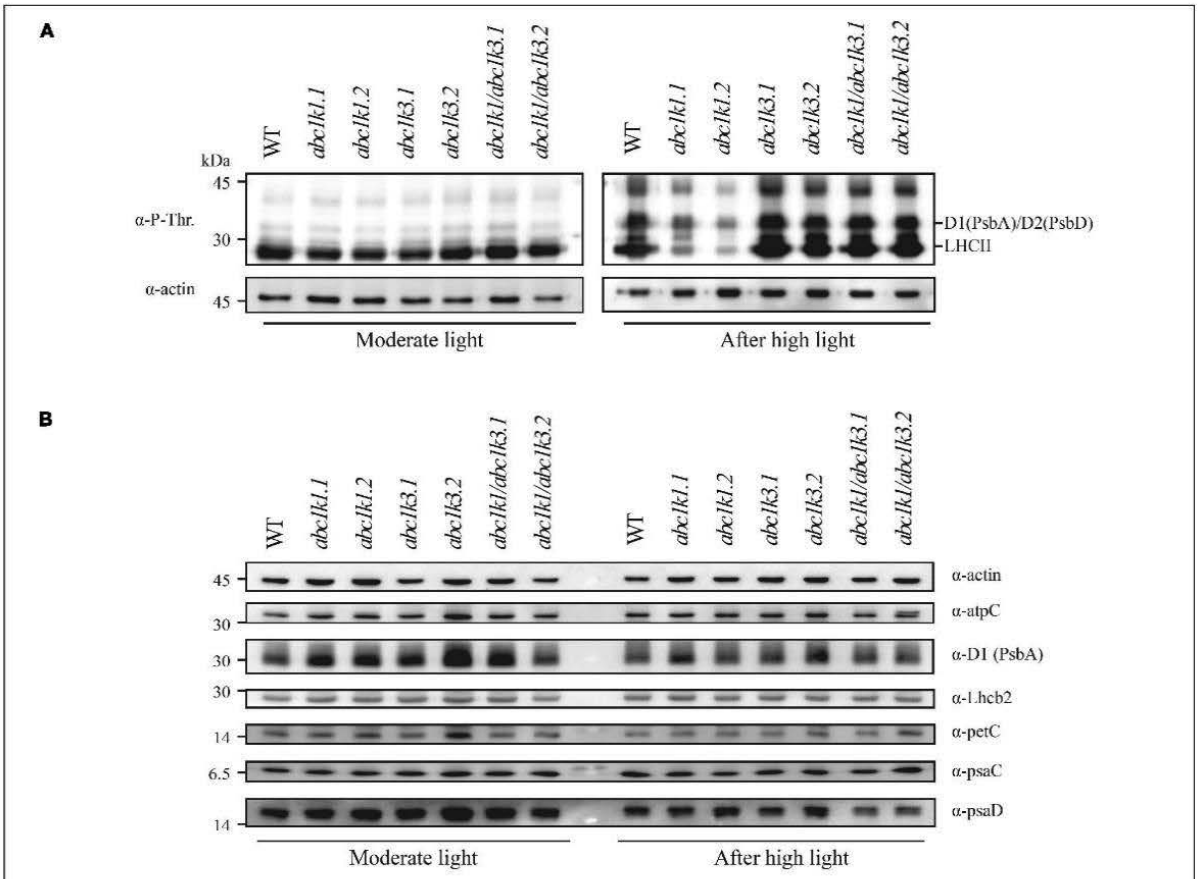

C

State transition quenching (qT)

	WT	*abc1k1.1*	*abc1k1.2*	*abc1k3.1*	*abc1k3.2*	*abc1k1/abc1k3.1*	*abc1k1/abc1k3.2*	*stn7/stn8*
ML	6,1 ± 1,2 [a]	3,8 ± 1,7 [b]	3,2 ± 2,4 [b]	6,1 ± 1,0 [a]	5,9 ± 1,3 [a]	6,0 ± 1,0 [a]	5,7 ± 0.9 [a]	**-3,8 ± 1,7** [c]
HL 3h	3,0 ± 1,2 [b]	**-2,1 ± 2,4** [c]	**-3,1 ± 1,9** [c]	2,4 ± 1,4 [b]	2,3 ± 1,0 [b]	3.0 ± 1.6 [a,b]	1.7 ± 2.6 [a,b,c]	**-11,0 ± 0,5** [d]

FIGURE 7 | Double mutant maintains thylakoid protein phosphorylation and state transitions after high light. **(A)** Total protein extracts of wild type (WT), *abc1k1.1, -2, abc1k3.1, -2,* and *abc1k1/abc1k3.1, -2* light-exposed leaves were separated by SDS PAGE, transferred on nitrocellulose membrane and decorated with anti-phosphothreonine antibody. The main thylakoid phospho-proteins are indicated on the right according to their size. Core photosystem II proteins D1 (PsbA) and D2 (PsbD) are indicated together due their poor resolution. **(B)** The accumulation of the principal photosynthetic complexes was assessed using antibodies against specific subunits of each complex: anti-Lhcb2 for the major LHCII, anti-D1 (PsbA) for PSII, anti-PetC for cytochrome *b6f*, anti-PsaD and anti-PsaC for PSI, and anti-AtpC for ATP synthase. Actin signal is shown as a loading control. **(C)** Fluorescence quenching related to the state transitions (qT) of wild type (WT), *abc1k1.1, -2, abc1k3.1, -2,* and *abc1k1/abc1k3.1, -2* under moderate light (120 μmol of photons m^{-2} s^{-1}) (ML) and after 3 h of high light (500 μmol of photons m^{-2} s^{-1}) (HL). qT was calculated from the maximal chlorophyll fluorescence measured after 10 min exposure to red light (660 nm) supplemented with far-red illumination (720 nm) "State 1" (FMST1) or to pure red light "State 2" (FMST2). Quenching related to state transition was calculated as qT = (FMST1 – FMST2)/FM. Each value represents the average of a pot containing 2–3 plants. Superscript letters are used to indicate statistically different groups ($p < 0.05$) by paired Student's *t*-test.

partially rescued in *abc1k1/abc1k3*, presumably by increasing the efficiency of the electron transfer in the ETC. In a previous report, the limitation of the electron transport capacity observed in *abc1k1* was linked to a depletion of the photoactive PQ pool (Pralon et al., 2019). However, the decrease in the number of electrons transported to PSI appeared to be more severe than the measured decrease in the size of the photoactive PQ pool. Therefore, it was hypothesized that the PQ mobility in the ETC plays an additional role in limiting the electron transport capacity. To investigate this hypothesis the energy fluxes along the ETC were analyzed by rapid fluorescence induction curves. The estimation of the number of electrons present in the ETC

before saturation, expressed as the Area/Fv (**Figure 4A**), was consistent with the P_{700} oxidation analysis (**Figure 3**). In fact, already under moderate light the normalized area was smaller in *abc1k1* mutant and larger in *abc1k3* in comparison to WT, consistent with *abc1k1* having limited electron transport and *abc1k3* having more carriers than the WT. In this condition, the *abc1k1/abc1k3* double mutant had an Area/Fv value in between those of the two single mutants, suggesting once again, a partial recovery of the photosynthetic electron transport. Upon exposure to high light only the *abc1k1* mutant showed a decrease in the number of available carriers; while all the other lines had a tendency to increase the Area/Fv value, compared to moderate light, indicating a better, or at least unchanged, electron transport capacity (**Figure 4A**). By analyzing the induction curve's principal steps, we can obtain hints regarding the different components that may be affected in the ETC. The first step, at 3 ms from the start of the saturating flash, was reported to be dependent of the Q_B redox state at the PSII and therefore linked to the redox state of the photoactive PQ pool (Tóth et al., 2007), which is also affected by the size of the photoactive PQ pool (Pralon et al., 2019). From the fluorescence value at 3 ms (F_J) it is possible to calculate the ΦET2o, the efficiency of the electron transport between Q_A and Q_B (which depends on the status of the photoactive PQ pool) (Strasser et al., 2010; Kalaji et al., 2014a,b). We observed that the ΦET2o is lower both in *abc1k1* and in *abc1k1/abc1k3*, suggesting a similar defect in the photoactive PQ pool. However, the defect appears to be somewhat milder in the double mutant compared to *abc1k1* (**Figure 4B**). The second step in the fluorescence rise occurs at 30 ms (F_I), and the level of the fluorescence recorded at this step is linked to the electron transport to the PSI final acceptors in the OJIP model (Strasser et al., 2010; Kalaji et al., 2014a,b). From the F_I value is also possible to calculate the electron transport efficiency, defined as ΦRE1o. Comparison of this efficiency revealed that *abc1k1* has a lower efficiency compared to the WT but that was not the case for *abc1k1/abc1k3*. In the latter, the ΦRE1o was the same as in the WT in moderate light, and was less affected upon the exposure to 3 h high light compared to *abc1k1* (**Figure 4C**). The *abc1k3* single mutation did not create any measurable defect in electron transport. On the contrary, the efficiency of the transport to PSI acceptors appeared to be even higher than in the WT, both under moderate light and after exposure to high light (**Figure 4C**). This suggests that the mutation of the *ABC1K3* gene leads to an increased efficiency in the electron mobility between PSII and PSI.

To support the fluorescence induction results we biochemically measured the size of the photoactive pool in the mutants exposed to moderate light and to high light. Consistent with the biophysical observations, the photoactive PQ pool was smaller in both *abc1k1* and *abc1k1/abc1k3* compared to the WT in moderate light condition (**Figure 5B**). Exposure to 3 h of high light had a limited effect on the size of the photoactive PQ pool in the four tested lines (**Figure 5B**). However, while the WT and the double *abc1k1/abc1k3* mutant display a tendency toward the increase of the photoactive PQ after 3 h of high light, we detected a slight decrease of the photoactive PQ pool in *abc1k1* as previously reported (Pralon et al., 2019). The depletion observed in this report was not significant as it was in the previous report, this may suggest that the photoactive PQ pool homeostasis relies on multiple factors (e.g., thylakoid organization, lipid distribution) and that ABC1K1, despite its prominent role, is not the only factor regulating the photoactive PQ pool size. A similar depletion of the photoactive PQ pool after 3 h of high light, was observed in *abc1k3* even though the relative photoactive PQ pool size was still larger than in *abc1k1*, and comparable to the WT (**Figure 5B**). On the contrary, the *abc1k1/abc1k3* double mutant constitutively displayed a small photoactive PQ pool that was not depleted by the exposure to high light (**Figure 5B**). This leads to the conclusion that the photoactive PQ pool size *per se* has a limited influence on photosynthetic efficiency, and that the photosynthetic defect becomes symptomatic only when PQ limitation is associated with an additional impairment in its mobility. Impaired PQ mobility may be the cause affecting the reoxidation of the photoactive PQ by PTOX, since it may require an exchange between grana stacks and stroma lamellae (**Figure 6A**; Stepien and Johnson, 2018). Furthermore, it would affect the exchange between the photoactive pool and the reservoir stored in the PGs necessary to maintain the photoactive PQ pool size (Pralon et al., 2019). We cannot exclude that the defect in the mobility and exchange between the different PQ pools stems from a defect in the thylakoid membrane composition. In fact, it has been previously reported that the mutation of *abc1k1* results in a lower amount of several prenyl lipids (Martinis et al., 2014) compared to the WT under control growth conditions (150 μmol of photons m^{-2} s^{-1}) as well as after several days of growth in high light (500 μmol of photons m^{-2} s^{-1}). However, the *abc1k3* mutant has a similar defect in the level of accumulation of these lipophilic compounds (Martinis et al., 2013). Therefore, no obvious correlation between the photosynthetic defect and the amount of the principal chloroplast lipids can be drawn at this stage.

A lower amount of total PQ, which decreased after 3 h of high light, was observed in *abc1k3* (**Figure 5A**). This decrease may be an indirect effect of the increased photosynthetic electron transport observed in *abc1k3* compared to WT. A possible explanation is that the amount or the redox state of PQ in the photoactive pool act as a signal to regulate PQ biosynthesis. This is supported also by previous reports showing a correlation between PQ biosynthesis and increase in light intensity (Zbierzak et al., 2010; Ksas et al., 2015). Consistent with this hypothesis, the increased relative PQ accumulation in the photoactive pool, observed in the *abc1k3* mutant under moderate light (**Figure 5B**), would alter this signal and therefore limit the biosynthesis resulting in a lower amount of total PQ (**Figures 5A**, **8**).

A crosstalk between photoactive PQ pool and biosynthesis would ensure the coupling of the photosynthetic electron transport efficiency with the production of a PQ reserve in the non-photoactive pool allowing fast adaptation to changing environmental conditions. It is necessary to point out that the decrease of total PQ after 3 h of high light was likely to be transitory since, under permissive light intensity, *abc1k3* was capable of restoring the total PQ amount to WT levels as previously shown (Martinis et al., 2013). We cannot exclude that ABC1K1 and ABC1K3 play an active role in this

signaling pathway, through still unidentified targets, therefore the mutation of these two kinases would result in a combined effect on the source of the signal, the photoactive PQ pool, as well as on the transmission of said signal.

Another feature linked to the *abc1k1* mutation was the loss of thylakoid protein phosphorylation. These phosphorylation events are mostly dependent on STN7 and STN8 kinases, activities of which depend on the redox status of the PQ pool (Aro and Ohad, 2003; Pesaresi et al., 2010; Puthiyaveetil, 2011; Puthiyaveetil et al., 2012). The mutation of *abc1k3* in the *abc1k1* background was sufficient to re-establish the phosphorylation of the thylakoid proteins to WT level after 3 h of high light. This observation has an important implication to understand the factors regulating the redox state of the photoactive PQ pool. In fact, the PQ pool redox state appears to be dependent also on the exchanges between the photoactive pool and storage sites and not only on the size of the photoactive pool and the activity of the ETC. We cannot exclude that protein phosphorylation has a positive feedback loop effect; in fact, the phosphorylation of the thylakoid proteins may favor their mobility in the membrane and by doing so increase also the mobility of the PQ between different portions of the thylakoid membrane (Kirchhoff et al., 2000; Fristedt et al., 2009; Kirchhoff, 2014). We also cannot exclude the involvement of the phosphorylation of other, less evident, targets such as CURT1b, the phosphorylation of which is also dependent on STN8 kinase (Trotta et al., 2019). By their phosphorylation level, the proteins imbedded in the thylakoid membrane may change the overall conformation of the membrane system and by this also the mobility and exchange of the PQ, and other lipids, between the photoactive pool and the reservoir (Armbruster et al., 2013). Moreover, ABC1K1 and ABC1K3 are also predicted to function as kinases; therefore, they may phosphorylate yet unknown target proteins leading to the regulation of the photosynthetic activity and potentially influencing membrane fluidity and/or thylakoid protein organization (Yokoyama et al., 2016).

The results lead us to propose the following model for the action of ABC1K1 and ABC1K3, being two kinases located at the plastoglobule (Vidi et al., 2006; Lundquist et al., 2012; Martinis et al., 2013, 2014). The role of ABC1K1 would be to promote the release, or the exchange of the PQ between the storage and the photoactive pool, while ABC1K3 would act in limiting such diffusion blocking this PQ flux (**Figure 8**). This model would explain the slightly bigger size of the photoactive pool in *abc1k3* and also the difference between *abc1k1* and *abc1k1/abc1k3*, the latter having a better photosynthetic performance since it is missing the ABC1K3 protein that would otherwise act as a "brake" to the PQ supply to the photoactive pool (**Figure 8**). To fully explain the observed results, we also have to assume that, without the activity of ABC1K1, the PQ tends to over-accumulate in the non-photoactive pool thus leading to a depletion of the photoactive pool. In this regard, the role of ABC1K1 is crucial to maintaining the photosynthetic efficiency by promoting the movement and accumulation of the PQ against its "passive" distribution. In contrast ABC1K3, acting as a brake to the mobilization of the non-photoactive pool, may have a more important role in other processes and phases of plant development when lipids need to be efficiently accumulated in the reserve compartments (e.g., senescence, fruit maturation). Previous reports describe a direct interaction between ABC1K1 and ABC1K3 (Lundquist et al., 2013). It is possible to hypothesize that this interaction allows a reciprocal regulation of the two kinases. For instance, a negative regulation of ABC1K3, mediated by ABC1K1, could partially explain the results of this report. In this scenario, the *abc1k1* mutation would cause a deregulation, or over activation, of the ABC1K3 kinase and this would then cause the photosynthetic defect. Following this model, the removal of ABC1K3, as in the double *abc1k1/abc1k3* mutant, would partially rescue the defect caused by the first mutation. It has

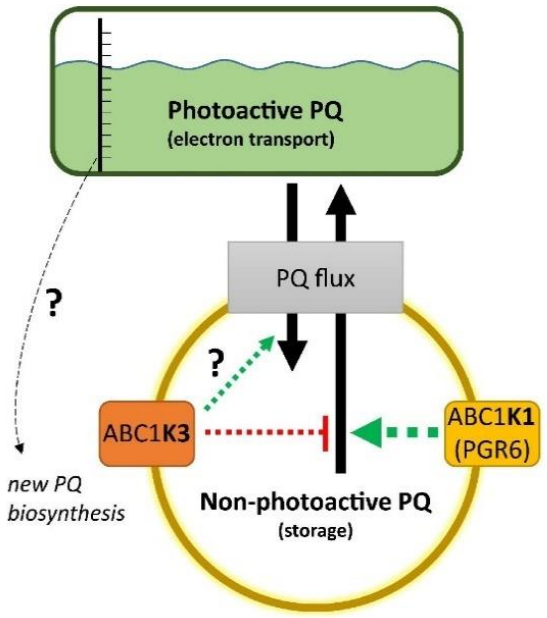

FIGURE 8 | Working model on the activity of ABC1K1 and ABC1K3 on the plastoquinone (PQ) redistribution. The two atypical kinases are enriched in the plastoglobule proteome, therefore presumably in the proximity of the non-photoactive PQ pool. The activity of the ABC1K1 promotes the mobilization of PQ toward the photoactive pool, while ABC1K3 counteracts this mobilization thus favoring the accumulation of PQ in the non-photoactive pool. In the absence of both kinases the PQ tends to accumulate in the non-photoactive pool, therefore a positive regulation of ABC1K3 on the flux from the photoactive to the non-photoactive pool is not essential, as highlighted by the question mark, but cannot be excluded in this model. The observation that in absence of both kinases PQ tends to accumulate in the non-photoactive pool suggests a prominent role of ABC1K1 in the PQ flux regulation (larger arrow). A not yet identified sensor of the size and/or the redox state of the photoactive PQ pool may serve to regulate the level of PQ biosynthesis. When the relative size of the photoactive pool is larger, and the electron transport more efficient as in the *abc1k3* mutant, the signal promoting PQ biosynthesis may be dimmed resulting in a lower amount of total PQ. The dashed arrows represent that the regulation of the PQ fluxes, mediated by the two atypical kinases, is likely to be indirect. Although the effect on PQ flux is opposite, the presented working model cannot exclude that the two atypical kinases act via separate mechanisms and that the impact observed on PQ mobility is a consequence of the alteration of their primary targets.

to be underlined that the physiological state of the double mutant *abc1k1/abc1k3* is still not optimal and that the absence of ABC1K3 only partially rescues the photosynthetic phenotype. This observation is thus consistent with previous reports showing that the double mutant, lacking both kinases, displays a stunted phenotype under prolonged stress conditions to which is unable to adapt (Lundquist et al., 2013).

CONCLUSION

In conclusion, we show that the *abc1k3* mutation allows a partial recovery of the *pgr6/abc1k1* phenotype. Consequently, ABC1K1 and ABC1K3 act in an opposite manner in order to cope with short-term high light. Therefore, we suggest that the system of the atypical kinases ABC1K1 and ABC1K3 allows a dynamic regulation of the PQ pool mobility and availability, which is fundamental for the plant to cope with variations in environmental conditions. In the working model ABC1K3 would act by limiting the distribution of PQ to the photoactive pool, while ABC1K1 acts in the opposite way. The role of ABC1K1 would be prominent considering that, without any regulation, the relative amount of PQ in the photoactive pool is lower, as is the case for the double *abc1k1/abc1k3* mutant. The opposing activities of these two atypical kinases would allow to equilibrate the amount of PQ, and potentially other lipids, between the storage compartments and the thylakoid membrane. Finally, a hypothetical signaling mechanism from the photoactive PQ pool to the PQ biosynthesis could explain the decreased amount of total PQ observed in *abc1k3* (**Figure 8**). Overall, the ABC1K1/ABC1K3 mechanism, by regulating lipid partitioning, could be important to allow plastid plasticity that is essential for the progression into different developmental stages of the plant life.

DATA AVAILABILITY STATEMENT

The raw data supporting the conclusions of this article will be made available by the authors, without undue reservation, to any qualified researcher.

AUTHOR CONTRIBUTIONS

TP, VS, PL, and FK designed the experiments. TP, JC, RP, BK, VS, PL, MH, and GF performed all the experiments. TP, VS, PL, MH, GF, and FK contributed to the analysis and the interpretation of the results. TP, PL, MH, GF, and FK wrote the manuscript.

FUNDING

This work was supported by the Swiss National Science Foundation (SNSF) grants 31003A_156998, 31003A_179417, and 31003A_176191. GF acknowledges support from the LabEX GRAL, ANR-10-LABX-49-01 financed within the University Grenoble Alpes graduate school (Ecoles Universitaires de Recherche) CBH-EUR-GS (ANR-17-EURE-0003).

ACKNOWLEDGMENTS

The Laboratory of Plant Physiology thanks Véronique Douet for her technical support during the project.

SUPPLEMENTARY MATERIAL

The Supplementary Material for this article can be found online at: https://www.frontiersin.org/articles/10.3389/fpls.2020.00337/full#supplementary-material

REFERENCES

Allen, J. F., Bennett, J., Steinback, K. E., and Arntzen, C. J. (1981). Chloroplast protein phosphorylation couples plastoquinone redox state to distribution of excitation energy between photosystems. *Nature* 291, 25–29. doi: 10.1038/291025a0

Armbruster, U., Labs, M., Pribil, M., Viola, S., Xu, W., Scharfenberg, M., et al. (2013). *Arabidopsis* CURVATURE THYLAKOID1 proteins modify thylakoid architecture by inducing membrane curvature. *Plant Cell* 25, 2661–2678. doi: 10.1105/tpc.113.113118

Aro, E. M., and Ohad, I. (2003). Redox regulation of thylakoid protein phosphorylation. *Antioxid. Redox Signal.* 5, 55–67. doi: 10.1089/152308603321223540

Aro, E. M., Virgin, I., and Andersson, B. (1993). Photoinhibition of photosystem II. Inactivation, protein damage and turnover. *Biochim. Biophys. Acta* 1143, 113–134. doi: 10.1016/0005-2728(93)90134-2

Austin, J. R. II, Frost, E., Vidi, P. A., Kessler, F., and Staehelin, L. A. (2006). Plastoglobules are lipoprotein subcompartments of the chloroplast that are permanently coupled to thylakoid membranes and contain biosynthetic enzymes. *Plant Cell* 18, 1693–1703. doi: 10.1105/tpc.105.039859

Bellafiore, S., Barneche, F., Peltier, G., and Rochaix, J. D. (2005). State transitions and light adaptation require chloroplast thylakoid protein kinase STN7. *Nature* 433, 892–895. doi: 10.1038/nature03286

Blackwell, M., Gibas, C., Gygax, S., Roman, D., and Wagner, B. (1994). The plastoquinone diffusion coefficient in chloroplasts and its mechanistic implications. *Biochim. Biophys. Acta Bioenerg.* 1183, 533–543. doi: 10.1016/0005-2728(94)90081-7

Block, A., Fristedt, R., Rogers, S., Kumar, J., Barnes, B., Barnes, J., et al. (2013). Functional modeling identifies paralogous solanesyl-diphosphate synthases that assemble the side chain of plastoquinone-9 in plastids. *J. Biol. Chem.* 288, 27594–27606. doi: 10.1074/jbc.M113.492769

Bonardi, V., Pesaresi, P., Becker, T., Schleiff, E., Wagner, R., Pfannschmidt, T., et al. (2005). Photosystem II core phosphorylation and photosynthetic acclimation require two different protein kinases. *Nature* 437, 1179–1182. doi: 10.1038/nature04016

Bousquet, I., Dujardin, G., and Slonimski, P. P. (1991). ABC1, a novel yeast nuclear gene has a dual function in mitochondria: it suppresses a cytochrome b mRNA translation defect and is essential for the electron transfer in the bc 1 complex. *EMBO J.* 10, 2023–2031. doi: 10.1002/j.1460-2075.1991.tb07732.x

Brasseur, G., Tron, P., Dujardin, G., Slonimski, P. P., and Brivet-Chevillotte, P. (1997). The nuclear ABC1 gene is essential for the correct conformation and functioning of the cytochrome bc1 complex and the neighbouring complexes II and IV in the mitochondrial respiratory chain. *Eur. J. Biochem.* 246, 103–111. doi: 10.1111/j.1432-1033.1997.t01-1-00103.x

Dall'Osto, L., Caffarri, S., and Bassi, R. (2005). A mechanism of nonphotochemical energy dissipation, independent from PsbS, revealed by a conformational

change in the antenna protein CP26. *Plant Cell* 17, 1217–1232. doi: 10.1105/tpc.104.030601

Dumas, L., Zito, F., Blangy, S., Auroy, P., Johnson, X., Peltier, G., et al. (2017). A stromal region of cytochrome b6f subunit IV is involved in the activation of the Stt7 kinase in *Chlamydomonas*. *Proc. Natl. Acad. Sci. U.S.A.* 114, 12063–12068. doi: 10.1073/pnas.1713343114

Ferretti, U., Ciura, J., Ksas, B., Rac, M., Sedlarova, M., Kruk, J., et al. (2018). Chemical quenching of singlet oxygen by plastoquinols and their oxidation products in *Arabidopsis*. *Plant J.* 95, 848–861. doi: 10.1111/tpj.13993

Finazzi, G., Rappaport, F., Furia, A., Fleischmann, M., Rochaix, J. D., Zito, F., et al. (2002). Involvement of state transitions in the switch between linear and cyclic electron flow in Chlamydomonas reinhardtii. *EMBO Rep.* 3, 280–285. doi: 10.1093/embo-reports/kvf047

Fristedt, R., Willig, A., Granath, P., Crèvecoeur, M., Rochaix, J. D., and Vener, A. V. (2009). Phosphorylation of photosystem II controls functional macroscopic folding of photosynthetic membranes in *Arabidopsis*. *Plant Cell* 21, 3950–3964. doi: 10.1105/tpc.109.069435

Gaude, N., Bréhélin, C., Tischendorf, G., Kessler, F., and Dormann, P. (2007). Nitrogen deficiency in *Arabidopsis* affects galactolipid composition and gene expression and results in accumulation of fatty acid phytyl esters. *Plant J.* 49, 729–739. doi: 10.1111/j.1365-313x.2006.02992.x

Gong, H. S., and Ohad, I. (1991). The PQ/PQH2 ratio and occupancy of photosystem II-QB site by plastoquinone control the degradation of D1 protein during photoinhibition in vivo. *J. Biol. Chem.* 266, 21293–21299.

Gruszka, J., Pawlak, A., and Kruk, J. (2008). Tocochromanols, plastoquinol, and other biological prenyllipids as singlet oxygen quenchers-determination of singlet oxygen quenching rate constants and oxidation products. *Free Radic. Biol. Med.* 45, 920–928. doi: 10.1016/j.freeradbiomed.2008.06.025

Hall, J. D., Barr, R., Al-Abbas, A. H., and Crane, F. L. (1972). The Ultrastructure of chloroplasts in mineral-deficient maize leaves. *Plant Physiol.* 50, 404–409. doi: 10.1104/pp.50.3.404

Houyoux, P.-A., Ghysels, B., Lecler, R., and Franck, F. (2011). Interplay between non-photochemical plastoquinone reduction and re-oxidation in pre-illuminated *Chlamydomonas reinhardtii*: a chlorophyll fluorescence study. *Photosynth. Res.* 110:13. doi: 10.1007/s11120-011-9686-5

Huang, H., Yang, M., Su, Y., Qu, L., and Deng, X. W. (2015). *Arabidopsis* atypical kinases ABC1K1 and ABC1K3 act oppositely to cope with photodamage under red light. *Mol Plant* 8, 1122–1124. doi: 10.1016/j.molp.2015.04.003

Ivanov, A. G., Rosso, D., Savitch, L. V., Stachula, P., Rosembert, M., Oquist, G., et al. (2012). Implications of alternative electron sinks in increased resistance of PSII and PSI photochemistry to high light stress in cold-acclimated *Arabidopsis thaliana*. *Photosynth. Res.* 113, 191–206. doi: 10.1007/s11120-012-9769-y

Joet, T., Genty, B., Josse, E. M., Kuntz, M., Cournac, L., and Peltier, G. (2002). Involvement of a plastid terminal oxidase in plastoquinone oxidation as evidenced by expression of the *Arabidopsis thaliana* enzyme in tobacco. *J. Biol. Chem.* 277, 31623–31630. doi: 10.1074/jbc.m203538200

Joliot, P., and Finazzi, G. (2010). Proton equilibration in the chloroplast modulates multiphasic kinetics of nonphotochemical quenching of fluorescence in plants. *Proc. Natl. Acad. Sci. U.S.A.* 107, 12728–12733. doi: 10.1073/pnas.1006399107

Joliot, P., and Joliot, A. (2006). Cyclic electron flow in C3 plants. *Biochim. Biophys. Acta* 1757, 362–368. doi: 10.1016/j.bbabio.2006.02.018

Kalaji, H. M., Oukarroum, A., Alexandrov, V., Kouzmanova, M., Brestic, M., Zivcak, M., et al. (2014a). Identification of nutrient deficiency in maize and tomato plants by *in vivo* chlorophyll *a* fluorescence measurements. *Plant Physiol. Biochem.* 81, 16–25. doi: 10.1016/j.plaphy.2014.03.029

Kalaji, H. M., Schansker, G., Ladle, R. J., Goltsev, V., Bosa, K., Allakhverdiev, S. I., et al. (2014b). Frequently asked questions about in vivo chlorophyll fluorescence: practical issues. *Photosynth. Res.* 122, 121–158. doi: 10.1007/s11120-014-0024-6

Kanwischer, M., Porfirova, S., Bergmüller, E., and Dörmann, P. (2005). Alterations in tocopherol cyclase activity in transgenic and mutant plants of *Arabidopsis* affect tocopherol content, tocopherol composition, and oxidative stress. *Plant Physiol.* 137, 713–723. doi: 10.1104/pp.104.054908

Karpinski, S., Reynolds, H., Karpinska, B., Wingsle, G., Creissen, G., and Mullineaux, P. (1999). Systemic signaling and acclimation in response to excess excitation energy in *Arabidopsis*. *Science* 284, 654–657. doi: 10.1126/science.284.5414.654

Kirchhoff, H. (2014). Diffusion of molecules and macromolecules in thylakoid membranes. *Biochim. Biophys. Acta Bioenerg.* 1837, 495–502. doi: 10.1016/j.bbabio.2013.11.003

Kirchhoff, H., Horstmann, S., and Weis, E. (2000). Control of the photosynthetic electron transport by PQ diffusion microdomains in thylakoids of higher plants. *Biochim. Biophys. Acta Bioenerg.* 1459, 148–168. doi: 10.1016/s0005-2728(00)00143-2

Kruk, J., and Karpinski, S. (2006). An HPLC-based method of estimation of the total redox state of plastoquinone in chloroplasts, the size of the photochemically active plastoquinone-pool and its redox state in thylakoids of *Arabidopsis*. *Biochim. Biophys. Acta* 1757, 1669–1675. doi: 10.1016/j.bbabio.2006.08.004

Ksas, B., Becuwe, N., Chevalier, A., and Havaux, M. (2015). Plant tolerance to excess light energy and photooxidative damage relies on plastoquinone biosynthesis. *Sci. Rep.* 5:10919. doi: 10.1038/srep10919

Ksas, B., Legeret, B., Ferretti, U., Chevalier, A., Pospisil, P., Alric, J., et al. (2018). The plastoquinone pool outside the thylakoid membrane serves in plant photoprotection as a reservoir of singlet oxygen scavengers. *Plant Cell Environ.* 41, 2277–2287. doi: 10.1111/pce.13202

Lavergne, J., and Joliot, P. (1991). Restricted diffusion in photosynthetic membranes. *Trends Biochem. Sci.* 16, 129–134. doi: 10.1016/0968-0004(91)90054-y

Lennon, A. M., Prommeenate, P., and Nixon, P. J. (2003). Location, expression and orientation of the putative chlororespiratory enzymes, Ndh and IMMUTANS, in higher-plant plastids. *Planta* 218, 254–260. doi: 10.1007/s00425-003-1111-7

Li, L., Aro, E. M., and Millar, A. H. (2018). Mechanisms of photodamage and protein turnover in photoinhibition. *Trends Plant Sci.* 23, 667–676. doi: 10.1016/j.tplants.2018.05.004

Li, Z., Wakao, S., Fischer, B. B., and Niyogi, K. K. (2009). Sensing and responding to excess light. *Annu. Rev. Plant Biol.* 60, 239–260. doi: 10.1146/annurev.arplant.58.032806.103844

Lichtenthaler, H. K., and Peveling, E. (1966). Plastoglobuli in different types of plastids from *Allium cepa* L. *Planta* 72, 1–13. doi: 10.1007/BF00388140

Lippold, F., vom Dorp, K., Abraham, M., Holzl, G., Wewer, V., Yilmaz, J. L., et al. (2012). Fatty acid phytyl ester synthesis in chloroplasts of *Arabidopsis*. *Plant Cell* 24, 2001–2014. doi: 10.1105/tpc.112.095588

Lohscheider, J. N., and Rio Bartulos, C. (2016). Plastoglobules in algae: a comprehensive comparative study of the presence of major structural and functional components in complex plastids. *Mar. Genomics* 28, 127–136. doi: 10.1016/j.margen.2016.06.005

Lundquist, P. K., Poliakov, A., Bhuiyan, N. H., Zybailov, B., Sun, Q., and van Wijk, K. J. (2012). The functional network of the *Arabidopsis* plastoglobule proteome based on quantitative proteomics and genome-wide coexpression analysis. *Plant Physiol.* 158, 1172–1192. doi: 10.1104/pp.111.193144

Lundquist, P. K., Poliakov, A., Giacomelli, L., Friso, G., Appel, M., McQuinn, R. P., et al. (2013). Loss of plastoglobule kinases ABC1K1 and ABC1K3 causes conditional degreening, modified prenyl-lipids, and recruitment of the jasmonic acid pathway. *Plant Cell* 25, 1818–1839. doi: 10.1105/tpc.113.111120

Martinis, J., Glauser, G., Valimareanu, S., and Kessler, F. (2013). A chloroplast ABC1-like kinase regulates vitamin E metabolism in *Arabidopsis*. *Plant Physiol.* 162, 652–662. doi: 10.1104/pp.113.218644

Martinis, J., Glauser, G., Valimareanu, S., Stettler, M., Zeeman, S. C., Yamamoto, H., et al. (2014). ABC1K1/PGR6 kinase: a regulatory link between photosynthetic activity and chloroplast metabolism. *Plant J.* 77, 269–283. doi: 10.1111/tpj.12385

Miyao, M. (1994). Involvement of active oxygen species in degradation of the D1 protein under strong illumination in isolated subcomplexes of photosystem II. *Biochemistry* 33, 9722–9730. doi: 10.1021/bi00198a043

Moejes, F. W., Matuszynska, A., Adhikari, K., Bassi, R., Cariti, F., Cogne, G., et al. (2017). A systems-wide understanding of photosynthetic acclimation in algae and higher plants. *J. Exp. Bot.* 68, 2667–2681. doi: 10.1093/jxb/erx137

Mollet, J., Delahodde, A., Serre, V., Chretien, D., Schlemmer, D., Lombes, A., et al. (2008). CABC1 gene mutations cause ubiquinone deficiency with cerebellar ataxia and seizures. *Am. J. Hum. Genet.* 82, 623–630. doi: 10.1016/j.ajhg.2007.12.022

Müller, P., Li, X. P., and Niyogi, K. K. (2001). Non-photochemical quenching. A response to excess light energy. *Plant Physiol.* 125, 1558–1566. doi: 10.1104/pp.125.4.1558

Munné-Bosch, S., and Alegre, L. (2002). Plant aging increases oxidative stress in chloroplasts. *Planta* 214, 608–615. doi: 10.1007/s004250100646

Nilkens, M., Kress, E., Lambrev, P., Miloslavina, Y., Müller, M., Holzwarth, A. R., et al. (2010). Identification of a slowly inducible zeaxanthin-dependent component of non-photochemical quenching of chlorophyll fluorescence generated under steady-state conditions in *Arabidopsis*. *Biochim. Biophys. Acta Bioenerg.* 1797, 466–475. doi: 10.1016/j.bbabio.2010.01.001

Nowicka, B., and Kruk, J. (2012). Plastoquinol is more active than alpha-tocopherol in singlet oxygen scavenging during high light stress of *Chlamydomonas reinhardtii*. *Biochim. Biophys. Acta* 1817, 389–394. doi: 10.1016/j.bbabio.2011.12.002

Pesaresi, P., Hertle, A., Pribil, M., Schneider, A., Kleine, T., and Leister, D. (2010). Optimizing photosynthesis under fluctuating light. *Plant Signal. Behav.* 5, 21–25. doi: 10.4161/psb.5.1.10198

Pesaresi, P., Pribil, M., Wunder, T., and Leister, D. (2011). Dynamics of reversible protein phosphorylation in thylakoids of flowering plants: the roles of STN7, STN8 and TAP38. *Biochim. Biophys. Acta* 1807, 887–896. doi: 10.1016/j.bbabio.2010.08.002

Pfannschmidt, T. (2003). Chloroplast redox signals: how photosynthesis controls its own genes. *Trends Plant Sci.* 8, 33–41. doi: 10.1016/s1360-1385(02)00005-5

Pfannschmidt, T., Nilsson, A., and Allen, J. F. (1999). Photosynthetic control of chloroplast gene expression. *Nature* 397:625. doi: 10.1038/17624

Poon, W. W., Davis, D. E., Ha, H. T., Jonassen, T., Rather, P. N., and Clarke, C. F. (2000). Identification of *Escherichia coli* ubiB, a gene required for the first monooxygenase step in ubiquinone biosynthesis. *J. Bacteriol.* 182, 5139–5146. doi: 10.1128/jb.182.18.5139-5146.2000

Pralon, T., Shanmugabalaji, V., Longoni, P., Glauser, G., Ksas, B., Collombat, J., et al. (2019). Plastoquinone homoeostasis by *Arabidopsis* proton gradient regulation 6 is essential for photosynthetic efficiency. *Commun. Biol.* 2:220. doi: 10.1038/s42003-019-0477-4

Puthiyaveetil, S. (2011). A mechanism for regulation of chloroplast LHC II kinase by plastoquinol and thioredoxin. *FEBS Lett.* 585, 1717–1721. doi: 10.1016/j.febslet.2011.04.076

Puthiyaveetil, S., Ibrahim, I. M., and Allen, J. F. (2012). Oxidation-reduction signalling components in regulatory pathways of state transitions and photosystem stoichiometry adjustment in chloroplasts. *Plant Cell Environ.* 35, 347–359. doi: 10.1111/j.1365-3040.2011.02349.x

Rintamaki, E., Kettunen, R., and Aro, E. M. (1996). Differential D1 dephosphorylation in functional and photodamaged photosystem II centers. Dephosphorylation is a prerequisite for degradation of damaged D1. *J. Biol. Chem.* 271, 14870–14875. doi: 10.1074/jbc.271.25.14870

Rintamaki, E., Salonen, M., Suoranta, U. M., Carlberg, I., Andersson, B., and Aro, E. M. (1997). Phosphorylation of light-harvesting complex II and photosystem II core proteins shows different irradiance-dependent regulation in vivo. Application of phosphothreonine antibodies to analysis of thylakoid phosphoproteins. *J. Biol. Chem.* 272, 30476–30482. doi: 10.1074/jbc.272.48.30476

Rochaix, J. D. (2007). Role of thylakoid protein kinases in photosynthetic acclimation. *FEBS Lett.* 581, 2768–2775. doi: 10.1016/j.febslet.2007.04.038

Rochaix, J. D. (2011). Regulation of photosynthetic electron transport. *Biochim. Biophys. Acta* 1807, 375–383. doi: 10.1016/j.bbabio.2010.11.010

Rochaix, J. D. (2013). Redox regulation of thylakoid protein kinases and photosynthetic gene expression. *Antioxid. Redox Signal.* 18, 2184–2201. doi: 10.1089/ars.2012.5110

Rottet, S., Devillers, J., Glauser, G., Douet, V., Besagni, C., and Kessler, F. (2016). Identification of plastoglobules as a site of carotenoid cleavage. *Front. Plant Sci.* 7:1855. doi: 10.3389/fpls.2016.01855

Ruban, A. V. (2016). Nonphotochemical chlorophyll fluorescence quenching: mechanism and effectiveness in protecting plants from photodamage. *Plant Physiol.* 170, 1903–1916. doi: 10.1104/pp.15.01935

Ruban, A. V. (2018). Light harvesting control in plants. *FEBS Lett.* 592, 3030–3039. doi: 10.1002/1873-3468.13111

Shapiguzov, A., Chai, X., Fucile, G., Longoni, P., Zhang, L., and Rochaix, J. D. (2016). Activation of the Stt7/STN7 Kinase through dynamic interactions with the cytochrome b6f complex. *Plant Physiol.* 171, 82–92. doi: 10.1104/pp.15.01893

Shapiguzov, A., Ingelsson, B., Samol, I., Andres, C., Kessler, F., Rochaix, J. D., et al. (2010). The PPH1 phosphatase is specifically involved in LHCII dephosphorylation and state transitions in *Arabidopsis*. *Proc. Natl. Acad. Sci. U.S.A.* 107, 4782–4787. doi: 10.1073/pnas.0913810107

Shikanai, T., Munekage, Y., Shimizu, K., Endo, T., and Hashimoto, T. (1999). Identification and characterization of *Arabidopsis* mutants with reduced quenching of chlorophyll fluorescence. *Plant Cell Physiol.* 40, 1134–1142. doi: 10.1093/oxfordjournals.pcp.a029498

Spicher, L., Glauser, G., and Kessler, F. (2016). Lipid antioxidant and galactolipid remodeling under temperature stress in tomato plants. *Front. Plant Sci.* 7:167. doi: 10.3389/fpls.2016.00167

Steinmuller, D., and Tevini, M. (1985). Composition and function of plastoglobuli : 1. Isolation and purification from chloroplasts and chromoplasts. *Planta* 163, 201–207. doi: 10.1007/BF00393507

Stepien, P., and Johnson, G. N. (2018). Plastid terminal oxidase requires translocation to the grana stacks to act as a sink for electron transport. *Proc. Natl. Acad. Sci. U.S.A.* 115, 9634–9639. doi: 10.1073/pnas.1719070115

Stirbet, A., Lazár, D., Kromdijk, J., and Govindjee (2018). Chlorophyll *a* fluorescence induction: can just a one-second measurement be used to quantify abiotic stress responses? *Photosynthetica* 56, 86–104. doi: 10.1007/s11099-018-0770-3

Strasser, R. J., Tsimilli-Michael, M., Qiang, S., and Goltsev, V. (2010). Simultaneous in vivo recording of prompt and delayed fluorescence and 820-nm reflection changes during drying and after rehydration of the resurrection plant *Haberlea rhodopensis*. *Biochim. Biophys. Acta* 1797, 1313–1326. doi: 10.1016/j.bbabio.2010.03.008

Suzuki, N., Koussevitzky, S., Mittler, R., and Miller, G. (2012). ROS and redox signalling in the response of plants to abiotic stress. *Plant Cell Environ.* 35, 259–270. doi: 10.1111/j.1365-3040.2011.02336.x

Sylak-Glassman, E. J., Malnoe, A., De Re, E., Brooks, M. D., Fischer, A. L., Niyogi, K. K., et al. (2014). Distinct roles of the photosystem II protein PsbS and zeaxanthin in the regulation of light harvesting in plants revealed by fluorescence lifetime snapshots. *Proc. Natl. Acad. Sci. U.S.A.* 111, 17498–17503. doi: 10.1073/pnas.1418317111

Taylor, A. O., and Craig, A. S. (1971). Plants under climatic stress: II. Low temperature, high light effects on chloroplast ultrastructure. *Plant Physiol.* 47, 719–725. doi: 10.1104/pp.47.5.719

Theis, J., and Schroda, M. (2016). Revisiting the photosystem II repair cycle. *Plant Signal. Behav.* 11:e1218587. doi: 10.1080/15592324.2016.1218587

Tikhonov, A. N. (2014). The cytochrome b6f complex at the crossroad of photosynthetic electron transport pathways. *Plant Physiol. Biochem.* 81, 163–183. doi: 10.1016/j.plaphy.2013.12.011

Tikkanen, M., Gollan, P. J., Suorsa, M., Kangasjarvi, S., and Aro, E. M. (2012). STN7 operates in retrograde signaling through controlling redox balance in the electron transfer chain. *Front. Plant Sci.* 3:277. doi: 10.3389/fpls.2012.00277

Tikkanen, M., Nurmi, M., Kangasjarvi, S., and Aro, E. M. (2008). Core protein phosphorylation facilitates the repair of photodamaged photosystem II at high light. *Biochim. Biophys. Acta* 1777, 1432–1437. doi: 10.1016/j.bbabio.2008.08.004

Tóth, S. Z., Schansker, G., and Strasser, R. J. (2007). A non-invasive assay of the plastoquinone pool redox state based on the OJIP-transient. *Photosynth. Res.* 93, 193. doi: 10.1007/s11120-007-9179-8

Trotta, A., Bajwa, A. A., Mancini, I., Paakkarinen, V., Pribil, M., and Aro, E. M. (2019). The role of phosphorylation dynamics of CURVATURE THYLAKOID 1B in plant thylakoid membranes. *Plant Physiol.* 181, 1615–1631. doi: 10.1104/pp.19.00942

Trotta, A., Suorsa, M., Rantala, M., Lundin, B., and Aro, E. M. (2016). Serine and threonine residues of plant STN7 kinase are differentially phosphorylated upon changing light conditions and specifically influence the activity and stability of the kinase. *Plant J.* 87, 484–494. doi: 10.1111/tpj.13213

Trouillard, M., Shahbazi, M., Moyet, L., Rappaport, F., Joliot, P., Kuntz, M., et al. (2012). Kinetic properties and physiological role of the plastoquinone terminal oxidase (PTOX) in a vascular plant. *Biochim. Biophys. Acta* 1817, 2140–2148. doi: 10.1016/j.bbabio.2012.08.006

van Wijk, K. J., and Kessler, F. (2017). Plastoglobuli: plastid microcompartments with integrated functions in metabolism, plastid developmental transitions, and environmental adaptation. *Annu. Rev. Plant Biol.* 68, 253–289. doi: 10.1146/annurev-arplant-043015-111737

Vasilikiotis, C., and Melis, A. (1994). Photosystem II reaction center damage and repair cycle: chloroplast acclimation strategy to irradiance stress. *Proc. Natl. Acad. Sci. U.S.A.* 91, 7222–7226. doi: 10.1073/pnas.91.15.7222

Vidi, P. A., Kanwischer, M., Baginsky, S., Austin, J. R., Csucs, G., Dormann, P., et al. (2006). Tocopherol cyclase (VTE1) localization and vitamin E accumulation in chloroplast plastoglobule lipoprotein particles. *J. Biol. Chem.* 281, 11225–11234. doi: 10.1074/jbc.m511939200

Wetzel, C. M., Jiang, C. Z., Meehan, L. J., Voytas, D. F., and Rodermel, S. R. (1994). Nuclear-organelle interactions: the immutans variegation mutant of *Arabidopsis* is plastid autonomous and impaired in carotenoid biosynthesis. *Plant J.* 6, 161–175. doi: 10.1046/j.1365-313x.1994.6020161.x

Yamori, W., and Shikanai, T. (2016). Physiological functions of cyclic electron transport around photosystem I in sustaining photosynthesis and plant growth. *Annu. Rev. Plant Biol.* 67, 81–106. doi: 10.1146/annurev-arplant-043015-112002

Yang, M., Huang, H., Zhang, C., Wang, Z., Su, Y., Zhu, P., et al. (2016). *Arabidopsis* atypical kinase ABC1K1 is involved in red light-mediated development. *Plant Cell Rep.* 35, 1213–1220. doi: 10.1007/s00299-016-1953-7

Yokoyama, R., Yamamoto, H., Kondo, M., Takeda, S., Ifuku, K., Fukao, Y., et al. (2016). Grana-localized proteins, RIQ1 and RIQ2, affect the organization of light-harvesting complex II and grana stacking in *Arabidopsis*. *Plant Cell* 28, 2261–2275. doi: 10.1105/tpc.16.00296

Ytterberg, A. J., Peltier, J. B., and van Wijk, K. J. (2006). Protein profiling of plastoglobules in chloroplasts and chromoplasts. A surprising site for differential accumulation of metabolic enzymes. *Plant Physiol.* 140, 984–997. doi: 10.1104/pp.105.076083

Zbierzak, A. M., Kanwischer, M., Wille, C., Vidi, P. A., Giavalisco, P., Lohmann, A., et al. (2010). Intersection of the tocopherol and plastoquinol metabolic pathways at the plastoglobule. *Biochem. J.* 425, 389–399. doi: 10.1042/BJ20090704

Zechmann, B. (2019). Ultrastructure of plastids serves as reliable abiotic and biotic stress marker. *PLoS One* 14:e0214811. doi: 10.1371/journal.pone.0214811

Conflict of Interest: The authors declare that the research was conducted in the absence of any commercial or financial relationships that could be construed as a potential conflict of interest.

3. General Conclusion

Plants have developed many mechanisms to cope with environmental changes and to maintain the efficiency of the photosynthesis inside the chloroplast. Photosynthesis is a highly complex bioenergetic mechanism and needs to be finely regulated in order to maintain celllar functions in various environmental conditions. For this reason, the chloroplast communicates continuously with the nucleus via a retrograde signaling system to regulate and coordinate the functions of both compartments. Plastoglobules, lipids droplets attached to the thylakoid membrane of the chloroplast, participate in chloroplast metabolism and in the maintenance of photosynthetic efficiency. Indeed, the ABC1K1 protein, localized inside plastoglobules, has been shown to be essential for plastoquinone homoeostasis thereby contributing to control photosynthetic electron transport. Consequently, the *abc1k1* mutant is defective in photosynthetic electron transport as well as NPQ (non-photochemical quenching). Interestingly, the *abc1k1* mutant displays a strong greening defect characterized by a pale green phenotype with a short hypocotyl under red light conditions. This phenotype is separable from the photosynthetic phenotype suggesting that ABC1K1 could have an additional role in chloroplast biogenesis especially under stressful light conditions.

Consequently, this PhD affords new insight into the role of the atypical ABC1K1 kinase in the regulation of chloroplast biogenesis and signaling under light stress conditions. Here, we showed that ABC1K1 interacts with the FTSH2/ EX1 signaling pathway to regulate the $^1O_2$ mediated retrograde signaling under red light conditions, when the PSII should be particularly excited.

This work demonstrates that the greening defect of *abc1k1* is not directly linked to the photosynthetic defect, but rather implicates a specific signal involving the degradation of Executer 1 (EX1) through the chloroplast protease FTSH. However, all the photosynthetic mutants tested, including *abc1k1*, had hypocotyls shorter than the wild type suggesting that the photosynthetic defects triggers other signals that, integrating with the phytochrome pathway, affect the hypocotyl elongation.

Our results suggest that the accumulation of EX1 protein in the *abc1k1* mutant leads to the arrest of chloroplast biogenesis during the early phase of the germination. This hypothesis is supported by the observation that the EX1 mutation in the *abc1k1* background results in a partial recovery of the *abc1k1* pale green phenotype under red light. Moreover, the discovery of a highly similar pale green phenotype for the *var2* (*ftsh2*) mutant under red light, which correlated with the accumulation of EX1, supports the hypothesis that the accumulation of EX1 itself constitutes a signal for the arrest of the chloroplast biogenesis.

During this PhD, we also showed that the *abc1k1* mutant displays a variegated phenotype under high light similar to that of the *var2* mutant, which also strongly suggested that ABC1K1 has a role in the chloroplast biogenesis regulation under light stress conditions (Pralon et al., 2019). Moreover, our work demonstrated that the *abc1k1* mutant is impaired in the dark-reoxidation of the plastoquinone pool, suggesting a defect in the mobility of photoactive plastoquinone in

this mutant. Interestingly, this defect is partially restored in the *abc1k1/abc1k3* mutant (Pralon et al., 2020).

We propose that the ABC1K1 protein may act as a sensor of $^1O_2$ in order to regulate the proteolysis of EX1 under stressful red or high light conditions. Even though there is no evidence that ABC1K1 directly senses $^1O_2$, a possible hypothesis would be that it senses the plastoquinone redox state which may act as proxy for the production of $^1O_2$ by PSII. In agreement with its role in plastoquinone homoeostasis, it is imaginable that ABC1K1 relays the redox state of the plastoquinone pool to induce EX1 degradation thereby promoting chloroplast biogenesis.

These results demonstrate a functional link between photosynthesis and chloroplast signaling and biogenesis. They identify an important contribution of plastoglobule proteins to this process. However, we still need to understand how and if ABC1K1 senses $^1O_2$ or the redox state of the plastoquinone pool to induce the EX1 signalling. The mechanisms of plastoquinone homoeostasis by ABC1K1 and its partner protein ABC1K3 remains unknown and needs to be elucidated in the future to better understand the molecular functions of ABC1K1 inside the chloroplast.

For the future perspectives, it will be interesting to confirm the link between ABC1K1 and the production of single oxygen by quantifying directly the accumulation of $^1O_2$ in *abc1k1* under red light and particularly in presence of DCMU using singlet oxygen green sensor (SOGS). The impact of the *abc1k1* mutation on the $^1O_2$ induced gene expression after 3 hours of red light should also allow us to determine whether ABC1K1 functions as a component of the $^1O_2$-mediated signaling under light stress conditions.

A second objective is to understand the link between ABC1K1-mediated plastoquinone homoeostasis and ABC1K1 signaling. How can the regulation of the plastoquinone pool by ABC1K1 affect the $^1O_2$-mediated signaling? To answer this question, it will be interesting to do some *in vitro* complementation experiments in *abc1k1* by adding exogenous plastoquinone to isolated thylakoids or by overexpressing enzymes involved in the biosynthesis of plastoquinone. To directly establish a link between ABC1K1 and the regulation of the plastoquinone pool, we can perform some binding experiments between ABC1K1 and the plastoquinone molecule.

In the pull-down experiment, we identified multiple subunits of the chloroplast NAD(P)H dehydrogenase (NDH) complex as a potential ABC1K1 interaction partners**.** The NDH complex being involved in the reduction of the plastoquinone pool through the cyclic electron flow. It will be interesting to determine to which extent the ABC1K1 protein regulates this complex and what the impact of the NDH complex is on the regulation of the plastoquinone pool.

To better understand the ABC1K1 molecular mechanisms, we should determine whether the ABC1K1 kinase activity is required for the protein functions by using *abc1k1* line complemented with a kinase mutant (ABC1K1 D400N). Similarly, we could also check if the phosphorylation state of ABC1K1 is important for its functions. We are currently segregating

abc1k1 lines that express ABC1K1 carrying point mutations in the phosphorylation sites to mimic a constitutively phosphorylated residues (ABC1K1 T604D T606D) or lacking phosphorylation sites (ABC1K1 T604A T606A) in both *abc1k1* and wild type backgrounds.

Since the EX1 protein has been identified as a potential ABC1K1 interaction partners, and seems to accumulate in the *abc1k1* mutant, we should confirm the interaction between the two proteins using bimolecular fluorescence complementation (BiFC) or a yeast two-hybrid experiment (for instance). The impact of EX1 accumulation on chloroplast biogenesis should also be analysed by overexpressing the EX1 protein in a wild type background or by trying to complement the *var2* mutant by the *ex1* mutation (for instance).

Finally, the role of the ABC1K3 protein in ABC1K1-mediated signalling should be elucidated. It will be interesting to understand why the *abc1k3* mutation complements the *abc1k1* phenotype. For example, we can analyse the interactions partners of ABC1K3 and complement *abc1k3* and *abc1k1/abc1k3* with an ABC1K3 protein mutated in the kinase domain (ABC1K3 D379N).

I think that these research questions would make very interesting projects for a future generation of PhD students and researchers in the field.

References

Adam, Z., Rudella, A., and van Wijk, K.J. (2006). Recent advances in the study of Clp, FtsH and other proteases located in chloroplasts. Current opinion in plant biology *9*, 234-240.

Aluru, M.R., Bae, H., Wu, D., and Rodermel, S.R. (2001). The Arabidopsis immutans mutation affects plastid differentiation and the morphogenesis of white and green sectors in variegated plants. Plant Physiol *127*, 67-77.

Amunts, A., Drory, O., and Nelson, N. (2007). The structure of a plant photosystem I supercomplex at 3.4 A resolution. Nature *447*, 58-63.

Andrès, C., Agne, B., and Kessler, F. (2010). The TOC complex: preprotein gateway to the chloroplast. Biochim Biophys Acta *1803*, 715-723.

Aro, E.M., Virgin, I., and Andersson, B. (1993). Photoinhibition of Photosystem II. Inactivation, protein damage and turnover. Biochim Biophys Acta *1143*, 113-134.

Aronsson, H., Schöttler, M.A., Kelly, A.l.A., Sundqvist, C., Dörmann, P., Karim, S., and Jarvis, P. (2008). Monogalactosyldiacylglycerol Deficiency in Arabidopsis Affects Pigment Composition in the Prolamellar Body and Impairs Thylakoid Membrane Energization and Photoprotection in Leaves Plant Physiology *148*, 580-592.

Austin, J.R., 2nd, Frost, E., Vidi, P.A., Kessler, F., and Staehelin, L.A. (2006a). Plastoglobules are lipoprotein subcompartments of the chloroplast that are permanently coupled to thylakoid membranes and contain biosynthetic enzymes. Plant Cell *18*, 1693-1703.

Austin, J.R., II, Frost, E., Vidi, P.-A., Kessler, F., and Staehelin, L.A. (2006b). Plastoglobules Are Lipoprotein Subcompartments of the Chloroplast That Are Permanently Coupled to Thylakoid Membranes and Contain Biosynthetic Enzymes. The Plant Cell *18*, 1693-1703.

Bailey, S., Thompson, E., Nixon, P.J., Horton, P., Mullineaux, C.W., Robinson, C., and Mann, N.H. (2002). A critical role for the Var2 FtsH homologue of Arabidopsis thaliana in the photosystem II repair cycle in vivo. J Biol Chem *277*, 2006-2011.

Balparda, M., Armas, A.M., Estavillo, G.M., Roschzttardtz, H., Pagani, M.A., and Gomez-Casati, D.F. (2020). The PAP/SAL1 retrograde signaling pathway is involved in iron homeostasis. Plant molecular biology *102*, 323-337.

Bellafiore, S., Barneche, F., Peltier, G., and Rochaix, J.D. (2005). State transitions and light adaptation require chloroplast thylakoid protein kinase STN7. Nature *433*, 892-895.

Ben Salem-Fnayou, A., Bouamama, B., Ghorbel, A., and Mliki, A. (2011). Investigations on the leaf anatomy and ultrastructure of grapevine (Vitis vinifera) under heat stress. Microscopy research and technique *74*, 756-762.

Block, A., Fristedt, R., Rogers, S., Kumar, J., Barnes, B., Barnes, J., Elowsky, C.G., Wamboldt, Y., Mackenzie, S.A., Redding, K., *et al.* (2013). Functional modeling identifies paralogous solanesyl-diphosphate synthases that assemble the side chain of plastoquinone-9 in plastids. J Biol Chem *288*, 27594-27606.

Block, M.A., Dorne, A.J., Joyard, J., and Douce, R. (1983). Preparation and characterization of membrane fractions enriched in outer and inner envelope membranes from spinach chloroplasts. II. Biochemical characterization. Journal of Biological Chemistry *258*, 13281-13286.

Blomqvist, L.A., Ryberg, M., and Sundqvist, C. (2008). Proteomic analysis of highly purified prolamellar bodies reveals their significance in chloroplast development. Photosynthesis Research *96*, 37-50.

Boudière, L., Michaud, M., Petroutsos, D., Rébeillé, F., Falconet, D., Bastien, O., Roy, S., Finazzi, G., Rolland, N., Jouhet, J., *et al.* (2014). Glycerolipids in photosynthesis: Composition, synthesis and trafficking. Biochimica et Biophysica Acta (BBA) - Bioenergetics *1837*, 470-480.

Bousquet, I., Dujardin, G., and Slonimski, P.P. (1991). ABC1, a novel yeast nuclear gene has a dual function in mitochondria: it suppresses a cytochrome b mRNA translation defect and is essential for the electron transfer in the bc 1 complex. *10*, 2023-2031.

Boyd, J.S., Mittelmeier, T.M., Lamb, M.R., and Dieckmann, C.L. (2011). Thioredoxin-family protein EYE2 and Ser/Thr kinase EYE3 play interdependent roles in eyespot assembly. Molecular biology of the cell *22*, 1421-1429.

Brasseur, G., Tron, G., Dujardin, G., Slonimski, P.P., and Brivet-Chevillotte, P. (1997). The nuclear ABC1 gene is essential for the correct conformation and functioning of the cytochrome bc1 complex and the neighbouring complexes II and IV in the mitochondrial respiratory chain. European journal of biochemistry *246*, 103-111.

Breyton, C. (2000). Conformational changes in the cytochrome b6f complex induced by inhibitor binding. J Biol Chem *275*, 13195-13201.

Caffarri S, Tibiletti T, Jennings RC, Santabarbara S. A comparison between plant photosystem I and photosystem II architecture and functioning. Curr Protein Pept Sci. 2014;15(4):296-331.

Carol, P., Stevenson, D., Bisanz, C., Breitenbach, J., Sandmann, G., Mache, R., Coupland, G., and Kuntz, M. (1999). Mutations in the Arabidopsis gene IMMUTANS cause a variegated phenotype by inactivating a chloroplast terminal oxidase associated with phytoene desaturation. Plant Cell *11*, 57-68.

Cazzaniga, S., Li, Z., Niyogi, K.K., Bassi, R., and Dall'Osto, L. (2012). The Arabidopsis szl1 mutant reveals a critical role of β-carotene in photosystem I photoprotection. Plant physiology *159*, 1745-1758.

Chattopadhyay, S., Ang, L.H., Puente, P., Deng, X.W., and Wei, N. (1998). Arabidopsis bZIP protein HY5 directly interacts with light-responsive promoters in mediating light control of gene expression. The Plant cell *10*, 673-683.

Chen, M., Choi, Y., Voytas, D., and Rodermel, S. (2000). Mutations in the Arabidopsis VAR2 locus cause leaf variegation due to the loss of chloroplast FtsH protease. The Plant Journal *22*, 303-313.

Chen, Z., and Gallie, D.R. (2012). Violaxanthin de-epoxidase is rate-limiting for non-photochemical quenching under subsaturating light or during chilling in Arabidopsis. Plant physiology and biochemistry : PPB *58*, 66-82.

Daum, B., and Kühlbrandt, W. (2011). Electron tomography of plant thylakoid membranes. J Exp Bot *62*, 2393-2402.

Do, T.Q., Hsu, A.Y., Jonassen, T., Lee, P.T., and Clarke, C.F. (2001). A Defect in Coenzyme Q Biosynthesis Is Responsible for the Respiratory Deficiency in Saccharomyces cerevisiae abc1Mutants*. Journal of Biological Chemistry *276*, 18161-18168.

Dogra, V., Duan, J., Lee, K.P., Lv, S., Liu, R., and Kim, C. (2017). FtsH2-Dependent Proteolysis of EXECUTER1 Is Essential in Mediating Singlet Oxygen-Triggered Retrograde Signaling in Arabidopsis thaliana. Front Plant Sci *8*, 1145.

Dogra, V., and Kim, C. (2020). Singlet Oxygen Metabolism: From Genesis to Signaling. Front Plant Sci *10*, 1640.

Estavillo, G.M., Crisp, P.A., Pornsiriwong, W., Wirtz, M., Collinge, D., Carrie, C., Giraud, E., Whelan, J., David, P., Javot, H., *et al.* (2011). Evidence for a SAL1-PAP Chloroplast Retrograde Pathway That Functions in Drought and High Light Signaling in Arabidopsis The Plant Cell *23*, 3992-4012.

Eugeni Piller, L., Abraham, M., Dörmann, P., Kessler, F., and Besagni, C. (2012a). Plastid lipid droplets at the crossroads of prenylquinone metabolism. Journal of Experimental Botany *63*, 1609-1618.

Eugeni Piller, L., Abraham, M., Dörmann, P., Kessler, F., and Besagni, C. (2012b). Plastid lipid droplets at the crossroads of prenylquinone metabolism. J Exp Bot *63*, 1609-1618.

Fork, D.C., and Herbert, S.K. (1993). Electron transport and photophosphorylation by Photosystem I in vivo in plants and cyanobacteria. Photosynth Res *36*, 149-168.

Fusco, G., and Minelli, A. (2010). Phenotypic plasticity in development and evolution: facts and concepts. Introduction. Philos Trans R Soc Lond B Biol Sci *365*, 547-556.

Galvez-Valdivieso, G., and Mullineaux, P.M. (2010). The role of reactive oxygen species in signalling from chloroplasts to the nucleus. Physiologia plantarum *138*, 430-439.

Gaude, N., Bréhélin, C., Tischendorf, G., Kessler, F., and Dörmann, P. (2007). Nitrogen deficiency in Arabidopsis affects galactolipid composition and gene expression and results in accumulation of fatty acid phytyl esters. Plant J *49*, 729-739.

Gould, S.B., Waller, R.F., and McFadden, G.I. (2008). Plastid evolution. Annual review of plant biology *59*, 491-517.

Greenwood, A.D., Leech, R.M., and Williams, J.P. (1963). The osmiophilic globules of chloroplasts: I. Osmiophilic globules as a normal component of chloroplasts and their isolation and composition in Vicia faba L. Biochimica et Biophysica Acta *78*, 148-162.
Grennan, A.K. (2008). Plastoglobule proteome. Plant physiology *147*, 443-445.

Grzyb, J.M., Solymosi, K., Strzałka, K., and Mysliwa-Kurdziel, B. (2013). Visualization and characterization of prolamellar bodies with atomic force microscopy. J Plant Physiol *170*, 1217-1227.

Gunning, B.E. (2001). Membrane geometry of "open" prolamellar bodies. Protoplasma *215*, 4-15.

Havaux, M. (2014). Carotenoid oxidation products as stress signals in plants. Plant J *79*, 597-606.

Havaux, M., Eymery, F.o., Porfirova, S., Rey, P., and Dörmann, P. (2005). Vitamin E Protects against Photoinhibition and Photooxidative Stress in Arabidopsis thaliana. The Plant Cell *17*, 3451-3469.

Herbstová, M., Tietz, S., Kinzel, C., Turkina, M.V., and Kirchhoff, H. (2012). Architectural switch in plant photosynthetic membranes induced by light stress. Proceedings of the National Academy of Sciences of the United States of America *109*, 20130-20135.

Holm, M., and Deng, X.W. (1999). Structural organization and interactions of COP1, a light-regulated developmental switch. Plant molecular biology *41*, 151-158.

Huang, H., Yang, M., Su, Y.e., Qu, L., and Deng, X.W. (2015). Arabidopsis Atypical Kinases ABC1K1 and ABC1K3 Act Oppositely to Cope with Photodamage Under Red Light. Mol Plant *8*, 1122-1124.

Järvi, S., Suorsa, M., and Aro, E.-M. (2015). Photosystem II repair in plant chloroplasts — Regulation, assisting proteins and shared components with photosystem II biogenesis. Biochimica et Biophysica Acta (BBA) - Bioenergetics *1847*, 900-909.

Jarvis, P. (2004). Organellar proteomics: chloroplasts in the spotlight. Current biology : CB *14*, R317-319.

Jun, L., Saiki, R., Tatsumi, K., Nakagawa, T., and Kawamukai, M. (2004). Identification and subcellular localization of two solanesyl diphosphate synthases from Arabidopsis thaliana. Plant Cell Physiol *45*, 1882-1888.

Junesch, U., and Gräber, P. (1991). The rate of ATP-synthesis as a function of ΔpH and Δψ catalyzed by the active, reduced H+-ATPase from chloroplasts. FEBS Letters *294*, 275-278.

Jung, H.-S., Crisp, P.A., Estavillo, G.M., Cole, B., Hong, F., Mockler, T.C., Pogson, B.J., and Chory, J. (2013). Subset of heat-shock transcription factors required for the early response of Arabidopsis to excess light. Proceedings of the National Academy of Sciences of the United States of America *110*, 14474-14479.

Jung, H.S., and Mockler, T.C. (2014). A new alternative in plant retrograde signaling. Genome biology *15*, 117.

Kambakam, S., Bhattacharjee, U., Petrich, J., and Rodermel, S. (2016). PTOX Mediates Novel Pathways of Electron Transport in Etioplasts of Arabidopsis. Mol Plant *9*, 1240-1259.

Karpinski, S., Reynolds, H., Karpinska, B., Wingsle, G., Creissen, G., and Mullineaux, P. (1999). Systemic signaling and acclimation in response to excess excitation energy in Arabidopsis. Science (New York, NY) *284*, 654-657.

Kato, Y., Miura, E., Ido, K., Ifuku, K., and Sakamoto, W. (2009). The Variegated Mutants Lacking Chloroplastic FtsHs Are Defective in D1 Degradation and Accumulate Reactive Oxygen Species. Plant Physiology *151*, 1790-1801.

Kato, Y., and Sakamoto, W. (2009). Protein quality control in chloroplasts: a current model of D1 protein degradation in the photosystem II repair cycle. Journal of biochemistry *146*, 463-469.

Kato, Y., and Sakamoto, W. (2018). FtsH Protease in the Thylakoid Membrane: Physiological Functions and the Regulation of Protease Activity. Front Plant Sci *9*.

Kato, Y., Sun, X., Zhang, L., and Sakamoto, W. (2012). Cooperative D1 Degradation in the Photosystem II Repair Mediated by Chloroplastic Proteases in Arabidopsis. Plant Physiology *159*, 1428-1439.

Keegstra, K., and Cline, K. (1999). Protein import and routing systems of chloroplasts. The Plant cell *11*, 557-570.

Keegstra, K., and Froehlich, J.E. (1999). Protein import into chloroplasts. Current opinion in plant biology *2*, 471-476.

Kemmerer, Z.A., Robinson, K.P., Schmitz, J.M., Manicki, M., Paulson, B.R., Jochem, A., Hutchins, P.D., Coon, J.J., and Pagliarini, D.J. (2021). UbiB proteins regulate cellular CoQ distribution in Saccharomyces cerevisiae. Nature Communications *12*, 4769.

Kessler, F., Schnell, D., and Blobel, G. (1999). Identification of proteins associated with plastoglobules isolated from pea (Pisum sativum L.) chloroplasts. Planta *208*, 107-113.

Kessler, F., and Schnell, D.J. (2004). Chloroplast protein import: solve the GTPase riddle for entry. Trends in cell biology *14*, 334-338.

Kessler, F., and Schnell, D.J. (2006). The Function and Diversity of Plastid Protein Import Pathways: A Multilane GTPase Highway into Plastids. Traffic *7*, 248-257.

Kim, C., and Apel, K. (2013). 1O2-Mediated and EXECUTER-Dependent Retrograde Plastid-to-Nucleus Signaling in Norflurazon-Treated Seedlings of Arabidopsis thaliana. Mol Plant *6*, 1580-1591.

Kim, C., Lee, K.P., Baruah, A., Nater, M., Göbel, C., Feussner, I., and Apel, K. (2009). $^{1}O_{2}$-mediated retrograde signaling during late embryogenesis predetermines plastid differentiation in seedlings by recruiting abscisic acid. Proc. Natl. Acad. Sci. U.S.A *106*, 9920-9924.

Kim, C., Meskauskiene, R., Zhang, S., Lee, K.P., Lakshmanan Ashok, M., Blajecka, K., Herrfurth, C., Feussner, I., and Apel, K. (2012). Chloroplasts of Arabidopsis Are the Source and a Primary Target of a Plant-Specific Programmed Cell Death Signaling Pathway. The Plant Cell *24*, 3026-3039.

Kleine, T., and Leister, D. (2016). Retrograde signaling: Organelles go networking. Biochimica et Biophysica Acta (BBA) - Bioenergetics *1857*, 1313-1325.

Koussevitzky, S., Nott, A., Mockler, T.C., Hong, F., Sachetto-Martins, G., Surpin, M., Lim, J., Mittler, R., and Chory, J. (2007). Signals from Chloroplasts Converge to Regulate Nuclear Gene Expression. Science. Science *316*, 715-719.

Küchler, M., Decker, S., Hörmann, F., Soll, J., and Heins, L. (2002). Protein import into chloroplasts involves redox-regulated proteins. EMBO J *21*, 6136-6145.

Laizet, Y., Pontier, D., Mache, R., and Kuntz, M. (2004). Subfamily Organization and Phylogenetic Origin of Genes Encoding Plastid Lipid-Associated Proteins of the Fibrillin Type. Journal of Genome Science and Technology *3*, 19-28.

Latowski, D., Kuczyńska, P., and Strzałka, K. (2011). Xanthophyll cycle--a mechanism protecting plants against oxidative stress. Redox Rep *16*, 78-90.

Lee, D.W., Lee, S., Lee, G.-j., Lee, K.H., Kim, S., Cheong, G.-W., and Hwang, I. (2005). Functional Characterization of Sequence Motifs in the Transit Peptide of Arabidopsis Small Subunit of Rubisco. Plant Physiology *140*, 466-483.

Lee, K.P., Kim, C., Landgraf, F., and Apel, K. (2007). EXECUTER1- and EXECUTER2-dependent transfer of stress-related signals from the plastid to the nucleus of Arabidopsis thaliana. Proceedings of the National Academy of Sciences of the United States of America *104*, 10270-10275.

Leivar, P., and Monte, E. (2014). PIFs: systems integrators in plant development. Plant Cell *26*, 56-78.

Li, L., and Yuan, H. (2013). Chromoplast biogenesis and carotenoid accumulation. Archives of biochemistry and biophysics *539*, 102-109.

Li, X.-P., Müller-Moulé, P., Gilmore, A.M., and Niyogi, K.K. (2002). PsbS-dependent enhancement of feedback de-excitation protects photosystem II from photoinhibition. Proceedings of the National Academy of Sciences *99*, 15222.

Li, X.P., Björkman, O., Shih, C., Grossman, A.R., Rosenquist, M., Jansson, S., and Niyogi, K.K. (2000). A pigment-binding protein essential for regulation of photosynthetic light harvesting. Nature *403*, 391-395.

Lichtenthaler, H.K. (1968). Verbreitung und relative Konzentration der lipophilen Plastidenchionone in grünen Pflanzen. Planta *81*, 140-152.

Lichtenthaler, H.K., and Peveling, E. (1966). [Osmiophilic lipid inclusions in the chloroplasts and in the cytoplasm of Hoya carnosa R. Br]. Die Naturwissenschaften *53*, 534.

Lindahl, M., Tabak, S., Cseke, L., Pichersky, E., Andersson, B., and Adam, Z. (1996). Identification, characterization, and molecular cloning of a homologue of the bacterial FtsH protease in chloroplasts of higher plants. J Biol Chem *271*, 29329-29334.

Lippold, F., vom Dorp, K., Abraham, M., Hölzl, G., Wewer, V., Yilmaz, J.L., Lager, I., Montandon, C., Besagni, C., Kessler, F., *et al.* (2012). Fatty Acid Phytyl Ester Synthesis in Chloroplasts of Arabidopsis The Plant Cell *24*, 2001-2014.

Liu, Z., Yan, H., Wang, K., Kuang, T., Zhang, J., Gui, L., An, X., and Chang, W. (2004). Crystal structure of spinach major light-harvesting complex at 2.72 Å resolution. Nature *428*, 287-292.

Loll, B., Kern, J., Saenger, W., Zouni, A., and Biesiadka, J. (2005). Towards complete cofactor arrangement in the 3.0 Å resolution structure of photosystem II. Nature *438*, 1040-1044.

Lundquist, P.K., Davis, J.I., and van Wijk, K.J. (2012a). ABC1K atypical kinases in plants: filling the organellar kinase void. Trends in Plant Science *17*, 546-555.

Lundquist, P.K., Poliakov, A., Bhuiyan, N.H., Zybailov, B., Sun, Q., and van Wijk, K.J. (2012b). The Functional Network of the Arabidopsis Plastoglobule Proteome Based on Quantitative Proteomics and Genome-Wide Coexpression Analysis. Plant Physiology *158*, 1172-1192.

Lundquist, P.K., Poliakov, A., Giacomelli, L., Friso, G., Appel, M., McQuinn, R.P., Krasnoff, S.B., Rowland, E., Ponnala, L., Sun, Q., *et al.* (2013). Loss of plastoglobule kinases ABC1K1 and ABC1K3 causes conditional degreening, modified prenyl-lipids, and recruitment of the jasmonic acid pathway. The Plant cell *25*, 1818-1839.

Mackender, R.O., and Leech, R.M. (1974). The Galactolipid, Phospholipid, and Fatty Acid Composition of the Chloroplast Envelope Membranes of Vicia faba. L. Plant physiology *53*, 496-502.

Manara, A., DalCorso, G., and Furini, A. (2016). The Role of the Atypical Kinases ABC1K7 and ABC1K8 in Abscisic Acid Responses. Front Plant Sci *7*, 366-366.

Manara, A., DalCorso, G., Guzzo, F., and Furini, A. (2015). Loss of the Atypical Kinases ABC1K7 and ABC1K8 Changes the Lipid Composition of the Chloroplast Membrane. Plant and Cell Physiology *56*, 1193-1204.

Manara, A., Dalcorso, G., Leister, D., Jahns, P., Baldan, B., and Furini, A. (2013). AtSIA1 AND AtOSA1: Two Abc1 proteins involved in oxidative stress responses and iron distribution within chloroplasts. The New phytologist *201*, 452-465.

Martin, W., Rujan, T., Richly, E., Hansen, A., Cornelsen, S., Lins, T., Leister, D., Stoebe, B., Hasegawa, M., and Penny, D. (2002). Evolutionary analysis of Arabidopsis, cyanobacterial, and chloroplast genomes reveals plastid phylogeny and thousands of cyanobacterial genes in the nucleus. Proc Natl Acad Sci U.S.A *99*, 12246-12251.

Martin, W., Stoebe, B., Goremykin, V., Hansmann, S., Hasegawa, M., and Kowallik, K.V. (1998). Gene transfer to the nucleus and the evolution of chloroplasts. Nature *393*, 162-165.

Martínez-García, J.F., Huq, E., and Quail, P.H. (2000). Direct Targeting of Light Signals to a Promoter Element-Bound Transcription Factor. Science *288*, 859-863.

Martinis, J., Glauser, G., Valimareanu, S., and Kessler, F. (2013). A Chloroplast ABC1-like Kinase Regulates Vitamin E Metabolism in Arabidopsis. Plant Physiology *162*, 652-662.

Martinis, J., Glauser, G., Valimareanu, S., Stettler, M., Zeeman, S.C., Yamamoto, H., Shikanai, T., and Kessler, F. (2014). ABC1K1/PGR6 kinase: a regulatory link between photosynthetic activity and chloroplast metabolism. The Plant Journal *77*, 269-283.

Mène-Saffrané, L., Jones, A.D., and DellaPenna, D. (2010). Plastochromanol-8 and tocopherols are essential lipid-soluble antioxidants during seed desiccation and quiescence in Arabidopsis. Proceedings of the National Academy of Sciences of the United States of America *107*, 17815-17820.

Meskauskiene, R., Nater, M., Goslings, D., Kessler, F., op den Camp, R., and Apel, K. (2001). FLU: A negative regulator of chlorophyll biosynthesis in Arabidopsis thaliana. Proc Natl Acad Sci U.S.A *98*, 12826-12831.

Mirkovic, T., Ostroumov, E. E., Anna, J. M., van Grondelle, R., Govindjee & Scholes, G. D. Light absorption and energy transfer in the antenna complexes of photosynthetic organisms. *Chem Rev* **117**, 249-293 (2017).

Miura, E., Kato, Y., and Sakamoto, W. (2010). Comparative transcriptome analysis of green/white variegated sectors in Arabidopsis yellow variegated2: responses to oxidative and other stresses in white sectors. J Exp Bot *61*, 2433-2445.

Mochizuki, N., Brusslan, J.A., Larkin, R., Nagatani, A., and Chory, J. (2001). Arabidopsis genomes uncoupled 5 (GUN5) mutant reveals the involvement of Mg-chelatase H subunit in plastid-to-nucleus signal transduction. Proceedings of the National Academy of Sciences of the United States of America *98*, 2053-2058.

Mollet, J., Delahodde, A., Serre, V., Chretien, D., Schlemmer, D., Lombes, A., Boddaert, N., Desguerre, I., de Lonlay, P., Ogier de Baulny, H., *et al.* (2008). CABC1 Gene Mutations Cause Ubiquinone Deficiency with Cerebellar Ataxia and Seizures. The American Journal of Human Genetics *82*, 623-630.

Müller, P., Li, X.P., and Niyogi, K.K. (2001). Non-photochemical quenching. A response to excess light energy. Plant physiology *125*, 1558-1566.

Munekage, Y., Hashimoto, M., and Miyake, C. (2004). Cyclic electron flow around photosystem I is essential for photosynthesis. Nature *700*.

Nacir, H., and Brehelin, C. (2013). When Proteomics Reveals Unsuspected Roles: The Plastoglobule Example. Front Plant Sci *4*, 114.

Neuwald, A.F., Aravind, L., Spouge, J.L., and Koonin, E.V. (1999). AAA+: A class of chaperone-like ATPases associated with the assembly, operation, and disassembly of protein complexes. Genome research *9*, 27-43.

Nilkens, M., Kress, E., Lambrev, P., Miloslavina, Y., Müller, M., Holzwarth, A., and Jahns, P. (2010). Identification of a slowly inducible zeaxanthin-dependent component of non-

photochemical quenching of chlorophyll fluorescence generated under steady-state conditions in Arabidopsis. Biochimica et biophysica acta *1797*, 466-475.

Nixon, P.J., Barker, M., Boehm, M., de Vries, R., and Komenda, J. (2005). FtsH-mediated repair of the photosystem II complex in response to light stress. J Exp Bot *56*, 357-363.

Okegawa, Y., Kobayashi, Y., and Shikanai, T. (2010). Physiological links among alternative electron transport pathways that reduce and oxidize plastoquinone in Arabidopsis. Plant J *63*, 458-468.

op den Camp, R.G.L., Przybyla, D., Ochsenbein, C., Laloi, C., Kim, C., Danon, A., Wagner, D., Hideg, E., Göbel, C., Feussner, I., *et al.* (2003). Rapid induction of distinct stress responses after the release of singlet oxygen in Arabidopsis. The Plant cell *15*, 2320-2332.

Ostersetzer, O., and Adam, Z. (1997). Light-stimulated degradation of an unassembled Rieske FeS protein by a thylakoid-bound protease: the possible role of the FtsH protease. The Plant cell *9*, 957-965.

Otsubo, M., Ikoma, C., Ueda, M., Ishii, Y., and Tamura, N. (2018). Functional Role of Fibrillin5 in Acclimation to Photooxidative Stress. Plant and Cell Physiology *59*, 1670-1682.

Page, M.T., McCormac, A.C., Smith, A.G., and Terry, M.J. (2017). Singlet oxygen initiates a plastid signal controlling photosynthetic gene expression. New phytol *213*, 1168-1180.

Pagliano, C., Nield, J., Marsano, F., Pape, T., Barera, S., Saracco, G., and Barber, J. (2014). Proteomic characterization and three-dimensional electron microscopy study of PSII-LHCII supercomplexes from higher plants. Biochim Biophys Acta *1837*, 1454-1462.

Pagliano, C., Saracco, G., and Barber, J. (2013). Structural, functional and auxiliary proteins of photosystem II. Photosynth Res *116*, 167-188.

Paila, Y.D., Richardson, L.G.L., and Schnell, D.J. (2015). New insights into the mechanism of chloroplast protein import and its integration with protein quality control, organelle biogenesis and development. Journal of molecular biology *427*, 1038-1060.

Pan, X., Li, M., Wan, T., Wang, L., Jia, C., Hou, Z., Zhao, X., Zhang, J., and Chang, W. (2011). Structural insights into energy regulation of light-harvesting complex CP29 from spinach. Nature Structural & Molecular Biology *18*, 309-315.

Park, E., Kim, Y., and Choi, G. (2018). Phytochrome B Requires PIF Degradation and Sequestration to Induce Light Responses across a Wide Range of Light Conditions. Plant Cell *30*, 1277-1292.

Patel, S., and Latterich, M. (1998). The AAA team: related ATPases with diverse functions. Trends in cell biology *8*, 65-71.

Perez-Riverol, Y., Csordas, A., Bai, J., Bernal-Llinares, M., Hewapathirana, S., Kundu, D.J., Inuganti, A., Griss, J., Mayer, G., Eisenacher, M., *et al.* (2019). The PRIDE database and related tools and resources in 2019: improving support for quantification data. Nucleic Acids Res *47*, D442-D450.

Petrillo, E., Godoy Herz, M.A., Fuchs, A., Reifer, D., Fuller, J., Yanovsky, M.J., Simpson, C., Brown, J.W., Barta, A., Kalyna, M., *et al.* (2014). A chloroplast retrograde signal regulates nuclear alternative splicing. Science (New York, NY) *344*, 427-430.

Pham, V.N., Kathare, P.K., and Huq, E. (2018). Phytochromes and Phytochrome Interacting Factors. Plant Physiol *176*, 1025-1038.

Pipitone, R., Eicke, S., Pfister, B., Glauser, G., Falconet, D., Uwizeye, C., Pralon, T., Zeeman, S.C., Kessler, F., and Demarsy, E. (2021). A multifaceted analysis reveals two distinct phases of chloroplast biogenesis during de-etiolation in Arabidopsis. eLife *10*.

Pogson, B.J., Woo, N.S., Förster, B., and Small, I.D. (2008). Plastid signalling to the nucleus and beyond. Trends in Plant Science *13*, 602-609.

Ponnu, J., and Hoecker, U. (2021). Illuminating the COP1/SPA Ubiquitin Ligase: Fresh Insights Into Its Structure and Functions During Plant Photomorphogenesis. Front Plant Sci *12*.

Poon, W.W., Davis, D.E., Ha, H.T., Jonassen, T., Rather, P.N., and Clarke, C.F. (2000). Identification of Escherichia coli ubiB, a gene required for the first monooxygenase step in ubiquinone biosynthesis. J Bacteriol *182*, 5139-5146.

Pospísil, P. (2009). Production of reactive oxygen species by photosystem II. Biochim Biophys Acta *1787*, 1151-1160.

Pospíšil, P. (2016). Production of Reactive Oxygen Species by Photosystem II as a Response to Light and Temperature Stress. Front Plant Sci *7*.

Pralon, T., Collombat, J., Pipitone, R., Ksas, B., Shanmugabalaji, V., Havaux, M., Finazzi, G., Longoni, P., and Kessler, F. (2020). Mutation of the Atypical Kinase ABC1K3 Partially Rescues the PROTON GRADIENT REGULATION 6 Phenotype in Arabidopsis thaliana. Front Plant Sci *11*, 337

Pralon, T., Shanmugabalaji, V., Longoni, P., Glauser, G., Ksas, B., Collombat, J., Desmeules, S., Havaux, M., Finazzi, G., and Kessler, F. (2019). Plastoquinone homoeostasis by Arabidopsis proton gradient regulation 6 is essential for photosynthetic efficiency. Commun Biol *2*, 220.

Ramel, F., Birtic, S., Cuiné, S., Triantaphylidès, C., Ravanat, J.-L., and Havaux, M. (2012a). Chemical Quenching of Singlet Oxygen by Carotenoids in Plants Plant Physiology *158*, 1267-1278.

Ramel, F., Birtic, S., Ginies, C., Soubigou-Taconnat, L., Triantaphylidès, C., and Havaux, M. (2012b). Carotenoid oxidation products are stress signals that mediate gene responses to singlet oxygen in plants. Proceedings of the National Academy of Sciences of the United States of America *109*, 5535-5540.

Rédei, G.P. (1967). Biochemical aspects of a genetically determined variegation in Arabidopsis. Genetics *56*, 431-443.

Reyes-Prieto, A., Weber, A.P., and Bhattacharya, D. (2007). The origin and establishment of the plastid in algae and plants. Annual review of genetics *41*, 147-168.

Richardson, L.G.L., Paila, Y.D., Siman, S.R., Chen, Y., Smith, M.D., and Schnell, D.J. (2014). Targeting and assembly of components of the TOC protein import complex at the chloroplast outer envelope membrane. Front Plant Sci *5*, 269-269.

Richter, M., Rühle, W., and Wild, A. (1990). Studies on the mechanism of photosystem II photoinhibition II. The involvement of toxic oxygen species. Photosynthesis Research *24*, 237-243.

Rochaix, J.D. (2011). Regulation of photosynthetic electron transport. Biochim Biophys Acta *1807*, 375-383.

Rockwell, N.C., Su, Y.S., and Lagarias, J.C. (2006). Phytochrome structure and signaling mechanisms. Annual review of plant biology *57*, 837-858.

Rossel, J.B., Walter, P.B., Hendrickson, L., Chow, W.S., Poole, A., Mullineaux, P.M., and Pogson, B.J. (2006). A mutation affecting ASCORBATE PEROXIDASE 2 gene expression reveals a link between responses to high light and drought tolerance. Plant, cell & environment *29*, 269-281.

Rossel, J.B., Wilson, I.W., and Pogson, B.J. (2002). Global Changes in Gene Expression in Response to High Light in Arabidopsis. Plant Physiology *130*, 1109-1120.

Rosso, D., Bode, R., Li, W., Krol, M., Saccon, D., Wang, S., Schillaci, L.A., Rodermel, S.R., Maxwell, D.P., and Hüner, N.P.A. (2009). Photosynthetic Redox Imbalance Governs Leaf Sectoring in the Arabidopsis thaliana Variegation Mutants immutans, spotty, var1, and var2 The Plant Cell *21*, 3473-3492.

Rottet, S., Besagni, C., and Kessler, F. (2015). The role of plastoglobules in thylakoid lipid remodeling during plant development. Biochimica et Biophysica Acta (BBA) - Bioenergetics *1847*, 889-899.

Sadali, N.M., Sowden, R.G., Ling, Q., and Jarvis, R.P. (2019). Differentiation of chromoplasts and other plastids in plants. Plant cell reports *38*, 803-818.

Sakamoto, W., Zaltsman, A., Adam, Z., and Takahashi, Y. (2003). Coordinated regulation and complex formation of yellow variegated1 and yellow variegated2, chloroplastic FtsH metalloproteases involved in the repair cycle of photosystem II in Arabidopsis thylakoid membranes. The Plant cell *15*, 2843-2855.

Scheeff, E.D., and Bourne, P.E. (2005). Structural evolution of the protein kinase-like superfamily. PLoS computational biology *1*, e49.

Schnell, D.J., Blobel, G., Keegstra, K., Kessler, F., Ko, K., and Soll, J. (1997). A consensus nomenclature for the protein-import components of the chloroplast envelope. Trends in cell biology *7*, 303-304.

Schnell, D.J., Kessler, F., and Blobel, G. (1994). Isolation of components of the chloroplast protein import machinery. Science (New York, NY) *266*, 1007-1012.

Shapiguzov, A., Ingelsson, B., Samol, I., Andres, C., Kessler, F., Rochaix, J.-D., Vener, A.V., and Goldschmidt-Clermont, M. (2010). The PPH1 phosphatase is specifically involved in LHCII dephosphorylation and state transitions in Arabidopsis. Proc Natl Acad Sci USA *107*, 4782-4787.

Shikanai, T., Munekage, Y., Shimizu, K., Endo, T., and Hashimoto, T. (1999). Identification and Characterization of Arabidopsis Mutants with Reduced Quenching of Chlorophyll Fluorescence. Plant and Cell Physiology *40*, 1134-1142.

Shikanai, T., and Yamamoto, H. (2017). Contribution of Cyclic and Pseudo-cyclic Electron Transport to the Formation of Proton Motive Force in Chloroplasts. Mol Plant *10*, 20-29.
Simkin, A., Gaffé, J., Alcaraz, J.-P., Carde, J.-P., Bramley, P., Fraser, P., and Kuntz, M. (2007a). Fibrillin influence on plastid ultrastructure and pigment content in tomato fruit. Phytochemistry *68*, 1545-1556.

Simkin, A.J., Gaffé, J., Alcaraz, J.P., Carde, J.P., Bramley, P.M., Fraser, P.D., and Kuntz, M. (2007b). Fibrillin influence on plastid ultrastructure and pigment content in tomato fruit. Phytochemistry *68*, 1545-1556.

Singh, D.K., Laremore, T.N., Smith, P.B., Maximova, S.N., and McNellis, T.W. (2012). Knockdown of FIBRILLIN4 gene expression in apple decreases plastoglobule plastoquinone content. PloS one *7*, e47547.

Singh, D.K., Maximova, S.N., Jensen, P.J., Lehman, B.L., Ngugi, H.K., and McNellis, T.W. (2010). FIBRILLIN4 is required for plastoglobule development and stress resistance in apple and Arabidopsis. Plant physiology *154*, 1281-1293.

Singh, D.K., and McNellis, T.W. (2011). Fibrillin protein function: the tip of the iceberg? Trends Plant Sci *16*, 432-441.

Sinvany-Villalobo, G., Davydov, O., Ben-Ari, G., Zaltsman, A., Raskind, A., and Adam, Z. (2004). Expression in multigene families. Analysis of chloroplast and mitochondrial proteases. Plant physiology *135*, 1336-1345.

Slesak, I., Libik, M., Karpinska, B., Karpinski, S., and Miszalski, Z. (2007). The role of hydrogen peroxide in regulation of plant metabolism and cellular signalling in response to environmental stresses. Acta biochimica Polonica *54*, 39-50.

Smith, M.D., Rounds, C.M., Wang, F., Chen, K., Afitlhile, M., and Schnell, D.J. (2004). atToc159 is a selective transit peptide receptor for the import of nucleus-encoded chloroplast proteins. J Cell Biol *165*, 323-334.

Solymosi, K., and Schoefs, B. (2010). Etioplast and etio-chloroplast formation under natural conditions: the dark side of chlorophyll biosynthesis in angiosperms. Photosynth Res *105*, 143-166.

Song, C., Mroginski, M.A., Lang, C., Kopycki, J., Gärtner, W., Matysik, J., and Hughes, J. (2018). 3D Structures of Plant Phytochrome A as Pr and Pfr From Solid-State NMR: Implications for Molecular Function. Front Plant Sci *9*, 498

Sprey, B., and Lichtenthaler, H.K. (1966). Zur Frage der Beziehungen zwischen Plastoglobuli und Thylakoidgenese in Gerstenkeimlingen. Zeitschrift für Naturforschung B. *21*, 697-699.

Spurr, A.R., and Harris, W.M. (1968). ULTRASTRUCTURE OF CHLOROPLASTS AND CHROMOPLASTS IN CAPSICUM ANNUUM I. THYLAKOID MEMBRANE CHANGES DURING FRUIT RIPENING. Am J Bot *55*, 1210-1224.

Stahl, W., and Sies, H. (2003). Antioxidant activity of carotenoids. Molecular Aspects of Medicine *24*, 345-351.

Standfuss, J., Terwisscha van Scheltinga, A.C., Lamborghini, M., and Kühlbrandt, W. (2005). Mechanisms of photoprotection and nonphotochemical quenching in pea light-harvesting complex at 2.5 A resolution. EMBO J *24*, 919-928.

Strand, Å., Asami, T., Alonso, J., Ecker, J.R., and Chory, J. (2003). Chloroplast to nucleus communication triggered by accumulation of Mg-protoporphyrinIX. Nature *421*, 79-83.

Sugiura, M. (1989). The Chloroplast Chromosomes in Land Plants. Annu Rev Cell Biol *5*, 51-70.

Susek, R.E., Ausubel, F.M., and Chory, J. (1993). Signal transduction mutants of arabidopsis uncouple nuclear CAB and RBCS gene expression from chloroplast development. Cell *74*, 787-799.

Szymańska, R., and Kruk, J. (2010). Plastoquinol is the Main Prenyllipid Synthesized During Acclimation to High Light Conditions in Arabidopsis and is Converted to Plastochromanol by Tocopherol Cyclase. Plant and Cell Physiology *51*, 537-545.

Terry, M.J., and Kendrick, R.E. (1999). Feedback inhibition of chlorophyll synthesis in the phytochrome chromophore-deficient aurea and yellow-green-2 mutants of tomato. Plant physiology *119*, 143-152.

Tevini, M., and Steinmüller, D. (1985). Composition and function of plastoglobuli : II. Lipid composition of leaves and plastoglobuli during beech leaf senescence. Planta *163*, 91-96.
Theis, J., and Schroda, M. (2016). Revisiting the photosystem II repair cycle. Plant signaling & behavior *11*, e1218587.

Tikhonov, A.N. (2014). The cytochrome b6f complex at the crossroad of photosynthetic electron transport pathways. Plant physiology and biochemistry : PPB *81*, 163-183.

Tikkanen, M., Nurmi, M., Kangasjärvi, S., and Aro, E.M. (2008). Core protein phosphorylation facilitates the repair of photodamaged photosystem II at high light. Biochim Biophys Acta *1777*, 1432-1437.

Timmis, J.N., Ayliffe, M.A., Huang, C.Y., and Martin, W. (2004). Endosymbiotic gene transfer: organelle genomes forge eukaryotic chromosomes. Nature reviews Genetics *5*, 123-135.

Torres-Romero, D., Gómez-Zambrano, Á., Serrato, A.J., Sahrawy, M., and Mérida, Á. (2020). Fibrillin 2 interacts with other proteins to protect photosystem II against abiotic stress in Arabidopsis thaliana. 2020.2010.2007.329979.

Triantaphylidès, C., Krischke, M., Hoeberichts, F.A., Ksas, B., Gresser, G., Havaux, M., Van Breusegem, F., and Mueller, M.J. (2008). Singlet Oxygen Is the Major Reactive Oxygen Species Involved in Photooxidative Damage to Plants. Plant Physiology *148*, 960-968.

Tripathi, S., Hoang, Q.T.N., Han, Y.-J., and Kim, J.-I. (2019). Regulation of Photomorphogenic Development by Plant Phytochromes. Int J Mol Sci *20*, 6165.

Tuquet, C., and Newman, D.W. (1980). Aging and regreening in soybean cotyledons. 1 Ultrastructural changes in plastids and plastoglobuli. Cytobios *29*, 43-59.

van Wijk, K.J., Roobol-Boza, M., Kettunen, R., Andersson, B., and Aro, E.M. (1997). Synthesis and assembly of the D1 protein into photosystem II: processing of the C-terminus and identification of the initial assembly partners and complexes during photosystem II repair. Biochemistry *36*, 6178-6186.

Vener, A.V., van Kan, P.J., Rich, P.R., Ohad, I., and Andersson, B. (1997). Plastoquinol at the quinol oxidation site of reduced cytochrome bf mediates signal transduction between light and protein phosphorylation: thylakoid protein kinase deactivation by a single-turnover flash. Proceedings of the National Academy of Sciences of the United States of America *94*, 1585-1590.

Vidi, P.A., Kanwischer, M., Baginsky, S., Austin, J.R., Csucs, G., Dormann, P., Kessler, F., and Brehelin, C. (2006). Tocopherol cyclase (VTE1) localization and vitamin E accumulation in chloroplast plastoglobule lipoprotein particles. J Biol Chem *281*, 11225-11234.

Vinyard, D.J., and Brudvig, G.W. (2017). Progress Toward a Molecular Mechanism of Water Oxidation in Photosystem II. Annual review of physical chemistry *68*, 101-116.

Wagner, D., Przybyla, D., Camp, R.o.d., Kim, C., Landgraf, F., Lee, K.P., Würsch, M., Laloi, C., Nater, M., Hideg, E., *et al.* (2004). The Genetic Basis of Singlet Oxygen-Induced Stress Responses of Arabidopsis thaliana. Science *306*, 1183-1185.

Walter, B., Hristou, A., Nowaczyk, M.M., and Schünemann, D. (2015). In vitro reconstitution of co-translational D1 insertion reveals a role of the cpSec-Alb3 translocase and Vipp1 in photosystem II biogenesis. The Biochemical journal *468*, 315-324.

Wang, L., Kim, C., Xu, X., Piskurewicz, U., Dogra, V., Singh, S., Mahler, H., and Apel, K. (2016). Singlet oxygen- and EXECUTER1-mediated signaling is initiated in grana margins and depends on the protease FtsH2. Proceedings of the National Academy of Sciences of the United States of America *113*, E3792-3800.

Wang, L., Leister, D., Guan, L., Zheng, Y., Schneider, K., Lehmann, M., Apel, K., and Kleine, T. (2020). The Arabidopsis SAFEGUARD1 suppresses singlet oxygen-induced stress responses by protecting grana margins. Proc Natl Acad Sci U.S.A *117*, 6918-6927.

Wetzel, C.M., Jiang, C.Z., Meehan, L.J., Voytas, D.F., and Rodermel, S.R. (1994). Nuclear-organelle interactions: the immutans variegation mutant of Arabidopsis is plastid autonomous and impaired in carotenoid biosynthesis. The Plant journal : for cell and molecular biology *6*, 161-175.

Whitelegge, J.P., Zhang, H., Aguilera, R., Taylor, R.M., and Cramer, W.A. (2002). Full subunit coverage liquid chromatography electrospray ionization mass spectrometry (LCMS+) of an oligomeric membrane protein: cytochrome b(6)f complex from spinach and the cyanobacterium Mastigocladus laminosus. Molecular & cellular proteomics : MCP *1*, 816-827.

Wilson, P.B., Estavillo, G.M., Field, K.J., Pornsiriwong, W., Carroll, A.J., Howell, K.A., Woo, N.S., Lake, J.A., Smith, S.M., Harvey Millar, A., *et al.* (2009). The nucleotidase/phosphatase SAL1 is a negative regulator of drought tolerance in Arabidopsis. The Plant Journal *58*, 299-317.

Woodson, Jesse D., Perez-Ruiz, Juan M., and Chory, J. (2011). Heme Synthesis by Plastid Ferrochelatase I Regulates Nuclear Gene Expression in Plants. Current Biology *21*, 897-903.

Xie, L.X., Hsieh, E.J., Watanabe, S., Allan, C.M., Chen, J.Y., Tran, U.C., and Clarke, C.F. (2011). Expression of the human atypical kinase ADCK3 rescues coenzyme Q biosynthesis and phosphorylation of Coq polypeptides in yeast coq8 mutants. Biochimica et Biophysica Acta (BBA) - Molecular and Cell Biology of Lipids *1811*, 348-360.

Xu, P., Roy, L.M., and Croce, R. (2017). Functional organization of photosystem II antenna complexes: CP29 under the spotlight. Biochimica et biophysica acta Bioenergetics *1858*, 815-822.

Yang, M., Huang, H., Zhang, C., Wang, Z., Su, Y., Zhu, P., Guo, Y., and Deng, X.W. (2016). Arabidopsis atypical kinase ABC1K1 is involved in red light-mediated development. Plant cell reports *35*, 1213-1220.

Yang, S., Zeng, X., Li, T., Liu, M., Zhang, S., Gao, S., Wang, Y., Peng, C., Li, L., and Yang, C. (2012). AtACDO1, an ABC1-like kinase gene, is involved in chlorophyll degradation and the response to photooxidative stress in Arabidopsis. J Exp Bot *63*, 3959-3973.

Yoon, H.S., Hackett, J.D., Ciniglia, C., Pinto, G., and Bhattacharya, D. (2004). A Molecular Timeline for the Origin of Photosynthetic Eukaryotes. Molecular Biology and Evolution *21*, 809-818.

Ytterberg, A.J., Peltier, J.B., and van Wijk, K.J. (2006). Protein profiling of plastoglobules in chloroplasts and chromoplasts. A surprising site for differential accumulation of metabolic enzymes. Plant Physiol *140*, 984-997.

Yu, F., Park, S., and Rodermel, S.R. (2004). The Arabidopsis FtsH metalloprotease gene family: interchangeability of subunits in chloroplast oligomeric complexes. The Plant journal : for cell and molecular biology *37*, 864-876.

Yu, F., Park, S., and Rodermel, S.R. (2005). Functional redundancy of AtFtsH metalloproteases in thylakoid membrane complexes. Plant physiology *138*, 1957-1966.

Zaltsman, A., Ori, N., and Adam, Z. (2005). Two Types of FtsH Protease Subunits Are Required for Chloroplast Biogenesis and Photosystem II Repair in Arabidopsis. The Plant Cell *17*, 2782-2790.

Zbierzak, A.M., Kanwischer, M., Wille, C., Vidi, P.A., Giavalisco, P., Lohmann, A., Briesen, I., Porfirova, S., Bréhélin, C., Kessler, F., *et al.* (2009). Intersection of the tocopherol and plastoquinol metabolic pathways at the plastoglobule. The Biochemical journal *425*, 389-399.

Zhang, D.-P. (2007). Signaling to the Nucleus with a Loaded GUN. Science (New York, NY) *316*, 700-701.

Zhang, L., Paakkarinen, V., van Wijk, K.J., and Aro, E.M. (1999). Co-translational assembly of the D1 protein into photosystem II. J Biol Chem *274*, 16062-16067.

Zhang, R., Wise, R.R., Struck, K.R., and Sharkey, T.D. (2010). Moderate heat stress of Arabidopsis thaliana leaves causes chloroplast swelling and plastoglobule formation. Photosynth Res *105*, 123-134.

Zhang, S., Apel, K., and Kim, C. (2014). Singlet oxygen-mediated and EXECUTER-dependent signalling and acclimation of Arabidopsis thaliana exposed to light stress. Philos Trans R Soc Lond B Biol Sci *369*, 20130227-20130227.

Zito, F., Finazzi, G., Delosme, R., Nitschke, W., Picot, D., and Wollman, F.A. (1999). The Qo site of cytochrome b6f complexes controls the activation of the LHCII kinase. EMBO J *18*, 2961-2969.

Acknowledgements

In the first place, I would like to thank my thesis director Professor Felix KESSLER for giving me the opportunity to do my PhD in the laboratory of plant physiology and for his support and enthusiasm during these five years.

I am grateful to Dr. Fiamma LONGONI for the help, support, corrections, ideas and stimulating discussion. I could not have hoped a better supervisor and this work would not have been possible without her.

I would like also to thank Dr. Michel HAVAUX and Dr. Brigitte KSAS (CEA, Cadarache, france) for their collaboration and their work about the analyze of lipid peroxydation.

I also thank Dr. Giovanni FINAZZI (CEA, Grenoble, France) and Pr. Joop Vermeer from the laboratory of cell and molecular biology of the University of Neuchâtel for their presence as members of my thesis committee.

I would like to thank Thibaut PRALON and Véronique DOUET for her support, help and discussions during all my PhD.

I am also grateful to Jenny PEGO MAGHALES for her work and his inestimable friendship, for the support and her contagious happiness.

A special thanks to all my colleagues for their help, happiness, support, discussion and for their incredible friendship. Thank you to Gent BALLABANI, Wayne ZITA, Hamed SATTARI VAYGHAN, Shamungabalaji VENTAKASALAM, Gautier PIZZOLON, Maryam FOROUGH, Mancy PHILIP, Segolène BRESSOUD and Bastien CALVIN.

I would like to acknowledge my boyfriend, Florian TRAVERSI, for his unconditional support and for always believing in me. Finally, the last but not least, I would like to thank my family, especially my father for his financial support during my studies, and for giving me the strength and the motivation to do this PhD. I am grateful to my sister and my mother for their continuous support.

Thank you all.